BULLETIN OF RUSSIAN STATE MEDICAL UNIVERSITY

BIOMEDICAL JOURNAL OF PIROGOV RUSSIAN NATIONAL RESEARCH MEDICAL UNIVERSITY

SUBMISSION http://vestnikrgmu.ru/login?lang=en
CORRESPONDENCE editor@vestnikrgmu.ru
COLLABORATION manager@vestnikrgmu.ru
ADDRESS ul. Ostrovityanova, d. 1, Moscow, Russia, 117997

Indexed in Scopus. CiteScore 2018: 0.16

Indexed in WoS. JCR 2018: 0.13

Five-year h-index is 3

Indexed in RSCI. IF 2017: 0.326

Listed in HAC 27.01.2016 (no. 1760)

Open access to archive

Issue DOI: 10.24075/brsmu.2019-05
The mass media registration certificate no. 012769 issued on July 29, 1994
Founder and publisher is Pirogov Russian National Research Medical University (Moscow, Russia)

Approved for print 31.10.2019
Circulation: 100 copies. Printed by Print.Formula
www.print-formula.ru

ВЕСТНИК РОССИЙСКОГО ГОСУДАРСТВЕННОГО МЕДИЦИНСКОГО УНИВЕРСИТЕТА

НАУЧНЫЙ МЕДИЦИНСКИЙ ЖУРНАЛ РНИМУ ИМ. Н. И. ПИРОГОВА

ГЛАВНЫЙ РЕДАКТОР Денис Ребриков, д. б. н., профессор

ЗАМЕСТИТЕЛЬ ГЛАВНОГО РЕДАКТОРА Александр Эттингер, д. м. н., профессор

РЕДАКТОРЫ Валентина Гейдебрехт, Лилия Егорова

ТЕХНИЧЕСКИЙ РЕДАКТОР Нина Тюрина

ПЕРЕВОДЧИКИ Екатерина Третьякова, Вячеслав Витюк

ДИЗАЙН И ВЕРСТКА Марина Доронина

ПОДАЧА РУКОПИСЕЙ http://vestnikrgmu.ru/login
ПЕРЕПИСКА С РЕДАКЦИЕЙ editor@vestnikrgmu.ru
СОТРУДНИЧЕСТВО manager@vestnikrgmu.ru
АДРЕС РЕДАКЦИИ ул. Островитянова, д. 1, г. Москва, 117997

Журнал включен в Scopus. CiteScore 2018: 0,16

Журнал включен в WoS. JCR 2018: 0,13

Индекс Хирша (h^5) журнала по оценке Google Scholar: 3

Журнал включен в РИНЦ. IF 2017: 0,326

Журнал включен в Перечень 27.01.2016 (№ 1760)

Здесь находится открытый архив журнала

DOI выпуска: 10.24075/vrgmu.2019-05
Свидетельство о регистрации средства массовой информации № 012769 от 29 июля 1994 г.
Учредитель и издатель — Российский национальный исследовательский медицинский университет имени Н. И. Пирогова (Москва, Россия)

Подписано в печать 31.10.2019
Тираж 100 экз. Отпечатано в типографии Print.Formula
www.print-formula.ru

BULLETIN OF RSMU **5, 2019**
ВЕСТНИК РГМУ

Contents
Содержание

CAR T-CELL THERAPY OF SOLID TUMORS: PROMISING APPROACHES TO MODULATING ANTITUMOR ACTIVITY OF CAR T CELLS

Kiseleva YaYu ✉, Shishkin AM, Ivanov AV, Kulinich TM, Bozhenko VK

Russian Scientific Center of Roentgenoradiology, Moscow, Russia

Adoptive immunotherapy that makes use of genetically modified autologous T cells carrying a chimeric antigen receptor (CAR) with desired specificity is a promising approach to the treatment of advanced or relapsed solid tumors. However, there are a number of challenges facing the CAR T-cell therapy, including the ability of the tumor to silence the expression of target antigens in response to the selective pressure exerted by therapy and the dampening of the functional activity of CAR T cells by the immunosuppressive tumor microenvironment. This review discusses the existing gene-engineering approaches to the modification of CAR T-cell design for 1) creating universal "switchable" synthetic receptors capable of attacking a variety of target antigens; 2) enhancing the functional activity of CAR T cells in the immunosuppressive microenvironment of the tumor by silencing the expression of inhibiting receptors or by stimulating production of cytokines.

Keywords: CAR T-cell therapy, solid tumors, chimeric antigen receptor, CAR T cells, universal CARs, immunosuppressive microenvironment

Author contribution: Kiseleva YaYu analyzed the literature, prepared the draft of the manuscript, created the figures; Shishkin AM analyzed the literature and revised the manuscript; Ivanov AV analyzed the literature and revised the manuscript; Kulinich TM revised the manuscript; Bozhenko VK revised the manuscript.

✉ **Correspondence should be addressed:** Yana Yu. Kiseleva
Profsoyuznaya, 86, Moscow, 117997; 89036728541 yana.kiseleva@gmail.com

Received: 03.10.2019 **Accepted:** 17.10.2019 **Published online:** 18.10.2019

DOI: 10.24075/brsmu.2019.066

CAR-ТЕРАПИЯ СОЛИДНЫХ ОПУХОЛЕЙ: ПЕРСПЕКТИВНЫЕ ПОДХОДЫ К МОДУЛИРОВАНИЮ ПРОТИВООПУХОЛЕВОЙ АКТИВНОСТИ CAR-T-ЛИМФОЦИТОВ

Я. Ю. Киселева ✉, А. М. Шишкин, А. В. Иванов, Т. М. Кулинич, В. К. Боженко

Российский научный центр рентгенорадиологии, Москва, Россия

Адоптивную иммунотерапию, использующую генно-модифицированные аутологичные Т-лимфоциты с искусственным рецептором заданной специфичности (CAR-терапию) рассматривают в качестве перспективного подхода к лечению солидных опухолей, как рецидивирующих, так и на поздних стадиях развития. При использовании этого вида терапии приходится сталкиваться с рядом проблем, таких как способность опухоли к отбору клеток со сниженной экспрессией антигенов-мишеней в ходе терапии и снижение функциональной активности CAR-T-лимфоцитов иммуносупрессивным микроокружением опухоли. В обзоре обсуждены существующие генно-инженерные подходы к модификации технологии получения CAR-T-лимфоцитов для: 1) создания универсальных искусственных рецепторов, способных в ходе иммунотерапии переключаться и атаковать различные антигены-мишени; 2) повышения функциональной активности CAR-T-лимфоцитов в условиях иммуносупрессивного микроокружения путем подавления экспрессии ингибирующих рецепторов или повышения продукции цитокинов.

Ключевые слова: CAR-терапия, солидные опухоли, химерный антигенный рецептор, CAR-T-клетки, универсальные CAR, иммуносупрессивное микроокружение

Информация о вкладе авторов: Я. Ю. Киселева — анализ литературы, написание рукописи, подготовка рисунков, редактирование; А. М. Шишкин и А. В. Иванов — анализ литературы, редактирование; Т. М. Кулинич и В. К. Боженко — редактирование.

✉ **Для корреспонденции:** Яна Юрьевна Киселева
ул. Профсоюзная, д. 86, г. Москва, 117997; yana.kiseleva@gmail.com

Статья получена: 03.10.2019 **Статья принята к печати:** 17.10.2019 **Опубликована онлайн:** 18.10.2019

DOI: 10.24075/vrgmu.2019.066

Traditional treatment options for malignancies, such as surgery, radiation therapy and chemotherapy, do not satisfy the criteria for therapeutic efficacy in patients with advanced or relapsed cancer. The need for more effective therapies has driven development of innovative treatment modalities, many of which harness the mechanisms of immune response [1]. One of them is adoptive immunotherapy that makes use of T-cell chimeric antigen receptors (CARs). Eligible patients receive an infusion of autologous T cells genetically modified *ex vivo* before the procedure to carry a synthetic receptor with a desired specificity on their surface. A CAR is a fusion protein composed of an extracellular single-chain variable immunoglobulin fragment (scFv) and T-cell intracellular signaling domains [2]. Unlike T-cell receptors that recognize antigens processed and embedded within the major histocompatibility complex, chimeric T-cell receptors target native (unprocessed) cell surface antigens associated with malignant cell transformation [3]. Despite the success of CAR T-cell therapy in fighting hematologic malignancies [4], its application to solid tumors has a few limitations related to the presence of tumor-associated antigens on the surface of healthy tissue cells and the ensuing adverse cytotoxicity [5, 6]. Another challenge is that malignant tumors are heterogenous and can evolve under selective pressure induced by immunotherapy, expressing fewer target antigens on their surface. In addition, once a CAR T cell reaches the tumor, it finds itself in the immunosuppressive microenvironment created by regulatory T cells, tumor-associated macrophages, myeloid-derived suppressor cells, some overexpressed immunosuppressive molecules (PD-L1, PD-L2, CD80, CD86), hypoxia, necrosis, and lack of nutrients [7].

In order to overcome these barriers, a variety of gene engineering approaches have been proposed to the modification of CAR T-cell manufacturing technology [7–9]. The most promising of them include 1) designing universal CARs capable of attacking a wide range of target antigens and 2) enhancing functional activity of CAR T cells in the immunosuppressive microenvironment of the tumor. This review focuses on genetically engineered universal CARs and the possibility of modulating antitumor activity of CAR T cells by downregulating the expression of inhibiting receptors and stimulating production of cytokines.

Universal CARs with an adaptor module

Since classic, i.e. currently used in clinical practice, CARs are monospecific, antigen loss provoked by therapy remains one of the crucial challenges facing CAR therapy. In order to cut down on manufacturing costs and effort involved in creating a CAR construct with new (yet fixed) specificity, as well as to expand the range of simultaneously or consecutively attacked targets, a modular design of the CAR T-cell system has been proposed in which the antigen-recognition and signaling domains are represented by two separate modules. The antigen-binding adaptor is a stand-alone molecule recognized by a CAR ectodomain. Such system can be functional only in the presence of all 3 components, including the target, the adaptor module and the effector CAR T cell. Its design allows controlled activation of CAR T cells and their rapid "switch-off" in case of toxic adverse events, such as the cytokine release syndrome. In addition, a modular CAR T cell can be easily redirected from one target to another, without having to start the engineering process all over in an attempt to obtain a cell with new antigen specificity. This concept lies behind the idea of a universal CAR system (UniCAR). This review looks at the most promising universal CAR systems developed so far.

A modular CAR system equipped with biotin-binding immunoreceptors

In this type of UniCAR T cells, the universal ectodomain is represented by avidin or streptavidin (Fig. 1A) that bind to biotinylated antigen-specific molecules (MAT, ScFv and other specific ligands that recognize the target antigen). The first UniCAR system exploited the interaction between biotin and avidin [10]. Its inventors demonstrated that T cells equipped with the biotin-binding immunoreceptor (BBIR), whose ectodomain was represented by an extracellularly modified avidin dimer, could bind to cancer cells pre-incubated with biotinylated antibodies, switch on and lyse the malignant target. The researchers showed that supraphysiological concentrations of biotin, which is present in human blood plasma, did not cause antigen-independent activation of modified CAR T cells and did not inhibit their activity. Biotinylated antibodies were also employed as adaptor modules in another UniCAR system described in [11]. Here, the role of the ectodomain component was played by a high-affinity streptavidin monomer (mSA2). Using biotinylated rituximab (anti-CD20 mAb) as an adaptor module, the researchers demonstrated that modified T cells were capable of switching on and lysing their targets in a dose-dependent manner *in vitro*. However, the immunogenicity of avidin/streptavidin remains an open question and can limit therapeutic applications of BBIR-based UniCAR T-cell systems [10, 11].

A modular CAR-system containing fluorescein isothiocyanate

In this modular system (Fig. 1B), the universal CAR T-cell ectodomain contains a variable scFv fragment that targets synthetic fluorescein isothiocyanate (FITC), a commonly used fluorescent probe for antibody labeling. Here, FITC is conjugated either to a monoclonal antibody (mAb) or to a receptor ligand that interacts with a target antigen on the surface of the malignant cell. This interaction results in a pseudoimmunological synapse formed between the anti-FITC CAR T cell and the tumor cell expressing the target antigen. Subsequently, the activated CAR T cells lyse the target. CAR T-cell constructs carrying FITC conjugated to mAb (trastuzumab, rituximab and cetuximab) were successfully tested against HER2-expressing cells (breast cancer), CD20 (B-cell lymphoma) and EGFR (pancreatic cancer) in NSG mice [12]. Just like BBIR-based UniCAR T cells, the immunogenicity of FITS is yet to be elucidated [12].

Modular CAR systems with neoepitopes

In this type of CAR systems, the adaptor module contains a neoepitope bound to antigen-specific scFv or Fab, whereas the CAR itself consists of an intracellular domain and an ectodomain (scFv) that recognizes the neoepitope. Neoepitopes are exogenous peptides not found in humans. So far, two modular neoepitope CAR T-cell systems have been developed; they rely on neoepitopes 5B9 and PNE (Fig. 1C).

5B9 is a non-immunogenic peptide 10 amino acids in length. Its sequence is a peptide motif present in the nuclear autoantigen La/SS-B typically found in patients with Sjögren's syndrome and systemic lupus erythematosus [13]. Initially, the developed 5B9-specific UniCAR system [14] was directed against antigens CD33 and CD123 expressed on acute myeloid leukemia cells. The researchers experimented with both mono- and bispecific antigen-recognizing modules conjugated to epitope 5B9. The targeted cells were effectively lysed both in the presence of two independent monomodules (scFv) and the bispecific module (bis-scFv) alone; the latter turned out to be even more effective. It was established that antigen-recognizing modules could effectively induce lysis

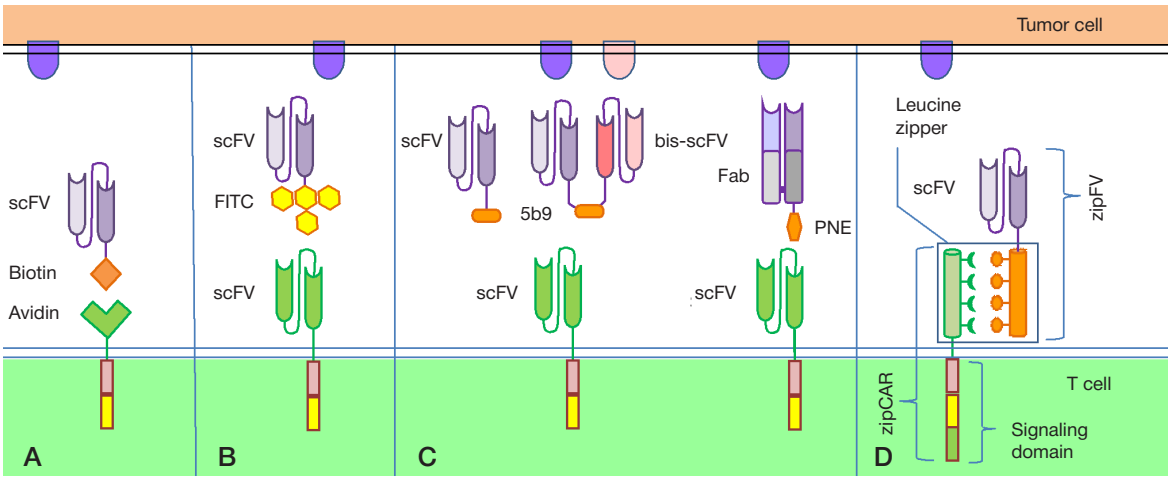

Fig. 1. Types of universal CARs. **A**. A modular CAR T-cell system with biotin-binding immunoreceptors. **B**. A modular CAR T-cell system with fluorescein isothiocyanate. **C**. A modular CAR T-cell system with neoepitopes (5B9, PNE). **D**. A modular CAR T-cell system with a leucine zipper motif (SUPRA CAR)

even at very low concentrations, regardless of antigen density on the surface of targeted cells [14]. Later, the efficacy of the 5B9-specific UniCAR-system against solid tumors was tested in cell and animal models of prostate cancer [15]. In this case, the neoepitope 5B9 was bound to scFv directed against prostate stem cell antigen (PSCA). The use of the 5B9-specific UniCAR system in NSG mice with high and low tumor burden significantly delayed tumor growth and improved animal survival. Interestingly, after the adaptor module was added to the co-cultured cancer and 5B9-specific UniCAR T cells, the expression of immunosuppressing PD-L1 and PD-L2 on the cancer cells and their PD-1 receptor on effector T cells significantly increased in comparison with the control cultured without the adaptor module [15]. Later, the same research team [16] published preclinical trial data on the successful application of PSCA- and PSMA-specific (prostate specific membrane antigen) 5B9-modules used in combination.

The other peptide known as PNE (peptide neoepitope) and exploited in a neoepitope UniCAR (Fig. 1C) was derived from GCN4, the transcription factor found in yeast. PNE contains 14 amino acid residues, is not found in humans and is expected to have low immunogenicity, according to the *in silico* analysis. Proposed in [17], the PNE-based adaptor module contained a PNE bound to a Fab fragment of therapeutic antibodies specific either for CD19 or for CD20. The universal CAR ectodomain contained scFv of highly specific 52SR4 mAb that recognize PNE. Using the mouse model of B-cell leukemia xenograft, the researchers demonstrated dose-dependent control over the activity of UniCAR T cells and their localization in tissue in the areas of malignant cell accumulation and cytokine secretion [17]. Interestingly, high doses of adaptor modules caused expansion of $CD45RA^{+}CD62L^{-}$ cells (TEMRA, terminal effector memory expressing CD45RA+), whereas low adaptor doses led to the prevalence of the $CD45RA^{-}CD62L^{+}$ phenotype (central memory cells) associated with prolonged persistence of CAR T cells and correlated with sustained remission in patients with acute myeloid leukemia or chronic lymphocyte leukemia [18]. The same research team developed a UniCAR-system with PNE targeting the HER2-expressing breast cancer cells [19]. The antigen-recognizing component of the adaptor module was represented by the Fab fragment of trastuzumab (clone 4D5). The study [19] demonstrated a dose-dependent cytotoxic effect exerted by the system *in vitro*, as well as complete resolution of lesions in NSG mice inoculated subcutaneously with breast cancer cell lines characterized by different levels of HER2 expression.

SUPRA CAR: a modular CAR-system with a leucine zipper motif component

One of the most promising universal CARs is known as SUPRA CAR (split, universal and programmable) and was proposed in [20] (Fig. 1D). It is a two-component system that relies on a leucine zipper motif to ensure the interaction between its parts. The zipper is composed of a universal receptor (zipCAR) expressed on the T-cell surface and an antitumor scFv adaptor (zipFv). The universal zipCAR receptor rises from the fusion of intracellular signaling domains (CD28, 4-1BB and CD3z) with the ectodomain containing a leucine zipper motif. The adaptor module zipFv consists of an antigen-specific scFv and a leucine zipper motif, which ensures its interaction with zipCAR and subsequent activation of T cells. Unlike “conventional” CARs with fixed specificity, the described construct allows redirecting the system against different antigen targets without preforming any extra manipulations on a patient’s immune cells. Another unique feature of SUPRA CAR is its tunability: it is possible to adjust the wide range of different parameters involved in modulating T-cell response and prevent T-cell overactivation. By varying such parameters as (1) affinity between leucine zipper motifs, (2) affinity between the tumor antigen and scFv, (3) zipFv concentrations, and (4) zipCAR expression, one can modulate the functional activity of T cells, including interferon gamma production [20]. In case of a cytokine storm occurring in response to CAR therapy, the activity of SUPRA CAR T cells can be dampened or completely inhibited by administering a competing low/high-affinity adaptor zipFv to the patient. The adaptor can dimerize with the leucine zipper domain of specific zipFv introduced into the patient’s organism in the previous step, and thus prevent it from binding to zipCAR. Besides, this system can perform such logic operations as A OR B or A AND NOT B. The former is used when there is a need to attack malignant cells carrying two target antigens, which is achieved by adding two zipFv adaptors specific for the two targets and capable of binding to zipCAR. The second logic operation is performed to mitigate adverse cytotoxic effects on healthy cells expressing the target antigen. The researchers demonstrated

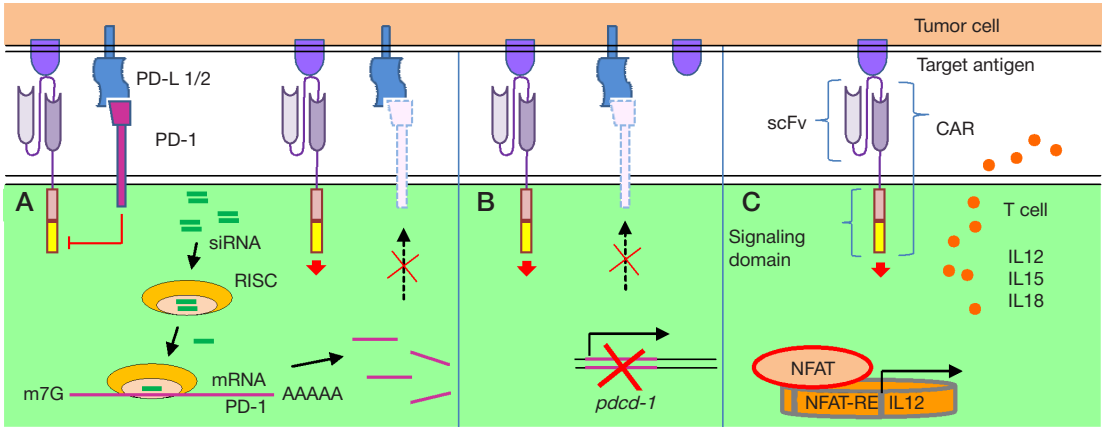

Fig. 2. A schematic showing modulation of antitumor activity of CAR T cells in the immunosuppressive tumor microenvironment. **A**. Silencing the expression of the *pdcd-1* gene in T lymphocytes by transfecting them with siRNA. The PD-1 receptor interacts with its ligands PD-L1/2 and inhibits the activating CAR signal. After transfection, siRNA duplexes interact with the RISC-binding complex (RNA-induced silencing complex); one of RNA strands is removed from the complex, whereas the other remains within RISC, binds to mRNA and initiates its degradation. This leads to a decline in the PD-1 expression on the cell surface. **B**. Knockout of the *pdcd-1* gene performed using CRISPR/Cas9 technology. **C**. TRUCKs: apart from CAR, a plasmid is introduced into the T cell, containing a NFAT responsive element (NFAT-RE) and sequences of genes coding for IL12, IL15 or IL18. The T cell is activated following the interaction between the CAR and the target antigen. This leads to dephosphorylation of NFAT transcription factor that relocates to the nucleus and triggers cytokine production by binding to NFAR-RE. Local secretion of the cytokine initiates immune response against cancer cells invisible for CAR T lymphocytes

the feasibility of sparing cells that carry 2 target antigens, one of which was tumor-associated and the other was non-tumor [20]. This effect can be achieved by using the zipFv adaptor that is specific for a non-tumor antigen but competes with zipCAR for binding to the leucine zipper domain of the zipFv adaptor specific for the tumor antigen. When bound to the target, the adaptors form dimers, meaning that zipFv specific for the tumor antigen can no longer interact with zipCAR. As a result, the induced cytotoxic response of T cells against healthy cells is weak. It was demonstrated that SUPRA CAR T cells can control tumor growth in NSG mice injected with SK-BR-3 breast cancer cells intraperitoneally or with Jurkat cells intravenously [20]. In order to reduce immunogenicity of the proposed system, the authors humanized leucine zippers using the corresponding sequences of human transcription factors [20].

Modulation of antitumor activity of CAR T cells in the immunosuppressive tumor microenvironment

The immunosuppressive microenvironment of solid tumors is one of the major factors preventing the positive outcome of CAR therapy. Coupled with the expression of inhibiting receptors on the surface of CAR T cells, it disrupts the efficacy of the latter [21]. The following 2 inhibiting receptors are worth noting: PD-1 (programmed cell death receptor) and CTLA-4 (cytotoxic T-cell-associated antigen 4); today, they are regarded as leading regulators of the immune system that control the activation of T cells and maintain peripheral tolerance [7, 22]. By interacting with CD80/86, CTLA-4 inhibits potentially autoreactive T cells in the early stage of naive T-cell activation, usually in lymph nodes [23], whereas PD1 bound to PD-L1/2 participates in the regulation of activated cells in later stages of immune response, exerting its effect in peripheral tissue [24]. Tumor cells expressing the corresponding ligands on their surface can harness those two receptors to inactivate tumor-specific lymphocytes, including CAR T cells, thus acquiring insensitivity to their attacks [22, 25]. Importantly, adoptive immunotherapy makes use of activated T cells. Their activation leads to overexpression of PD-1 and CTLA-4, which makes T cells even more susceptible to the immunosuppressive effect of the tumor [25].

The unwanted interaction between the ligand and the receptor can be blocked by mAb specific for this receptor or ligand [26]. Since 2011, therapeutic regimens for metastatic melanoma adopted in the USA have included ipilimumab, the monoclonal antibody that blocks CTLA-4 [27]. Clinical trials have demonstrated the efficacy of immunotherapy with PD-1 and PD-L1 inhibitors in patients with melanoma [28]. It should be noted that the combination therapy with anti-PD-1 (nivolumab) and anti-CTLA-4 (ipilimumab) improved progression-free survival and increased the objective response rate in patients with melanoma who had not received any previous treatment, as compared with monotherapy [29]. Today, a number of anti-mAb have been approved for treating melanoma, non-small cell lung cancer, bladder cancer, and some other types of cancers, including nivolumab, pembrolizumab, atezolizumab, avelumab, and durvalumab [27]. However, these drugs induce a wide range of side effects called immune-related adverse events, including autoimmune thyroiditis, hepatitis, colitis, myocarditis, etc. [30]. Apparently, immunomediated adverse effects are related to non-specific activation of immunocompetent cells, limiting the therapeutic application of such drugs [30].

An alternative approach to the modification of functional activity of CAR T cells is based on silencing the expression of inhibiting receptors on their surface through genetic modification of T cells ex vivo in addition to the introduction of an antigen-specific CAR receptor into the cell. This can be done by simultaneously transfecting the T cell with siRNA (small interfering RNA) (Fig. 2A) and DNA/RNA coding for the antigen-specific receptor [22], or by using genome editing tools, such as CRISPR/Cas9 [31] (Fig. 2B). A study [32] has demonstrated that CTLA-4 mRNA expression can be successfully silenced in the peripheral blood lymphocytes of patients with chronic hepatitis B using the siRNA-based technology. It should be noted though that in the mentioned experiment specific CAR receptors were not introduced into the cells. Another recent study has shown that transfection of T-cells with mRNA coding for the second-generation CAR-receptor specific for the melanoma antigen CSPG4 and two siRNAs inhibiting PD-1 and CTLA-4 leads to a decline in the expression of surface PD-1 and intracellular CTLA-4 in T lymphocytes [25]. The researchers observed a statistically significant increase in the cytotoxic effect of modified T lymphocytes on melanoma cells transfected with PD-L1- or CD80-encoding plasmids, in comparison with the control [25]. CRISPR/Cas9-based genome editing has been recently applied to suppress the expression of PD-1 and CTLA-4 [31, 33]. The CRISPR/Cas9 technology can be successfully used to silence the PD-1-encoding gene in CAR T cells; this significantly enhances their antitumor activity both *in vitro* and *in vivo* [33]. It has been shown that three genes, including PD-1 [31], and 4 genes, including PD-1 and CTLA-4 [34], can be simultaneously silenced in CAR T cells using the CRISPR/Cas9 technology.

Another approach to overcoming the immunosuppressive activity of tumor environment and attacking tumor cells that have stopped expressing the target antigen on their surface lies in enabling T cells to increase production of cytokines directly in target tissue upon their activation through the interaction between CAR and the target cell. Such modified cytokine-producing CAR T cells are referred to as TRUCKs: T cells Redirected for Universal Cytokine Killing [35] (Fig. 2C). They have proved to be highly effective in delivering cytokines to the tumor microenvironment. Experiments in mouse models have demonstrated that accumulation of IL12 in malignant tissue following adoptive transfer of tumor-specific IL12-secreting cells improves the cytolytic activity of T lymphocytes [36] and stimulates activation and recruitment of innate immunity cells to the tumor site [37]. Secretion of IL12 locally affects myeloid suppressor cells, dysfunctional dendritic cells and alternatively activated macrophages and reprograms them into functional antigen-presenting cells that can present tumor-associated antigens to tumor-infiltrating lymphocytes (TIL), causing regression of large tumor lesions [38]. Clinical trials conducted in patients with metastatic melanoma treated with autologous TIL expressing IL12 under the “supervision” of regulatory NFAT (NFAT stands for nuclear factor of activated T cells) have demonstrated an objective clinical effect in 10 out of 16 patients treated with lower cell doses than recommended in the standard protocol [39]. However, many patients recruited for the trial developed serious side effects, such as severe hepatotoxicity and hemodynamic instability; therefore, the trial was terminated [39]. Pronounced cytotoxicity of TCR T cells with NFAT-regulated expression of IL12 has been detected *in vivo* in the experiments in mice [40]. Another research group has achieved a positive therapeutic outcome (the absence of toxicity *in vivo*) by controlling the IL12 expression with the TET-On promotor sensitive to doxycycline [45]. Transient expression of IL12 was enough to inhibit the growth of B16F10 melanoma without provoking systemic cytotoxicity.

There have been studies investigating the effect of the increased IL15 and IL18 expression on the antitumor activity of CAR T cells and TCR T cells. It has been established that IL15 improves survival and promotes proliferation of ex vivo modified CAR T cells redirected against CD19 (in leukemia/lymphoma) [42] and IL13Rα2 (in glioblastoma) [43]. Using the melanoma mouse model, the researchers have demonstrated that administration of modified TCR T cells with NFAT-regulated expression of IL18 was safe (no adverse toxicity was observed), resulted in the expansion of CD8-cells in the lesion and increased antitumor activity [40]. CD4 CAR T cells secreting IL18 have been shown to activate CD8 T-cells that, in turn, proliferate and enhance the antitumor response in mice with induced B16F10 melanoma [44]. CAR T cells secreting IL18 trigger acute Th1 immune response in the tumor, which results in improved survival of mice with pancreatic and lung cancer [45].

CONCLUSION

At present, CAR T-cell therapy is successfully used in clinical practice in patients with hematologic malignancies. However, this positive experience cannot be extrapolated to solid tumors because of the adverse events associated with CAR T-cell toxicity against healthy cells and the inhibiting effect of the immunosuppressive tumor microenvironment on the functional activity of CAR T cells. A few solutions have been proposed, including universal CARs that can be quickly redirected against a new antigen target and CAR T cells that have been genetically modified to resist the immunosuppressive effect of the tumor microenvironment. Results of extensive research in this field instill hope for creating an arsenal of effective and therapeutically safe CAR T cells that can be used to treat solid tumors.

References

1. Palucka AK, Coussens LM. The Basis of Oncoimmunology. Cell. 2016; 164 (6): 1233–47. DOI: 10.1016/j.cell.2016.01.049. PubMed PMID: 26967289; PubMed Central PMCID: PMC4788788.
2. Jena B, Dotti G, Cooper LJ. Redirecting T-cell specificity by introducing a tumor-specific chimeric antigen receptor. Blood. 2010; 116 (7): 1035–44. DOI: 10.1182/blood-2010-01-043737. PubMed PMID: 20439624; PubMed Central PMCID: PMC2938125.
3. Klebanoff CA, Rosenberg SA, Restifo NP. Prospects for gene-engineered T cell immunotherapy for solid cancers. Nature medicine. 2016; 22 (1): 26–36. DOI: 10.1038/nm.4015. PubMed PMID: 26735408; PubMed Central PMCID: PMC6295670.
4. Park JH, Geyer MB, Brentjens RJ. CD19-targeted CAR T-cell therapeutics for hematologic malignancies: interpreting clinical outcomes to date. Blood. 2016; 127 (26): 3312–20. DOI: 10.1182/blood-2016-02-629063. PubMed PMID: 27207800; PubMed Central PMCID: PMC4929923.
5. Liu B, Yan L, Zhou M. Target selection of CAR T cell therapy in accordance with the TME for solid tumors. American journal of cancer research. 2019; 9 (2): 228–41. PubMed PMID: 30906625; PubMed Central PMCID: PMC6405971.
6. Bonifant CL, Jackson HJ, Brentjens RJ, Curran KJ. Toxicity and management in CAR T-cell therapy. Molecular therapy oncolytics. 2016; (3): 16011. DOI: 10.1038/mto.2016.11. PubMed PMID: 27626062; PubMed Central PMCID: PMC5008265.
7. Tahmasebi S, Elahi R, Esmaeilzadeh A. Solid Tumors Challenges and New Insights of CAR T Cell Engineering. Stem cell reviews and reports. 2019; 15 (5): 619–36. DOI: 10.1007/s12015-019-09901-7. PubMed PMID: 31161552.
8. Minutolo NG, Hollander EE, Powell DJ, Jr. The Emergence of Universal Immune Receptor T Cell Therapy for Cancer. Frontiers in oncology. 2019; (9): 176. DOI: 10.3389/fonc.2019.00176. PubMed PMID: 30984613; PubMed Central PMCID: PMC6448045.
9. Stoiber S, Cadilha BL, Benmebarek MR, Lesch S, Endres S, Kobold S. Limitations in the Design of Chimeric Antigen Receptors for Cancer Therapy. Cells. 2019; 8 (5). DOI: 10.3390/cells8050472. PubMed PMID: 31108883; PubMed Central PMCID: PMC6562702.
10. Urbanska K, Lanitis E, Poussin M, Lynn RC, Gavin BP, Kelderman S, et al. A universal strategy for adoptive immunotherapy of cancer through use of a novel T-cell antigen receptor. Cancer research. 2012; 72 (7): 1844–52. DOI: 10.1158/0008-5472.CAN-11-3890. PubMed PMID: 22315351; PubMed Central PMCID: PMC3319867.
11. Lohmueller JJ, Ham JD, Kvorjak M, Finn OJ. mSA2 affinity-enhanced biotin-binding CAR T cells for universal tumor targeting. Oncoimmunology. 2017; 7 (1): e1368604. DOI: 10.1080/2162402X.2017.1368604. PubMed PMID: 29296519; PubMed Central PMCID: PMC5739565.
12. Tamada K, Geng D, Sakoda Y, Bansal N, Srivastava R, Li Z, et al. Redirecting gene-modified T cells toward various cancer types using tagged antibodies. Clinical cancer research: an official journal of the American Association for Cancer Research. 2012; 18 (23): 6436–45. DOI: 10.1158/1078-0432.CCR-12-1449. PubMed PMID: 23032741.
13. Koristka S, Cartellieri M, Arndt C, Bippes CC, Feldmann A, Michalk I, et al. Retargeting of regulatory T cells to surface-inducible autoantigen La/SS-B. Journal of autoimmunity. 2013; (42): 105–16. DOI: 10.1016/j.jaut.2013.01.002. PubMed PMID: 23352111.
14. Cartellieri M, Feldmann A, Koristka S, Arndt C, Loff S, Ehninger A, et al. Switching CAR T cells on and off: a novel modular platform for retargeting of T cells to AML blasts. Blood cancer journal. 2016; 6 (8): e458. DOI: 10.1038/bcj.2016.61. PubMed PMID: 27518241; PubMed Central PMCID: PMC5022178 directed to CD33, La and the UniCAR platform technology. AE, SL and MC are employed by GEMoaB and CPT, respectively. The other authors declare no conflict of interest.
15. Pishali Bejestani E, Cartellieri M, Bergmann R, Ehninger A, Loff S, Kramer M, et al. Characterization of a switchable chimeric antigen receptor platform in a pre-clinical solid tumor model. Oncoimmunology. 2017; 6 (10): e1342909. DOI: 10.1080/2162402X.2017.1342909. PubMed PMID: 29123951; PubMed Central PMCID: PMC5665068.
16. Feldmann A, Arndt C, Bergmann R, Loff S, Cartellieri M, Bachmann D, et al. Retargeting of T lymphocytes to PSCA- or PSMA positive prostate cancer cells using the novel modular chimeric antigen receptor platform technology "UniCAR". Oncotarget. 2017; 8 (19): 31368–85. DOI: 10.18632/oncotarget.15572. PubMed PMID: 28404896; PubMed Central PMCID: PMC5458214.
17. Rodgers DT, Mazagova M, Hampton EN, Cao Y, Ramadoss NS, Hardy IR, et al. Switch-mediated activation and retargeting of CAR-T cells for B-cell malignancies. Proceedings of the National Academy of Sciences of the United States of America. 2016; 113 (4): E459–68. DOI: 10.1073/pnas.1524155113. PubMed PMID: 26759369; PubMed Central PMCID: PMC4743815.
18. Riddell SR, Sommermeyer D, Berger C, Liu LS, Balakrishnan A, Salter A, et al. Adoptive therapy with chimeric antigen receptor-modified T cells of defined subset composition. Cancer journal. 2014; 20 (2): 141–4. DOI: 10.1097/PPO.0000000000000036. PubMed PMID: 24667960; PubMed Central PMCID: PMC4149222.
19. Cao Y, Rodgers DT, Du J, Ahmad I, Hampton EN, Ma JS, et al. Design of Switchable Chimeric Antigen Receptor T Cells Targeting Breast Cancer. Angewandte Chemie. 2016; 55 (26): 7520–4. DOI: 10.1002/anie.201601902. PubMed PMID: 27145250; PubMed Central PMCID: PMC5207029.
20. Cho JH, Collins JJ, Wong WW. Universal Chimeric Antigen Receptors for Multiplexed and Logical Control of T Cell Responses. Cell. 2018; 173 (6): 1426–38. DOI: 10.1016/j.

cell.2018.03.038. PubMed PMID: 29706540; PubMed Central PMCID: PMC5984158.
21. Scarfo I, Maus MV. Current approaches to increase CAR T cell potency in solid tumors: targeting the tumor microenvironment. Journal for immunotherapy of cancer. 2017; (5): 28. DOI: 10.1186/s40425-017-0230-9. PubMed PMID: 28331617; PubMed Central PMCID: PMC5359946.
22. Sioud M. Releasing the Immune System Brakes Using siRNAs Enhances Cancer Immunotherapy. Cancers. 2019; 11 (2). DOI: 10.3390/cancers11020176. PubMed PMID: 30717461.
23. Boutros C, Tarhini A, Routier E, Lambotte O, Ladurie FL, Carbonnel F, et al. Safety profiles of anti-CTLA-4 and anti-PD-1 antibodies alone and in combination. Nature reviews Clinical oncology. 2016; 13 (8): 473–86. DOI: 10.1038/nrclinonc.2016.58. PubMed PMID: 27141885.
24. Hugo W, Zaretsky JM, Sun L, Song C, Moreno BH, Hu-Lieskovan S, et al. Genomic and Transcriptomic Features of Response to Anti-PD-1 Therapy in Metastatic Melanoma. Cell. 2016; 165 (1): 35–44. DOI: 10.1016/j.cell.2016.02.065. PubMed PMID: 26997480; PubMed Central PMCID: PMC4808437.
25. Simon B, Harrer DC, Schuler-Thurner B, Schaft N, Schuler G, Dorrie J, et al. The siRNA-mediated downregulation of PD-1 alone or simultaneously with CTLA-4 shows enhanced in vitro CAR-T-cell functionality for further clinical development towards the potential use in immunotherapy of melanoma. Experimental dermatology. 2018; 27 (7): 769–78. DOI: 10.1111/exd.13678. PubMed PMID: 29704887.
26. Martinez M, Moon EK. CAR T Cells for Solid Tumors: New Strategies for Finding, Infiltrating, and Surviving in the Tumor Microenvironment. Frontiers in immunology. 2019; (10): 128. DOI: 10.3389/fimmu.2019.00128. PubMed PMID: 30804938; PubMed Central PMCID: PMC6370640.
27. Vivot A, Jacot J, Zeitoun JD, Ravaud P, Crequit P, Porcher R. Clinical benefit, price and approval characteristics of FDA-approved new drugs for treating advanced solid cancer, 2000–2015. Annals of oncology: official journal of the European Society for Medical Oncology. 2017; 28 (5): 1111–6. DOI: 10.1093/annonc/mdx053. PubMed PMID: 28453694.
28. Medina PJ, Adams VR. PD-1 Pathway Inhibitors: Immuno-Oncology Agents for Restoring Antitumor Immune Responses. Pharmacotherapy. 2016; 36 (3): 317–34. DOI: 10.1002/phar.1714. PubMed PMID: 26822752; PubMed Central PMCID: PMC5071694.
29. Larkin J, Chiarion-Sileni V, Gonzalez R, Grob JJ, Cowey CL, Lao CD, et al. Combined Nivolumab and Ipilimumab or Monotherapy in Untreated Melanoma. The New England journal of medicine. 2015; 373 (1): 23–34. DOI: 10.1056/NEJMoa1504030. PubMed PMID: 26027431; PubMed Central PMCID: PMC5698905.
30. Postow MA, Sidlow R, Hellmann MD. Immune-Related Adverse Events Associated with Immune Checkpoint Blockade. The New England journal of medicine. 2018; 378 (2): 158–68. DOI: 10.1056/NEJMra1703481. PubMed PMID: 29320654.
31. Ren J, Liu X, Fang C, Jiang S, June CH, Zhao Y. Multiplex Genome Editing to Generate Universal CAR T Cells Resistant to PD1 Inhibition. Clinical cancer research: an official journal of the American Association for Cancer Research. 2017; 23 (9): 2255–66. DOI: 10.1158/1078-0432.CCR-16-1300. PubMed PMID: 27815355; PubMed Central PMCID: PMC5413401.
32. Yu Y, Wu H, Tang Z, Zang G. CTLA4 silencing with siRNA promotes deviation of Th1/Th2 in chronic hepatitis B patients. Cellular & molecular immunology. 2009; 6 (2): 123–7. DOI: 10.1038/cmi.2009.17. PubMed PMID: 19403062; PubMed Central PMCID: PMC4002649.
33. Rupp LJ, Schumann K, Roybal KT, Gate RE, Ye CJ, Lim WA, et al. CRISPR/Cas9-mediated PD-1 disruption enhances anti-tumor efficacy of human chimeric antigen receptor T cells. Scientific reports. 2017; 7 (1): 737. DOI: 10.1038/s41598-017-00462-8. PubMed PMID: 28389661; PubMed Central PMCID: PMC5428439.
34. Ren J, Zhang X, Liu X, Fang C, Jiang S, June CH, et al. A versatile system for rapid multiplex genome-edited CAR T cell generation. Oncotarget. 2017; 8 (10): 17002–11. DOI: 10.18632/oncotarget.15218. PubMed PMID: 28199983; PubMed Central PMCID: PMC5370017.
35. Knochelmann HM, Smith AS, Dwyer CJ, Wyatt MM, Mehrotra S, Paulos CM. CAR T Cells in Solid Tumors: Blueprints for Building Effective Therapies. Frontiers in immunology. 2018; (9): 1740. DOI: 10.3389/fimmu.2018.01740. PubMed PMID: 30140266; PubMed Central PMCID: PMC6094980.
36. Kerkar SP, Muranski P, Kaiser A, Boni A, Sanchez-Perez L, Yu Z, et al. Tumor-specific CD8+ T cells expressing interleukin-12 eradicate established cancers in lymphodepleted hosts. Cancer research. 2010; 70 (17): 6725–34. DOI: 10.1158/0008-5472.CAN-10-0735. PubMed PMID: 20647327; PubMed Central PMCID: PMC2935308.
37. Pegram HJ, Lee JC, Hayman EG, Imperato GH, Tedder TF, Sadelain M, et al. Tumor-targeted T cells modified to secrete IL12 eradicate systemic tumors without need for prior conditioning. Blood. 2012; 119 (18): 4133–41. DOI: 10.1182/blood-2011-12-400044. PubMed PMID: 22354001; PubMed Central PMCID: PMC3359735.
38. Kerkar SP, Goldszmid RS, Muranski P, Chinnasamy D, Yu Z, Reger RN, et al. IL12 triggers a programmatic change in dysfunctional myeloid-derived cells within mouse tumors. The Journal of clinical investigation. 2011; 121 (12): 4746–57. DOI: 10.1172/JCI58814. PubMed PMID: 22056381; PubMed Central PMCID: PMC3226001.
39. Zhang L, Morgan RA, Beane JD, Zheng Z, Dudley ME, Kassim SH, et al. Tumor-infiltrating lymphocytes genetically engineered with an inducible gene encoding interleukin-12 for the immunotherapy of metastatic melanoma. Clinical cancer research: an official journal of the American Association for Cancer Research. 2015; 21 (10): 2278–88. DOI: 10.1158/1078-0432.CCR-14-2085. PubMed PMID: 25695689; PubMed Central PMCID: PMC4433819.
40. Kunert A, Chmielewski M, Wijers R, Berrevoets C, Abken H, Debets R. Intra-tumoral production of IL18, but not IL12, by TCR-engineered T cells is non-toxic and counteracts immune evasion of solid tumors. Oncoimmunology. 2017; 7 (1): e1378842. DOI: 10.1080/2162402X.2017.1378842. PubMed PMID: 29296541; PubMed Central PMCID: PMC5739571.
41. Alsaieedi A, Holler A, Velica P, Bendle G, Stauss HJ. Safety and efficacy of Tet-regulated IL12 expression in cancer-specific T cells. Oncoimmunology. 2019; 8 (3): 1542917. DOI: 10.1080/2162402X.2018.1542917. PubMed PMID: 30723575; PubMed Central PMCID: PMC6350686.
42. Hoyos V, Savoldo B, Quintarelli C, Mahendravada A, Zhang M, Vera J, et al. Engineering CD19-specific T lymphocytes with interleukin-15 and a suicide gene to enhance their anti-lymphoma/leukemia effects and safety. Leukemia. 2010; 24 (6): 1160–70. DOI: 10.1038/leu.2010.75. PubMed PMID: 20428207; PubMed Central PMCID: PMC2888148.
43. Krenciute G, Prinzing BL, Yi Z, Wu MF, Liu H, Dotti G, et al. Transgenic Expression of IL15 Improves Antiglioma Activity of IL13Ralpha2-CAR T Cells but Results in Antigen Loss Variants. Cancer immunology research. 2017; 5 (7): 571–81. DOI: 10.1158/2326-6066.CIR-16-0376. PubMed PMID: 28550091; PubMed Central PMCID: PMC5746871.
44. Hu B, Ren J, Luo Y, Keith B, Young RM, Scholler J, et al. Augmentation of Antitumor Immunity by Human and Mouse CAR T Cells Secreting IL18. Cell reports. 2017; 20 (13): 3025–33. DOI: 10.1016/j.celrep.2017.09.002. PubMed PMID: 28954221; PubMed Central PMCID: PMC6002762.
45. Chmielewski M, Abken H. CAR T Cells Releasing IL18 Convert to T-Bet(high) FoxO1(low) Effectors that Exhibit Augmented Activity against Advanced Solid Tumors. Cell reports. 2017; 21 (11): 3205–19. DOI: 10.1016/j.celrep.2017.11.063. PubMed PMID: 29241547.

Литература

1. Palucka AK, Coussens LM. The Basis of Oncoimmunology. Cell. 2016; 164 (6): 1233–47. DOI: 10.1016/j.cell.2016.01.049. PubMed PMID: 26967289; PubMed Central PMCID: PMC4788788.
2. Jena B, Dotti G, Cooper LJ. Redirecting T-cell specificity by introducing a tumor-specific chimeric antigen receptor. Blood. 2010; 116 (7): 1035–44. DOI: 10.1182/blood-2010-01-043737. PubMed PMID: 20439624; PubMed Central PMCID: PMC2938125.
3. Klebanoff CA, Rosenberg SA, Restifo NP. Prospects for gene-engineered T cell immunotherapy for solid cancers. Nature medicine. 2016; 22 (1): 26–36. DOI: 10.1038/nm.4015. PubMed PMID: 26735408; PubMed Central PMCID: PMC6295670.
4. Park JH, Geyer MB, Brentjens RJ. CD19-targeted CAR T-cell therapeutics for hematologic malignancies: interpreting clinical outcomes to date. Blood. 2016; 127 (26): 3312–20. DOI: 10.1182/blood-2016-02-629063. PubMed PMID: 27207800; PubMed Central PMCID: PMC4929923.
5. Liu B, Yan L, Zhou M. Target selection of CAR T cell therapy in accordance with the TME for solid tumors. American journal of cancer research. 2019; 9 (2): 228–41. PubMed PMID: 30906625; PubMed Central PMCID: PMC6405971.
6. Bonifant CL, Jackson HJ, Brentjens RJ, Curran KJ. Toxicity and management in CAR T-cell therapy. Molecular therapy oncolytics. 2016; (3): 16011. DOI: 10.1038/mto.2016.11. PubMed PMID: 27626062; PubMed Central PMCID: PMC5008265.
7. Tahmasebi S, Elahi R, Esmaeilzadeh A. Solid Tumors Challenges and New Insights of CAR T Cell Engineering. Stem cell reviews and reports. 2019; 15 (5): 619–36. DOI: 10.1007/s12015-019-09901-7. PubMed PMID: 31161552.
8. Minutolo NG, Hollander EE, Powell DJ, Jr. The Emergence of Universal Immune Receptor T Cell Therapy for Cancer. Frontiers in oncology. 2019; (9): 176. DOI: 10.3389/fonc.2019.00176. PubMed PMID: 30984613; PubMed Central PMCID: PMC6448045.
9. Stoiber S, Cadilha BL, Benmebarek MR, Lesch S, Endres S, Kobold S. Limitations in the Design of Chimeric Antigen Receptors for Cancer Therapy. Cells. 2019; 8 (5). DOI: 10.3390/cells8050472. PubMed PMID: 31108883; PubMed Central PMCID: PMC6562702.
10. Urbanska K, Lanitis E, Poussin M, Lynn RC, Gavin BP, Kelderman S, et al. A universal strategy for adoptive immunotherapy of cancer through use of a novel T-cell antigen receptor. Cancer research. 2012; 72 (7): 1844–52. DOI: 10.1158/0008-5472.CAN-11-3890. PubMed PMID: 22315351; PubMed Central PMCID: PMC3319867.
11. Lohmueller JJ, Ham JD, Kvorjak M, Finn OJ. mSA2 affinity-enhanced biotin-binding CAR T cells for universal tumor targeting. Oncoimmunology. 2017; 7 (1): e1368604. DOI: 10.1080/2162402X.2017.1368604. PubMed PMID: 29296519; PubMed Central PMCID: PMC5739565.
12. Tamada K, Geng D, Sakoda Y, Bansal N, Srivastava R, Li Z, et al. Redirecting gene-modified T cells toward various cancer types using tagged antibodies. Clinical cancer research: an official journal of the American Association for Cancer Research. 2012; 18 (23): 6436–45. DOI: 10.1158/1078-0432.CCR-12-1449. PubMed PMID: 23032741.
13. Koristka S, Cartellieri M, Arndt C, Bippes CC, Feldmann A, Michalk I, et al. Retargeting of regulatory T cells to surface-inducible autoantigen La/SS-B. Journal of autoimmunity. 2013; (42): 105–16. DOI: 10.1016/j.jaut.2013.01.002. PubMed PMID: 23352111.
14. Cartellieri M, Feldmann A, Koristka S, Arndt C, Loff S, Ehninger A, et al. Switching CAR T cells on and off: a novel modular platform for retargeting of T cells to AML blasts. Blood cancer journal. 2016; 6 (8): e458. DOI: 10.1038/bcj.2016.61. PubMed PMID: 27518241; PubMed Central PMCID: PMC5022178 directed to CD33, La and the UniCAR platform technology. AE, SL and MC are employed by GEMoaB and CPT, respectively. The other authors declare no conflict of interest.
15. Pishali Bejestani E, Cartellieri M, Bergmann R, Ehninger A, Loff S, Kramer M, et al. Characterization of a switchable chimeric antigen receptor platform in a pre-clinical solid tumor model. Oncoimmunology. 2017; 6 (10): e1342909. DOI: 10.1080/2162402X.2017.1342909. PubMed PMID: 29123951; PubMed Central PMCID: PMC5665068.
16. Feldmann A, Arndt C, Bergmann R, Loff S, Cartellieri M, Bachmann D, et al. Retargeting of T lymphocytes to PSCA- or PSMA positive prostate cancer cells using the novel modular chimeric antigen receptor platform technology "UniCAR". Oncotarget. 2017; 8 (19): 31368–85. DOI: 10.18632/oncotarget.15572. PubMed PMID: 28404896; PubMed Central PMCID: PMC5458214.
17. Rodgers DT, Mazagova M, Hampton EN, Cao Y, Ramadoss NS, Hardy IR, et al. Switch-mediated activation and retargeting of CAR-T cells for B-cell malignancies. Proceedings of the National Academy of Sciences of the United States of America. 2016; 113 (4): E459–68. DOI: 10.1073/pnas.1524155113. PubMed PMID: 26759369; PubMed Central PMCID: PMC4743815.
18. Riddell SR, Sommermeyer D, Berger C, Liu LS, Balakrishnan A, Salter A, et al. Adoptive therapy with chimeric antigen receptor-modified T cells of defined subset composition. Cancer journal. 2014; 20 (2): 141–4. DOI: 10.1097/PPO.0000000000000036. PubMed PMID: 24667960; PubMed Central PMCID: PMC4149222.
19. Cao Y, Rodgers DT, Du J, Ahmad I, Hampton EN, Ma JS, et al. Design of Switchable Chimeric Antigen Receptor T Cells Targeting Breast Cancer. Angewandte Chemie. 2016; 55 (26): 7520–4. DOI: 10.1002/anie.201601902. PubMed PMID: 27145250; PubMed Central PMCID: PMC5207029.
20. Cho JH, Collins JJ, Wong WW. Universal Chimeric Antigen Receptors for Multiplexed and Logical Control of T Cell Responses. Cell. 2018; 173 (6): 1426–38. DOI: 10.1016/j.cell.2018.03.038. PubMed PMID: 29706540; PubMed Central PMCID: PMC5984158.
21. Scarfo I, Maus MV. Current approaches to increase CAR T cell potency in solid tumors: targeting the tumor microenvironment. Journal for immunotherapy of cancer. 2017; (5): 28. DOI: 10.1186/s40425-017-0230-9. PubMed PMID: 28331617; PubMed Central PMCID: PMC5359946.
22. Sioud M. Releasing the Immune System Brakes Using siRNAs Enhances Cancer Immunotherapy. Cancers. 2019; 11 (2). DOI: 10.3390/cancers11020176. PubMed PMID: 30717461.
23. Boutros C, Tarhini A, Routier E, Lambotte O, Ladurie FL, Carbonnel F, et al. Safety profiles of anti-CTLA-4 and anti-PD-1 antibodies alone and in combination. Nature reviews Clinical oncology. 2016; 13 (8): 473–86. DOI: 10.1038/nrclinonc.2016.58. PubMed PMID: 27141885.
24. Hugo W, Zaretsky JM, Sun L, Song C, Moreno BH, Hu-Lieskovan S, et al. Genomic and Transcriptomic Features of Response to Anti-PD-1 Therapy in Metastatic Melanoma. Cell. 2016; 165 (1): 35–44. DOI: 10.1016/j.cell.2016.02.065. PubMed PMID: 26997480; PubMed Central PMCID: PMC4808437.
25. Simon B, Harrer DC, Schuler-Thurner B, Schaft N, Schuler G, Dorrie J, et al. The siRNA-mediated downregulation of PD-1 alone or simultaneously with CTLA-4 shows enhanced in vitro CAR-T-cell functionality for further clinical development towards the potential use in immunotherapy of melanoma. Experimental dermatology. 2018; 27 (7): 769–78. DOI: 10.1111/exd.13678. PubMed PMID: 29704887.
26. Martinez M, Moon EK. CAR T Cells for Solid Tumors: New Strategies for Finding, Infiltrating, and Surviving in the Tumor Microenvironment. Frontiers in immunology. 2019; (10): 128. DOI: 10.3389/fimmu.2019.00128. PubMed PMID: 30804938; PubMed Central PMCID: PMC6370640.
27. Vivot A, Jacot J, Zeitoun JD, Ravaud P, Crequit P, Porcher R. Clinical benefit, price and approval characteristics of FDA-approved new drugs for treating advanced solid cancer, 2000–2015. Annals of oncology: official journal of the European Society for Medical Oncology. 2017; 28 (5): 1111–6. DOI: 10.1093/annonc/mdx053. PubMed PMID: 28453694.
28. Medina PJ, Adams VR. PD-1 Pathway Inhibitors: Immuno-Oncology Agents for Restoring Antitumor Immune Responses. Pharmacotherapy. 2016; 36 (3): 317–34. DOI: 10.1002/phar.1714. PubMed PMID: 26822752; PubMed Central PMCID: PMC5071694.
29. Larkin J, Chiarion-Sileni V, Gonzalez R, Grob JJ, Cowey CL, Lao CD, et al. Combined Nivolumab and Ipilimumab or Monotherapy

in Untreated Melanoma. The New England journal of medicine. 2015; 373 (1): 23–34. DOI: 10.1056/NEJMoa1504030. PubMed PMID: 26027431; PubMed Central PMCID: PMC5698905.
30. Postow MA, Sidlow R, Hellmann MD. Immune-Related Adverse Events Associated with Immune Checkpoint Blockade. The New England journal of medicine. 2018; 378 (2): 158–68. DOI: 10.1056/NEJMra1703481. PubMed PMID: 29320654.
31. Ren J, Liu X, Fang C, Jiang S, June CH, Zhao Y. Multiplex Genome Editing to Generate Universal CAR T Cells Resistant to PD1 Inhibition. Clinical cancer research: an official journal of the American Association for Cancer Research. 2017; 23 (9): 2255–66. DOI: 10.1158/1078-0432.CCR-16-1300. PubMed PMID: 27815355; PubMed Central PMCID: PMC5413401.
32. Yu Y, Wu H, Tang Z, Zang G. CTLA4 silencing with siRNA promotes deviation of Th1/Th2 in chronic hepatitis B patients. Cellular & molecular immunology. 2009; 6 (2): 123–7. DOI: 10.1038/cmi.2009.17. PubMed PMID: 19403062; PubMed Central PMCID: PMC4002649.
33. Rupp LJ, Schumann K, Roybal KT, Gate RE, Ye CJ, Lim WA, et al. CRISPR/Cas9-mediated PD-1 disruption enhances anti-tumor efficacy of human chimeric antigen receptor T cells. Scientific reports. 2017; 7 (1): 737. DOI: 10.1038/s41598-017-00462-8. PubMed PMID: 28389661; PubMed Central PMCID: PMC5428439.
34. Ren J, Zhang X, Liu X, Fang C, Jiang S, June CH, et al. A versatile system for rapid multiplex genome-edited CAR T cell generation. Oncotarget. 2017; 8 (10): 17002–11. DOI: 10.18632/oncotarget.15218. PubMed PMID: 28199983; PubMed Central PMCID: PMC5370017.
35. Knochelmann HM, Smith AS, Dwyer CJ, Wyatt MM, Mehrotra S, Paulos CM. CAR T Cells in Solid Tumors: Blueprints for Building Effective Therapies. Frontiers in immunology. 2018; (9): 1740. DOI: 10.3389/fimmu.2018.01740. PubMed PMID: 30140266; PubMed Central PMCID: PMC6094980.
36. Kerkar SP, Muranski P, Kaiser A, Boni A, Sanchez-Perez L, Yu Z, et al. Tumor-specific CD8+ T cells expressing interleukin-12 eradicate established cancers in lymphodepleted hosts. Cancer research. 2010; 70 (17): 6725–34. DOI: 10.1158/0008-5472.CAN-10-0735. PubMed PMID: 20647327; PubMed Central PMCID: PMC2935308.
37. Pegram HJ, Lee JC, Hayman EG, Imperato GH, Tedder TF, Sadelain M, et al. Tumor-targeted T cells modified to secrete IL12 eradicate systemic tumors without need for prior conditioning. Blood. 2012; 119 (18): 4133–41. DOI: 10.1182/blood-2011-12-400044. PubMed PMID: 22354001; PubMed Central PMCID: PMC3359735.
38. Kerkar SP, Goldszmid RS, Muranski P, Chinnasamy D, Yu Z, Reger RN, et al. IL12 triggers a programmatic change in dysfunctional myeloid-derived cells within mouse tumors. The Journal of clinical investigation. 2011; 121 (12): 4746–57. DOI: 10.1172/JCI58814. PubMed PMID: 22056381; PubMed Central PMCID: PMC3226001.
39. Zhang L, Morgan RA, Beane JD, Zheng Z, Dudley ME, Kassim SH, et al. Tumor-infiltrating lymphocytes genetically engineered with an inducible gene encoding interleukin-12 for the immunotherapy of metastatic melanoma. Clinical cancer research: an official journal of the American Association for Cancer Research. 2015; 21 (10): 2278–88. DOI: 10.1158/1078-0432.CCR-14-2085. PubMed PMID: 25695689; PubMed Central PMCID: PMC4433819.
40. Kunert A, Chmielewski M, Wijers R, Berrevoets C, Abken H, Debets R. Intra-tumoral production of IL18, but not IL12, by TCR-engineered T cells is non-toxic and counteracts immune evasion of solid tumors. Oncoimmunology. 2017; 7 (1): e1378842. DOI: 10.1080/2162402X.2017.1378842. PubMed PMID: 29296541; PubMed Central PMCID: PMC5739571.
41. Alsaieedi A, Holler A, Velica P, Bendle G, Stauss HJ. Safety and efficacy of Tet-regulated IL12 expression in cancer-specific T cells. Oncoimmunology. 2019; 8 (3): 1542917. DOI: 10.1080/2162402X.2018.1542917. PubMed PMID: 30723575; PubMed Central PMCID: PMC6350686.
42. Hoyos V, Savoldo B, Quintarelli C, Mahendravada A, Zhang M, Vera J, et al. Engineering CD19-specific T lymphocytes with interleukin-15 and a suicide gene to enhance their anti-lymphoma/leukemia effects and safety. Leukemia. 2010; 24 (6): 1160–70. DOI: 10.1038/leu.2010.75. PubMed PMID: 20428207; PubMed Central PMCID: PMC2888148.
43. Krenciute G, Prinzing BL, Yi Z, Wu MF, Liu H, Dotti G, et al. Transgenic Expression of IL15 Improves Antiglioma Activity of IL13Ralpha2-CAR T Cells but Results in Antigen Loss Variants. Cancer immunology research. 2017; 5 (7): 571–81. DOI: 10.1158/2326-6066.CIR-16-0376. PubMed PMID: 28550091; PubMed Central PMCID: PMC5746871.
44. Hu B, Ren J, Luo Y, Keith B, Young RM, Scholler J, et al. Augmentation of Antitumor Immunity by Human and Mouse CAR T Cells Secreting IL18. Cell reports. 2017; 20 (13): 3025–33. DOI: 10.1016/j.celrep.2017.09.002. PubMed PMID: 28954221; PubMed Central PMCID: PMC6002762.
45. Chmielewski M, Abken H. CAR T Cells Releasing IL18 Convert to T-Bet(high) FoxO1(low) Effectors that Exhibit Augmented Activity against Advanced Solid Tumors. Cell reports. 2017; 21 (11): 3205–19. DOI: 10.1016/j.celrep.2017.11.063. PubMed PMID: 29241547.

CORRELATED DYNAMICS OF SERUM IGE AND IGE$^+$ CLONOTYPE COUNT WITH ALLERGEN AIR LEVEL IN SEASONAL ALLERGIC RHINITIS

Mikelov AI[1,2], Staroverov DB[2], Komech EA[2,3], Lebedev YB[2,3], Chudakov DM[1,2,3], Zvyagin IV[2,3] ✉

[1] Skoltech, Moscow, Russia

[2] Shemyakin-Ovchinnikov Institute of Bioorganic Chemistry, Moscow, Russia

[3] Pirogov Russian National Research Medical University, Moscow, Russia

Mechanisms of maintenance of immunological memory in the chronic course of seasonal allergic rhinitis remain poorly understood. The detailed understanding of these mechanisms is required for design of new approaches for allergy treatment. It is known that the level of allergen-specific IgE antibodies (sIgE), which play a key role in the development of the disease, is increased in patients with seasonal allergic rhinitis during pollination season. This study aimed to investigate the dynamics of serum IgE levels and characteristics of the clonal repertoire of IgE-secreting lymphocytes depending on the intensity of the patient's contact with the allergen. For three patients, allergic to birch pollen (22, 22, and 28 y.o.), we measured total IgE and birch pollen specific IgE levels at 6 time points with 2 week interval during the birch pollination season. Immunoglobulin heavy chain gene (IGH) clonal repertoire data for several B-cell subpopulations at different time points were obtained for one patient. We observe growth of the sIgE level (91%, 37%, and 64% compared to the baseline) at the peak of pollination season in all three donors. Initial increase in sIgE and total IgE levels coincides with the birch pollination initiation; sIgE and total IgE levels correlate with the birch pollen air level (sIgE: $R^2 = 0.98$ at $p < 0.05$; total IgE: $R^2 = 0.95$ at $p < 0.05$). We detected IgE clonotypes only in samples obtained during the birch pollination, which indicates an increase of IGE-expressing cells concentration during this period. The frequency of IgE clonotypes was extremely low compared to that of the clonotypes of other isotypes (IgE — 0.01%, IgM — 48.4%, IgD — 14%, IgG — 17.4%, IgA — 19.8%). Hypermutation and phylogenetic analysis of the sequences from the 13 detected IgE-containing clonal groups showed that these IgE clonotypes could originate from IgG as a result of sequential isotype-switching.

Keywords: allergic rhinitis, allergen-specific IgE, birch pollen, seasonal dynamics, immunoglobulin clonal repertoire

Funding: the study was supported by the Grant Council of the President of the Russian Federation (grant MK6000.2018.4).

Acknowledgments: we are very grateful to all the donors who participated in the study.

Author contribution: Mikelov AI — ELISA, preparation of IGH cDNA libraries, sequencing data and results analysis, research design, drafting the manuscript; Staroverov DB — cell subpopulations isolation (flow cytometry); Komech EA — blood samples collection, cell subpopulations isolation (flow cytometry); Lebedev YB — results analysis and discussion, advisory support; Chudakov DM — results analysis and discussion, advisory support (cDNA libraries preparation); Zvyagin IV — preparation of IGH cDNA libraries, sequencing data and results analysis, research design, drafting the manuscript, research organization.

Compliance with ethical standards: the study was conducted in full compliance with the requirements of the 2013 Helsinki Declaration; all donors signed a voluntary informed consent to participate in the study. Blood samples were taken by qualified medical personnel in the certified clinic ("Invitro").

✉ **Correspondence should be addressed:** Ivan V. Zvyagin
Miklukho-Maklaya, 16/10, Moscow, 117997; izvyagin@gmail.com

Received: 09.10.2019 **Accepted:** 23.10.2019 **Published online:** 31.10.2019

DOI: 10.24075/brsmu.2019.072

СОГЛАСОВАННАЯ ДИНАМИКА СЫВОРОТОЧНОГО IGE И ЧИСЛЕННОСТИ IGE$^+$-КЛОНОТИПОВ С УРОВНЕМ ПЫЛЬЦЫ В ВОЗДУХЕ ПРИ ПОЛЛИНОЗЕ

А. И. Микелов[1,2], Д. Б. Староверов[2], Е. А. Комеч[2,3], Ю. Б. Лебедев[2,3], Д. М. Чудаков[1,2,3], И. В. Звягин[2,3] ✉

[1] Сколковский институт науки и технологий, Москва, Россия

[2] Институт биоорганической химии имени М. М. Шемякина и Ю. А. Овчинникова, Москва, Россия

[3] Российский национальный исследовательский университет имени Н. И. Пирогова, Москва, Россия

Механизмы поддержания иммунологической памяти, обусловливающей хроническое течение сезонного аллергического ринита у человека, слабо изучены. Рациональный дизайн новых подходов к терапии аллергических заболеваний требует детального понимания этих механизмов. Известно, что уровень аллергенспецифичных антител класса IgE (sIgE), являющихся ключевым агентом в развитии данного заболевания, повышен у пациентов с поллинозом в период цветения. Целью работы было изучить динамику сывороточного уровня IgE и характеристик клонального репертуара IgE-секретирующих лимфоцитов в зависимости от интенсивности контакта пациента с аллергеном. Для трех пациентов (22, 22 и 28 лет) с аллергией на березовую пыльцу были измерены уровни общего IgE и sIgE к березовой пыльце в 6 временных точках с интервалом в 2 недели, включая период пыления березы. Для одного донора получены данные о клональном репертуаре генов тяжелых цепей иммуноглобулинов (IGH) субпопуляций B-клеточного ряда. Прирост уровня sIgE в период пыления составил 91%, 37% и 64% по сравнению с исходным у трех доноров. Момент начала роста уровня sIgE и общего IgE и его динамика согласуются с ростом концентрации аллергена (sIgE: $R^2 = 0{,}98$ при $p < 0{,}05$; IgE общий: $R^2 = 0{,}95$ при $p < 0{,}05$). IgE-клонотипы обнаружены только в образцах, взятых в период цветения березы, что свидетельствует о росте их концентрации в этот период. Доля IgE-клонотипов оказалась крайне низкой по сравнению с клонотипами других изотипов (IgE — 0,01%, IgM — 48,4%, IgD — 14%, IgG — 17,4%, IgA — 19,8%). Оценка числа гипермутаций и филогенетический анализ последовательностей внутри 13 обнаруженных IgE-содержащих клональных групп показали возможность происхождения IgE-клонотипов из IgG в результате смены изотипа.

Ключевые слова: аллергический риноконъюнктивит, аллергенспецифичный IgE, пыльца березы, сезонная динамика, клональный репертуар иммуноглобулинов

Финансирование: исследование выполнено при поддержке Совета по грантам Президента Российской Федерации (грант МК6000.2018.4).

Благодарности: выражаем большую признательность всем донорам, принявшим участие в исследовании.

Информация о вкладе авторов: А. И. Микелов — определение уровня антител, подготовка библиотек кДНК IGH, анализ данных секвенирования и полученных результатов, дизайн исследования, подготовка рукописи; Д. Б. Староверов — выделение клеточных субпопуляций с помощью проточной цитофлюорометрии; Е. А. Комеч — сбор образцов крови, выделение клеточных субпопуляций с помощью проточной цитофлюорометрии; Ю. Б. Лебедев — анализ и обсуждение полученных результатов, консультативная поддержка; Д. М. Чудаков — анализ и обсуждение полученных результатов, консультативная поддержка подготовки библиотек кДНК; И. В. Звягин — подготовка библиотек кДНК IGH, анализ данных секвенирования и полученных результатов, дизайн исследования, подготовка рукописи, организация исследования.

Соблюдение этических стандартов: исследование проведено в полном соответствии с требованиями Хельсинской декларации 2013 г.; все доноры подписали добровольное информированное согласие на участие в исследовании. Забор образцов крови выполнен квалифицированным медицинским персоналом в сертифицированных кабинетах компании «ИНВИТРО».

✉ **Для корреспонденции:** Иван Владимирович Звягин
ул. Миклухо-Маклая, д. 16/10, г. Москва, 117997; izvyagin@gmail.com

Статья получена: 09.10.2019 **Статья принята к печати:** 23.10.2019 **Опубликована онлайн:** 31.10.2019

DOI: 10.24075/vrgmu.2019.072

Seasonal allergic rhinoconjunctivitis (SAR), or seasonal allergic rhinitis, is one of the most common allergies. According to various studies, 17 to 28% of the population of Europe suffer from this disease [1]. A significant part of SAR patients (8–16% of the total population) react to tree pollen, and birch pollen is the most common tree-produced allergen [2]. Same as other types of allergy, SAR is a chronic disease for most patients, and the probability of development of concomitant pathologies, such as asthma and food allergies, is quite high. While the most widely used therapeutic agents only aim to alleviate the symptoms (antihistamine and glucocorticosteroid drugs, mast cell membrane stabilizers), allergen-specific immunotherapy is the only currently practiced approach to SAR treatment that is designed to bring a long-term change in the chronic course of the disease. This is a long-term therapy that requires strict patient compliance and yields complete disappearance of the symptoms only in some patients [3]. Therefore, development of the new therapeutic approaches designed to prevent SAR from turning chronic is an extremely urgent task.

Rational design of such approaches requires a deep understanding of the mechanisms of maintenance of immunological memory that determine chronic course of allergy. A number of recent unsuccessful clinical trials of the allergic rhinitis treatment modalities demonstrate that the currently available information about these mechanisms is insufficient [4, 5]. Basic research efforts implying deeper investigation of the mechanisms of immunological memory preservation, which turns the allergy chronic, is a necessary basis both for the development of the new approaches to SAR treatment and improvement of the existing therapies.

It is known that IgE, a class E immunoglobulin, is one of the key agents in the development of an allergic response. However, there is little information about cell subpopulations producing IgE in allergic rhinitis patients: their localization, lifespan and required survival factors are not clear. Recently, using a mouse model of food allergy it was demonstrated, that shortly after sensitization IgE-secreting plasma cells can be found in the bone marrow and have a limited lifespan (up to 1 year) [6]. IgE class antibodies can remain bound at mast cell membranes for up to 100 days. It was also shown that at least some of the long-term immunological memory that turns allergy chronic is maintained by the subpopulation of IgG1$^+$ allergen-specific memory B-lymphocytes, which serves as a "reservoir" from which the population of IgE producers is replenished in case of contact with the allergen [6, 7].

This study aimed to investigate the dynamics of serum IgE levels in greater detail compared to the previous research efforts [8–10]. We enrolled patients allergic to birch pollen and studied the dependence of the aforementioned dynamics on the intensity of their contact with the allergen that is the derivative of the pollen concentration in air. As part of the study, we sought to identify the time point that, relative to the moment of contact with the allergen, marks replenishment of the IgE secreting cell fraction. We also aimed to characterize the subpopulation of IgE-secreting plasmablast and plasma cells aand describe their relationship to other isotypes and memory B-cell population during seasonal exacerbation of the disease.

METHODS

Patient cohort and collection of serum samples

The studied cohort included three patients (22, 22, and 28 years old). The inclusion criteria were: 1) any gender; 2) previously diagnosed seasonal birch pollen allergic rhinitis; 3) no bronchial asthma; 4) no other chronic inflammatory, autoimmune, oncological and infectious diseases. The exclusion criteria were: 1) ongoing or recently finished allergen-specific immunotherapy course; 2) vaccination during the study period. Venous blood samples were taken in medical laboratories and by medical personnel of the Invitro CDL chain of labs; the personnel used the Vacuette Serum Gel Z and Vacuette K3EDTA tubes (BD Biosciences; USA). Further experimental work was carried out in the research laboratory of the Institute of Bioorganic Chemistry, Russian Academy of Science.

To measure the total level of IgE and the level of birch and alder pollen-specific IgE we collected the patients' blood samples every fortnight from March to May 2019, thus taking 6 samples from each donor. From one of the donors (28 years old) we also collected four additional serum samples collected in March and May 2017, and in March and May 2018.

ELISA

We followed the protocol provided by the tube manufacturer (BD Biosciences; USA) to isolate blood serum. To establish the total IgE level and the level of birch and alder pollen-specific IgE we used the commercially available ELISA kits (Alkor Bio; Russia) according to the manufacturer's protocol. Hidex Sense reader (Hidex Oy; Finland) was used to measure the optical density. Each serum sample was measured in two independent replicates.

Isolation of subpopulations of memory B-lymphocytes, plasmablasts and plasma cells

For one of the donors (28 years old), we obtained samples of three cell B-cell subpopulations: memory B-lymphocytes, plasmablasts and peripheral blood plasma cells. These samples were collected at three time points, March and May 2017 and March 2018.

Peripheral blood mononuclear cells from whole blood were isolated using standard Ficoll density gradient protocol: centrifugation at 310g for 20 min, Eppendorf 5804 centrifuge (Eppendorf; Germany). Then, the cells were stained with the set of fluorescently-labeled antibodies: anti-CD19-APC, anti-CD20-VioBlue, anti-CD27-VioBright FITC, anti-CD138-PE-Vio770 (Myltenyi Biotec; USA). Next, using the fluorescence-activated sorting equipment (BD FacsAria III, BD Biosciences; USA) we isolated the target B-cell subpopulations: memory B-lymphocytes (CD19$^+$ CD20$^+$ CD27$^+$), plasmablasts (CD20$^-$ CD19$^+$ CD27^{++} CD138$^-$) and plasma cells (CD20$^-$ CD19$^{low/-}$ CD27$^+$ CD138$^+$). At each time point, we collected two samples of memory B-lymphocytes (50,000 cells), plasmablasts and plasma cells (1000 and 500 cells, respectively).

Sequencing and analysis of B-cell receptor repertoires

Preparing the immunoglobulin (IgH) heavy chain cDNA libraries, we followed the previously published protocol [11] with some modifications. At the reverse transcription stage we introduced the adapter with a unique molecular identifier (UMI) and sample-specific barcode (Table 1). Further amplification was done in two stages using the primers described in Table 1. For sequencing we used Illumina Hiseq 2000/2500 (Illumina; USA) in pair-end mode with 310 + 310 read length.

MIGEC software [12] was used for raw data set demultiplexing and consensus assembling on the basis of unique molecular identifier and sample-specific barcode sequences [12]. MIXCR software [13] was used to annotate the V-, D-, J-, and C-segments,

to identify the unique clonal IGH sequences (clonotypes) and to assess the level of hypermutations. To assemble the IGH clonal sequences, we used the IGH cDNA sequences supported by at least two reads based on the UMIs analysis. Clonotypes were defined by the nucleotide sequence of the immunoglobulin heavy chain starting from V segment framework region 1 (FR1) to the end of the J segment, with respect to the antibody isotype determined by the 5' fragment of the C segment 15–16 nucleotides long. R programming language [14] was used for IGH clonal repertoire analysis, statistical processing of the results and regression analysis; the Figures were prepared using the ggplot2 package [15]. Change-O software [16] was used to identify the clonal groups on the basis of the following criteria: one clonal group contains IGH sequences which have the same CDR3 length and IGH V-segment, and at least 85% of CDR3 nucleotide sequence identity 15% R. Phylogenetic analysis was performed using MEGA 7 software [17] (maximum likelihood phylogenetic trees, evolutionary GTR model).

Regression analysis

Regression model was used to test whether there is a relation between the birch pollen sIgE serum level dynamics and the allergen air level. Table 2 shows the data used for the model. Regression equation:

$$sIgE\_level = b + k1 \times pollen\_level + k2 \times donorMRK + k3 \times donorLK,$$

where sIgE_level is a dependent variable, representing serum level of the birch pollen-specific IgE; pollen_level — predictor variable, representing average level of birch pollen in the air (class) registered through the two weeks before sampling blood to measure the serum IgE level; donor MRK — dummy variable, can be 1 (MRK donor) and 0 (not MRK donor); donorLK — dummy variable, can be 1 (donor LK) and 0 (donor not LK); b is the intercept of the regression model that reflects the basic level of the dependent variable, relating to MS donor; $k1$, $k2$, $k3$ are the regression coefficients ($k1$ reflects the change in the dependent variable when the pollen level in the air changes by one pollination class; $k2$ reflects the difference in the basic level of birch pollen-specific IgE between MRK and MS donors; $k3$ reflects the difference in the basic level of birch pollen-specific IgE between LK and MS donors.

Calculated coefficients: $b = 207.813$ ($p < 0.01$); $k1 = 6.474$ ($p < 0.05$); $k2 = -194.4$ ($p < 0.01$); $k3 = -208.15$ ($p < 0.01$). Adjusted $R^2 = 0.98$; $p < 0.01$; F test.

Similarly, we used a regression model to analyze the relation between the serum IgE level dynamics and the air level of birch pollen. Total IgE serum level was selected as the dependent variable; predictor variables were the same as in the described model for sIgE. For the model where the total IgE serum level is the dependent variable, the coefficients were as follows: $b = 1299.05$ ($p < 0.01$); $k2 = -1056.4$ ($p < 0.01$); $k1 = 51.45$ ($p < 0.05$); $k3 = -1313.65$ ($p < 0.01$). Adjusted $R^2 = 0.95$; $p < 0.01$; F test.

Pollen monitoring data

Pollen monitoring data for Moscow were obtained from open sources (Allergophone). Table 3 is the pollination classification table that shows the number of pollen grains per cubic meter of air for each class.

Table 1. Sequences of oligonucleotide primers used for IGH cDNA libraries

Primer name	Description	Sequence
cDNA synthesis		
SmartMK	Template-switch adapter for cDNA synthesis. *U* = dU, rG-riboG, *N* — A/G/C/T nucleotides	CAGUGGUAUCAACGCAGAGUACNNNNNNUTGAAAUNNNNNNUCTT(rG)4
hIGG_r1	Isotype-specific primer, IgG	GAAGTAGTCCTTGACCAGGCA
hIGM_r1	Isotype-specific primer, IgM	GTGATGGAGTCGGGAAGGAAG
hIGA_r1	Isotype-specific primer, IgA	GCGACGACCACGTTCCCATCT
hIGD_r1	Isotype-specific primer, IgD	GGACCACAGGGCTGTTATC
hIGE_r1	Isotype-specific primer, IgE	AGTCACGGAGGTGGCATTG
PCR amplification, step 1		
M1ss	Forward primer	AAGCAGTGGTATCAACGCA
hIGG_r2	Isotype-specific reverse primer, IgG/IgE	CCAGGGGGAAGACCGATG
hIGA_r2	Isotype-specific reverse primer, IgA	CTCAGCGGGAAGACCTTG
hIGM_r2	Isotype-specific reverse primer, IgM	ACGAGGGGGAAAAGGGTTG
hIGD_r2	Isotype-specific reverse primer, IgD	CCTGATATGATGGGGAACAC
hIGE_r2	Isotype-specific reverse primer, IgE	GTCAAGGGGAAGACGGATG
PCR amplification step 2		
M1s_long_i7	Forward primer *	CAAGCAGAAGACGGCATACGAGAT(i7)GTCTCGTGGGCTCGGAGATGTGTATAAGAGACAGTGGTATCAACGCAGAG
hIGD_r2_long_i5	Isotype-specific reverse primer, IgD *	AATGATACGGCGACCACCGAGATCTACAC(i5)TCGTCGGCAGCGTCAGATGTGTATAAGAGACAGATATGATGGGGAACAC
hIGM_r2_long_i5	Isotype-specific reverse primer, IgM *	AATGATACGGCGACCACCGAGATCTACAC(i5)TCGTCGGCAGCGTCAGATGTGTATAAGAGACAGAGGGGGAAAAGGGTTG
hIGA_r2_long_i5	Isotype-specific reverse primer, IgA *	AATGATACGGCGACCACCGAGATCTACAC(i5)TCGTCGGCAGCGTCAGATGTGTATAAGAGACAGCAGCGGGAAGACCTTG
hIGGE_r2_long_i5	Isotype-specific reverse primer, IgG/IgE *	AATGATACGGCGACCACCGAGATCTACAC(i5)TCGTCGGCAGCGTCAGATGTGTATAAGAGACAGARGGGGAAGACSGATG

Note: * (i5) and (i7) — sequences 8 nucleotides in length, which are sample-specific barcodes.

RESULTS

The total and birch pollen-specific IgE serum levels increased as the birch pollen level grew in the air

We measured total and birch pollen-specific serum IgE levels at 6 time points before and after the start of birch pollination season. The absolute values reflecting serum levels of both specific (Fig. 1A) and total IgE (Fig. 1B) significantly differ among patients, and the individual differences significantly exceed differences between IgE levels of the same donor at different time points. In all donors, the absolute values of both birch pollen sIgE and total IgE increased between time point 1 and time point 6. The level of birch pollen-specific IgE correlates with the total IgE level in each donor; it exceeds the reference level at all time points (Fig. 1).

The change in the levels of birch-pollen sIgE and total IgE registered through the period of the study is significantly smaller than the differences in the total and specific IgE serum levels between donors (coefficient of variation between all time points, one donor, birch pollen-sIgE: MS — 0.130, MRK — 0.228, LK — 0.282; total IgE: MS — 0.189, MRK — 0.154, LK — 0.485; the smallest variation coefficient between donors, sIgE — 1.39, total IgE — 1.17). Taking this into account, in order to characterize the seasonal dynamics of total IgE and sIgE in serum we considered these levels with regards to the initial level of total IgE and sIgE, measured before the birch pollination season had started (time point 1). For each donor, each total and birch pollen-specific IgE level measurement was normalized to the corresponding values of total and birch pollen-specific IgE level at time point 1.

Our findings are consistent with the previously published research on the seasonal dynamics of serum levels of IgE specific to other pollen allergens [8–10]: birch pollen-sIgE level grows significantly between the off-season time point (1) and the season peak time point (6). The dynamics of birch pollen sIgE correlates with the level of birch pollen in the air (Fig. 2). The maximum increase of sIgE was observed at the peak of the birch pollen level, between time points 3 and 5: the increase reached 90.7% for donor LK, for MRK — 63.7%, for MS — 36.9%.

A linear regression model was developed to statistically test the hypothesis that the level of birch pollen in the air and the serum level of birch pollen-specific IgE are related. According to the model, a high proportion of variance of the dependent variable (sIgE level) depends on the selected predictors (adjusted R^2 = 0.98), i.e. pollen air level and donor identifier (the latter accounts for significant differences in the absolute sIgE level between donors). All coefficients are significantly not equal to 0, ($p < 0.05$ for all coefficients), and the coefficient at the predictor-variable reflecting birch pollen air level is greater than 0 ($k1$ = 6.47), which serves as a statistical confirmation of the consistency of serum sIgE level dynamics with the birch pollen air level. Similarly, the regression model for total IgE level also demonstrates that its level grows together with the growth of the allergen's concentration in the air (adjusted R^2 = 0.95; $p < 0.05$ for each of the coefficients).

It should be noted that a relatively small (compared to the maximums registered through the observation period) birch pollen sIgE level increase occurs before the start of pollination season or when the allergen concentration is low (time points 1–3). The possible reasons could be a random fluctuation in birch pollen sIgE level (two out of three donors exhibited the absolute level increase below 1 IU/ml between time points 1–2 and 2–3) or a contact of the patient with birch pollen that occurred early, before pollen level growth was registered by pollen monitoring stations. Such an increase in the birch pollen sIgE level can also be the result of its cross-reactivity to alder pollen antigens as alder pollination season precedes birch pollination season and there is a high level of structural similarity between birch and alder pollen antigens. To assess the contribution of cross-reactive IgE we measured the level of alder pollen sIgE in all collected serum samples (Fig. 3). In all donors, the level of alder

Table 2. Data used to build the regression models. Birch pollen-specific and total IgE levels, averaged level of birch pollen in the air between corresponding time points

Time point	Donor	Birch pollen sIgE serum level, IU/ml	Total IgE serum level, IU/ml	Av. level of birch pollen in the air, class
1	MS	178.4	1066.3	0.00
2	MS	192.4	1148.9	0.00
3	MS	202.7	1275.9	0.07
4	MS	232	1419.7	1.07
5	MS	243.1	1469.4	3.83
6	MS	244.3	1779.9	2.13
1	MRK	15.7	273.7	0.00
2	MRK	17.4	245.9	0.00
3	MRK	17.6	288.5	0.07
4	MRK	23	293.1	1.07
5	MRK	27.1	358.3	3.83
6	MRK	25.7	362.2	2.13
1	LK	5.4	26.2	0.00
2	LK	6.4	31.2	0.00
3	LK	6.1	28.2	0.07
4	LK	6.2	44.8	1.07
5	LK	9.6	69.1	3.83
6	LK	10.3	78.7	2.13

Table 3. Pollination level — pollination classes according to the volume of pollen in the air

Amount of pollen grains per 1 m^3 of air	0	1–10	11–100	101–1000	1001–5000	> 5000
Class	0	1	2	3	4	5

pollen sIgE followed birch pollen air level more than alder pollen air level. Alder pollen sIgE peaked between time points 4 and 5, when the concentration of birch pollen in the air was at its maximum, but not at time points 1 and 2, when alder pollen level showed most of its growth. Therefore, we can assume a high level of birch pollen sIgE cross-reactivity to alder pollen antigens in all participating donors.

In 2 donors (MRK, LK), birch pollen sIgE grew slightly (<1 IU/ml) while alder pollen sIgE went down. Thus, the insignificant increase in birch pollen sIgE level shown for MRK and LK donors cannot be explained by its cross-reactivity to alder pollen sIgE. In MS donor, we registered growing alder pollen sIgE between time points 1 and 2, which may explain the increase in birch pollen sIgE level before the beginning of the birch pollination season.

The abundance of IgE-expressing cells in peripheral blood B-cell subpopulations is relatively low and increases during seasonal exacerbation of allergies

Based on the data obtained from the mouse model of food allergy, we can assume that birch pollen sIgE serum level and total IgE level grow with the increase of the number of IgE-producing cells. In order to assess the seasonal dynamics of IgE$^+$ cell abundance in different B-cell subpopulations, we analyzed the immunoglobulin heavy chain (IGH) clonal repertoires of memory B-cells, plasmablasts and plasma cells from peripheral blood at three time points (1_2017, 3_2018 — time points outside the birch pollination season, 2_2017 — season peak).

For all three time points, sequencing yielded a total of 50,550,291 reads representing 1,616,747 unique IGH cDNA molecules. To eliminate the majority of errors in determining the clonal sequence, we included only those IGH cDNA sequences which were supported by at least two independent reads. A total of 116,437 IGH clonotypes were identified (a clonotype is defined as unique nucleotide sequence of IGH starting from the framework region (FR1) of the V segment to the end of the J segment, with antibody isotype determined on the basis of 5' fragment of C segment). IgE clonotypes were extremely rare (~0.01% out of all detected clonotypes). For comparison, the frequency of IgM clonotypes was 48.4%, IgD — 14%, IgG — 17.4%, IgA — 19.8%.

All IGE$^+$ clonotypes were detected in IGH repertoires of memory B-lymphocytes, plasmablasts and long-lived plasma cells exclusively in samples obtained during the birch pollination

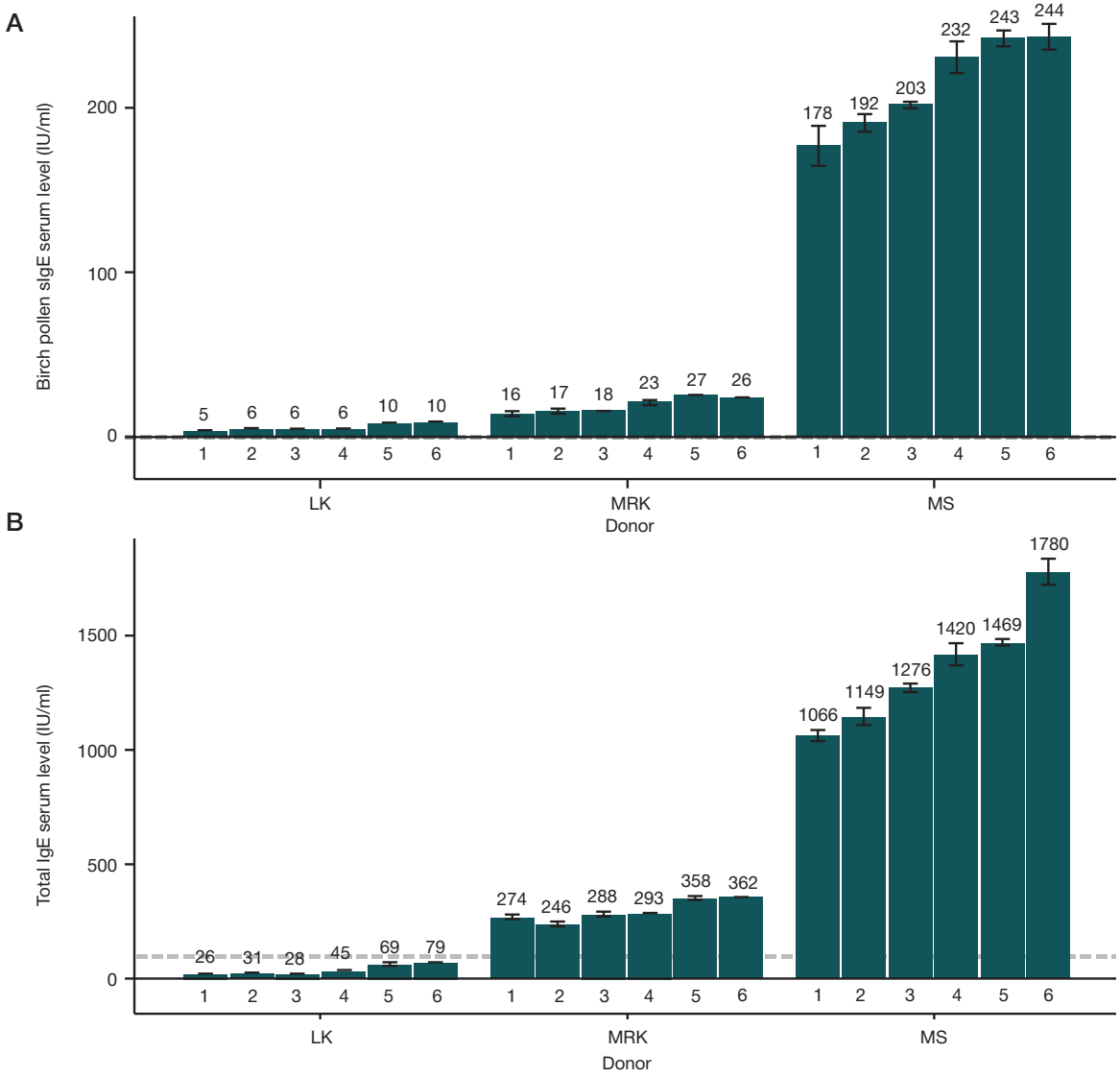

Fig. 1. Level of birch pollen-specific IgE (**A**) and total IgE (**B**) for three donors (LK, MRK, MS) with seasonal allergic rhinoconjunctivitis at six time points (1–6). Horizontal dashed line represents the reference level of corresponding antibodies in a healthy adult donor's serum (<0.35 IU/ml for sIgE, <100 IU/ml for general IgE). Error bars reflect difference between minimum and maximum measurement values

season (Fig. 4), while the sample size (in the number of cells) for each subpopulation does not differ between time points. This result demonstrates the increase in abundance of IGE$^+$ cells in the patient's peripheral blood during birch pollination season.

The technology applied to prepare immunoglobulin heavy chain cDNA libraries allows estimating the number of hypermutations along the entire length of the IGH sequence, from the FR1 region to 5' fragment of the constant region. For each clonotype, we identified the number of hypermutations and compared it between clonotypes with different isotypes. As expected, the lowest level of hypermutations was detected among IgD and IgM clonotypes (median — 2.3 and 3.7 bp per 100 bp of the V segment sequence, respectively), while a higher level — among IgG and IgA clonotypes (median — 6.8 and 7.1 bp per 100 bp of the V segment sequence, respectively) (Fig. 5), which are typically expressed in B-lymphocytes that matured in germinal centers. The average number of hypermutations of IgE clonotypes was not lower (median — 7.4 bp per 100 bp of the V segment sequence) compared to that of IgG and IgA clonotypes. Similar level of hypermutations between IgE and IgG clonotypes may reflect the origination of the IgE clonotypes of antibody-secreting cell subpopulations from memory IgG$^+$ B lymphocytes, but also does not exclude the independent isotype switching and accumulation of hypermutations in IgE$^+$ and IgG$^+$ B lymphocytes.

To analyze the relationship between IgE clonotypes in immunoglobulin heavy chain repertoires and clonotypes of other isotypes in greater detail we applied the previously described approach for identification of sets of clonotypes most likely derived from a single precursor and having a similar but not necessarily identical nucleotide sequence encoding a variable domain of the B-cell receptor heavy chain (clonal groups) [16]. A total of 13 IgE-containing clonal groups were identified; they included 154 clonotypes. In 4 of them we have identified clonotypes of other isotypes: IgG — 82, IgA — 19, IgM — 4 and IgD — 1. Phylogenetic analysis that we did for clonotypes of each of these clonal groups reveals a close relationship between IgE and IgG clonotypes (Fig. 6): for most IgE clonotypes, the closest neighbour in the phylogenetic tree was an IgG clonotype. It should be noted that in each of the considered IgE-containing clonal groups there were IgG-clonotypes representing the IgG$^+$ fraction of memory B-lymphocytes.

DISCUSSION

Previously published studies describe an increase in the serum level of total and allergen-specific IgE during the seasonal allergic rhinitis exacerbation [8–10]. However, these studies present the serum levels seasonal dynamics data

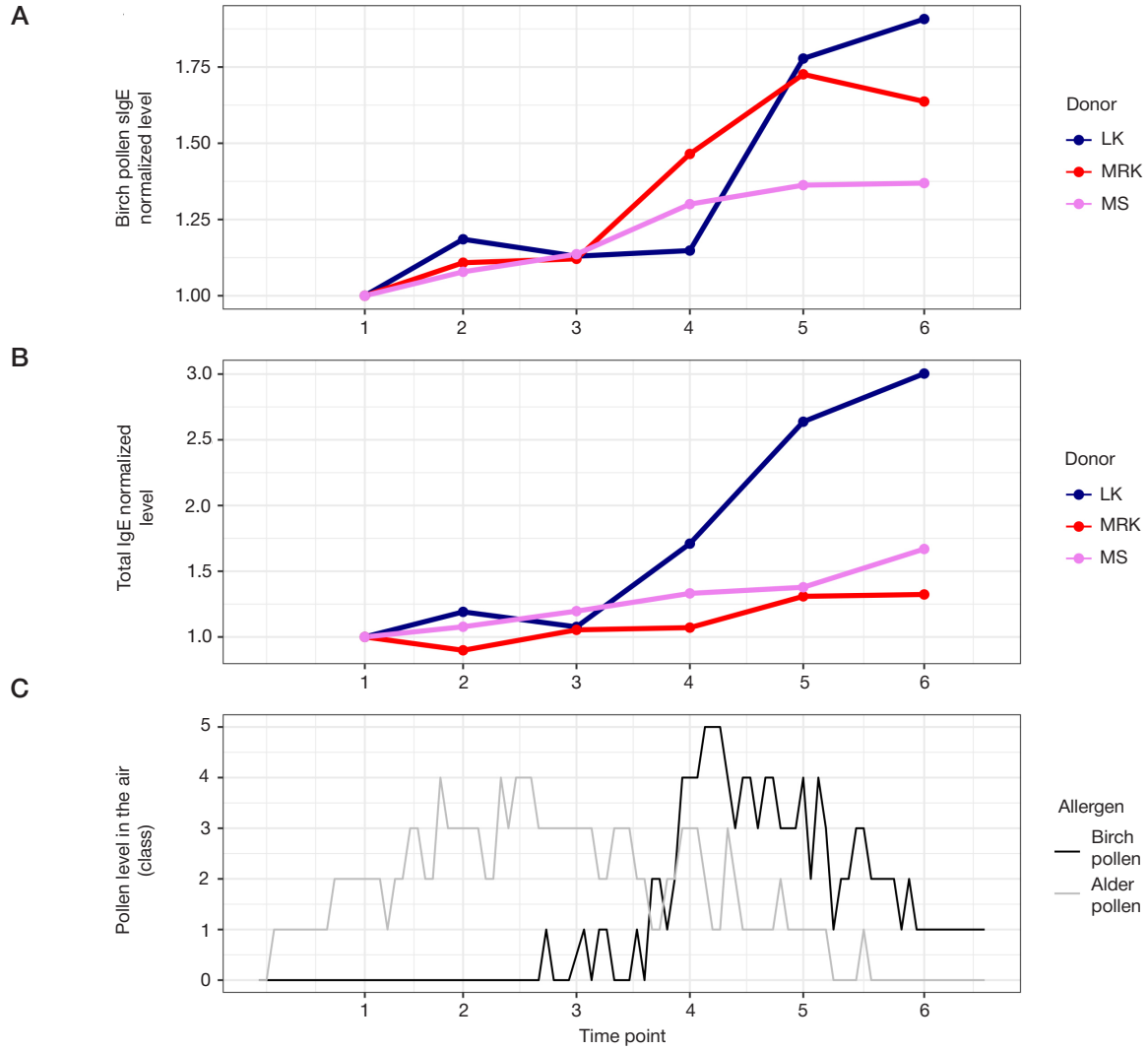

Fig. 2. Serum IgE level and birch pollen air level dynamics. **A**. Birch pollen sIgE serum level at each time point, normalized to the level of birch pollen sIgE at time point 1 for the corresponding donor. **B**. Total sIgE serum level at each time point, normalized to the level of total sIgE at time point 1 for the corresponding donor. **C**. Birch pollen level in the air

that were collected once every several months. Moreover, no connection was made to the air level of pollen that causes the allergy. In this work, we measured serum levels of total IgE and birch pollen/alder pollen-specific IgE with a higher time resolution (immunoglobulin levels were measured once a fortnight) during a period including the birch pollination commencement. Collation of the immunoglobulin levels and air level of the pollen at each time point allowed to demonstrate a correlation between birch pollen concentration in the air and level of birch pollen-specific and total IgE. Interestingly, all donors had the alder pollen sIgE growing together with the concentration of birch pollen in the air, but not with the level of alder pollen. Most likely, this is due to the birch pollen sIgE's cross-reactivity to alder pollen antigens; this fact may indicate that the donors that participated in our study lack specific antibodies to unique alder epitopes. However, since we did not register the alder pollen sIgE level before alder pollination season (it was a little over a week away from the beginning of sIgE level registration, and within this week the alder pollen air concentration was as low as 1–10 grains per 1 m^3), we cannot exclude the possibility of alder pollen sIgE peaking during this season (time points 1–3).

In all donors, birch pollen sIgE and total IgE levels began growing at the same time when the concentration of birch pollen in the air started to increase. This simultaneity may be the result of the growing count of IgE-secreting plasmablasts and plasma cells differentiating from memory B-lymphocytes in response to stimulation by the allergen. Analysis of the IGH repertoire dynamics and properties of sequences of identified IGH clonotypes generally confirms this assumption. The data obtained show that the abundance of peripheral blood IgE-expressing plasmablasts and plasma cells grows when birch starts pollinating, which reflects the active differentiation process of B-lymphocytes. The high level of hypermutations observed in IgE clonotypes is the sign of a long history of receptor selection in germination centers, which suggests that these IgE-secreting cells may originate from memory B-lymphocytes.

Overall, the obtained results allow assuming that the long-term immunological memory maintenance model proposed for food allergies [6] may also be valid for seasonal allergic rhinitis. In this model, the long-lived IgE-secreting plasma cells have a limited life span (~100 days in the mouse model), while memory IgG1 B-lymphocytes serve as the long-term "reservoir" from which the pool of IgE-secreting plasma cells is replenished. The replenishment occurs when the patient contacts the allergen, the process itself implies rapid proliferation, isotype switching, and differentiation of memory IgG1 B-lymphocytes under the action of Th2-associated cytokines (IL4, IL13, etc.). The previously published study of the B-cell receptor repertoires in respiratory allergies [18] did not allocate clonotypes to specific subpopulations, however, there were indications of clonal connections between IgG and IgE clonotypes in the peripheral blood immunoglobulin heavy chain repertoires, which is an indirect confirmation of correctness of the model suggested by R. Jiménez-Saiz and co-authors. The phylogenetic analysis of IgE-containing clonal groups, which was part of our study, demonstrates that the IgE-secreting plasma cells may originate from memory IgG^+ B lymphocytes in allergic rhinoconjunctivitis patients. However, the analysis does not exclude other IgE-producers origination patterns.

Our results also do not exclude the possibility of serum IgE level increase being caused by the boost in production and secretion of antibodies by existing IgE-secreting plasma cells. The average lifespan of IgE^+ plasma cells in human red bone marrow remains unexplored. Allergic rhinitis patients exhibit high IgE concentration in serum even outside the pollination season, which suggests the lifespan exceeding the time between two pollination seasons. However, taking into account the previously published data on correlation between

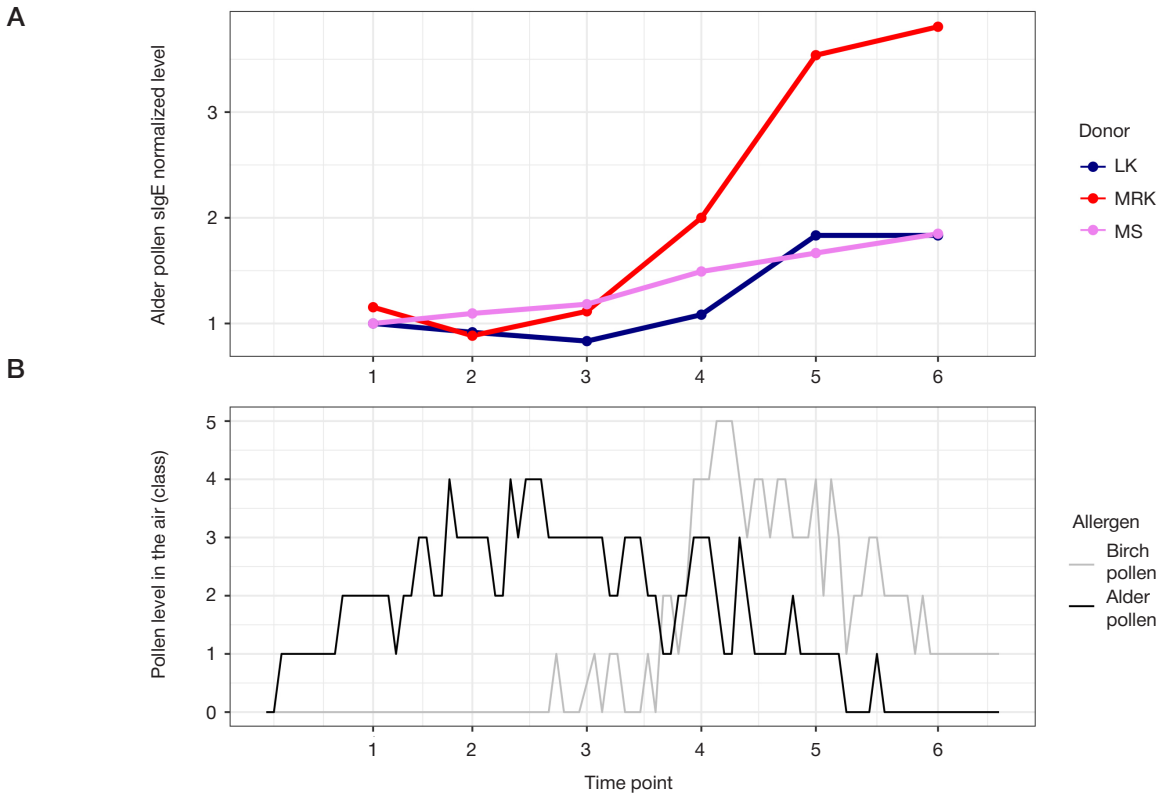

Fig. 3. Dynamics of alder pollen-specific IgE level and concentration of pollen in the air. **A**. Alder pollen sIgE serum level at each time point, normalized to the level of alder pollen sIgE at time point 1 for the corresponding donor. **B**. Pollen level in the air

serum IgE and peripheral blood IgE$^+$ plasma cells count [19], the growing number of IgE-secreting cells seems to be a more likely explanation for growth of IgE and sIgE levels, which is consistent with the results of this work.

CONCLUSIONS

Compared to the previously published study, we monitored the level of antibodies in serum at a higher temporal resolution, which allowed to demonstrate that level of sIgE starts to increase at the same time with the increase of birch pollen in air for patients with seasonal birch pollen allergy. The dynamics of total and allergen-specific IgE correlates with the level of birch pollen in the air.

Combined with the data obtained by other researchers in a mouse model of food allergy, our results of high-throughput sequencing and analysis of repertoires of cells of B-cell lineage suggest that this growth is most likely caused by the growing abundance of IgE-secreting plasma cells. The analysis of IGH nucleotide sequences of IgE-containing clonal groups of different B cell subpopulations showed a high similarity of IgE and IgG clonotypes and presence of IgG clonotypes representing the IgG$^+$ memory B lymphocyte fraction in these groups, which suggests that IgE-secreting cells could originate from a pool of IgG$^+$ B lymphocytes.

The small sample size does not allow to generalize the revealed characteristics to all patients since there is an alleged variety in endotypes of allergic rhinoconjunctivitis. The results we obtained in our study highlight similarities in the long-term immune memory maintenance mechanisms for SAR and food allergies. To validate this assumption, it is necessary to conduct

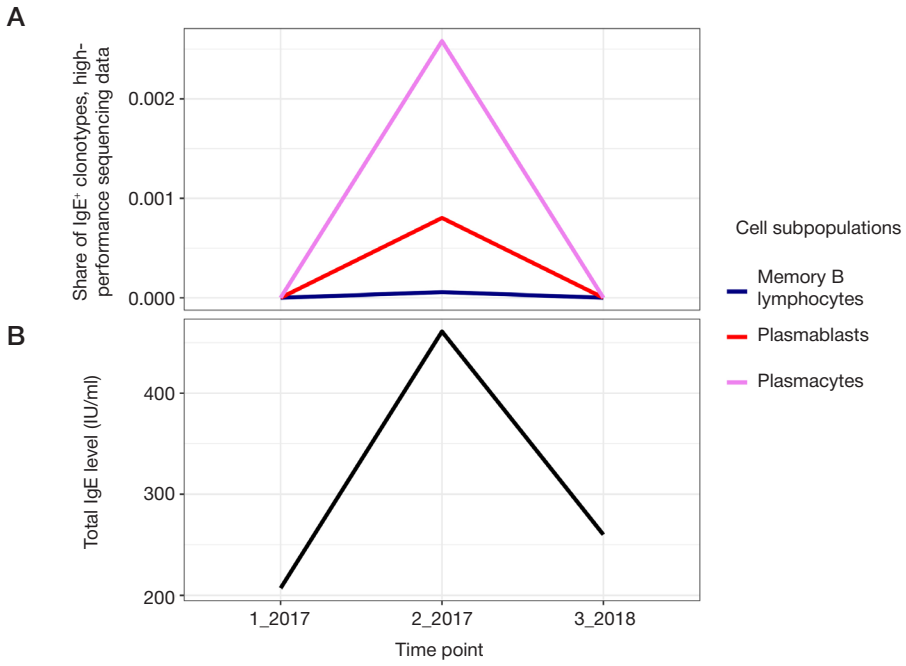

Fig. 4. B cell clonal repertoire dynamics. **A**. Abundance of IgE-clonotypes as revealed by high-throughput sequencing of immunoglobulin heavy chain repertoires for three subpopulations of peripheral blood cells: memory B lymphocytes, plasmablasts and plasma cells. **B**. Serum level of total IgE at the corresponding time points

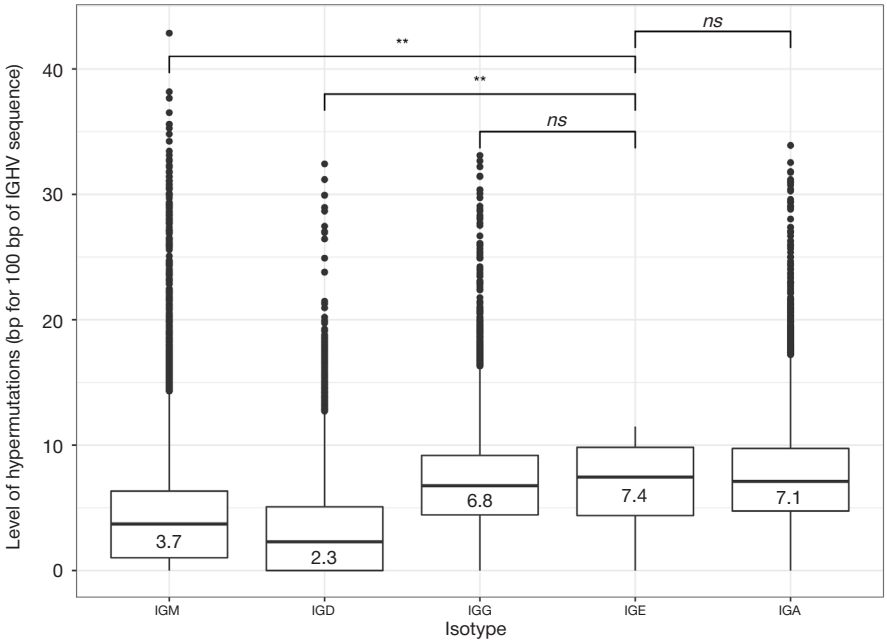

Fig. 5. Level of hypermutations (per 100 bp of IGHV sequence) calculated from high-throughput IGH repertoire sequencing data. IGM (n = 55 865), IGD (n = 15 834), IGG (n = 20 321), IGE (n = 13), IGA (n = 23 955). (** — $p < 0.01$; *ns* — not significant; Wilcoxon rank-sum test)

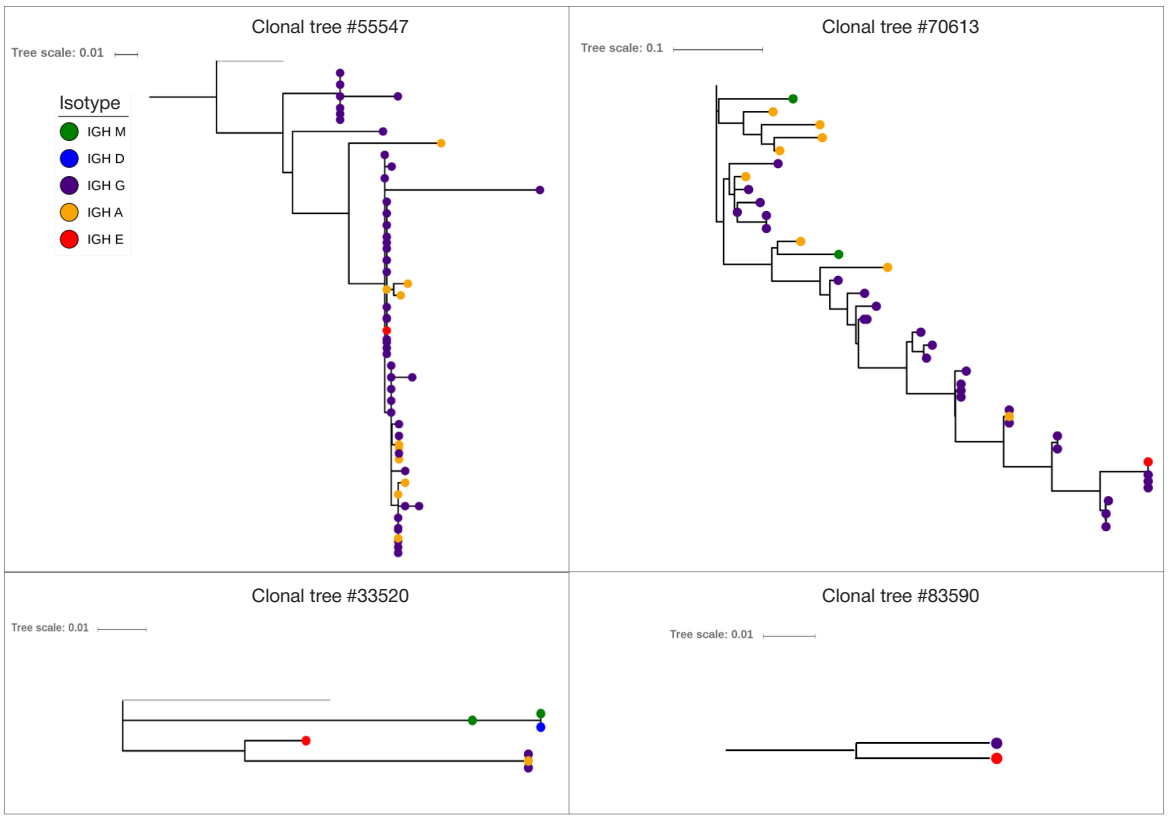

Fig. 6. Phylogenetic trees for IgE-containing clonal groups with clonotypes of different isotypes. Each dot represents a unique IGH clonotype. Clonotypes of different isotypes are color coded (dark blue — IgG, red — IgE, orange — IgA, green — IgM, blue — IgD). Length of the branches reflects distance between nodes according to the number of mutations between sequences. "Tree scale" reflects the scale used to build the tree

further research with larger cohorts and more elaborate clinical characterization of patients. Such research efforts are needed to develop new therapies aimed at breaking the allergen-specific immunological memory. For example, such new therapy may imply blocking isotype switching to IgE during differentiation of IgG^+ allergen-specific memory B cells, which is achievable through suppressing the effect of Th2 T cell cytokines by using a monoclonal antibody to IL4R. The obtained information on the dynamics of serum antibodies level with changing the allergen air concentration facilitates further investigation of the seasonal dynamics of concentration of IgE-secreting allergen-specific cells.

References

1. Bauchau V, Durham SR. Prevalence and rate of diagnosis of allergic rhinitis in Europe. European Respiratory Journal. 2004; 24 (5): 758–64. https://doi.org/10.1183/09031936.04.00013904.
2. Biedermann T, Winther L, Till SJ, Panzner P, Knulst A, Valovirta E. Birch pollen allergy in Europe. Allergy. 2019; 74 (7): all.13758. https://doi.org/10.1111/all.13758.
3. Penagos M, Eifan AO, Durham SR, Scadding GW. Duration of Allergen Immunotherapy for Long-Term Efficacy in Allergic Rhinoconjunctivitis. Current Treatment Options in Allergy. 2018; 5 (3): 275–90. https://doi.org/10.1007/s40521-018-0176-2.
4. Balbino B, Conde E, Marichal T, Starkl P, Reber LL. Approaches to target IgE antibodies in allergic diseases. Pharmacology & Therapeutics. 2018; (191): 50–64. https://doi.org/10.1016/j.pharmthera.2018.05.015.
5. Rudulier CD, Tonti E, James E, Kwok WW, Larché M. Modulation of CRTh2 expression on allergen specific T cells following peptide immunotherapy. Allergy. 2019; all.13867. https://doi.org/10.1111/all.13867.
6. Jiménez-Saiz R, Chu DK, Mandur TS, Walker TD, Gordon ME, Chaudhary R, et al. Lifelong memory responses perpetuate humoral TH2 immunity and anaphylaxis in food allergy. Journal of Allergy and Clinical Immunology. 2017; 140 (6): 1604–15. https://doi.org/10.1016/j.jaci.2017.01.018.
7. Jiménez-Saiz R, Bruton K, Koenig JF, Waserman S, Jordana M. The IgE memory reservoir in food allergy. The Journal of Allergy and Clinical Immunology. 2018; 142 (5): 1441–3. https://doi.org/10.1016/j.jaci.2018.08.029.
8. Beeh K, Beier J, Buhl R. Seasonal variations of serum-IgE and potential impact on dose-calculation of omalizumab (rhuMab-E25, anti-IgE). Pneumologie. 2004; 58 (08): 546–51. https://doi.org/10.1055/s-2004-818483.
9. Sato K, Nakazawa T, Sahashi N, Kochibe N. Yearly and Seasonal Changes of Specific IgE to Japanese Cedar Pollen in a Young Population. Annals of Allergy, Asthma & Immunology. 1997; 79 (1): 57–61. https://doi.org/10.1016/S1081-1206(10)63085-2.
10. Gleich GJ, Jacob GL, Yunginger JW, Henderson LL. Measurement of the absolute levels of IgE antibodies in patients with ragweed hay fever. Journal of Allergy and Clinical Immunology. 1977; 60 (3): 188–98. https://doi.org/10.1016/0091-6749(77)90123-3.
11. Turchaninova MA, Davydov A, Britanova OV, Shugay M, Bikos V, Egorov ES, et al. High-quality full-length immunoglobulin profiling with unique molecular barcoding. Nature Protocols. 2016; 11 (9): 1599–616. https://doi.org/10.1038/nprot.2016.093.
12. Shugay M, Britanova OV, Merzlyak EM, Turchaninova MA, Mamedov IZ, Tuganbaev TR, et al. Towards error-free profiling of immune repertoires. Nature Methods. 2014; (11): 653. http://dx.doi.org/10.1038/nmeth.2960.
13. Bolotin DA, Poslavsky S, Mitrophanov I, Shugay M, Mamedov IZ, Putintseva EV, et al. MiXCR: software for comprehensive adaptive immunity profiling. Nature Methods. 2015; (12): 380.

https://doi.org/10.1038/nmeth.3364.
14. R Core Team. R: A language and environment for statistical computing. R Foundation for Statistical Computing. Vienna, Austria. 2013. URL http://www.R-project.org/.
15. Wickham H. ggplot2: Elegant Graphics for Data Analysis. New York: Springer-Verlag, 2016. Retrieved from https://ggplot2.tidyverse.org.
16. Gupta NT, Vander Heiden JA, Uduman M, Gadala-Maria D, Yaar G, Kleinstein SH. Change-O: a toolkit for analyzing large-scale B cell immunoglobulin repertoire sequencing data. Bioinformatics. 2015; 31 (20): 3356–8. DOI: 10.1093/bioinformatics/btv359.
17. Sudhir Kumar, Glen Stecher, Koichiro Tamura. MEGA7: Molecular Evolutionary Genetics Analysis Version 7.0 for Bigger Datasets, Molecular Biology and Evolution. 2016; 33 (7): 1870–4. https://doi.org/10.1093/molbev/msw054.
18. Looney TJ, Lee JY, Roskin KM, Hoh RA, King J, Glanville J, et al. Human B-cell isotype switching origins of IgE. Journal of Allergy and Clinical Immunology. 2016; 137 (2): 579–86. https://doi.org/10.1016/j.jaci.2015.07.014.
19. Horst A, Hunzelmann N, Arce S, Herber M, Manz RA, Radbruch A, et al. Detection and characterization of plasma cells in peripheral blood: Correlation of IgE$^+$ plasma cell frequency with IgE serum titre. Clinical and Experimental Immunology. 2002; 130 (3): 370–8. https://doi.org/10.1046/j.1365-2249.2002.02025.x.

Литература

1. Bauchau V, Durham SR. Prevalence and rate of diagnosis of allergic rhinitis in Europe. European Respiratory Journal. 2004; 24 (5): 758–64. https://doi.org/10.1183/09031936.04.00013904.
2. Biedermann T, Winther L, Till SJ, Panzner P, Knulst A, Valovirta E. Birch pollen allergy in Europe. Allergy. 2019; 74 (7): all.13758. https://doi.org/10.1111/all.13758.
3. Penagos M, Eifan AO, Durham SR, Scadding GW. Duration of Allergen Immunotherapy for Long-Term Efficacy in Allergic Rhinoconjunctivitis. Current Treatment Options in Allergy. 2018; 5 (3): 275–90. https://doi.org/10.1007/s40521-018-0176-2.
4. Balbino B, Conde E, Marichal T, Starkl P, Reber LL. Approaches to target IgE antibodies in allergic diseases. Pharmacology & Therapeutics. 2018; (191): 50–64. https://doi.org/10.1016/j.pharmthera.2018.05.015.
5. Rudulier CD, Tonti E, James E, Kwok WW, Larché M. Modulation of CRTh2 expression on allergen specific T cells following peptide immunotherapy. Allergy. 2019; all.13867. https://doi.org/10.1111/all.13867.
6. Jiménez-Saiz R, Chu DK, Mandur TS, Walker TD, Gordon ME, Chaudhary R, et al. Lifelong memory responses perpetuate humoral TH2 immunity and anaphylaxis in food allergy. Journal of Allergy and Clinical Immunology. 2017; 140 (6): 1604–15. https://doi.org/10.1016/j.jaci.2017.01.018.
7. Jiménez-Saiz R, Bruton K, Koenig JF, Waserman S, Jordana M. The IgE memory reservoir in food allergy. The Journal of Allergy and Clinical Immunology. 2018; 142 (5): 1441–3. https://doi.org/10.1016/j.jaci.2018.08.029.
8. Beeh K, Beier J, Buhl R. Seasonal variations of serum-IgE and potential impact on dose-calculation of omalizumab (rhuMab-E25, anti-IgE). Pneumologie. 2004; 58 (08): 546–51. https://doi.org/10.1055/s-2004-818483.
9. Sato K, Nakazawa T, Sahashi N, Kochibe N. Yearly and Seasonal Changes of Specific IgE to Japanese Cedar Pollen in a Young Population. Annals of Allergy, Asthma & Immunology. 1997; 79 (1): 57–61. https://doi.org/10.1016/S1081-1206(10)63085-2.
10. Gleich GJ, Jacob GL, Yunginger JW, Henderson LL. Measurement of the absolute levels of IgE antibodies in patients with ragweed hay fever. Journal of Allergy and Clinical Immunology. 1977; 60 (3): 188–98. https://doi.org/10.1016/0091-6749(77)90123-3.
11. Turchaninova MA, Davydov A, Britanova OV, Shugay M, Bikos V, Egorov ES, et al. High-quality full-length immunoglobulin profiling with unique molecular barcoding. Nature Protocols. 2016; 11 (9): 1599–616. https://doi.org/10.1038/nprot.2016.093.
12. Shugay M, Britanova OV, Merzlyak EM, Turchaninova MA, Mamedov IZ, Tuganbaev TR, et al. Towards error-free profiling of immune repertoires. Nature Methods. 2014; (11): 653. http://dx.doi.org/10.1038/nmeth.2960.
13. Bolotin DA, Poslavsky S, Mitrophanov I, Shugay M, Mamedov IZ, Putintseva EV, et al. MiXCR: software for comprehensive adaptive immunity profiling. Nature Methods. 2015; (12): 380. https://doi.org/10.1038/nmeth.3364.
14. R Core Team. R: A language and environment for statistical computing. R Foundation for Statistical Computing. Vienna, Austria. 2013. URL http://www.R-project.org/.
15. Wickham H. ggplot2: Elegant Graphics for Data Analysis. New York: Springer-Verlag, 2016. Retrieved from https://ggplot2.tidyverse.org.
16. Gupta NT, Vander Heiden JA, Uduman M, Gadala-Maria D, Yaar G, Kleinstein SH. Change-O: a toolkit for analyzing large-scale B cell immunoglobulin repertoire sequencing data. Bioinformatics. 2015; 31 (20): 3356–8. DOI: 10.1093/bioinformatics/btv359.
17. Sudhir Kumar, Glen Stecher, Koichiro Tamura. MEGA7: Molecular Evolutionary Genetics Analysis Version 7.0 for Bigger Datasets, Molecular Biology and Evolution. 2016; 33 (7): 1870–4. https://doi.org/10.1093/molbev/msw054.
18. Looney TJ, Lee JY, Roskin KM, Hoh RA, King J, Glanville J, et al. Human B-cell isotype switching origins of IgE. Journal of Allergy and Clinical Immunology. 2016; 137 (2): 579–86. https://doi.org/10.1016/j.jaci.2015.07.014.
19. Horst A, Hunzelmann N, Arce S, Herber M, Manz RA, Radbruch A, et al. Detection and characterization of plasma cells in peripheral blood: Correlation of IgE$^+$ plasma cell frequency with IgE serum titre. Clinical and Experimental Immunology. 2002; 130 (3): 370–8. https://doi.org/10.1046/j.1365-2249.2002.02025.x.

THE ACCURACY OF PREDICTING EYE AND HAIR PIGMENTATION BASED ON GENETIC MARKERS IN RUSSIAN POPULATIONS

Balanovsky OP[1,2,3], Petrushenko VS[1,2,4], Gorin IO[1,2,4], Kagazezheva ZhA[1,2], Markina NV[2], Kostryukova ES[5], Leybova NA[6], Maurer AM[7], Balanovska EV[1,3] ✉

[1] Research Centre for Medical Genetics, Moscow, Russia
[2] Vavilov Institute of General Genetics, Moscow, Russia
[3] Biobank of North Eurasia, Moscow, Russia
[4] Moscow Institute of Physics and Technology, Moscow, Russia
[5] Federal Research and Clinical Center of Physical-Chemical Medicine, Moscow, Russia
[6] Institute of Anthropology and Ethnography, Moscow, Russia
[7] Anuchin Research Institute and Museum of Anthropology, Moscow, Russia

Prediction of eye and hair color from DNA is being increasingly employed in forensic medicine and the studies of ancient populations. HIrisPlex-S is a prediction tool that was developed using the data collected from Dutch donors and verified for some other European populations. The accuracy of its predictions for other world populations has not been studied yet. Unlike the majority of other world populations, Russian populations are characterized not only by dark but also by light color eyes and hair and therefore pose a special interest in this respect. The aim of this work was to determine the accuracy of eye and hair color predictions for Russian populations. We studied 144 representatives of indigenous populations of Russia (Avars, Aleuts, Buryats, Itelmens, Karelians, Koryaks, Maris, Nanais, Russians, Rutulians, Chuvashes, Chukchi, Evenks, and Evens). Anthropological photos were taken of all individuals. Based on the photos, the anthropologists identified eye and hair color phenotypes. SNP-markers were genotyped using the HIrisPlex panel. Based on the genotypes, the phenotypes were predicted and subsequently compared to the actual phenotypes. We obtained a series of HIrisPlex accuracy indicators for the populations inhabiting the European part of Russia and Siberia. On the whole, prediction accuracy was satisfactory, although a bit lower than for West European populations. Further research could look for additional markers increasing the accuracy of predictions for Russian populations.

Keywords: eye color, hair color, genetic markers, prediction, gene pool, indigenous people, HIrisPlex-S

Funding: the study was supported by the Ministry of Science and Education of the Russian Federation (State contract 011–17 dated 26.09.2017) as part of the Union State Research and Technical Project *DNA-based identification*, which included genotyping and phenotyping of European samples and preparation of this manuscript, and the State assignment of the Ministry of Science and Higher Education of the Russian Federation for the Research Centre for Medical Genetics (phenotyping of Siberian samples, creating a database, data analysis).

Acknowledgements: we thank all donors participating in our study. DNA samples and anthropological images were provided by the Biobank of North Eurasia.

Author contribution: Balanovska EV — supervision and study design; Petrushenko VS, Gorin IO — bioinformatic analysis, literature analysis, manuscript preparation; Maurer AM, Leybova NA — phenotyping of the samples; Kagazezheva ZhA — phenotyping of the samples, photography, photo processing, tabular data processing; Balanovsky OP, Markina NV — manuscript preparation; Kostryukova ES — genotyping.

Compliance with ethical standards: the study was approved by the Ethics Committee of the Research Centre for Medical Genetics (Protocol No 3/1 dated September 5, 2018). The samples used in this work were obtained from a population genetic study. Informed consent was obtained from all study participants.

✉ **Correspondence should be addressed:** Elena V. Balanovska
Moskvorechie, 1, Research Centre for Medical Genetics, Moscow, 115522; balanovska@mail.ru

Received: 22.10.2019 **Accepted:** 26.10.2019 **Published online:** 28.10.2019
DOI: 10.24075/brsmu.2019.069

ТОЧНОСТЬ ПРЕДИКЦИИ ПИГМЕНТАЦИИ ВОЛОС И ГЛАЗ ПО ГЕНЕТИЧЕСКИМ МАРКЕРАМ ДЛЯ ПОПУЛЯЦИЙ РОССИИ

О. П. Балановский[1,2,3], В. С. Петрушенко[1,2,4], И. О. Горин[1,2,4], Ж. А. Кагазежева[1,2], Н. В. Маркина[2], Е. С Кострюкова[5], Н. А. Лейбова[6], А. М. Маурер[7], Е. В. Балановская[1,3] ✉

[1] Медико-генетический научный центр, Москва, Россия
[2] Институт общей генетики имени Н. И. Вавилова Российской академии наук, Москва, Россия
[3] Биобанк Северной Евразии, Москва, Россия
[4] Московский физико-технический институт (Научно-исследовательский университет), Москва, Россия
[5] Федеральный научно-клинический центр физико-химической медицины, Москва, Россия
[6] Институт этнологии и антропологии Российской академии наук, Москва, Россия
[7] Научно-исследовательский институт и музей антропологии имени Д. Н. Анучина, Москва, Россия

Предикция цвета глаз и волос по генотипу становится распространенным инструментом в судебно-медицинской экспертизе и в исследованиях древних популяций. Для этого широко используется панель HIrisPlex-S, разработанная на выборке голландцев и верифицированная для некоторых других популяций Западной Европы. Однако точность ее предсказаний для представителей других регионов мира не изучена. Особый интерес представляют популяции России, в которых (в отличие от большинства других популяций мира) присутствуют не только темные, но и светлые оттенки цвета волос и глаз. Целью работы было определить точность предикции цвета глаз и волос для популяций России. Мы изучили 144 представителя коренного населения России (аварцев, алеутов, бурят, ительменов, карел, коряков, марийцев, нанайцев, русских, рутульцев, чувашей, чукчей, эвенков, эвенов). Для всех индивидов были сделаны антропологические фотографии. На основании фотографий эксперты-антропологи проводили определение цвета глаз и волос. Для тех же индивидов проводили генотипирование SNP-маркеров панели HIrisPlex. На основании генотипов предсказывали фенотипы и предсказанные фенотипы сопоставляли с реальными. Получена серия показателей точности HIrisPlex для популяций Европейской части России и Сибири. В целом точность оказалась удовлетворительной, хотя и несколько сниженной по сравнению с точностью для популяций Западной Европы. В будущих исследованиях возможно провести поиск дополнительных маркеров, повышающих точность предикции для популяций России.

Ключевые слова: цвет глаз, цвет волос, генетические маркеры, предикция, генофонд, коренное население, HIrisPlex-S

Финансирование: исследование выполнено при финансовой поддержке Министерства науки и образования РФ (Госконтракт № 011–17 от 26.09.2017) в рамках научно-технической программы Союзного государства «ДНК-идентификация» (работы по генотипированию, по фенотипированию европейских образцов, подготовке текста статьи) и Государственного задания Министерства науки и высшего образования РФ для Медико-генетического научного центра им. академика Н. П. Бочкова (работы по фенотипированию сибирских образцов, созданию базы данных, анализу данных).

Благодарности: благодарим всех доноров образцов. Коллекция ДНК и антропологических фотографий предоставлена АНО «Биобанк Северной Евразии».

Информация о вкладе авторов: Е. В. Балановская — дизайн и руководство исследованием; В. С. Петрушенко и И. О. Горин — биоинформатический анализ и анализ литературы, написание текста статьи; А. М. Маурер, Н. А. Лейбова — фенотипирование образцов; Ж. А. Кагазежева — фенотипирование образцов, фотографирование и обработка фотографий, работа с табличными данными; О. П. Балановский и Н. В. Маркина — написание текста статьи; Е. С. Кострюкова — генотипирование.

Соблюдение этических стандартов: исследование одобрено этическим комитетом Медико-генетического научного центра (протокол № 3/1 от 5 сентября 2018 г.), выполнено на образцах, полученных в ходе популяционно-генетического обследования генофонда; все обследуемые подписали добровольное информированное согласие.

✉ **Для корреспонденции:** Елена Владимировна Балановская
ул. Москворечье, д. 1, Медико-генетический научный центр, г. Москва, 115522; balanovska@mail.ru

Статья получена: 22.10.2019 **Статья принята к печати:** 26.10.2019 **Опубликована онлайн:** 28.10.2019
DOI: 10.24075/vrgmu.2019.069

In the last decade, prediction of eye and hair color from DNA has paved its way into forensic medicine and population genetics. Today, it is possible to predict the physical appearance of an unknown person from their biological sample. Phenotype prediction is used to help crime investigations, identify disaster victims, study DNA samples of ancient populations, conduct genetic genealogy analysis, etc. So far, there have been abounding studies [1–10] that have identified a number of key genes and genetic sites involved in pigmentation. The most critical of them were included in the HIrisPlex panel and its expanded version HIrisPlex-S [8–11]. Genotyping of 25 DNA markers (SNPs and indels) included in HIrisPlex [10] helps to rapidly and reliably predict eye and hair color; HIrisPlex-S analyzes these 25 polymorphisms + 16 more predictive of skin color.

Original publications on HIrisPlex [8–11] demonstrate that the system generates reliable results for European populations. HIrisPlex was developed using European datasets, primarily Dutch, and verified in Polish, Greek and Irish populations. The accuracy of HIrisPlex-based prediction has not been tested yet in the populations inhabiting other parts of the world. Because the majority of non-Europeans have dark eyes and dark hair, such tests will not have any informative value in most other non-European continents. However, in some populations living on the border between Europe and Asia (Altai region, the Caucasus, regions to the East of the Ural Mountains), both dark and light hair/eye phenotypes are common. Genetically, such individuals can significantly differ from Western Europeans [12]; this means that the range of genetic markers determining their hair/eye pigmentation may also be different. Even populations of the Ural region, which are genetically closer to Western Europeans than to the inhabitants of the Caucasus and Western Siberia, are more genetically distant from the Dutch as compared to Irish, Polish and Greek populations, whose specimens were used for HIrisPlex verification.

The aim of this work was to evaluate predictive power of HIrisPlex-S for eye and hair color prediction for the populations of North Eurasia using biological samples and photos of indigenous peoples taken during our expedition fieldwork.

METHODS

Sample collection and phenotyping

As part of the field study of gene pools conducted by our team [13], we took images of the indigenous populations of Russia and bordering countries. The populations included in the study were examined during a few expeditions in 2015-2019. The following inclusion criteria were applied: 1) age over 18 years; 2) 4 ancestors (two grandfathers and 2 grandmothers) identifying themselves as belonging to the studied ethnic group; 3) the anthropological image of a participant; 4) written informed consent to participate. Exclusion criteria were as follows: 1) the lack of enough images preventing reliable identification of eye and hair color; 2) incomplete profile of the genotyped markers.

The study was carried out in 144 individuals representing the following populations:

1) European Russia — Russian, Mari, Chuvash, Karelian, Rutulian, Avar (n = 66, 65 males and 1 female);

2) Siberia and Far East — Buryat, Evenk, Even, Nanai, Koryak, Itelmen, Chukchi, Aleut (n = 78, 45 males and 33 females).

Eye/hair color was identified from the obtained photos by 3 experts; 2 of the experts were physical anthropologists with extensive experience in phenotyping; the other one was a geneticist specially trained in phenotyping. The experts worked independently. If the results were inconsistent with each other, the phenotyping procedure was repeated: this time, the experts worked together in order to reach a consensus. Eye color (dark, blue or intermediate) was successfully determined for 144 study participants. Hair color identification was successful in fewer cases because it was impossible to tell the natural hair color of most women from the photos and because some men had grey hair or were bald. Phenotyping results are shown in Table 1.

Genotyping and prediction of eye and hair color from genotypes

DNA was isolated from blood/saliva samples by classic phenol-chloroform extraction [14]. Genotyping was done using an Infinium Omni5Exome-4 v1.3 BeadChip kit (Illumina; USA) and an iScan array scanner. The quality of genotyping data was analyzed in GenomeStudio v2.0 (Illumina; USA). For all samples, the call rate (CR) was over 0.99, suggesting that the obtained data were suitable for further analysis. The BeadChip array can genotype over 4 million SNPs; the data it generates can be used in a variety of different studies. Genotypes matching 29 markers for eye/hair/skin color prediction included in the HirisPlex panel were extracted from the obtained array of genotyping data. The HIrisPlex-S panel contains a total of 25 predictive DNA markers for eye/hair color and 16 DNA markers for skin color. Of them, we successfully genotyped 19 markers of eye/hair color and 10 markers of skin color. The HIrisPlex panel allows prediction from a partial genotyping profile (a few obligatory markers are critical, others merely improve the accuracy of prediction), therefore a set of 19 out of 25 markers is sufficient to achieve good quality of prediction with HIrisPlex (predictive markers of skin color were not accounted for in our study). Nevertheless, clarification should be provided about the excluded marker rs312262906. Without it, predictions were generated only for eye color but not for hair color. The rs312262906 polymorphism causes a reading frame shift in the MC1R gene and is associated with red hair color. According to ExAC, the frequency of this polymorphism reaches 0.0038 in European populations and is 0.0000 (< 0.0001) in Asian populations; therefore, the probability of occurrence of at least 2 alternative alleles in our sample was negligible. This allowed us to assign the 0/0 genotype to this marker for all samples in order to predict hair color.

Genotypes were shortlisted using PLINK 1.9 [15]. The obtained genotypes are presented in Table 2.

HIrisPlex-S and the online webtool of the Department of Genetic Identification (Erasmus MC) [16] generated predictions for eye color (light, intermediate, or dark) and hair color (red, light, intermediate, or dark) for all the samples.

Evaluation of eye/hair color prediction accuracy

Phenotypes predicted by HIrisPlex from the obtained genotypes were compared to the actual phenotypes identified by the anthropologists from the images taken during our expeditions; quality metrics were calculated for all 144 samples. The constructed 5-grade scales for eye/hair pigmentation were converted into conventional 3-grade scales in order to make phenotyping results suitable for comparison with HIrisPlex-S data.

To analyze the accuracy of HIrisPlex-S-based predictions, the following quality metrics were calculated:

– precision (the ratio of true positives to the total number of positive predictions);

Table 1. Phenotypes (eye and hair color) identified from anthropological images

Sample	Metapopulation	Ethnicity	Sex	Age at the time of sample	Hair color	Eye color
FES-0001	Siberia	evenk	m	63	not analyzed	dark
FES-0002	Siberia	nanai	m	33	dark	dark
FES-0003	Siberia	nanai	m	42	dark	dark
FES-0004	Siberia	nanai	m	29	dark	dark
FES-0005	Siberia	nanai	m	58	dark	dark
FES-0006	Siberia	nanai	m	62	dark	light
FES-0007	Siberia	nanai	m	68	dark	dark
FES-0008	Siberia	nanai	m	64	not analyzed	dark
FES-0009	Siberia	nanai	m	52	dark	dark
FES-0010	Siberia	nanai	m	55	dark	dark
FES-0011	Siberia	nanai	m	46	not analyzed	dark
FES-0012	Siberia	nanai	m	51	dark	dark
FES-0013	Siberia	even	m	52	intermediate	light
FES-0014	Siberia	even	m	21	dark	light
FES-0015	Siberia	even	m	39	dark	dark
FES-0016	Siberia	even	m	21	dark	dark
FES-0017	Siberia	even	m	20	dark	dark
FES-0018	European Russia	bashkir	m	64	not analyzed	dark
FES-0019	Siberia	buryat	m	76	not analyzed	dark
FES-0020	Siberia	buryat	m	68	not analyzed	dark
FES-0021	Siberia	buryat	m	50	dark	dark
FES-0022	Siberia	buryat	m	68	dark	dark
FES-0023	European Russia	chuvash	m	33	intermediate	light
FES-0024	European Russia	chuvash	m	51	blond	light
FES-0025	European Russia	chuvash	m	53	intermediate	light
FES-0026	European Russia	chuvash	m	42	dark	light
FES-0027	European Russia	chuvash	m	41	dark	dark
FES-0028	European Russia	chuvash	m	36	red	light
FES-0029	European Russia	chuvash	m	55	not analyzed	dark
FES-0030	European Russia	chuvash	m	45	dark	dark
FES-0031	European Russia	chuvash	m	33	red	dark
FES-0032	European Russia	chuvash	m	46	intermediate	dark
FES-0033	European Russia	chuvash	m	32	intermediate	dark
FES-0034	European Russia	chuvash	m	41	not analyzed	light
FES-0035	European Russia	chuvash	m	49	intermediate	dark
FES-0036	European Russia	chuvash	m	53	not analyzed	dark
FES-0037	European Russia	chuvash	m	46	intermediate	dark
FES-0038	European Russia	chuvash	m	57	dark	dark
FES-0039	European Russia	chuvash	m	42	not analyzed	light
FES-0040	European Russia	chuvash	m	47	red	light
FES-0041	European Russia	chuvash	m	23	intermediate	light
FES-0042	European Russia	avar	m	52	not analyzed	dark
FES-0043	European Russia	avar	m	55	not analyzed	light
FES-0044	European Russia	avar	m	20	intermediate	light
FES-0045	European Russia	rutulian	m	36	not analyzed	dark
FES-0046	European Russia	rutulian	m	38	dark	dark
FES-0047	European Russia	rutulian	m	83	not analyzed	dark
FES-0048	European Russia	rutulian	m	57	not analyzed	dark
FES-0049	European Russia	rutulian	m	55	dark	dark
FES-0050	European Russia	rutulian	m	56	dark	dark
FES-0051	European Russia	rutulian	m	65	not analyzed	dark
FES-0052	Siberia	even	f	46	not analyzed	dark

Continuation of Table 1

Sample	Metapopulation	Ethnicity	Sex	Age at the time of sample	Hair color	Eye color
FES-0053	Siberia	koryak	f	74	not analyzed	dark
FES-0054	Siberia	even	m	50	dark	dark
FES-0055	Siberia	even	f	18	not analyzed	dark
FES-0056	Siberia	even	f	56	not analyzed	dark
FES-0057	Siberia	even	f	51	not analyzed	dark
FES-0058	Siberia	chukchi	f	47	not analyzed	dark
FES-0059	Siberia	koryak	f	68	not analyzed	dark
FES-0060	Siberia	itelmen	f	56	not analyzed	dark
FES-0061	Siberia	koryak	f	56	not analyzed	dark
FES-0062	Siberia	koryak	f	34	not analyzed	dark
FES-0063	Siberia	even	m	63	not analyzed	dark
FES-0064	Siberia	even	f	66	not analyzed	dark
FES-0065	Siberia	kamchadal	f	82	not analyzed	dark
FES-0066	Siberia	itelmen	m	62	intermediate	dark
FES-0067	Siberia	itelmen	f	53	not analyzed	dark
FES-0068	Siberia	aleut	f	66	not analyzed	dark
FES-0069	Siberia	aleut	f	35	not analyzed	dark
FES-0070	Siberia	aleut	m	42	dark	dark
FES-0071	Siberia	aleut	f	72	not analyzed	dark
FES-0072	Siberia	aleut	f	69	not analyzed	dark
FES-0073	Siberia	aleut	m	63	dark	dark
FES-0074	Siberia	aleut	f	53	not analyzed	dark
FES-0075	Siberia	koryak	m	59	not analyzed	dark
FES-0076	Siberia	koryak	m	62	dark	dark
FES-0077	Siberia	chukchi	f	69	not analyzed	dark
FES-0078	Siberia	koryak	m	69	dark	dark
FES-0079	Siberia	koryak	m	43	dark	light
FES-0080	Siberia	koryak	m	55	dark	dark
FES-0081	Siberia	koryak	f	52	not analyzed	dark
FES-0082	Siberia	koryak	f	55	not analyzed	dark
FES-0083	Siberia	even	f	55	not analyzed	dark
FES-0084	Siberia	koryak	f	57	not analyzed	dark
FES-0085	Siberia	chukchi	m	27	dark	dark
FES-0086	Siberia	even	m	48	not analyzed	light
FES-0087	Siberia	chukchi	m	58	dark	dark
FES-0088	Siberia	chukchi	m	58	dark	dark
FES-0089	Siberia	chukchi	m	56	not analyzed	dark
FES-0090	Siberia	koryak	f	31	not analyzed	dark
FES-0091	Siberia	even	m	35	dark	dark
FES-0092	Siberia	chukchi	m	34	dark	dark
FES-0093	Siberia	itelmen	f	59	not analyzed	dark
FES-0094	Siberia	itelmen	f	58	not analyzed	dark
FES-0095	Siberia	itelmen	m	49	dark	dark
FES-0096	Siberia	itelmen	f	70	not analyzed	dark
FES-0097	Siberia	itelmen	m	38	dark	dark
FES-0098	Siberia	itelmen	f	60	not analyzed	dark
FES-0099	Siberia	itelmen	f	60	not analyzed	dark
FES-0100	Siberia	itelmen	m	20	dark	dark
FES-0101	Siberia	itelmen	f	55	not analyzed	dark
FES-0102	Siberia	itelmen	f	40	not analyzed	dark
FES-0103	Siberia	itelmen	m	39	dark	dark
FES-0104	Siberia	itelmen	f	56	not analyzed	dark

End of Table 1

Sample	Metapopulation	Ethnicity	Sex	Age at the time of sample	Hair color	Eye color
FES-0105	Siberia	itelmen	f	71	not analyzed	dark
FES-0106	Siberia	itelmen	m	59	not analyzed	dark
FES-0107	Siberia	itelmen	f	47	not analyzed	dark
FES-0108	Siberia	itelmen	m	58	dark	dark
FES-0109	European Russia	mari	m	64	not analyzed	dark
FES-0110	European Russia	mari	m	56	dark	light
FES-0111	European Russia	mari	m	59	not analyzed	dark
FES-0112	European Russia	mari	m	38	dark	light
FES-0113	European Russia	mari	m	49	intermediate	light
FES-0114	European Russia	mari	m	58	dark	dark
FES-0115	European Russia	mari	m	50	dark	light
FES-0116	European Russia	mari	m	54	dark	dark
FES-0117	European Russia	mari	m	46	dark	intermediate
FES-0118	European Russia	mari	m	45	dark	light
FES-0119	European Russia	mari	m	70	not analyzed	dark
FES-0120	European Russia	mari	m	66	dark	intermediate
FES-0121	European Russia	mari	m	66	not analyzed	light
FES-0122	European Russia	mari	m	23	red	intermediate
FES-0123	European Russia	mari	m	51	blond	intermediate
FES-0124	European Russia	mari	m	37	red	light
FES-0125	European Russia	mari	m	58	not analyzed	dark
FES-0126	European Russia	mari	m	64	intermediate	light
FES-0127	European Russia	mari	m	61	not analyzed	dark
FES-0128	European Russia	mari	m	57	intermediate	dark
FES-0129	European Russia	russian	m	59	dark	light
FES-0130	European Russia	russian	m	34	intermediate	light
FES-0131	European Russia	russian	m	34	dark	light
FES-0132	European Russia	russian	m	40	dark	dark
FES-0133	European Russia	russian	m	32	dark	light
FES-0134	European Russia	russian	m	52	intermediate	light
FES-0135	European Russia	russian	m	30	dark	dark
FES-0136	European Russia	russian	m	41	dark	light
FES-0137	European Russia	karelian	m	75	intermediate	light
FES-0138	European Russia	karelian	m	79	not analyzed	light
FES-0139	European Russia	karelian	m	70	not analyzed	light
FES-0140	European Russia	karelian	m	66	intermediate	light
FES-0141	European Russia	karelian	f	79	not analyzed	light
FES-0142	European Russia	karelian	m	68	dark	light
FES-0143	European Russia	karelian	m	59	not analyzed	light
FES-0144	European Russia	karelian	m	62	dark	light

– recall (the ratio of true positives to the sum of true positives and false negatives in the class);

– accuracy (the proportion of correct predictions);

– F_1 score (the harmonic mean of precision and recall),

– AUC (area under curve) for ROC-curves (the true positive rate plotted against the false-positive rate at various threshold settings).

Quality metrics values are provided in Tables 3 and 4.

RESULTS

We photographed 144 representatives of the indigenous populations inhabiting European Russia and Siberia. Their DNA samples were genotyped for the markers included in the HirisPlex panel. Phenotyping and genotyping data obtained for each study participant were saved to a combined database.

To evaluate the quality of eye/hair color prediction by HIrisPlex-S in new populations phenotyped in advance, we predicted eye and hair color from their genotypes using the online webtool [16]. Results of eye color prediction for each individual case are shown in Table 5. Tables 1 and 5 allow comparing the observed and predicted phenotypes for each individual sample. Prediction quality metrics for the entire dataset are provided in Table 3.

In our study, AUC values, the most widely used quality metric, ranged between 0.89 and 0.59 for different phenotypic classes, averaging 0.79. For Russian populations, AUC values

Table 2. Genotypes of markers included in the HIrisPlex panel for eye and hair color prediction

RS	rs11547464	rs1805005	rs1805006	rs1805007	rs2228479	rs1110400	rs28777	rs12821256	rs4959270	rs12203592	rs1042602	rs1800407	rs2402130	rs12913832
Color prediction	Eyes and hair	Eyes and hair	Eyes and hair	Eyes and hair	Eyes and hair	Eyes and hair	Eyes and hair	Eyes and hair	Eyes and hair	Eyes and hair	Eyes and hair	Eyes and hair	Eyes and hair	Eyes and hair
CHROM	16	16	16	16	16	16	5	12	6	6	11	15	14	15
POS	89986091	89985844	89985918	89986117	89985940	89986130	33958959	89328335	457748	396321	88911696	28230318	92801203	28365618
REF	G	C	C	G	G	A	C	A	C	G	C	G	A	A
ALT	A	A	A	A	A	G	A	G	A	A	A	A	G	G
FES-0001	0/0	0/1	0/0	0/0	0/0	0/0	0/0	0/0	0/0	0/0	0/0	0/0	0/0	0/0
FES-0002	0/0	0/0	0/0	0/0	0/0	0/0	0/0	0/0	1/1	0/0	0/0	0/0	0/0	0/0
FES-0003	0/0	0/0	0/0	0/0	0/0	0/0	0/0	0/0	0/0	0/0	0/0	0/0	0/0	0/0
FES-0004	0/0	0/0	0/0	0/0	0/0	0/0	0/0	0/0	0/0	0/0	0/0	0/0	0/0	0/0
FES-0005	0/0	0/0	0/0	0/0	0/0	0/0	0/0	0/0	0/0	0/0	0/0	0/0	0/1	0/1
FES-0006	0/0	0/0	0/0	0/0	0/0	0/0	0/0	0/0	0/0	0/0	0/0	0/0	0/0	0/1
FES-0007	./.	0/1	0/0	./.	0/1	0/0	0/0	0/0	0/0	0/0	0/0	0/0	0/0	0/0
FES-0008	0/0	0/0	0/0	0/0	0/0	0/0	0/0	0/0	0/0	0/0	0/0	0/0	0/0	0/0
FES-0009	0/0	0/0	0/0	0/0	0/0	0/0	0/0	0/0	0/0	0/0	0/0	0/0	0/0	0/0
FES-0010	0/0	0/0	0/0	0/0	0/0	0/0	0/0	0/0	0/0	0/0	0/0	0/0	0/0	0/0
FES-0011	0/0	0/0	0/0	0/0	0/0	0/0	0/0	0/0	0/1	0/0	0/0	0/0	0/0	0/0
FES-0012	0/0	0/0	0/0	0/0	0/1	0/0	0/0	0/0	1/1	0/0	0/0	0/0	0/0	0/0
FES-0013	0/0	0/0	0/0	0/0	0/0	0/0	0/0	0/0	0/1	0/0	0/0	0/0	0/0	0/0
FES-0014	0/0	0/0	0/0	0/0	0/1	0/0	0/0	0/0	0/1	0/0	0/0	0/0	0/1	0/0
FES-0015	0/0	0/0	0/0	0/0	0/0	0/0	0/0	0/0	1/1	0/0	0/0	0/0	0/1	0/0
FES-0016	0/0	0/0	0/0	0/0	0/1	0/0	0/0	0/0	0/1	0/0	0/0	0/0	0/1	0/0
FES-0017	0/0	0/0	0/0	0/0	0/1	0/0	0/0	0/0	0/0	0/0	0/0	0/0	0/1	0/0
FES-0018	0/0	0/0	0/0	0/0	0/0	0/0	0/1	0/0	0/0	0/0	1/1	0/0	0/0	0/1
FES-0019	0/0	0/0	0/0	0/0	0/0	0/0	0/1	0/0	0/1	0/0	0/0	0/0	0/0	0/0
FES-0020	0/0	0/0	0/0	0/0	0/1	0/0	0/0	0/0	1/1	0/1	0/0	0/0	0/0	0/0
FES-0021	0/0	0/0	0/0	0/0	0/0	0/0	0/0	0/0	0/1	0/0	0/0	0/0	0/0	0/0
FES-0022	0/0	0/0	0/0	0/0	0/0	0/0	0/1	0/0	0/1	0/0	0/0	0/0	0/0	0/0
FES-0023	0/0	0/0	0/0	0/0	0/0	0/0	1/1	0/0	1/1	0/1	0/1	0/0	0/1	0/1
FES-0024	0/0	0/0	0/0	0/0	0/0	0/0	1/1	0/1	0/0	0/0	0/1	0/0	0/0	1/1
FES-0025	0/0	0/0	0/0	0/1	0/0	0/0	1/1	0/0	0/1	0/1	0/0	0/0	0/0	0/1
FES-0026	0/0	0/0	0/0	0/0	0/0	0/0	1/1	0/0	0/0	0/0	0/1	0/0	0/1	1/1
FES-0027	0/0	0/0	0/0	0/0	0/0	0/0	0/1	0/1	0/0	0/0	0/0	./.	0/0	0/0
FES-0028	0/0	0/0	0/0	0/1	0/0	0/0	0/1	0/0	0/1	0/0	0/1	0/0	0/0	1/1
FES-0029	0/0	0/1	0/0	0/1	./.	0/0	./.	0/0	1/1	0/0	0/0	0/0	0/0	0/1
FES-0030	0/0	0/0	0/0	0/1	0/0	0/0	0/1	0/0	0/0	0/0	0/0	0/0	0/0	0/1
FES-0031	0/0	0/0	0/0	0/0	0/0	0/0	1/1	0/0	0/0	0/0	0/0	0/1	0/0	0/1
FES-0032	0/0	0/0	0/0	0/0	0/1	0/0	1/1	0/0	0/1	1/1	0/1	0/0	0/1	0/1
FES-0033	0/0	0/0	0/0	0/0	0/1	0/0	1/1	0/0	0/1	0/0	0/1	0/0	0/1	0/1
FES-0034	0/0	0/0	0/0	0/0	0/1	0/0	1/1	0/0	0/1	0/0	0/0	0/0	0/0	0/1
FES-0035	0/0	0/0	0/0	0/0	0/0	0/0	1/1	0/0	1/1	0/0	0/1	0/0	0/0	0/1
FES-0036	0/0	0/0	0/0	0/0	0/1	0/0	1/1	0/0	0/1	0/0	0/1	0/0	0/0	0/1
FES-0037	0/0	0/0	0/0	0/0	0/0	0/0	1/1	0/0	1/1	0/1	0/0	0/0	0/0	0/1
FES-0038	0/0	0/0	0/0	0/0	0/0	0/0	1/1	0/0	0/0	0/0	0/0	0/1	0/0	0/1
FES-0039	0/0	0/0	0/0	0/0	0/0	0/0	1/1	0/1	0/1	0/0	0/1	0/0	0/1	1/1
FES-0040	0/0	0/0	0/0	0/0	0/0	0/0	1/1	0/0	0/0	0/1	0/0	0/0	0/0	1/1
FES-0041	0/0	0/0	0/0	0/0	0/0	0/0	1/1	0/0	0/1	0/1	0/0	0/0	0/1	1/1
FES-0042	0/0	0/0	0/0	0/0	0/0	0/0	./.	0/0	1/1	0/0	0/1	0/0	0/0	0/1
FES-0043	0/0	0/0	0/0	0/0	0/0	0/0	1/1	0/0	0/0	0/0	0/0	0/1	0/1	0/1
FES-0044	0/0	0/0	0/0	0/0	0/0	0/0	1/1	0/0	0/0	0/0	0/1	0/0	0/1	1/1
FES-0045	0/0	0/0	0/0	0/0	0/0	0/0	1/1	0/0	0/0	0/0	0/1	0/0	0/1	0/0
FES-0046	0/0	0/0	0/0	0/0	0/1	0/0	0/1	0/1	1/1	0/0	0/1	0/0	0/0	0/0
FES-0047	0/0	0/1	0/0	0/0	0/0	0/0	1/1	0/0	0/1	0/0	0/0	0/0	0/1	0/1
FES-0048	0/0	0/0	0/0	0/0	0/0	0/0	1/1	0/0	0/1	0/1	0/0	0/1	0/1	0/1
FES-0049	0/0	0/0	0/0	0/0	0/0	0/0	./.	0/0	0/1	0/0	0/0	0/0	0/0	0/0
FES-0050	0/0	0/0	0/0	0/0	0/0	0/0	1/1	0/0	0/0	0/0	0/1	0/0	0/1	0/0
FES-0051	0/0	0/0	0/0	0/0	0/0	0/0	1/1	0/0	0/1	0/0	0/0	0/1	0/0	0/1
FES-0052	0/0	0/0	0/0	0/0	0/0	0/0	0/1	./.	0/0	0/0	0/0	0/0	0/0	0/0
FES-0053	0/0	0/0	0/0	0/0	0/0	0/0	0/1	./.	0/0	0/0	0/0	0/0	0/1	0/0

Continuation of Table 2

rs2378249	rs12896399	rs1393350	rs683	rs3114908	rs1800414	rs10756819	rs17128291	rs1129038	rs1667394	rs1126809	rs1470608	rs1426654	rs6059655	rs8051733
Eyes and hair	Eyes and hair	Eyes and hair	Eyes and hair	Eyes and hair	Skin	Skin	Skin	Skin	Skin	Skin	Skin	Skin	Skin	Skin
20	14	11	9	16	15	9	14	15	15	11	15	15	20	16
33218090	92773663	89011046	12709305	89383725	28197037	16858084	92882826	28356859	28530182	89017961	28288121	48426484	32665748	90024206
A	C	G	C	G	A	A	A	G	A	G	A	A	G	A
G	A	A	A	A	G	G	G	A	G	A	C	G	A	G
0/0	0/0	0/0	0/0	1/1	0/0	1/1	1/1	0/0	1/1	0/0	0/0	1/1	0/0	0/0
1/1	0/0	0/0	0/0	0/0	0/1	0/0	0/0	0/0	0/1	0/0	0/0	1/1	0/0	0/0
0/0	0/0	0/0	0/0	0/0	0/0	0/1	0/0	0/0	0/1	0/0	0/1	1/1	0/0	0/0
0/0	0/1	0/0	0/0	0/0	0/0	0/0	0/0	0/0	0/1	0/0	0/0	0/1	0/0	0/0
0/0	0/0	0/0	0/0	0/1	0/0	0/0	0/1	0/1	0/0	0/0	0/1	0/1	0/0	0/0
0/0	0/1	0/0	0/0	0/0	0/0	0/1	0/0	0/1	0/0	0/0	0/1	0/1	0/0	0/0
0/0	0/0	0/0	0/0	./.	./.	0/1	0/0	./.	0/1	./.	0/0	1/1	0/0	0/1
0/0	0/1	0/0	0/0	0/0	0/0	0/1	0/0	0/0	0/1	./.	0/0	1/1	0/0	0/0
0/0	0/1	0/0	0/0	0/0	0/0	0/0	0/0	0/0	1/1	./.	0/0	1/1	0/0	0/0
0/1	0/1	0/0	0/0	0/0	0/0	0/1	0/0	0/0	0/1	./.	0/0	1/1	0/0	0/0
0/1	0/1	0/0	0/0	0/0	0/0	0/0	0/0	0/0	0/1	./.	0/0	1/1	0/0	1/1
0/0	0/0	0/0	0/0	0/1	0/0	0/0	0/0	0/0	1/1	./.	0/0	1/1	0/0	0/1
0/1	0/1	0/0	0/1	0/1	0/0	0/0	0/0	0/0	0/1	0/0	0/0	1/1	0/0	0/0
0/0	0/1	0/0	0/0	0/1	0/0	0/0	0/0	0/0	0/1	0/0	0/0	1/1	0/0	0/1
0/1	0/0	0/0	0/0	0/1	0/0	0/1	0/1	0/0	0/1	0/0	0/0	1/1	0/0	0/0
0/1	0/1	0/0	0/0	0/1	0/0	0/0	0/0	0/0	0/1	0/0	0/1	1/1	0/0	0/1
0/1	0/0	0/0	0/0	0/0	0/0	1/1	0/0	0/0	0/0	0/0	0/0	1/1	0/0	0/1
0/0	0/0	0/0	0/1	1/1	0/0	0/1	0/0	0/1	0/1	./.	0/1	0/0	0/0	0/0
1/1	0/0	0/1	0/1	0/1	1/1	0/0	0/0	0/0	1/1	./.	0/0	0/1	0/0	0/0
0/1	0/0	0/0	0/0	0/1	0/0	0/1	0/0	0/0	0/0	./.	0/1	0/0	0/0	1/1
0/1	0/0	0/1	0/0	0/0	0/0	0/1	0/0	0/0	0/1	./.	0/0	0/1	0/0	0/0
0/1	0/0	0/0	0/0	1/1	0/0	0/1	0/0	0/0	0/1	./.	0/0	0/1	0/0	0/0
0/1	0/0	0/0	1/1	0/1	0/0	1/1	0/0	0/1	0/1	./.	1/1	0/0	0/0	0/0
0/0	0/0	0/1	1/1	0/1	0/0	1/1	0/0	1/1	0/0	./.	1/1	0/0	0/0	0/1
0/0	0/0	0/0	0/1	1/1	0/0	0/1	0/0	0/1	0/0	./.	0/1	0/1	0/0	1/1
0/0	0/0	0/1	0/1	0/0	0/0	0/1	0/1	1/1	0/0	./.	0/1	0/0	0/0	0/0
0/0	0/0	0/0	0/1	0/0	0/0	0/0	1/1	0/0	0/1	./.	0/1	0/0	0/0	0/0
0/1	1/1	0/0	0/1	0/1	0/0	0/1	0/1	1/1	0/0	./.	1/1	0/0	0/1	0/1
0/0	0/1	0/1	1/1	0/0	0/0	0/0	0/0	0/1	0/0	./.	./.	0/0	0/0	0/1
0/0	0/0	0/0	0/1	0/1	0/0	1/1	0/0	0/1	0/0	./.	0/1	0/1	0/0	0/1
0/0	0/0	0/0	1/1	0/0	0/0	0/0	0/0	0/1	0/1	./.	1/1	0/0	0/0	0/0
0/0	0/0	0/0	1/1	0/1	0/0	0/1	0/1	0/1	0/0	0/0	0/1	0/0	0/0	0/1
0/0	0/0	0/0	1/1	0/1	0/0	1/1	0/0	0/1	0/1	0/0	0/1	0/0	0/0	0/1
0/1	0/1	0/0	0/1	1/1	0/0	0/1	0/0	0/1	0/1	0/0	0/1	0/0	0/0	0/1
0/1	0/0	0/1	1/1	0/1	0/0	0/0	0/0	0/1	0/1	0/1	0/1	0/0	0/0	0/0
0/1	0/1	0/0	0/1	0/1	0/0	0/0	0/0	0/1	0/1	0/0	0/1	0/0	0/0	0/1
0/0	0/1	0/0	0/1	1/1	0/0	0/1	0/0	0/1	0/1	0/0	0/1	0/0	0/0	0/0
0/0	0/1	0/0	0/1	0/0	0/0	1/1	0/1	0/1	0/1	0/0	1/1	0/0	0/0	0/0
1/1	0/1	0/0	0/1	0/0	0/0	0/0	0/0	1/1	0/0	0/0	1/1	0/0	0/0	0/0
0/0	0/1	0/1	0/1	0/1	0/0	0/1	0/0	1/1	0/0	0/1	1/1	0/0	0/0	0/0
0/0	0/0	0/0	1/1	0/0	0/0	0/0	0/0	1/1	0/0	0/0	1/1	0/0	0/0	0/0
0/1	0/0	0/0	0/0	0/1	0/0	0/1	0/0	0/1	0/1	0/0	1/1	0/0	0/0	0/1
0/1	0/0	0/1	1/1	0/0	0/0	1/1	0/0	0/1	0/1	0/0	1/1	0/0	0/0	0/1
0/0	0/0	0/1	0/1	0/0	0/0	0/1	0/0	./.	0/0	0/0	0/1	0/0	0/0	0/0
0/0	0/0	0/0	0/1	0/0	0/0	1/1	0/0	0/0	1/1	0/0	0/0	0/0	0/0	0/0
0/0	0/0	0/0	1/1	0/0	0/0	0/0	0/0	0/0	0/0	0/0	0/1	0/0	0/0	1/1
0/0	0/0	0/1	0/1	0/1	0/0	0/1	0/0	0/1	0/1	0/0	0/1	0/0	0/0	0/0
0/0	0/0	0/0	0/1	0/0	0/0	0/1	0/0	0/1	0/1	0/0	1/1	0/0	0/0	0/0
0/1	0/0	0/0	0/0	0/0	0/0	0/0	0/0	./.	0/0	0/0	1/1	0/0	0/0	0/0
0/0	0/0	0/0	0/1	0/0	0/0	0/1	0/0	0/0	0/0	0/0	1/1	0/0	0/0	0/1
0/0	0/1	0/1	0/0	0/1	0/0	0/0	0/0	0/1	0/0	0/0	1/1	0/0	0/0	0/0
1/1	1/1	0/0	0/0	0/0	0/0	0/1	0/0	0/0	1/1	0/0	0/0	1/1	0/0	0/0
0/0	0/0	0/0	0/1	0/0	0/0	0/1	0/1	0/0	0/0	0/0	0/0	1/1	0/0	0/0

Continuation of Table 2

RS	rs11547464	rs1805005	rs1805006	rs1805007	rs2228479	rs1110400	rs28777	rs12821256	rs4959270	rs12203592	rs1042602	rs1800407	rs2402130	rs12913832
Color prediction	Eyes and hair	Eyes and hair	Eyes and hair	Eyes and hair	Eyes and hair	Eyes and hair	Eyes and hair	Eyes and hair	Eyes and hair	Eyes and hair	Eyes and hair	Eyes and hair	Eyes and hair	Eyes and hair
CHROM	16	16	16	16	16	16	5	12	6	6	11	15	14	15
POS	89986091	89985844	89985918	89986117	89985940	89986130	33958959	89328335	457748	396321	88911696	28230318	92801203	28365618
REF	G	C	C	G	G	A	C	A	C	G	C	G	A	A
ALT	A	A	A	A	A	G	A	G	A	A	A	A	G	G
FES-0054	0/0	0/0	0/0	0/0	0/1	0/0	0/0	./.	0/0	0/0	0/0	0/0	0/0	0/0
FES-0055	0/0	0/0	0/0	0/0	0/1	0/0	0/1	./.	0/1	0/1	0/0	0/0	0/1	0/0
FES-0056	0/0	0/0	0/0	0/0	0/0	0/0	0/0	./.	0/1	0/0	0/0	0/0	0/0	0/0
FES-0057	0/0	0/0	0/0	0/0	0/0	0/0	0/0	./.	0/1	0/0	0/0	0/0	0/0	0/0
FES-0058	0/0	0/0	0/0	0/0	0/0	0/0	0/1	./.	0/0	0/0	0/0	0/0	0/1	0/0
FES-0059	0/0	0/0	0/0	0/0	0/1	0/0	0/0	./.	1/1	0/0	0/0	0/0	0/0	0/0
FES-0060	0/0	0/0	0/0	0/0	0/0	0/0	0/0	./.	0/0	0/0	0/0	0/0	0/0	0/0
FES-0061	0/0	0/0	0/0	0/0	0/0	0/0	0/0	./.	0/0	0/0	0/0	0/0	0/0	0/0
FES-0062	0/0	0/0	0/0	0/0	0/1	0/0	0/0	./.	0/1	0/0	0/0	0/0	0/0	0/0
FES-0063	0/0	0/0	0/0	0/0	0/1	0/0	0/0	./.	0/0	0/0	0/0	0/0	0/0	0/0
FES-0064	0/0	0/0	0/0	0/0	0/1	0/0	0/0	./.	0/0	0/0	0/0	0/0	0/0	0/0
FES-0065	0/0	0/0	0/0	0/0	0/1	0/0	0/1	./.	0/0	0/0	0/0	0/0	0/0	0/1
FES-0066	0/0	0/0	0/0	0/0	0/0	0/0	1/1	./.	1/1	0/0	0/0	0/0	0/0	0/0
FES-0067	0/0	0/0	0/0	0/0	0/1	0/0	0/1	./.	0/0	0/0	0/0	0/0	0/0	0/0
FES-0068	0/0	0/0	0/0	0/0	0/0	0/0	1/1	./.	0/0	0/0	0/0	0/0	0/0	0/0
FES-0069	0/0	0/0	0/0	0/0	0/0	0/0	0/1	./.	1/1	0/0	0/1	0/0	0/0	1/1
FES-0070	0/0	0/0	0/0	0/0	0/1	0/0	0/0	./.	0/1	0/0	0/0	0/0	0/0	0/1
FES-0071	0/0	0/0	0/0	0/0	0/1	0/0	1/1	./.	0/1	0/0	0/0	0/0	0/1	0/1
FES-0072	0/0	0/0	0/0	0/0	0/0	0/0	1/1	./.	0/1	0/0	0/0	0/0	0/0	0/0
FES-0073	0/0	0/0	0/0	0/0	0/0	0/0	0/1	./.	0/1	0/0	0/0	0/0	0/1	0/1
FES-0074	0/0	0/0	0/0	0/0	0/0	0/0	1/1	./.	1/1	0/0	0/0	0/0	0/0	0/1
FES-0075	0/0	0/0	0/0	0/0	0/0	0/0	0/0	./.	0/0	0/0	0/0	0/0	0/0	0/0
FES-0076	0/0	0/0	0/0	0/0	0/1	0/0	0/0	./.	0/0	0/0	0/0	0/0	0/0	0/0
FES-0077	0/0	0/0	0/0	0/0	0/0	0/0	0/0	./.	0/1	0/0	0/0	0/0	0/0	0/0
FES-0078	0/0	0/0	0/0	0/0	0/0	0/0	0/0	./.	0/0	0/0	0/0	0/0	0/0	0/0
FES-0079	0/0	0/0	0/0	0/0	0/0	0/0	0/0	./.	0/0	0/0	0/0	0/0	0/1	0/0
FES-0080	0/0	./.	0/0	0/0	0/0	0/0	0/0	./.	0/1	0/0	0/0	0/0	0/0	0/0
FES-0081	0/0	0/0	0/0	0/0	0/0	0/0	0/0	./.	0/0	0/0	0/0	0/0	0/0	0/0
FES-0082	0/0	0/0	0/0	0/0	0/0	0/0	0/0	./.	0/1	0/0	0/0	0/0	0/0	0/0
FES-0083	0/0	0/0	0/0	0/0	1/1	0/0	0/0	0/0	0/1	0/0	0/0	0/0	0/1	0/0
FES-0084	0/0	0/0	0/0	0/0	0/0	0/0	0/1	0/0	0/0	0/0	0/1	0/0	0/0	0/0
FES-0085	0/0	0/0	0/0	0/0	0/0	0/0	0/1	0/0	0/1	0/0	0/0	0/0	0/0	0/0
FES-0086	0/0	0/0	0/0	0/0	0/0	0/0	0/0	0/0	0/1	0/0	0/0	0/0	0/0	0/0
FES-0087	0/0	0/0	0/0	0/0	0/0	0/0	0/1	0/0	1/1	0/0	0/0	0/0	0/0	0/0
FES-0088	0/0	0/0	0/0	0/0	0/0	0/0	1/1	0/0	0/0	0/0	0/0	0/0	0/0	0/0
FES-0089	0/0	0/0	0/0	0/0	0/0	0/0	0/1	0/0	0/0	0/0	0/0	0/0	0/0	0/0
FES-0090	0/0	0/0	0/0	0/0	./.	0/0	0/0	0/0	0/0	0/0	./.	0/0	0/0	0/0
FES-0091	0/0	0/0	0/0	0/0	0/1	0/0	0/0	0/0	1/1	0/1	0/0	0/0	0/0	0/1
FES-0092	0/0	0/0	0/0	0/0	0/0	0/0	1/1	0/0	0/0	0/0	0/0	0/0	0/0	0/0
FES-0093	0/0	0/0	0/0	0/0	0/1	0/0	0/1	0/0	1/1	0/0	0/1	0/0	0/0	0/0
FES-0094	0/0	0/0	0/0	0/0	0/0	0/0	0/0	0/0	1/1	0/0	0/0	0/0	0/0	0/0
FES-0095	0/0	0/0	0/0	0/0	0/0	0/0	0/0	0/0	0/0	0/0	0/0	0/0	0/0	0/0
FES-0096	0/0	0/0	0/0	0/0	0/1	0/0	0/0	0/0	0/0	0/0	0/0	0/0	0/1	0/0
FES-0097	0/0	0/0	0/0	0/0	0/1	0/0	0/0	0/0	0/0	0/0	0/0	0/0	0/0	0/0
FES-0098	0/0	0/0	0/0	0/0	0/0	0/0	0/0	0/0	1/1	0/0	0/0	0/0	0/0	0/0
FES-0099	0/0	0/0	0/0	0/0	0/0	0/0	0/1	0/0	0/0	0/0	0/0	0/0	0/0	0/0
FES-0100	0/0	0/0	0/0	0/0	0/0	0/0	0/0	0/0	0/1	0/0	0/0	0/0	0/1	0/1
FES-0101	0/0	0/0	0/0	0/0	0/0	0/0	0/0	0/0	0/1	0/0	0/0	0/0	0/0	0/0
FES-0102	0/0	0/0	0/0	0/0	0/1	0/0	0/0	0/0	0/1	0/0	0/0	0/0	0/0	0/0
FES-0103	0/0	0/0	0/0	0/0	0/1	0/0	0/1	0/0	0/1	0/0	0/0	0/0	0/1	0/0
FES-0104	0/0	0/0	0/0	0/0	0/0	0/0	0/1	0/0	0/0	0/0	0/0	0/0	0/0	0/0
FES-0105	0/0	0/0	0/0	0/0	0/0	0/0	0/0	0/0	0/0	0/0	0/0	0/0	0/0	0/0
FES-0106	0/0	0/0	0/0	0/0	0/0	0/0	0/0	0/0	0/0	0/0	0/0	0/0	0/0	0/0

Continuation of Table 2

rs2378249	rs12896399	rs1393350	rs683	rs3114908	rs1800414	rs10756819	rs17128291	rs1129038	rs1667394	rs1126809	rs1470608	rs1426654	rs6059655	rs8051733
Eyes and hair	Eyes and hair	Eyes and hair	Eyes and hair	Eyes and hair	Skin	Skin	Skin	Skin	Skin	Skin	Skin	Skin	Skin	Skin
20	14	11	9	16	15	9	14	15	15	11	15	15	20	16
33218090	92773663	89011046	12709305	89383725	28197037	16858084	92882826	28356859	28530182	89017961	28288121	48426484	32665748	90024206
A	C	G	C	G	A	A	A	G	A	G	A	A	G	A
G	A	A	A	A	G	G	G	A	G	A	C	G	A	G
0/1	0/0	0/0	0/0	0/0	0/0	0/1	0/1	0/0	1/1	0/0	0/0	0/1	0/0	0/1
0/0	0/0	0/0	0/0	0/0	0/0	1/1	0/0	0/0	1/1	0/0	0/0	1/1	0/0	0/1
0/1	0/1	0/0	0/0	0/0	0/0	0/0	0/0	0/0	0/1	0/0	0/0	1/1	0/0	0/0
0/0	1/1	0/0	0/0	0/1	0/0	0/1	0/1	0/0	1/1	0/0	0/0	0/1	0/0	0/0
0/0	0/1	0/0	0/0	0/0	0/0	0/0	0/1	0/0	0/1	0/0	0/1	0/1	0/0	0/0
0/1	0/0	0/0	0/0	0/0	0/0	1/1	0/0	0/0	1/1	0/0	0/0	1/1	0/0	0/1
0/0	1/1	0/0	0/1	1/1	0/0	0/0	0/0	0/0	0/1	0/0	0/0	1/1	0/0	0/0
0/1	1/1	0/0	0/0	0/0	0/0	0/0	0/0	0/0	1/1	0/0	0/0	./.	0/0	0/0
0/1	0/0	0/0	0/0	0/0	0/0	0/1	1/1	0/0	0/1	0/0	0/0	1/1	0/0	0/1
0/1	0/0	0/0	0/0	1/1	0/0	1/1	0/0	0/0	1/1	0/0	0/0	1/1	0/0	0/1
0/0	0/1	0/0	0/0	0/1	0/0	0/0	0/0	0/0	1/1	0/0	0/0	1/1	0/0	0/1
0/1	1/1	0/0	0/1	0/1	0/0	0/1	0/0	0/1	0/0	0/0	0/1	0/1	0/0	0/0
1/1	0/1	0/0	0/0	1/1	0/0	1/1	0/0	0/0	0/0	0/0	0/1	1/1	0/0	0/0
0/0	1/1	0/0	0/0	0/1	0/1	0/1	0/0	0/0	0/1	0/0	0/0	0/1	0/0	0/1
1/1	0/0	0/0	0/1	0/1	0/0	0/1	0/0	0/0	1/1	0/1	1/1	0/1	0/0	0/0
0/1	0/0	0/0	0/1	1/1	0/0	0/0	0/0	1/1	0/0	0/0	1/1	0/1	0/0	0/0
0/0	0/0	0/0	0/0	0/1	0/0	0/1	0/0	0/1	0/1	0/0	0/1	1/1	0/0	0/1
0/1	0/1	0/0	0/1	0/1	0/0	0/1	0/0	0/1	0/0	0/0	1/1	0/1	0/0	0/1
0/0	1/1	0/0	0/1	0/0	0/0	0/1	0/0	0/0	1/1	0/0	0/0	0/1	0/0	0/0
0/0	0/0	0/0	0/1	0/0	0/0	0/1	0/0	0/1	0/1	0/0	0/1	0/1	0/0	0/0
0/0	0/1	1/1	0/0	1/1	0/0	0/0	0/0	0/1	0/0	./.	1/1	0/0	0/0	0/0
0/0	0/0	0/0	0/0	0/1	0/0	0/0	0/0	0/0	0/0	0/0	0/0	1/1	0/0	0/0
0/0	0/1	0/0	0/0	0/0	0/0	1/1	0/1	0/0	0/0	0/0	0/0	1/1	0/0	0/1
0/0	0/1	0/0	0/0	0/1	0/0	0/1	0/0	0/0	0/1	0/0	0/1	1/1	0/0	0/0
0/1	0/0	0/0	0/0	0/1	0/0	0/0	0/0	0/0	0/0	0/0	0/0	1/1	0/0	0/0
0/1	0/0	0/0	0/0	0/1	0/0	0/1	0/0	0/0	0/0	0/0	0/0	1/1	0/0	0/0
0/1	0/0	0/0	0/0	1/1	0/0	0/1	0/0	0/0	0/1	0/0	0/0	1/1	0/0	0/0
0/1	1/1	0/0	0/0	0/0	0/0	1/1	0/0	0/0	0/1	0/0	0/0	1/1	0/0	0/0
0/1	0/1	0/0	0/0	0/1	0/1	0/1	0/0	0/0	0/1	0/0	0/0	1/1	0/0	0/0
0/1	0/0	0/0	0/0	1/1	0/0	0/1	0/0	0/0	0/0	./.	0/0	1/1	0/0	1/1
0/0	0/1	0/0	0/1	0/0	0/0	0/0	0/0	0/0	0/1	./.	0/1	0/1	0/0	0/0
0/0	0/0	0/0	0/1	0/0	0/0	0/1	0/0	0/0	1/1	./.	0/0	0/1	0/0	0/0
0/1	0/1	0/0	0/0	0/0	0/0	1/1	0/0	0/0	1/1	./.	0/0	0/1	0/0	0/0
0/1	0/0	0/0	0/0	1/1	0/0	0/1	0/0	0/0	0/1	./.	0/1	1/1	0/0	0/0
0/0	0/1	0/0	0/0	0/1	0/1	0/0	0/1	0/0	0/1	./.	0/0	1/1	0/0	0/0
1/1	0/0	0/0	0/0	0/1	0/0	0/1	0/0	0/0	0/0	./.	0/0	0/1	0/0	0/0
0/0	0/1	0/0	0/0	0/0	0/0	0/0	0/0	0/0	0/1	./.	0/0	1/1	0/0	0/1
0/0	1/1	0/0	0/0	0/0	0/0	0/0	0/0	0/1	0/0	./.	0/1	0/1	0/0	0/0
0/0	0/1	0/0	0/0	0/1	0/0	0/1	0/0	0/0	0/1	./.	0/0	0/1	0/0	0/0
0/0	0/1	0/0	0/1	1/1	0/0	0/1	0/0	0/0	0/1	./.	0/0	1/1	0/0	0/1
0/0	1/1	0/0	0/1	0/0	0/0	0/1	0/0	0/0	0/1	./.	0/0	1/1	0/0	0/0
0/1	0/1	0/0	0/1	0/1	0/0	0/1	0/1	0/0	1/1	./.	0/0	1/1	0/0	0/0
0/0	0/1	0/0	0/0	0/1	0/0	0/1	0/0	0/0	0/0	./.	0/1	1/1	0/0	0/1
0/0	0/0	0/0	0/1	0/0	0/0	0/1	0/0	0/0	0/1	./.	0/0	1/1	0/0	0/1
0/1	1/1	0/0	0/0	0/0	0/0	1/1	0/0	0/0	1/1	./.	0/0	1/1	0/0	0/0
1/1	0/0	0/0	0/1	0/0	0/0	1/1	0/0	0/0	0/1	./.	0/0	1/1	0/0	0/0
1/1	0/1	0/0	0/1	0/0	0/0	1/1	0/1	0/1	0/0	./.	0/1	0/1	0/1	0/0
0/1	0/0	0/0	0/0	0/0	0/0	0/0	0/0	0/0	0/1	./.	0/1	1/1	0/0	0/0
0/1	0/1	0/0	0/1	0/0	0/0	0/1	0/0	0/0	1/1	./.	0/0	0/1	0/0	0/1
1/1	0/1	0/0	0/0	0/1	0/0	0/1	0/0	0/0	0/0	./.	0/0	1/1	0/1	0/1
0/1	0/1	0/0	0/0	0/1	0/0	0/1	0/0	0/0	0/0	./.	0/0	1/1	0/0	0/0
0/0	0/0	0/0	0/0	0/0	0/0	0/0	0/1	0/0	0/1	./.	0/0	1/1	0/0	0/0
0/0	0/0	0/0	0/1	0/1	0/0	0/0	0/0	0/0	0/1	./.	0/0	1/1	0/0	0/0

Continuation of Table 2

RS	rs11547464	rs1805005	rs1805006	rs1805007	rs2228479	rs1110400	rs28777	rs12821256	rs4959270	rs12203592	rs1042602	rs1800407	rs2402130	rs12913832
Color prediction	Eyes and hair	Eyes and hair	Eyes and hair	Eyes and hair	Eyes and hair	Eyes and hair	Eyes and hair	Eyes and hair	Eyes and hair	Eyes and hair	Eyes and hair	Eyes and hair	Eyes and hair	Eyes and hair
CHROM	16	16	16	16	16	16	5	12	6	6	11	15	14	15
POS	89986091	89985844	89985918	89986117	89985940	89986130	33958959	89328335	457748	396321	88911696	28230318	92801203	28365618
REF	G	C	C	G	G	A	C	A	C	G	C	G	A	A
ALT	A	A	A	A	A	G	A	G	A	A	A	A	G	G
FES-0107	0/0	0/0	0/0	0/0	0/1	0/0	0/1	0/0	0/0	0/0	0/0	0/0	0/0	0/0
FES-0108	0/0	0/0	0/0	0/0	0/1	0/0	0/0	0/0	0/1	0/0	0/0	0/0	0/1	0/0
FES-0109	0/0	0/0	0/0	0/1	0/0	0/0	0/1	0/0	0/1	0/0	0/1	0/0	0/0	0/0
FES-0110	0/0	0/0	0/0	0/0	0/0	0/0	0/1	0/0	0/1	0/0	0/1	0/0	0/0	0/1
FES-0111	0/0	0/0	0/0	0/0	0/0	0/0	1/1	0/0	0/1	0/1	0/0	0/0	0/0	0/1
FES-0112	0/0	0/0	0/0	0/0	0/0	0/0	0/1	0/0	0/0	0/0	0/0	0/0	0/0	0/1
FES-0113	0/0	0/0	0/0	0/0	0/1	0/0	0/1	0/0	0/0	0/0	0/0	0/0	0/0	0/1
FES-0114	0/0	0/0	0/0	0/0	0/0	0/0	1/1	0/0	0/1	0/0	0/1	0/0	0/0	0/1
FES-0115	0/0	0/0	0/0	0/0	0/1	0/0	0/1	0/0	0/0	0/0	0/0	0/0	0/0	0/1
FES-0116	0/0	0/0	0/0	0/0	0/0	0/0	0/1	0/1	0/1	0/1	0/1	0/0	0/0	0/0
FES-0117	0/0	0/0	0/0	0/0	0/0	0/0	1/1	0/0	1/1	0/0	0/0	0/0	0/0	0/1
FES-0118	0/0	0/0	0/0	0/0	0/1	0/0	0/1	0/0	0/0	0/0	0/0	0/0	0/1	1/1
FES-0119	0/0	0/1	0/0	0/0	0/1	0/0	1/1	0/0	0/1	0/1	0/1	0/1	0/0	0/0
FES-0120	0/0	0/0	0/0	0/0	0/0	0/0	0/1	0/0	0/0	0/0	0/0	0/0	0/0	1/1
FES-0121	0/0	0/0	0/0	0/0	0/0	0/0	1/1	0/0	1/1	0/0	0/0	0/0	0/0	1/1
FES-0122	0/0	0/0	0/0	0/0	1/1	0/0	1/1	0/0	0/1	0/0	0/0	0/0	0/0	0/1
FES-0123	0/0	0/0	0/0	0/0	0/0	0/0	1/1	0/0	0/1	0/0	1/1	0/0	0/0	0/1
FES-0124	0/0	0/0	0/0	0/0	0/1	0/0	1/1	0/0	0/0	0/0	0/1	0/0	0/0	1/1
FES-0125	0/0	0/0	0/0	0/0	0/1	0/0	1/1	0/0	0/1	0/0	0/1	0/0	0/0	0/1
FES-0126	0/1	0/1	./.	./.	0/1	0/0	0/1	0/0	0/0	0/0	0/0	0/0	0/0	0/1
FES-0127	0/0	0/0	0/0	0/0	0/1	0/0	0/1	0/1	0/0	0/0	0/0	0/0	0/0	0/0
FES-0128	0/0	0/0	0/0	0/0	0/0	0/0	1/1	0/0	0/0	0/0	1/1	0/0	0/0	0/1
FES-0129	0/0	0/0	0/0	0/0	0/0	0/1	0/1	./.	1/1	0/1	0/1	0/0	./.	1/1
FES-0130	0/0	0/0	0/0	0/0	0/0	0/0	1/1	0/0	1/1	0/0	0/0	0/0	0/0	1/1
FES-0131	0/0	0/0	0/0	0/0	0/0	0/0	1/1	0/0	0/1	0/0	0/1	0/1	0/0	1/1
FES-0132	0/0	0/0	0/0	0/0	0/0	0/0	0/1	0/0	0/0	0/0	0/0	0/0	0/0	0/1
FES-0133	0/0	0/0	0/0	0/0	0/0	0/0	0/1	0/0	0/0	0/0	0/1	0/0	0/0	1/1
FES-0134	0/0	0/0	0/0	0/0	0/0	0/0	1/1	0/0	0/0	0/0	0/1	0/0	0/1	1/1
FES-0135	1/1	1/1	1/1	0/1	./.	0/0	./.	0/0	./.	0/1	0/1	0/1	0/1	0/1
FES-0136	0/0	0/0	0/0	0/0	0/0	0/0	1/1	0/0	1/1	0/1	0/0	0/0	0/1	1/1
FES-0137	0/0	0/0	0/0	0/0	0/1	0/0	1/1	0/0	0/1	0/0	1/1	0/0	0/1	1/1
FES-0138	0/0	0/0	0/0	0/0	0/0	0/0	1/1	0/0	0/1	0/0	0/1	0/0	0/1	1/1
FES-0139	0/0	./.	0/0	0/0	0/0	0/0	1/1	0/0	0/1	0/0	0/0	0/0	0/0	1/1
FES-0140	0/0	0/0	0/0	0/0	0/1	0/0	1/1	0/0	0/1	0/0	0/1	0/0	0/0	1/1
FES-0141	0/0	0/0	0/0	0/0	0/1	0/0	1/1	0/1	0/1	0/1	0/1	0/1	0/0	1/1
FES-0142	0/0	0/0	0/0	0/1	0/0	0/0	1/1	0/0	0/1	0/1	0/1	0/1	0/0	1/1
FES-0143	0/0	0/0	0/0	0/0	0/0	0/0	1/1	0/0	0/0	0/0	0/0	0/0	0/0	1/1
FES-0144	0/0	0/0	0/0	0/0	0/0	0/0	1/1	0/0	0/1	0/0	0/0	0/0	0/0	1/1

are a bit lower than those observed in Western Europeans (0.89). For example, AUC for light eye color is 0.94 for Western Europeans vs 0.89 for Russians. A decrease in AUC values can be observed for all eye and hair color phenotypes represented in our study. Of note, prediction quality metrics for intermediate eye color and light hair color are not provided in this article because these 2 phenotypes were underrepresented in our sample. If necessary, they can be calculated using the data from Tables 1 and 5. Their values turned out to be even lower than in Western European populations, but due to a very small sample size of these 2 phenotypic classes (< 5 individuals), the obtained results cannot be considered reliable.

Russian populations are very heterogeneous genetically. We purposefully included genetically contrasting groups of indigenous populations of European Russia and Siberia in the sample. Table 4 describes the quality of eye color prediction by HIrisPlex for these 2 metapopulations (the quality of hair color prediction was not evaluated due to a small sample size, see Methods). The accuracy of eye color prediction for the populations of European Russia was close to the prediction accuracy for the pooled sample. There was some decline in accuracy, in comparison with Western European samples, but, on the whole, the accuracy of prediction was satisfactory (AUC about 0.8). For Siberian populations, prediction quality was much poorer (AUC = 0.6).

DISCUSSION

The collection of anthropological images of the indigenous peoples of Russia laid the foundation for our study. The photos

End of Table 2

rs2378249	rs12896399	rs1393350	rs683	rs3114908	rs1800414	rs10756819	rs17128291	rs1129038	rs1667394	rs1126809	rs1470608	rs1426654	rs6059655	rs8051733
Eyes and hair	Eyes and hair	Eyes and hair	Eyes and hair	Eyes and hair	Skin	Skin	Skin	Skin	Skin	Skin	Skin	Skin	Skin	Skin
20	14	11	9	16	15	9	14	15	15	11	15	15	20	16
33218090	92773663	89011046	12709305	89383725	28197037	16858084	92882826	28356859	28530182	89017961	28288121	48426484	32665748	90024206
A	C	G	C	G	A	A	A	G	A	G	A	A	G	A
G	A	A	A	A	G	G	G	A	G	A	C	G	A	G
1/1	1/1	0/0	0/0	0/0	0/0	0/1	0/0	0/0	0/1	./.	0/0	1/1	0/0	0/1
0/1	0/0	0/0	0/0	0/0	0/0	1/1	0/1	0/0	1/1	./.	0/1	0/1	0/0	0/0
0/0	0/0	0/0	0/0	0/1	0/0	1/1	0/1	0/0	1/1	0/0	0/0	0/0	0/0	0/1
0/0	0/0	0/0	0/0	0/1	0/0	0/0	0/0	0/1	0/1	0/0	0/1	0/0	0/0	0/0
0/0	0/0	0/0	1/1	0/0	0/0	0/1	0/0	0/1	0/1	0/0	0/1	0/1	0/0	0/1
0/0	0/0	0/0	0/1	0/0	0/0	0/1	0/0	0/1	0/0	0/0	1/1	0/0	0/0	0/0
0/0	0/1	0/1	1/1	0/1	0/0	0/0	0/0	0/1	0/1	0/1	0/1	0/0	0/0	0/1
0/0	0/1	0/0	0/1	1/1	0/0	1/1	0/0	0/1	0/0	0/0	0/1	0/0	0/0	0/0
0/0	0/1	0/1	1/1	0/1	0/0	0/0	0/0	0/1	0/1	0/1	0/1	0/0	0/0	0/1
0/1	0/1	0/0	0/1	0/0	0/0	0/1	0/0	0/0	1/1	0/0	0/0	0/0	0/0	0/1
0/0	0/0	0/0	0/1	0/1	0/0	0/0	0/0	0/1	0/0	0/0	0/1	0/0	0/0	0/1
0/1	0/0	0/1	1/1	0/0	0/0	0/0	0/1	1/1	0/0	0/1	1/1	0/0	0/0	0/1
0/0	0/0	0/0	1/1	0/1	0/0	0/0	0/0	0/0	1/1	0/0	0/1	1/1	0/1	0/0
0/0	0/0	0/1	0/0	0/0	0/0	0/1	0/0	1/1	0/0	0/1	1/1	0/0	0/0	0/0
0/0	1/1	0/1	0/1	0/0	0/0	0/0	0/0	1/1	0/0	0/1	1/1	0/0	0/0	1/1
0/0	0/0	0/0	0/1	0/1	0/0	0/0	0/0	0/1	0/0	0/0	0/1	0/0	0/0	1/1
0/0	0/1	0/0	0/1	1/1	0/0	0/1	0/0	0/1	0/1	0/0	0/1	0/0	0/0	0/1
0/1	1/1	0/0	0/0	0/1	0/0	0/0	0/1	1/1	0/0	0/0	1/1	0/0	0/1	0/1
0/1	0/0	0/0	0/1	0/1	0/0	0/0	0/0	0/1	0/0	0/0	0/1	0/0	0/0	1/1
0/0	0/0	0/1	./.	0/1	0/0	1/1	0/1	0/1	./.	0/1	./.	0/0	0/0	0/0
0/0	0/1	0/0	0/1	0/1	0/0	0/1	0/0	0/0	0/1	0/0	0/1	0/0	0/0	1/1
0/1	0/1	0/0	0/0	0/1	0/0	0/1	0/1	0/1	0/0	0/0	0/1	0/0	0/1	0/1
0/0	0/1	0/0	1/1	0/1	0/0	0/1	0/0	1/1	0/0	./.	1/1	0/0	./.	0/1
0/0	0/1	0/0	0/1	0/0	0/0	0/1	0/0	1/1	0/0	0/0	1/1	0/0	0/0	0/0
0/0	0/0	0/0	0/1	0/1	0/0	0/0	0/0	1/1	0/0	0/0	1/1	0/0	0/0	0/0
0/1	0/1	0/1	1/1	1/1	0/0	0/1	0/0	0/1	0/0	0/1	1/1	0/0	0/0	0/1
0/0	0/1	0/0	0/1	0/0	0/0	0/0	0/0	1/1	0/0	0/0	1/1	0/0	0/0	0/1
0/1	0/0	0/0	0/1	0/1	0/0	0/1	./.	1/1	0/0	0/0	1/1	0/0	0/0	0/0
0/1	0/1	0/1	0/1	./.	./.	./.	0/0	1/1	0/1	1/1	0/1	0/0	1/1	0/0
0/0	0/1	0/1	0/0	0/1	0/0	0/1	0/0	1/1	0/0	0/1	0/1	0/0	0/0	0/0
0/0	0/1	0/0	0/1	0/1	0/0	0/0	0/0	1/1	0/0	0/0	1/1	0/0	0/0	1/1
0/0	0/0	0/0	1/1	0/0	0/0	0/1	1/1	1/1	0/0	0/0	1/1	0/0	0/0	0/1
0/1	0/0	0/1	1/1	0/1	0/0	0/1	0/0	1/1	0/0	0/1	1/1	0/0	0/0	0/1
0/1	0/1	0/0	1/1	0/0	0/0	0/1	0/0	1/1	0/0	0/0	0/1	0/0	0/0	0/1
0/1	1/1	0/0	0/1	0/1	0/0	0/1	0/0	0/1	0/0	0/0	1/1	0/0	0/0	0/1
0/0	0/0	0/0	0/1	1/1	0/0	0/1	0/0	1/1	0/0	0/0	1/1	0/0	0/0	0/1
0/0	0/1	0/0	1/1	0/0	0/0	0/1	0/0	1/1	0/0	0/0	0/1	0/0	0/0	0/0
0/0	0/1	0/0	0/1	1/1	0/0	0/1	0/0	1/1	0/0	0/0	1/1	0/0	0/0	0/1

taken in 3 planes in accordance with anthropological standards are a valuable resource for research into the associations between phenotypic traits and genotypes. In this study, such images were used to identify eye and hair color. The fact that phenotyping was independently conducted by 3 different experts and the availability of photos for verification render the results of our study reliable and reproducible.

For genotyping, we used the most comprehensive, state-of-the art, popular HirisPlex-S system that has proven its accuracy in the studies of modern and ancient Western European populations [8, 11, 17]. HirisPlex-S prediction accuracy for the populations outside Western Europe was evaluated by comparing the observed phenotypes identified from the photos to the phenotypes predicted from DNA. Of all quality metrics (Table 3), AUC posed the greatest interest because AUC values characterizing HIrisPlex performance are available for Western European populations [16]. So, we were able to directly compare the accuracy of HIrisPlex predictions between Western European and Russian populations.

On the whole, the values of prediction quality metrics obtained for the majority of phenotypic classes (Table 3) were quite high (0.6–0.9), suggesting that use of HIrisPlex in Russian populations is justified. None of the systems predicting phenotypes from DNA is 100% accurate; for some classes, HIrisPlex prediction accuracy is below 0.9 even for Western European populations. In our opinion, this study has demonstrated the fitness of HIrisPlex for use in Russian populations and its satisfactory accuracy of prediction. However, HIrisPlex prediction accuracy is lower for Russian populations than for Western Europeans (0.8 vs 0.9 on average). Therefore,

Table 3. Parameters of prediction accuracy of HIrisPlex for Western European populations and Russia

	Western European populations	Russia			
	AUC	AUC	Precision	Accuracy	Recall
Light eye color	0.94	0.89	0.89	0.88	0.63
Intermediate eye color	0.74	–	–	–	–
Dark eye color	0.95	0.89	0.85	0.87	0.98
Red hair color	0.93	0.59	0.33	0.92	0.2
Blond hair color	0.81	–	–	–	–
Intermediate hair color	0.74	0.72	0.32	0.66	0.56
Dark hair color	0.86	0.84	0.94	0.68	0.57

Table 4. Prediction accuracy of HIrisPlex for Russian regions

	European Russia	Siberia
Light eyes	0.89	0.57
Dark eyes	0.86	0.56

we believe that HIrisPlex can be used in Russian populations but still recommend to account for the detected decline in accuracy when interpreting the obtained data.

In our study, Russian populations were divided into 2 datasets: European Russia and Siberia. Previous population genetic studies [18, 19] revealed that these metapopulations are contrasting in terms of their genetic origin. They also turned out to be contrasting in terms of phenotype prediction quality, which was considerably lower for Siberia (Table 4). The data in Tables 1 and 5 demonstrate that HIrisPlex predicts dark eyes for almost all Siberian samples, although some representatives of Siberian populations have light color eyes; the division into light and intermediate shades is arbitrary, but even so, the color of their eyes is not dark as predicted by HIrisPlex. Perhaps, light color eyes sometimes seen in indigenous Siberian populations is associated with other alleles or other genes, as compared to Europeans, meaning that the system based on Western European datasets cannot correctly predict light (not dark) color of eyes in those populations. A decrease in the prediction accuracy for the inhabitants of European Russia may have the same nature, but because this population is genetically closer to the populations of Western Europe, the differences in the allele spectrum and the decrease in prediction accuracy are not so pronounced. This can inspire new research aimed at identifying additional genetic markers that could improve the accuracy of prediction of pigmentation phenotypes from genotypes.

CONCLUSIONS

The analysis of correlations between genotypes and eye/hair pigmentation phenotypes of Russian populations aided by the widely used HIrisPlex-S panel confirmed its fitness for use in these

Table 5. Phenotypes (eye and hair color) predicted from genotypes included in the HIrisPlex panel

Sample	Predicted eye color	Predicted hair color
FES-0001	dark	not analyzed
FES-0002	dark	dark
FES-0003	dark	dark
FES-0004	dark	dark
FES-0005	dark	dark
FES-0006	dark	dark
FES-0007	dark	not predicted
FES-0008	dark	not analyzed
FES-0009	dark	dark
FES-0010	dark	dark
FES-0011	dark	not analyzed
FES-0012	dark	dark
FES-0013	dark	dark
FES-0014	dark	dark
FES-0015	dark	dark
FES-0016	dark	dark
FES-0017	dark	dark
FES-0018	dark	not analyzed
FES-0019	dark	not analyzed
FES-0020	dark	not analyzed

Continuation of Table 5

Sample	Predicted eye color	Predicted hair color
FES-0021	dark	dark
FES-0022	dark	dark
FES-0023	dark	intermediate
FES-0024	light	blond
FES-0025	dark	intermediate
FES-0026	light	blond
FES-0027	dark	intermediate
FES-0028	light	red
FES-0029	dark	not analyzed
FES-0030	dark	intermediate
FES-0031	dark	blond
FES-0032	dark	intermediate
FES-0033	dark	intermediate
FES-0034	dark	not analyzed
FES-0035	dark	intermediate
FES-0036	dark	not analyzed
FES-0037	dark	intermediate
FES-0038	dark	blond
FES-0039	light	not analyzed
FES-0040	light	intermediate
FES-0041	light	intermediate
FES-0042	dark	not analyzed
FES-0043	dark	not analyzed
FES-0044	light	blond
FES-0045	dark	not analyzed
FES-0046	dark	intermediate
FES-0047	dark	not analyzed
FES-0048	dark	not analyzed
FES-0049	dark	dark
FES-0050	dark	intermediate
FES-0051	dark	not analyzed
FES-0052	dark	not analyzed
FES-0053	dark	not analyzed
FES-0054	dark	dark
FES-0055	dark	not analyzed
FES-0056	dark	not analyzed
FES-0057	dark	not analyzed
FES-0058	dark	not analyzed
FES-0059	dark	not analyzed
FES-0060	dark	not analyzed
FES-0061	dark	not analyzed
FES-0062	dark	not analyzed
FES-0063	dark	not analyzed
FES-0064	dark	not analyzed
FES-0065	dark	not analyzed
FES-0066	dark	intermediate
FES-0067	dark	not analyzed
FES-0068	dark	not analyzed
FES-0069	light	not analyzed
FES-0070	dark	dark
FES-0071	dark	not analyzed

Continuation of Table 5

Sample	Predicted eye color	Predicted hair color
FES-0072	dark	not analyzed
FES-0073	dark	intermediate
FES-0074	dark	not analyzed
FES-0075	dark	not analyzed
FES-0076	dark	dark
FES-0077	dark	not analyzed
FES-0078	dark	dark
FES-0079	dark	dark
FES-0080	dark	dark
FES-0081	dark	not analyzed
FES-0082	dark	not analyzed
FES-0083	dark	not analyzed
FES-0084	dark	not analyzed
FES-0085	dark	dark
FES-0086	dark	not analyzed
FES-0087	dark	dark
FES-0088	dark	dark
FES-0089	dark	not analyzed
FES-0090	dark	not analyzed
FES-0091	dark	dark
FES-0092	dark	dark
FES-0093	dark	not analyzed
FES-0094	dark	not analyzed
FES-0095	dark	dark
FES-0096	dark	not analyzed
FES-0097	dark	dark
FES-0098	dark	not analyzed
FES-0099	dark	not analyzed
FES-0100	dark	intermediate
FES-0101	dark	not analyzed
FES-0102	dark	not analyzed
FES-0103	dark	dark
FES-0104	dark	not analyzed
FES-0105	dark	not analyzed
FES-0106	dark	not analyzed
FES-0107	dark	not analyzed
FES-0108	dark	dark
FES-0109	dark	not analyzed
FES-0110	dark	intermediate
FES-0111	dark	not analyzed
FES-0112	dark	intermediate
FES-0113	dark	dark
FES-0114	dark	intermediate
FES-0115	dark	dark
FES-0116	dark	intermediate
FES-0117	dark	intermediate
FES-0118	light	intermediate
FES-0119	dark	not analyzed
FES-0120	light	intermediate
FES-0121	light	not analyzed
FES-0122	dark	blond

End of Table 5

Sample	Predicted eye color	Predicted hair color
FES-0123	dark	intermediate
FES-0124	light	blond
FES-0125	dark	not analyzed
FES-0126	dark	not predicted
FES-0127	dark	not analyzed
FES-0128	dark	intermediate
FES-0129	light	intermediate
FES-0130	light	blond
FES-0131	light	blond
FES-0132	dark	intermediate
FES-0133	light	intermediate
FES-0134	light	blond
FES-0135	light	red
FES-0136	light	intermediate
FES-0137	light	blond
FES-0138	light	not analyzed
FES-0139	light	not analyzed
FES-0140	light	blond
FES-0141	light	not analyzed
FES-0142	light	red
FES-0143	light	not analyzed
FES-0144	light	blond

previously unstudied populations, although its prediction accuracy was lower than in Western European datasets that had served as a basis for this classifier. A decrease in accuracy (from 0.94 to 0.89) is not that dramatic for the populations of European Russia, as compared to Siberian samples. This decrease might be associated with an impact of population-specific SNPs well-represented in the populations of North Eurasia but rarely found in Western Europe and, therefore, not included in the HIrisPlex-S panel.

References

1. Bouakaze C, Keyser C, Crubezy E, Montagnon D, Ludes B. Pigment phenotype and biogeographical ancestry from ancient skeletal remains: inferences from multiplexed autosomal SNP analysis. Int J Legal Med. 2009; 123 (4): 315–25.
2. Branicki W, Brudnik U, Kupiec T, Wolanska-Nowak P, Szczerbinska A, Wojas-Pelc A. Association of polymorphic sites in the OCA2 gene with eye colour using the tree scanning method. Ann Hum Genet. 2008; 72 (Pt 2): 184–92.
3. Candille SI, Absher DM, Beleza S, Bauchet M, McEvoy B, Garrison NA, et al. Genome-wide association studies of quantitatively measured skin, hair, and eye pigmentation in four European populations. PLoS One. 2012; 7 (10): e48294.
4. Han J, Kraft P, Nan H, Guo Q, Chen C, Qureshi A, et al. A genome-wide association study identifies novel alleles associated with hair color and skin pigmentation. PLoS Genet. 2008; 4 (5): e1000074.
5. Lippert C, Sabatini R, Maher MC, Kang EY, Lee S, Arikan O, et al. Identification of individuals by trait prediction using whole-genome sequencing data. Proc Natl Acad Sci USA. 2017; 114 (38): 10166–71.
6. Liu F, van Duijn K, Vingerling JR, Hofman A, Uitterlinden AG, Janssens AC, et al. Eye color and the prediction of complex phenotypes from genotypes. Curr Biol. 2009; 19 (5): R192–3.
7. Maronas O, Sochtig J, Ruiz Y, Phillips C, Carracedo A, Lareu MV. The genetics of skin, hair, and eye color variation and its relevance to forensic pigmentation predictive tests. Forensic Sci Rev. 2015; 27 (1): 13–40.
8. Walsh S, Chaitanya L, Clarisse L, Wirken L, Draus-Barini J, Kovatsi L, et al. Developmental validation of the HIrisPlex system: DNA-based eye and hair colour prediction for forensic and anthropological usage. Forensic Sci Int Genet. 2014; 9: 150–61.
9. Walsh S, Kayser M. A Practical Guide to the HIrisPlex System: Simultaneous Prediction of Eye and Hair Color from DNA. Methods Mol Biol. 2016; (1420): 213–31.
10. Walsh S, Liu F, Wollstein A, Kovatsi L, Ralf A, Kosiniak-Kamysz A, et al. The HIrisPlex system for simultaneous prediction of hair and eye colour from DNA. Forensic Sci Int Genet. 2013; 7 (1): 98–115.
11. Chaitanya L, Breslin K, Zuñiga S, Wirken L, Pośpiech E, Kukla-Bartoszek M, et al. The HIrisPlex-S system for eye, hair and skin colour prediction from DNA: Introduction and forensic developmental validation. Forensic Sci Int Genet. 2018; (35): 123–35.
12. Pagani L, Lawson DJ, Jagoda E, Mörseburg A, Eriksson A, Mitt M, et al. Genomic analyses inform on migration events during the peopling of Eurasia. Nature. 2016 Oct 13; 538 (7624): 238–42. DOI: 10.1038/nature19792.
13. Balanovska EV, ZHabagin MK, Agdzhoyan AT, CHukhryayeva MI, Markina NV, Balaganskaya OA, et al. Populyatsionnyye biobanki: printsipy organizatsii i perspektivy primeneniya v genogeografii i personalizirovannoy meditsine. Genetika. 2016; (12): 1371–87. Russian.
14. Powell R, Gannon F. Purification of DNA by phenolextraction and ethanol precipitation. Practical Approach Series. Oxford: Oxford University Press, 2002.
15. Chang CC, Chow CC, Tellier LCAM, Vattikuti S, Purcell SM, Lee JJ. Second-generation PLINK: rising to the challenge of larger and richer datasets. GigaScience. 2015 December; 4 (1):

s13742-015-0047-8. DOI: 10.1186/s13742-015-0047-8.
16. Department of Genetic Identification of Erasmus MC. HIrisPlex-S Eye, Hair and Skin Colour DNA Phenotyping Webtool. [software]. Available from: https://hirisplex.erasmusmc.nl/.
17. Draus-Barini J, Walsh S, Pospiech E, Kupiec T, Glab H, Branicki W, et al. Bona fide colour: DNA prediction of human eye and hair colour from ancient and contemporary skeletal remains. Investigative Genetics. 2013 January; (4): 3. DOI: 10.1186/2041-2223-4-3.
18. Jeong C, Balanovsky O, Lukianova E, Kahbatkyzy N, Flegontov P, Zaporozhchenko V, et al. The genetic history of admixture across inner Eurasia. Nat Ecol Evol. 2019 Jun; 3 (6): 966–76. DOI: 10.1038/s41559-019-0878-2.
19. Triska P, Chekanov N, Stepanov V, Khusnutdinova EK, Kumar GPA, Akhmetova V, et al. Between Lake Baikal and the Baltic Sea: genomic history of the gateway to Europe. BMC Genet. 2017 Dec 28; 18 (Suppl 1): 110. DOI: 10.1186/s12863-017-0578-3.

Литература

1. Bouakaze C, Keyser C, Crubezy E, Montagnon D, Ludes B. Pigment phenotype and biogeographical ancestry from ancient skeletal remains: inferences from multiplexed autosomal SNP analysis. Int J Legal Med. 2009; 123 (4): 315–25.
2. Branicki W, Brudnik U, Kupiec T, Wolanska-Nowak P, Szczerbinska A, Wojas-Pelc A. Association of polymorphic sites in the OCA2 gene with eye colour using the tree scanning method. Ann Hum Genet. 2008; 72 (Pt 2): 184–92.
3. Candille SI, Absher DM, Beleza S, Bauchet M, McEvoy B, Garrison NA, et al. Genome-wide association studies of quantitatively measured skin, hair, and eye pigmentation in four European populations. PLoS One. 2012; 7 (10): e48294.
4. Han J, Kraft P, Nan H, Guo Q, Chen C, Qureshi A, et al. A genome-wide association study identifies novel alleles associated with hair color and skin pigmentation. PLoS Genet. 2008; 4 (5): e1000074.
5. Lippert C, Sabatini R, Maher MC, Kang EY, Lee S, Arikan O, et al. Identification of individuals by trait prediction using whole-genome sequencing data. Proc Natl Acad Sci USA. 2017; 114 (38): 10166–71.
6. Liu F, van Duijn K, Vingerling JR, Hofman A, Uitterlinden AG, Janssens AC, et al. Eye color and the prediction of complex phenotypes from genotypes. Curr Biol. 2009; 19 (5): R192–3.
7. Maronas O, Sochtig J, Ruiz Y, Phillips C, Carracedo A, Lareu MV. The genetics of skin, hair, and eye color variation and its relevance to forensic pigmentation predictive tests. Forensic Sci Rev. 2015; 27 (1): 13–40.
8. Walsh S, Chaitanya L, Clarisse L, Wirken L, Draus-Barini J, Kovatsi L, et al. Developmental validation of the HIrisPlex system: DNA-based eye and hair colour prediction for forensic and anthropological usage. Forensic Sci Int Genet. 2014; 9: 150–61.
9. Walsh S, Kayser M. A Practical Guide to the HIrisPlex System: Simultaneous Prediction of Eye and Hair Color from DNA. Methods Mol Biol. 2016; (1420): 213–31.
10. Walsh S, Liu F, Wollstein A, Kovatsi L, Ralf A, Kosiniak-Kamysz A, et al. The HIrisPlex system for simultaneous prediction of hair and eye colour from DNA. Forensic Sci Int Genet. 2013; 7 (1): 98–115.
11. Chaitanya L, Breslin K, Zuñiga S, Wirken L, Pośpiech E, Kukla-Bartoszek M, et al. The HIrisPlex-S system for eye, hair and skin colour prediction from DNA: Introduction and forensic developmental validation. Forensic Sci Int Genet. 2018; (35): 123–35.
12. Pagani L, Lawson DJ, Jagoda E, Mörseburg A, Eriksson A, Mitt M, et al. Genomic analyses inform on migration events during the peopling of Eurasia. Nature. 2016 Oct 13; 538 (7624): 238–42. DOI: 10.1038/nature19792.
13. Балановская Е. В., Жабагин М. К., Агджоян А. Т., Чухряева М. И., Маркина Н. В., Балаганская О. А. и др. Популяционные биобанки: принципы организации и перспективы применения в геногеографии и персонализированной медицине. Генетика. 2016; (12): 1371–87.
14. Powell R, Gannon F. Purification of DNA by phenolextraction and ethanol precipitation. Practical Approach Series. Oxford: Oxford University Press, 2002.
15. Chang CC, Chow CC, Tellier LCAM, Vattikuti S, Purcell SM, Lee JJ. Second-generation PLINK: rising to the challenge of larger and richer datasets. GigaScience. 2015 December; 4 (1): s13742-015-0047-8. DOI: 10.1186/s13742-015-0047-8.
16. Department of Genetic Identification of Erasmus MC. HIrisPlex-S Eye, Hair and Skin Colour DNA Phenotyping Webtool. [software]. Available from: https://hirisplex.erasmusmc.nl/.
17. Draus-Barini J, Walsh S, Pospiech E, Kupiec T, Glab H, Branicki W, et al. Bona fide colour: DNA prediction of human eye and hair colour from ancient and contemporary skeletal remains. Investigative Genetics. 2013 January; (4): 3. DOI: 10.1186/2041-2223-4-3.
18. Jeong C, Balanovsky O, Lukianova E, Kahbatkyzy N, Flegontov P, Zaporozhchenko V, et al. The genetic history of admixture across inner Eurasia. Nat Ecol Evol. 2019 Jun; 3 (6): 966–76. DOI: 10.1038/s41559-019-0878-2.
19. Triska P, Chekanov N, Stepanov V, Khusnutdinova EK, Kumar GPA, Akhmetova V, et al. Between Lake Baikal and the Baltic Sea: genomic history of the gateway to Europe. BMC Genet. 2017 Dec 28; 18 (Suppl 1): 110. DOI: 10.1186/s12863-017-0578-3.

FRIEDREICH ATAXIA: *FXN* GENE EXPRESSION AND ITS RELATIONSHIP WITH DNA METHYLATION PATTERN

Fedotova EYu ✉, Abramycheva NYu, Nuzhny EP, Ershova MV, Klyushnikov SA, Illarioshkin SN

Research Center of Neurology, Moscow, Russia

Friedreich ataxia (FRDA) is the most common autosomal recessive ataxia associated with the non-coding GAA tandem repeats expansion in the *FXN* gene. Transcription impairment and frataxin protein deficiency are the key features of the disease pathogenesis. Our research was aimed to study the *FXN* gene mRNA expression as well as to carry out the clinical, genetic and epigenetic correlation analysis in a group of patients with homozygous expansion, in a group of their relatives with heterozygous expansion and in a control group. The *FXN* mRNA level was determined using the real-time polymerase chain reaction. Methylation pattern of CpG sites was evaluated by direct bisulfite sequencing. As a result of the study, the threshold values were obtained between the FRDA patients group, the group of heterozygous carriers and the control group (15 and 79%, respectively). The clinical and genetic features comparison with the *FXN* expression level revealed no significant correlation. When comparing gene expression with an epigenetic profile, it was found that hypermethylation of a number of CpG sites upstream of the trinucleotide repeats and some non-CpG sites downstream of the region of repeats inhibited expression. Thus, the identified methylated sites may be considered as a target for epigenome editing to increase the *FXN* transcription and, consequently, for target therapy of the disease.

Keywords: Friedreich ataxia, gene expression, epigenetics, DNA methylation, non-CpG methylation, DNA diagnostics, target therapy

Funding: the study is supported by grant of the Russian Science Foundation (project № 17-75-20211).

Author contribution: all authors contributed to the study and preparation of the article equally, read and approved the final version before publishing.

Compliance with ethical standards: the study was approved by the Ethics Committee of Research Center of Neurology (protocol № 11–3/17 dated October 18, 2017). Informed consent was obtained from all study participants.

✉ **Correspondence should be addressed:** Ekaterina Yu. Fedotova
Volokolamskoe shosse, 80, Moscow, 125367; ekfedotova@gmail.com

Received: 22.08.2019 **Accepted:** 13.09.2019 **Published online:** 25.09.2019

DOI: 10.24075/brsmu.2019.062

БОЛЕЗНЬ ФРИДРЕЙХА: ЭКСПРЕССИЯ ГЕНА *FXN* И ЕЕ ВЗАИМОСВЯЗЬ С ОСОБЕННОСТЯМИ МЕТИЛИРОВАНИЯ ДНК

Е. Ю. Федотова ✉, Н. Ю. Абрамычева, Е. П. Нужный, М. В. Ершова, С. А. Клюшников, С. Н. Иллариошкин

Научный центр неврологии, Москва, Россия

Болезнь Фридрейха (БФ) — наиболее частая аутосомно-рецессивная атаксия, связанная с экспансией тандемных некодирующих GAA-повторов в гене *FXN*. Нарушение транскрипции и недостаточность белка фратаксина являются ключевыми звеньями патогенеза заболевания. Целью работы было исследовать экспрессию мРНК гена *FXN* и провести анализ клинических, генетических и эпигенетических корреляций в группе пациентов с гомозиготной экспансией повторов, в группе их родственников с гетерозиготной экспансией и в контрольной группе. Уровень мРНК гена *FXN* определяли с помощью полимеразной цепной реакции в реальном времени. Паттерн метилирования CpG-сайтов оценивали методом прямого секвенирования после бисульфитной обработки. В результате работы получены разграничительные значения между группой пациентов БФ, группой гетерозиготных носителей и контрольной группой (15 и 79% соответственно). При проведении клинико-генетических сопоставлений с уровнем экспрессии *FXN* значимых корреляций выявлено не было. При сопоставлении экспрессии гена с эпигенетическим профилем было установлено, что экспрессия подавляется при гиперметилировании ряда CpG-сайтов выше области тринуклеотидных повторов и некоторых не-CpG-сайтов ниже области повторов. Таким образом, выявленные сайты могут быть рассмотрены в качестве точки приложения таргетного эпигенетического редактирования для увеличения транскрипции *FXN* и, следовательно, для таргетной терапии заболевания.

Ключевые слова: болезнь Фридрейха, экспрессия гена, эпигенетика, метилирование ДНК, не-CpG-метилирование, ДНК-диагностика, таргетная терапия

Финансирование: работа выполнена при поддержке гранта РНФ (номер проекта 17-75-20211).

Информация о вкладе авторов: все авторы внесли равнозначный вклад в проведение исследования и подготовку статьи, прочли и одобрили ее финальную версию перед публикацией.

Соблюдение этических стандартов: исследование одобрено этическим комитетом ФГБНУ НЦН (протокол № 11–3/17 от 18 октября 2017 г.). Все пациенты подписали информированное согласие на участие в исследовании.

✉ **Для корреспонденции:** Екатерина Юрьевна Федотова
Волоколамское ш., д. 80, г. Москва; ekfedotova@gmail.com

Статья получена: 22.08.2019 **Статья принята к печати:** 13.09.2019 **Опубликована онлайн:** 25.09.2019

DOI: 10.24075/vrgmu.2019.062

Friedreich ataxia (FRDA) is the most common autosomal recessive ataxia associated with the GAA trinucleotide repeat expansions in intron 1 of the *FXN* gene [1, 2]. The molecular basis of the disease is the gene product deficiency (mitochondrial protein, frataxin) [3]. Large expansion containing hundreds of nucleotides observed in patients with FRDA inhibits transcription of the corresponding *FXN* mRNA [2].

A number of studies show that in the DNA critical locus containing the *FXN* gene, heterochromatin (inactive chromatin) is formed in presence of expansion demonstrating the transcription suppression [4]. This corresponds to histone modifications: acetylation decrease and trimethylation increase shown in patients with FRDA [5–7]. Along with the histone modification, other epigenetic phenomena are also observed: DNA hypermethylation in promoter region and in the intron 1 upstream of the GAA expansion (UP-GAA), as well as DNA hypomethylation in the intron 1 downstream of the GAA expansion (DOWN-GAA). It is known that cytosine methylation

in the cytosine-guanine dinucleotide pair (CpG) of the promoter leads to the gene expression decrease, i.e., DNA methylation in the UP-GAA region presumably inhibits transcription of *FXN* and leads to a decrease in the frataxin level [8].

DNA methylation and histone modification are interconnected epigenetic mechanisms. In particular, DNA methylation level may be an important predictive marker for histone deacetylases inhibitors. Clinical trials of the latter are conducted with the aim of epigenetic therapy of FRDA. At the same time it is believed that in patients with FRDA, DNA methylation is primary in relation to histone modification [9].

In recent years papers emerged investigating the significance of so-called non-CpG methylation in which cytosine paired with nucleotides other than guanine (adenine, thymine, cytosine) was methylated. The highest level of non-CpG methylation was observed in stem cells and cells of the nervous system [10, 11], which suggested the special role of this epigenetic modification in the nervous system functions in normal and pathological conditions. To date, non-CpG methylation in FRDA patients has not been investigated.

Our research was aimed to study the *FXN* gene mRNA expression as well as to conduct the clinical, genetic and epigenetic correlation analysis in patients with FRDA and in heterozygous *FXN* mutation carriers.

METHODS

The study was conducted in the 5th Neurological Department of the Research Center of Neurology from 2017 to 2019. A group of patients with FRDA and confirmed homozygous GAA repeat expansion in the *FXN* gene was surveyed (n = 8; 3 women and 5 men). The average age of patients was 29.9 ± 9.5 years, the average age of onset was 13.8 ± 6.7 years, the disease duration was 16.0 ± 9.3 years. Inclusion criteria for the group of patients with FRDA: clinical diagnosis and positive results of molecular genetic testing (homozygous GAA tandem repeat expansion in introne 1 of the *FXN* gene). Average number of the GAA repeats in the short allele in the group was 506.0 ± 232.0 (GAA1), in the long allele the average number was 718.8 ± 143.8 (GAA2). Clinical examination of patients was performed using the SARA scale (mean score for the group 23.1 ± 11.4) and the Montreal Cognitive Assessment (MoCA) test (mean score 24.6 ± 2.7). Cardiomyopathy (5/8), carbohydrate metabolism impairment (3/8), scoliosis and foot deformities (6/8) were also determined. Exclusion criteria: no clinical diagnosis.

The group of patients was compared with the group of heterozygous *FXN* gene mutation carriers designated hereinafter as GAA heterozygotes (n = 6; 5 women and 1 man). This group included the first-degree relatives of patients with FRDA. Comparison group included older people (53.7 ± 19.6 years) compared to patients with FRDA (because of the parents of patients). For heterozygous patients the inclusion criterion was presence of the GAA expansion in the heterozygous state. The length of the expanded *FXN* allele in the group was 664.0 ± 283.7 repeats (GAA2). Control group (n = 10) with no GAA repeat expansion in the *FXN* gene was comparable in gender and age to the main group.

Genomic DNA samples were isolated from peripheral blood leukocytes using the Wizard Genomic DNA Purification Kit (Promega; USA). The GAA repeat expansion in the FXN gene was determined using the polymerase chain reaction (PCR) with subsequent separation of amplicons using the agarose gel.

Methylation pattern was determined by direct bisulfite sequencing of the corresponding DNA regions using the EZ DNA Methylation Kit (Zymo Research; USA) according to the manufacturer's instructions. For each subject, the methylation level of CpG sites was determined in three main significant regions of the *FXN* gene: promoter region, UP-GAA region and DOWN-GAA region. 16 CpG sites in the promoter region of *FXN*, 67 CpG sites in the UP-GAA region and 21 CpG sites in the DOWN-GAA region were explored (numeration starts from the 5' end of the corresponding region). The degree of the site methylation was calculated by the ratio of the blue peak height (methylated cytosine, C) to the total height of the blue and red peaks (methylated and non- methylated cytosine, C + T).

Along with the CpG sites search and analysis of non-CpG sites methylation were performed. In non-CpG sites methylated cytosine was a precursor of adenine, thymine or cytosine (mCA, mCT, mCC respectively).

The *FXN* expression level (the amount of mRNA of the *FXN* gene) was measured the by real-time PCR (RT-PCR) in the studied samples according to the following scheme. Peripheral blood samples were placed in the tubes with EDTA. Blood samples were pre-treated with a special buffer for red blood cells lysis, Buffer EL (QIAGEN; Germany), aliquoted and stored at –80 °C. To isolate genomic RNA, the RNeasy Plus Mini Kit (QIAGEN; Germany) was used according to the manufacturer's protocol. Total cDNA from RNA samples was isolated using a kit for reverse transcription and cDNA amplification (Eurogen; Russia) with the addition of oligo (dT) primer, aliquoted and stored at –20 °C. The *FXN* gene mRNA level in the studied samples was determined by the threshold cycle using the RT-PCR method with intercalating SYBR Green dye, normalized to the *GAPDH* reference gene. The $2^{(-\Delta\Delta Ct)}$ formula was used as a method of calculating the level of expression.

Statistical analysis was carried out using the IBM SPSS Statistics 23 software (IBM; USA). The nonparametric methods were used: Mann–Whitney U test and Spearman rank correlation test. ROC curve analysis was performed using the MedCalc 18 software (MedCalc Software; Belgium).

RESULTS

FXN gene expression in homozygous and heterozygous expansion carriers

In the group of FRDA patients homozygous for the GAA repeat expansion the expression level was 0.05 [0.00; 0.127]. In the group of the patients relatives heterozygous for the expansion the expression level was 0.57 [0.54; 0.66], and in the control group it was 1.016 [0.847; 1.214]. The differences between the groups were significant ($p < 0.05$).

ROC curve analysis was performed based on the overlapping values of expression level obtained for the control group and for the group of GAA heterozygotes. The area under the curve for the analyzed indicator was 0.986. For the demarcation threshold value equal to 0.79, specificity was 95% and sensitivity was 93%. In the ROC curve analysis of the gene expression evaluation in the groups of GAA heterozygotes and GAA homozygotes the area under the curve was 0.934. For the demarcation threshold value equal to 0.15, specificity was 93% and sensitivity was 87%.

Clinical comparison

FXN expression was correlated with clinical data in the group of patients with FRDA. Correlation analysis did not reveal relationship between the expression level and the age of patients, the onset age and the duration of the disease, the SARA scale score

and the MoCA test score ($p > 0.05$). According to the obtained data, expression level was not associated with cardiomyopathy, impaired carbohydrate metabolism or bone deformities ($p > 0.05$).

In the comparison group among the relatives of patients the least *FXN* expression level was observed in the heterozygous GAA expansion carrier (750 GAA repeats) aged 72 (patient's mother). The subject had a history of long-term endocrinopathy (severe type 2 diabetes mellitus). In the GAA heterozygotes group there were no other patients with diabetes mellitus.

Genetic comparison

Correlation between the *FXN* mRNA expression level and the expanded allele length was studied. In the group of patients with FRDA expression was not associated with the shorter GAA1 allele length (no statistical significance) or with the longer GAA2 allele length. In the group of GAA heterozygotes no relationship between the expression level and the expanded GAA2 allele length was revealed.

Epigenetic comparison

The search for non-CpG sites was performed in all studied regions. Two non-CpG sites were identified in the promoter region, in the UP-GAA region there were no non-CpG sites, DOWN-GAA region contained 15 non-CpG sites.

Correlation analysis of the FRDA patients group revealed positive correlation between the *FXN* mRNA expression level and the CpG-54 site of the UP-GAA region methylation level ($r = 0.782$; $p = 0.037$). Negative correlation between the *FXN* expression level and the methylation level of three non-CpG sites of the DOWN-GAA region was revealed: non-CpG-7a ($r = –0.788$; $p = 0.035$), non-CpG-7b ($r = –0.795$; $p = 0.032$) and non-CpG-8a ($r = –0.875$; $p = 0.009$). No relationship of the methylation level of these non-CpG sites with the length of GAA1 or GAA2 was detected. At the same time, in adjacent CpG sites, methylation did not correlate with expression, but depended on the length of the expanded allele (Table 1).

In the comparison group among the GAA heterozygotes, correlation between the expression level and the CpG-13 methylation level in the promoter region was detected ($r = –0.947$; $p = 0.017$), as well as correlation between the expression level and the CpG-3 methylation level in the DOWN-GAA region ($r = –0.894$; $p = 0.041$).

Given the small number of subjects in the groups, we calculated correlations in a combined group of patients, relatives and healthy volunteers, adjusted for the group. The revealed correlations between the *FXN* expression level and the individual sites methylation level are presented in Table 2. Summarizing the results, it can be noted that negative correlation between gene expression and methylation in the promoter and UP-GAA region and positive correlation between gene expression and methylation in the DOWN-GAA region were revealed for CpG sites, whereas in the DOWN-GAA region negative correlation was detected for non-CpG sites.

Methylated cytosine in the non-CpG sites was a precursor of the following nucleotides: mCCC (site 5a), mCTT (site 7a), mCCC (site 7b), mCAG (site 8a), mCAT (site 8b), mCTG (site 10b).

In the combined group, the degree of methylation of non-CpG sites of the DOWN-GAA region did not correlate with the expansion length (GAA1, GAA2) — similar to the group of FRDA patients.

DISCUSSION

Frataxin protein deficiency in patients with FRDA has a systemic effect and leads to different neurological and extraneurological manifestations [1, 9]. The severity of genetic changes in patients with FRDA (the expansion length of GAA repeats) can only partially explain the variety of clinical manifestations associated with the disorder (variable onset age and rate of progression, clinical manifestation features, polyneuropathy and corticospinal tract involvement, severity of cardiomyopathy, carbohydrate

Table 1. Correlation of the *FXN* gene expression level and the shorter allele repeat expansion length with the methylation level of DOWN-GAA region non-CpG sites and adjacent CpG sites in patients with FRDA

Site identificators	Correlation# of methylation level with expression	Correlation# of methylation level with GAA1 length	Nucleotides following the methylated cytosine	Cytosine position (GRCh38)
CpG-7	–	–0.901*	mCG	chr9:69.037.380
non-CpG-7a	–0.788*	–	mCTT	chr9:69.037.382
non-CpG-7b	–0.795*	–	mCCC	chr9:69.037.388
CpG-8	–	–0.836*	mCG	chr9:69.037.390
non-CpG-8a	–0.875*	–	mCAG	chr9:69.037.397
CpG-9	–	–0.772*	mCG	chr9:69.037.420
CpG-10	–	–0.791*	mCG	chr9:69.037.434

Note: # — Spearman's rank correlation coefficient (r); * — $p < 0.05$; «–» — no correlation; mC — methylated cytosine.

Table 2. Correlation of the *FXN* gene level expression and the methylation level of sites in all studied regions in a combined cohort adjusted for the group

Promoter: negative correlations	DOWN-GAA: positive correlations
– CpG-5 ($r = –0.511$)* – CpG-13 ($r = –0.542$)* – CpG-16 ($r = –0.511$)*	– CpG-2 ($r = 0.567$)* – CpG-12 ($r = 0.520$)*
UP-GAA: negative correlations	**DOWN-GAA: negative correlations**
– CpG-43 ($r = –0.615$)* – CpG-44 ($r = –0.508$)* – CpG-45 ($r = –0.533$)*	– non-CpG-5a ($r = –0.514$)* – non-CpG-7a ($r = –0.571$)* – non-CpG-7b ($r = –0.506$)* – non-CpG-8a ($r = –0.625$)* – non-CpG-8b ($r = –0.644$)* – non-CpG-10b ($r = –0.540$)*

Note: * — $p < 0.05$.

metabolism disorders etc.). As a consequence, the search for such a wide phenotypic polymorphism explanation was carried out by studying the factors and processes which regulate the implementation of genetic information: DNA methylation, histone modification, spatial organization of DNA, antisense transcripts and non-coding RNA. Due to the complexity and versatility of the processes caused by intron GAA expansion, it has not yet been possible to identify the main targets, the impact on which would help us to solve the problem of frataxin deficiency and impaired transcription of *FXN*, and, therefore, offer an effective therapeutic strategy. The focus of our study was on one of the epigenetic factors, DNA methylation. This factor seems promising in the view of studies in the field of targeted epigenetic editing, which may allow restoration of the impaired transcription, as it was demonstrated by the example of the *FMR1* gene trinucleotide repeats expansion [12–14].

Results of the *FXN* expression degree investigation were presented in a number of foreign papers. Thus, in one of the papers, the level of *FXN* mRNA in patients with FRDA was reduced to 19% and in heterozygous carriers to 53% of the control level. At the same time, the mRNA level correlated with the level of frataxin, the age of the onset and the length of expansion [15]. In another study, comparable results were obtained. It was also demonstrated that mRNA level and the level of frataxin protein were relatively stable over time and changed against the background of epigenetic therapy (inhibitor of histone deacetylases) effect. In other words, the mRNA level is a measurable and variable indicator that can be used in clinical trials [16].

Our analysis of *FXN* gene expression also revealed a significant decrease in mRNA level in patients with homozygous GAA expansion (below 15%) in relation to the control group, as well as in the group of relatives with heterozygous repeat expansion (below 79%). However, in our study, statistically significant correlation with neither clinical nor genetic characteristics was detected, most likely due to the small sample size. At the same time, it is noteworthy that in the group of heterozygotes the lowest level of *FXN* mRNA was detected in a patient with type 2 diabetes mellitus. Possibly, a low level of expression of mRNA and frataxin protein in heterozygotes may be markers of the carbohydrate metabolism disorders observed in patients with FRDA which can also be detected in their relatives (heterozygous mutation carriers) [17, 18].

There are few papers on DNA methylation studies in patients with FRDA [8, 19–23]. Nevertheless, FRDA is considered a model disease characterized with a special type of trinucleotide repeat expansion (both alleles are in the non-coding, regulatory region of the gene) [20]. In two papers, hypermethylation of several sites was discovered in the UP-GAA region in patients with FRDA [21, 22]. Other researchers also noted UP-GAA hypermethylation and detected DOWN-GAA hypomethylation in patients' peripheral blood cells, in the brain and myocardium [23], which confirmed the systemic effect of the GAA repeat expansion and the information value of data obtained for peripheral blood leukocytes. In another study, in addition to UP-GAA hypermethylation and DOWN-GAA hypomethylation, a large sample of patients with FRDA demonstrated a negative correlation between the methylation level of one UP-CpG site and the *FXN* mRNA level [8]. mRNA level also correlated with GAA repeats number, onset age and symptoms severity. In our previously published paper [19] hypermethylation of the UP-GAA region and hypomethylation of the DOWN-GAA region in patients with FRDA were confirmed, a direct relationship between the degree of methylation of UP-GAA region sites and the expansion length of homozygous mutation carriers, as well as inverse relationship between the degree of methylation of DOWN-GAA region sites with expansion length in heterozygous mutation carriers were detected.

Our present study is the continuation of the previous studies. The study is aimed to investigate the FXN epigenetic profile effect on the corresponding mRNA expression. Comparing the results of previous and present studies, it can be noted that hypermethylation of individual CpG sites located upstream of the repeats region (promoter and UP-GAA) is associated with a lower mRNA level and a larger number of GAA tandem repeats in the FXN gene. Hypomethylation of individual CpG sites in the DOWN-GAA region is associated with a lower mRNA level and a larger number of GAA tandem repeats.

As it is mentioned above, non-CpG methylation in patients with FRDA has not yet been investigated. The functional significance of non-CpG sites is discussed. However, it is now clear that it is very important for expression regulation [24]. Non-CpG sites are predominantly located in the regions with lower density of CpG sites, i.e., usually inside the gene. Methylation of non-CpG inside the gene is associated with a decrease in its expression. It is believed that compared to CpG methylation of non-CpG sites is more susceptible to changes that occur during the development and under the influence of various environmental factors [25]. Thus, in neurons at the embryo stage, non-CpG sites are almost not methylated. Non-CpG methylation occurs during development. It is neurons that account for the largest part of adult non-CpG methylation, less for glia, stem cells, gametes. Non-CpG methylation is almost absent in other cells. Estimated ratio of non-CpG methylation to CpG methylation in neurons is 1 : 3. Most often, the first occurs in the CpA dinucleotide, to a lesser extent in the CpT dinucleotide, and even less in CpC. It is believed that the function of non-CpG methylation depends on the molecular context. Thus, methylation of cytosine in the mCAC sequence can lead to a decrease in gene expression, while methylation in mCAG can lead to its increase [10, 11].

In our study 2 non-CpG sites were identified in the promoter region, in UP-GAA there were no non-CpG sites, DOWN-GAA region contained 15 non-CpG sites. For comparison, the incidence of CpG in the same sequenced regions was as follows: 16 CpG in the promoter, 67 CpG in the UP-GAA and 21 CpG in the DOWN-GAA region. The provided data demonstrate that the higher the density of CpG, the lower the occurrence of non-CpG, and vice versa. Approximate, conditional ratio of non-CpG to CpG is 1 : 6. It should be reminded, that the study was performed on blood leukocytes with a lower proportion of non-CpG, and not on neurons.

No correlation between the methylation level of two non-CpG sites in the *FXN* promoter region and the mRNA level was detected. A cluster of interconnected, adjacent non-CpG sites was identified in the DOWN-GAA region, methylation of which negatively correlates with the mRNA level. There was no relationship between the methylation level and the GAA expansion length. The unidirectional effect of all 6 detected non-CpG sites on the expression did not depend on the context, it was shown in the CpA (mCAC, mCAG), CpT (mCTT, mCTG), and CpC (2 mCCC) configurations.

In the combined cohort, in contrast to non-CpG methylation, the level of CpG methylation in DOWN-GAA demonstrated direct associative relationship with the mRNA level, which suggested a possible multidirectional effect of those two types of methylation. Another difference between the types may be the dependence on the length of GAA expansion: it is present in CpG methylation, whereas in the case of non-CpG it cannot

be detected. Therefore, the non-CpG methylation can modify the expression of *FXN* regardless of a genetic defect.

The identified cluster of closely located non-CpG sites, methylation of which is associated with the decrease in the *FXN* gene transcription, is in the distance from the regulatory sequences and binding sites of known and studied in patients with FRDA transcription factors, CTCF, SRF, TFAP2, EGR3, E-box (all transcription factors lie inside the promoter and the UP-GAA region) [26, 27]. The region of the detected non-CpG cluster, being inside the DOWN-GAA region, is a part of the Alu (SINE) element. The functional significance of the latter is not clear completely, however, removal of the element leads to a significant impairment of *FXN* transcription [4, 21]. This once again confirms the possible significance of non-CpG methylation in this region for transcription.

CONCLUSION

The paper presents a comparison of the clinical parameters, the degree of expansion of GAA repeats, and the epigenetic characteristics of the *FXN* gene with the mRNA level in the group of patients with FRDA, in the group of their heterozygous relatives, and in the control group. *FXN* methylation sites significant for expression were identified. For a number of CpG sites in the promoter region and in the UP-GAA region, a negative correlation between methylation and the level of gene expression was determined, as well as for a number of non-CpG sites in the DOWN-GAA region. Thus, the identified hypermethylated cluster of non-CpG sites may be considered the application point for targeted epigenome editing needed for the *FXN* transcription increase, and, consequently, for FRDA target therapy.

References

1. Illarioshkin SN., Ershova MV. Ataksiya Fridreykha. V knige: Illarioshkin SN, Rudenskaya GE, Ivanova-Smolenskaya IA., Markova ED, Klyushnikov SA. Nasledstvennye ataksii i paraplegii. M., 2006; s.49–113. Russian.
2. Burk K. Friedreich ataxia: current status and future prospects. Cerebellum Ataxias. 2017; (4): 4.
3. Deutsch EC, Oglesbee D, Greeley NR, Lynch DR. Usefulness of frataxin immunoassays for the diagnosis of Friedreich ataxia. J Neurol Neurosurg Psychiatry. 2014; 85 (9): 994–1002.
4. Yandim C, Natisvivli T, Festenstein R. Gene regulation and epigenetics in Friedreich's ataxia. Journal of neurochemistry. 2013: 126 (Suppl. 1): 21–42.
5. Herman D, Jenssen K, Burnett R, Soragni E, Perlman SL, Gottesfeld JM. Histone deacetylase inhibitors reverse gene silencing in Friedreich's ataxia. Nat Chem Biol. 2006; 2 (10): 551–8.
6. Sandi C, Sandi M, Virmouni SA, Al-Mahdawi S, Pook MA. Epigenetic-based therapies for Friedreich ataxia. Frontiers in Genetics. 2014; (5): 165.
7. Soragni E, Miao W, Iudicello M, Jacoby D, De Mercanti S, Clerico M, et al. Epigenetic therapy for Friedreich ataxia. Ann Neurol. 2014; 76 (4): 489–508.
8. Evans-Galea MV, Carrodus N, Rowley SM, Corben LA, Tai G, Saffery R, et al. FXN methylation predicts expression and clinical outcome in Friedreich ataxia. Ann Neurol. 2012; 71 (4): 487–97.
9. Blair IA, Farmer J, Hersch S, Larkindale J, Lynch DR, Napierala J, et al. The current state of biomarker research for Friedreich's ataxia: a report from the 2018 FARA biomarker meeting. Future Sci OA. 2019; 5 (6): FSO398.
10. He Y, Ecker JR. Non-CG methylation in the human genome. Annu Rev Genomics Hum Genet. 2015; (16): 55–77.
11. Jang HS, Shin WJ, Lee JE, Do JT. CpG and non-CpG methylation in epigenetic gene regulation and brain function. Genes. 2017; (8): e148.
12. Liu XS, Wu H, Krzisch M, Wu X, Graef J, Muffat J, et al. Rescue of Fragile X syndrome neurons by DNA methylation editing of the FMR1 gene. Cell. 2018; (172): 979–92.
13. Lau C-H, Suh Y. In vivo epigenome editing and transcriptional modulation using CRISPR technology. Transgenic Res. 2018; 27 (6): 489–509.
14. Gomez JA, Beitnere U, Segal DJ. Live-animal epigenome editing: Convergence of novel techniques. Trends Genet. 2019; 35 (7): 527–41.
15. Sacca F, Puoro G, Antenora A, Marsili A, Denaro A, Piro R, et al. A combined nucleic acid and protein analysis in Friedreich ataxia: Implications for diagnosis, pathogenesis and clinical trial design. PLoS ONE. 2011; 6 (3): e17627.
16. Plasterer HL, Deutsch EC, Belmonte M, Egan E, Lynch DR, Rusche JR. Development of frataxin gene expression measures for the evaluation of experimental treatment in Friedreich's ataxia. PLoS ONE. 2013; 8 (5): e63958.
17. Hebinck J, Hardt C, Schols L, Vorgerd M, Briedigkeit L, Kahn CR, Ristow M. Heterozygous expansion of the GAA tract of the X25/frataxin gene is associated with insulin resistance in humans. Diabetes. 2000; 49 (9): 1604–7.
18. McCormick A, Farmer J, Perlman S, Delatycki M, Wilmot G, Matthews K, et al. Impact of diabetes in the Friedreich ataxia clinical outcome measures study. Annals of Clinical and Translational Neurology. 2017; 4 (9): 622–31.
19. Abramycheva NYu, Fedotova EYu, Nuzhniy EP, Nikolaeva NS, Klyushnikov SA, Ershova MV, i dr. Epigenetika bolezni Fridreykha: metilirovanie oblasti ekspansii (GAA)n-povtorov gena FXN. Vestnik Rossiyskoy akademii meditsinskikh nauk. 2019; 74 (2): 80–7.
20. Essebier A, Wolf PV, Cao MD, Carroll BJ, Balasubramanian S, Boden M. Statistical enrichment of epigenetic states around triplet repeats that can undergo expansions. Front Neurosci. 2016; (10): 92.
21. Greene E, Mahishi L, Entezam L, Kumari D, Usdin K. Repeat-induced epigenetic changes in intron 1 of the frataxin gene and its consequences in Friedreich ataxia. Nucleic Acids Research. 2007; 35 (10): 3383–90.
22. Castaldo I, Pinelli M, Monticelli A, Acquaviva F, Giacchetti M, Filla A, et al. DNA methylation in intron 1 of the frataxin gene is related to GAA repeat length and age of onset in Friedreich ataxia patients. J Med Genet. 2008; 45 (12): 808–12.
23. Al-Mahdawi S, Pinto RM, Ismail O, Varshney D, Lymperi S, Sandi C, et al. The Friedreich ataxia GAA repeat expansion mutation induces comparable epigenetic changes in human and transgenic mouse brain and heart tissues. Hum Mol Genet. 2008; (17): 735–46.
24. Patil V, Ward RL, Hesson LB. The evidence for functional non-CpG methylation in mammalian cells. Epigenetics. 2014; 9 (6): 823–28.
25. Fuso A, Lucarelli M. CpG and non-CpG methylation in the diet-epigenetics-neurodegeneration connection. Curr Nutr Rep. 2019; 8 (2): 74–82.
26. Li K, Singh A, Crooks DR, Dai X, Cong Z, Pan L, et al. Expression of human frataxin is regulated by transcription factors SRF and TFAP2. PLoS ONE. 2010; 5 (8): e12286.
27. Al-Mahdawi S, Sandi C, Pinto RM, Pook MA. Friedreich ataxia patient tissues exhibit increased 5-hydroxymethylcytosine modification and decreased CTCF binding at the FXN locus. PLoS ONE. 2013; 8 (9): e74956.

Литература

1. Иллариошкин С. Н., Ершова М. В. Атаксия Фридрейха. В книге: Иллариошкин С. Н., Руденская Г. Е., Иванова-Смоленская И. А., Маркова Е. Д., Клюшников С. А. Наследственные атаксии и параплегии. М., 2006; с. 49–113.
2. Burk K. Friedreich ataxia: current status and future prospects. Cerebellum Ataxias. 2017; (4): 4.
3. Deutsch EC, Oglesbee D, Greeley NR, Lynch DR. Usefulness of frataxin immunoassays for the diagnosis of Friedreich ataxia. J Neurol Neurosurg Psychiatry. 2014; 85 (9): 994–1002.
4. Yandim C, Natisvivli T, Festenstein R. Gene regulation and epigenetics in Friedreich's ataxia. Journal of neurochemistry. 2013: 126 (Suppl. 1): 21–42.
5. Herman D, Jenssen K, Burnett R, Soragni E, Perlman SL, Gottesfeld JM. Histone deacetylase inhibitors reverse gene silencing in Friedreich's ataxia. Nat Chem Biol. 2006; 2 (10): 551–8.
6. Sandi C, Sandi M, Virmouni SA, Al-Mahdawi S, Pook MA. Epigenetic-based therapies for Friedreich ataxia. Frontiers in Genetics. 2014; (5): 165.
7. Soragni E, Miao W, Iudicello M, Jacoby D, De Mercanti S, Clerico M, et al. Epigenetic therapy for Friedreich ataxia. Ann Neurol. 2014; 76 (4): 489–508.
8. Evans-Galea MV, Carrodus N, Rowley SM, Corben LA, Tai G, Saffery R et al. FXN methylation predicts expression and clinical outcome in Friedreich ataxia. Ann Neurol. 2012; 71 (4): 487–97.
9. Blair IA, Farmer J, Hersch S, Larkindale J, Lynch DR, Napierala J et al. The current state of biomarker research for Friedreich's ataxia: a report from the 2018 FARA biomarker meeting. Future Sci OA. 2019; 5 (6): FSO398.
10. He Y, Ecker JR. Non-CG methylation in the human genome. Annu Rev Genomics Hum Genet. 2015; (16): 55–77.
11. Jang HS, Shin WJ, Lee JE, Do JT. CpG and non-CpG methylation in epigenetic gene regulation and brain function. Genes. 2017; (8): e148.
12. Liu XS, Wu H, Krzisch M, Wu X, Graef J, Muffat J, et al. Rescue of Fragile X syndrome neurons by DNA methylation editing of the FMR1 gene. Cell. 2018; (172): 979–92.
13. Lau C-H, Suh Y. In vivo epigenome editing and transcriptional modulation using CRISPR technology. Transgenic Res. 2018; 27 (6): 489–509.
14. Gomez JA, Beitnere U, Segal DJ. Live-animal epigenome editing: Convergence of novel techniques. Trends Genet. 2019; 35 (7): 527–41.
15. Sacca F, Puoro G, Antenora A, Marsili A, Denaro A, Piro R, et al. A combined nucleic acid and protein analysis in Friedreich ataxia: Implications for diagnosis, pathogenesis and clinical trial design. PLoS ONE. 2011; 6 (3): e17627.
16. Plasterer HL, Deutsch EC, Belmonte M, Egan E, Lynch DR, Rusche JR. Development of frataxin gene expression measures for the evaluation of experimental treatment in Friedreich's ataxia. PLoS ONE. 2013; 8 (5): e63958.
17. Hebinck J, Hardt C, Schols L, Vorgerd M, Briedigkeit L, Kahn CR, Ristow M. Heterozygous expansion of the GAA tract of the X25/frataxin gene is associated with insulin resistance in humans. Diabetes. 2000; 49 (9): 1604–7.
18. McCormick A, Farmer J, Perlman S, Delatycki M, Wilmot G, Matthews K, et al. Impact of diabetes in the Friedreich ataxia clinical outcome measures study. Annals of Clinical and Translational Neurology. 2017; 4 (9): 622–31.
19. Абрамычева Н. Ю., Федотова Е. Ю., Нужный Е. П., Николаева Н. С., Клюшников С. А., Ершова М. В. и др. Эпигенетика болезни Фридрейха: метилирование области экспансии (GAA)n-повторов гена FXN. Вестник Российской академии медицинских наук. 2019; 74 (2): 80–7.
20. Essebier A, Wolf PV, Cao MD, Carroll BJ, Balasubramanian S, Boden M. Statistical enrichment of epigenetic states around triplet repeats that can undergo expansions. Front Neurosci. 2016; (10): 92.
21. Greene E, Mahishi L, Entezam L, Kumari D, Usdin K. Repeat-induced epigenetic changes in intron 1 of the frataxin gene and its consequences in Friedreich ataxia. Nucleic Acids Research. 2007; 35 (10): 3383–90.
22. Castaldo I, Pinelli M, Monticelli A, Acquaviva F, Giacchetti M, Filla A, et al. DNA methylation in intron 1 of the frataxin gene is related to GAA repeat length and age of onset in Friedreich ataxia patients. J Med Genet. 2008; 45 (12): 808–12.
23. Al-Mahdawi S, Pinto RM, Ismail O, Varshney D, Lymperi S, Sandi C et al. The Friedreich ataxia GAA repeat expansion mutation induces comparable epigenetic changes in human and transgenic mouse brain and heart tissues. Hum Mol Genet. 2008; (17): 735–46.
24. Patil V, Ward RL, Hesson LB. The evidence for functional non-CpG methylation in mammalian cells. Epigenetics. 2014; 9 (6): 823–28.
25. Fuso A, Lucarelli M. CpG and non-CpG methylation in the diet-epigenetics-neurodegeneration connection. Curr Nutr Rep. 2019; 8 (2): 74–82.
26. Li K, Singh A, Crooks DR, Dai X, Cong Z, Pan L, et al. Expression of human frataxin is regulated by transcription factors SRF and TFAP2. PLoS ONE. 2010; 5 (8): e12286.
27. Al-Mahdawi S, Sandi C, Pinto RM, Pook MA. Friedreich ataxia patient tissues exhibit increased 5-hydroxymethylcytosine modification and decreased CTCF binding at the FXN locus. PLoS ONE. 2013; 8 (9): e74956.

EFFECTS OF CARNOSINE AND LIPOIC ACID IN THE LATE STAGE OF PARKINSON'S DISEASE IN RATS

Berezhnoy DS, Fedorova TN, Kulikova OI ✉, Stavrovskaya AV, Abaimov DA, Gushchina AS, Olshansky AS, Voronkov DN, Stvolinsky SL

Research Center of Neurology, Moscow, Russia

The late stage of Parkinson's disease is characterized by massive neuronal loss in the substantia nigra (SN) and degeneration of the dopaminergic innervation in the striatum. There is a need to assess the neuroprotective effect of antioxidants (AO) at this stage of the disease. The aim of our study was to assess the efficacy of two AO, carnosine and lipoic acid (LA), in the rat model of late-stage parkinsonism. The pathology was induced by a unilateral injection of 6-hydroxydopamine (6-OHDA) into the SN of the right brain hemisphere. AO were administered 4 times, starting on day 14 following the injection of the toxin. We investigated the effect of the injected drugs on the behavior of rats, the loss of neurons in the SN and the metabolism of biogenic neurotransmitter amines. Both AO dampened the development of 6-OHDA-induced neurological and behavioral symptoms. 6-OHDA induced a 90% drop (p = 0.01) in the levels of dopamine (DA) and its metabolites in the right striatum and caused death of over 95% of neurons (p = 0.01) in the SN of the right hemisphere (p = 0.01). AO did not have a significant effect on the number of neurons in the SN but caused an increase in the levels of DA metabolites, as compared to their levels in the animals exposed to 6-OHDA. Elevated DA (a 5.8-fold increase, p = 0.007) was observed only in the animals treated with carnosine. LA stimulated a 23% decline in serotonin levels (p = 0.06) and a 36% increase (p = 0.009) in its metabolite, 5-hydroxyindolacetic acid (5-HIAA). We conclude that although carnosine and LA did not have a direct neuroprotective effect, they could relieve the symptoms. This suggests that these AO could be used as an adjunctive component to antiparkinsonian therapy.

Keywords: parkinsonism, Wistar rats, carnosine, lipoic acid, neurotransmitters, behavioral tests

Author contribution: Berezhnoy DS analyzed the literature; planned the study; acquired, analyzed and interpreted the obtained data; prepared the draft of the manuscript and revised its final version. Fedorova TN analyzed the literature; planned the study; analyzed and interpreted the obtained data; revised the manuscript. Kulikova OI analyzed the literature; planned the study; acquired, analyzed and interpreted the obtained data; revised the manuscript. Stavrovskaya AV analyzed the literature; planned the study; acquired, analyzed and interpreted the obtained data; prepared the draft of the manuscript. Abaimov DA acquired, analyzed and interpreted the obtained data; prepared the draft of the manuscript. Gushchina AS planned the study; acquired, analyzed and interpreted the obtained data; prepared the draft of the manuscript. Olshansky AS acquired and analyzed the data; prepared the draft of the manuscript. Voronkov DN acquired analyzed and interpreted the obtained data; prepared the draft of the manuscript. Stvolinsky SL planned the study; acquired, analyzed and interpreted the obtained data; prepared the draft of the manuscript.

Compliance with ethical standards: all experiments involving the use of animals were conducted in full compliance with the international Guide for the Care and Use of Laboratory Animals.

✉ **Correspondence should be addressed:** Olga I. Kulikova
Volokolamskoe shosse, 80, Moscow, 125367; kulikova@neurology.ru

Received: 12.08.2019 **Accepted:** 30.08.2019 **Published online:** 18.09.2019

DOI: 10.24075/brsmu.2019.060

ДЕЙСТВИЕ КАРНОЗИНА И ЛИПОЕВОЙ КИСЛОТЫ В МОДЕЛИ ПОЗДНЕЙ СТАДИИ БОЛЕЗНИ ПАРКИНСОНА У КРЫС

Д. С. Бережной, Т. Н. Федорова, О. И. Куликова ✉, А. В. Ставровская, Д. А. Абаимов, А. С. Гущина, А. С. Ольшанский, Д. Н. Воронков, С. Л. Стволинский

Научный центр неврологии, Москва, Россия

Оценка эффективности антиоксидантных (АО) препаратов при введении на поздней стадии экспериментального паркинсонизма в условиях тотальной гибели нейронов черной субстанции (ЧС) и нарушений дофаминергической иннервации стриатума является актуальной проблемой. Целью исследования было оценить эффективность АО карнозина и липоевой кислоты (ЛК) в модели поздней стадии паркинсонизма. Паркинсонизм индуцировали у крыс с помощью унилатерального стереотаксического введения 6-гидроксидофамина (ГДА) в ЧС правого полушария. АО вводили 4 раза, начиная с 14-го дня после введения токсина. Изучали влияние препаратов на поведение, гибель нейронов ЧС и метаболизм медиаторов-моноаминов. Оба препарата снижали развитие неврологической симптоматики и нарушения поведения, вызванные ГДА. Введение ГДА приводило к снижению уровня дофамина (ДА) и его метаболитов в правом стриатуме на 90% (p = 0,01) и гибели более 95% нейронов в ЧС правого полушария (p = 0,01). АО значимо не влияли на количество нейронов в ЧС, но увеличивали содержание метаболитов ДА относительно животных, получавших ГДА, при этом повышение содержания ДА (в 5,8 раз; p = 0,007) наблюдали только у животных, получавших карнозин. Введение ЛК способствовало снижению серотонина на 23% (p = 0,006) и его метаболита 5-гидроксииндолуксусной кислоты (ГИУК) на 36% (p = 0,009). Таким образом, при отсутствии прямого нейропротекторного эффекта было обнаружено симптоматическое действие карнозина и ЛК, что обосновывает возможность их использования в качестве дополнительной терапии болезни Паркинсона.

Ключевые слова: паркинсонизм, крысы линии Wistar, карнозин, липоевая кислота, нейромедиаторы, физиологическое тестирование

Информация о вкладе авторов: Д. С. Бережной — анализ литературы, планирование исследования, подготовка черновика рукописи и финального варианта статьи; Т. Н. Федорова — анализ литературы, планирование исследования, подготовка финального варианта статьи; О. И. Куликова — анализ литературы, планирование исследования, подготовка финального варианта статьи; А. В. Ставровская — анализ литературы, планирование исследования, подготовка черновика рукописи; Д. А. Абаимов — подготовка черновика рукописи; А. С. Гущина — планирование исследования, подготовка черновика рукописи; А. С. Ольшанский — подготовка черновика рукописи; Д. Н. Воронков — подготовка черновика рукописи; С. Л. Стволинский — планирование исследования, подготовка черновика рукописи; все авторы участвовали в сборе, анализе и интерпретации данных.

Соблюдение этических стандартов: все эксперименты с животными проводили в соответствии с международными правилами работы с лабораторными животными.

✉ **Для корреспонденции:** Куликова Ольга Игоревна
Волоколамское ш., д. 80, г. Москва, 125367; kulikova@neurology.ru

Статья получена: 12.08.2019 **Статья принята к печати:** 30.08.2019 **Опубликована онлайн:** 18.09.2019

DOI: 10.24075/vrgmu.2019.060

Parkinson's disease (PD) is a progressive neurodegenerative disorder characterized by the loss of dopaminergic neurons in the substantia nigra pars compacta (SNpc). There is no cure for PD, and the available treatments are symptomatic. This creates the need for effective neuroprotective agents capable of slowing or stopping the progression of the disease [1, 2].

6-Hydroxydopamine (6-OHDA) is a selective catecholaminergic neurotoxin that gives rise to free radicals and inhibits complexes I and IV of the mitochondrial electron transport chain [3]. This compound is often used to induce PD in animal models. 6-OHDA injected into the SN of rats causes death of almost all striatal dopaminergic neurons and their terminals within 10 to 14 days after the injection [4]. Antioxidants (AO) administered to experimental animals before the injection or immediately after brain surgery have a remarkable neuroprotective effect [5], possibly resulting from their direct interaction with free radicals generated during 6-OHDA oxidation and, to some extent, from the effect they have on 6-OHDA autoxidation [6]. AO do not prevent the development of the pathology as such, but rather inactivate the neurotoxin that triggers the disease.

Carnosine and alpha-lipoic acid (LA) have been shown to be protective against neuronal damage in the early stage of induced parkinsonism in rats [7]. Bearing that in mind, it would be interesting to assess the efficacy of these AO in later stages of PD when neuronal loss has already occurred and the dopaminergic innervation of the striatum has suffered some degeneration. This is when the definitive diagnosis is usually made and treatment starts.

The objective of this study was to assess the effect of carnosine and LA on rat behavior and the neurochemical parameters of rat brain in the late stage of 6-OHDA-induced parkinsonism.

METHODS

The study was conducted in 40 3-month old outbred male Wistar rats weighing 250 to 300 g. The animals were housed under standard conditions (the 12/12 light/dark cycle) and had free access to food and water.

The rats were divided into 4 groups. Three experimental groups received a 3 µl injection of 0.05% ascorbic acid solution containing 12 µg of 6-OHDA (Sigma; USA) into the substantia nigra at the start of the experiment. The control group consisted of sham-operated animals (n = 9) that received an equal amount of the solvent (0.05% ascorbic acid). The stereotaxic coordinates for the injection were as follows: AP = –4.8; L = 1.9; V = 8.0 [8]. For surgery, the rats were anesthetized with intramuscular injections of Zoletil 100 (3 mg/100g) and xylazine (3 mg/kg); premedication with 0.04 mg/kg atropine was administered subcutaneously 10 to 15 min before xylazine. On days 14, 16, 18, and 20 following the 6-OHDA injection, the sham-operated animals (n = 9) received intraperitoneal injections of 0.9% NaCl solution (this group will be referred to as 6-OHDA+NaCl); groups 2 and 3 (n = 11 and n = 11, respectively) received intraperitoneal injections of 50 mg/kg carnosine (Swedlight AB; Sweden) and 50 mg/kg LA (Chem–Implex Int`l Inc.; USA), respectively. Below, these 2 groups will be referred to as 6-OHDA+ carnosine and 6-OHDA+LA.

The open field (OF) and the tapered beam walking (BW) tests were carried out on days 21 and 22 after the 6-OHDA injection to assess the behavior and locomotor activity of the animals. Because not all of them were able to make it to the end of the walking beam, we used an additional scale to assess their neurotic-like behavior (Table 1) [9] On day 25, the animals were decapitated using a guillotine (Open Science, Russia), their brains were removed and chilled on ice; the dorsal striatum of the left and right brain hemispheres and the SN-containing midbrain fragment were isolated for further histopathologic examination and immunostaining, respectively. The obtained samples were stored in liquid nitrogen.

Quantification of dopaminergic neurons

The number of dopaminergic neurons in the SN of the control animals and the 6-OHDA+NaCl group was estimated using an

Table 1. Points scored on the scale for assessing the neurotic-like behavior demonstrated in the beam walking test. The table describes the types and variations of different behaviors and the score for each type

Behaviors	Elements	Score
Self-grooming	Nose-cheeks	1
	Nose-cheeks-ears	2
	Nose-cheeks-ears-belly	3
	Nose-cheeks-ears-belly-back	4
	-//- + self-biting	5
Movements		
Head	Sniffing	1
	Left and right turns	2
	Chewing	3
	Licking	3
Body	Turn	3
	Backing	4
	Freezing	5
Hangs over the beam	Head	1
	Half of the body	2
Stops on the walking beam		3
Slips		2
Hiccups		4

immunofluorescence staining technique for determining tyrosine hydroxylase (TH) content in the studied tissue [10]. TH is the key enzyme involved in dopamine synthesis. The specimens fixed in 4% formalin were soaked in sucrose and subsequently immersed in the O.C.T. Tissue Tek compound (Sigma; USA). Frozen frontal sections prepared from the specimens were 12 μm thick in the SN region. The sections were incubated with 1 : 800 monoclonal rabbit anti-tyrosine hydroxylase antibodies (T8700, Sigma; USA) in a humidity chamber at room temperature for 24 h. The binding of primary antibodies was visualized using goat CF488-conjugated antirabbit antibodies (Sigma, 1 : 500). The sections were mounted in the FluoroShield media (Sigma; USA), coverslipped and photographed under a Nikon Eclipse Ni-u microscope (Nikon; USA) at ×10 magnification. At least 8–10 sections per animal were studied, the distance between slices was 36–48 μm. Neuronal bodies were counted in the field of view in ImageJ (NIH; USA).

Concentrations of amine neurotransmitters and their metabolites

The neurotransmitter amines and their metabolites measured in our study included dopamine (DA), 3,4-dihydroxyphenylacetic acid (DOPAC), homovanillic acid (HVA), 3-methoxytyramine (3-MT), noradrenalin (NA), serotonin (5-HT), and 5-hydroxyindoleacetic acid (5-HIAA). Their levels were determined in the right and left striatum using high-performance liquid chromatography with electrochemical detection (HPLC-ED). Measurements were done using a System Gold High-Performance Liquid Chromatograph (Beckman Coulter Inc.; USA) equipped with an amperometric detector RECIPE EC 3000 (Recipe GmbH; Germany). The excised brain tissue was homogenized in 20 volumes of 0.1 N HClO4 supplemented with 0.5 nmol/ml dioxybenzylamine, which was used as an internal standard. The tissue was centrifuged at 10,000 g for 10 min. The supernatant was removed and analyzed [7].

Statistical analysis

The obtained data were processed in Statistica 10.0 (Dell. Inc.; USA). Significance of differences was assessed with ANOVA and Tukey's HSD. The samples were compared using paired Student's *t*-test and Mann–Whitney U test, depending on the normality of data distribution. The differences were considered significant at $p < 0.05$. The results are presented below as a mean value ± the standard error (M ± *m*).

RESULTS

Analysis of neurological symptoms

The beam walking test revealed pronounced behavioral symptoms in the rats that had been exposed to 6-OHDA ($F(3.36) = 10.54$; $p = 0.001$). All rodents from the control group successfully got to the end of the walking beam; the time it took them to cover the whole distance was 13.88 ± 1.73 seconds on average. However, only 3 of 11 animals from the 6-OHDA+NaCl group were able to reach the safety platform. Other rats demonstrated freezing behavior and could not finish the test. Therefore, we used an additional scale to assess the neurotic-like behavior of the animals (Table 2). The rats that had received carnosine or LA did not have pronounced neurological symptoms. The post hoc analysis revealed no significant differences between any of these groups and the controls. At the same time, the differences between these 2 groups and the 6-OHDA+NaCl group were significant (Table 2).

No significant changes in horizontal activity were observed between the experimental groups in the OF test ($F(3.36) = 1.83$; $p = 0.16$). However, paired sample comparison demonstrated significant differences between the control and the 6-OHDA+NaCl groups (7.97 ± 0.42 and 4.21 ± 0.77, respectively; $p = 0.001$). ANOVA suggested a change in vertical activity ($F(3.36) = 3.04$; $p = 0.04$). The post hoc analysis revealed that vertical activity was low only in the 6-OHDA+NaCl group, in contrast to the animals who had been treated with carnosine or LA (Table 2).

Quantification of dopaminergic neurons

The number of dopaminergic neurons in SNpc was inferred from the immunohistochemical localization of TH, the marker of dopamine neurons. Staining for TH was indicative of neuronal loss in the midbrain sections of all animals injected with 6-OHDA ($F(3.10) = 6.33$; $p = 0.01$) (Fig. 1); it also showed that AO had produced no therapeutic effect ($F(2.8) = 0.51$; $p = 0.61$). For example, the examined regions of SNpc of the control animals contained an average of 166 ± 48 neurons, whereas all rats exposed to 6-OHDA had only 4 ± 2 neurons ($p = 0.01$). These findings confirm the validity of our experimental model.

Concentrations of amine neurotransmitters and their metabolites

ANOVA results suggested that the levels of major amine neurotransmitters and their metabolites were changed in the right striatum only, where the neurotoxin had been injected ($F(21.81) = 3.29$; $p = 0.001$), in comparison with the left brain hemisphere ($F(21.69) = 1.15$; $p = 0.32$). However, paired comparison of the 6-OHDA+NaCl and control groups revealed a significant increase in DOPAC (by 19.0 ± 5.3%) and HVA (by 19.1 ± 3.8%) concentrations in the left-brain hemisphere following the 6-OHDA injection (Fig. 2). Carnosine brought DOPAC levels down to the values registered in the control group.

The levels of DA and its major metabolites in the right striatum plummeted by an average of 90% in all animals

Table 2. The effects of carnosine and lipoic acid (LA) on rat performance in the tapered beam walking (BW) test and the open field (OF) test. The table shows the results of the post hoc Tukey's HSD test

	BW score	Horizontal activity in OF (distance, m)	Vertical activity in OF (rearings, number of)
Control group	5.13 ± 0.64	7.97 ± 0.42	11.88 ± 1.61
6-OHDA + NaCl	13.60 ± 1.53#	4.21 ± 0.77	4.20 ± 1.52#
6-OHDA + Carnosine	7.18 ± 1.05*	6.32 ± 1.38	8.64 ± 1.50
6-OHDA + LA	5.27 ± 1.27*	6.16 ± 1.14	9.90 ± 2.29

Note: * — difference from the 6-OHDA + NaCl group is significant, $p < 0.05$; # — difference from the control group is significant, $p < 0.05$.

exposed to the neurotoxin regardless of the therapy they had received (Fig. 3). 3-MT concentrations demonstrated a less pronounced decline (by 58%, on average).

Serotonin levels did not change significantly. 5-HIAA, one of serotonin metabolites, was elevated by 38% in the experimental groups, as compared to the controls (Fig. 4).

A 5.8-fold ($p = 0.007$) increase in the striatal DA content was observed in the animals treated with carnosine, relative to the 6-OHDA+NaCl group. The levels of DA metabolites (DOPAC and HVA) were elevated 3.4-fold ($p = 0.04$) and 8.8-fold ($p = 0.01$), respectively, following carnosine administration. LA injections caused a 4.7-fold ($p = 0.03$) and a 7.4-fold ($p = 0.04$) increase in DOPAC and HVA, respectively (Fig. 3). The tested AO induced no changes in 3-MT levels. There was a 23% ($p = 0.006$) and 36% ($p = 0.009$) decline in the concentrations of serotonin and its metabolite 5-HIAA, respectively, relative to the 6-OHDA+NaCl group. Carnosine did not have any effect on the levels of serotonin or its metabolites.

DISCUSSION

We attempted to comprehensively assess the effect of carnosine and LA on the performance of rats with induced parkinsonism in the behavioral tests and on the metabolism of DA and serotonin in the striatum. The pathology was induced by a unilateral injection of 6-OHDA into the SN; the first injection of AO was made on day 14 after surgery to prevent their effect on the autoxidation of the toxin and the occurred neuronal loss.

The death of neurons and ipsilateral striatal denervation were confirmed by immunohistochemistry (immunostaining of dopaminergic neurons in SN) and a significant decline in DA and its metabolites in the striatum of the right brain hemisphere, where the toxin had been injected. Regardless of the treatment applied, DA and its metabolites were lower in the animals exposed to 6-OHDA than in the control group. At the same time, carnosine and LA affected DA metabolism and caused an increase in DA metabolites, in comparison with the group of untreated 6-OHDA-exposed animals. However, DA levels were significantly elevated only in the group of animals treated with carnosine. Serotonin and 5-HIAA concentrations were lower in the group treated with LA than in the untreated 6-OHDA-exposed group. Considering that serotonin stimulates neurochemical mechanisms promoting motor dysfunction in PD and that low serotonergic neurotransmission in the basal ganglia has an antiparkinsonian effect [11], the impact of LA on serotonergic innervation may contribute to the improvement of motor function in parkinsonism.

Physiological tests revealed that neurological deficit and behavioral symptoms were significantly attenuated in the animals treated with both tested antioxidants. Four injections of carnosine and LA on days 14 through 20 of the experiment prevented the development of 6-OHDA-induced neurotic symptoms.

Studies involving the use of rat models of toxin-induced parkinsonism have demonstrated neuroprotective effects of both carnosine [12] and lipoic acid [13]. These drugs restored the antioxidant brain status and reduced peroxide oxidation. Besides, lipoic acid improved motor function in the affected animals [13]. However, in the studies cited above the drugs and the toxin were administered simultaneously and the loss of neurons in the SN was not assessed. This complicated interpretation of the results and left open the question about

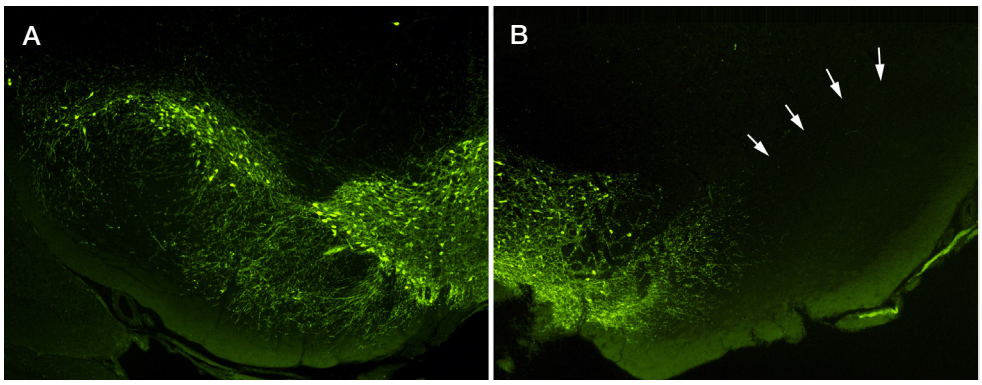

Fig. 1. Immunostaining for tyrosine hydroxylase in the SN of rats following the intranigral injection of 6-hydroxydopamine. **A**. Left brain hemisphere of an animal injected with saline. **B**. Right brain hemisphere of an animal injected with 6-OHDA. Arrows point to the region of neuronal loss in the SN at x10 magnification

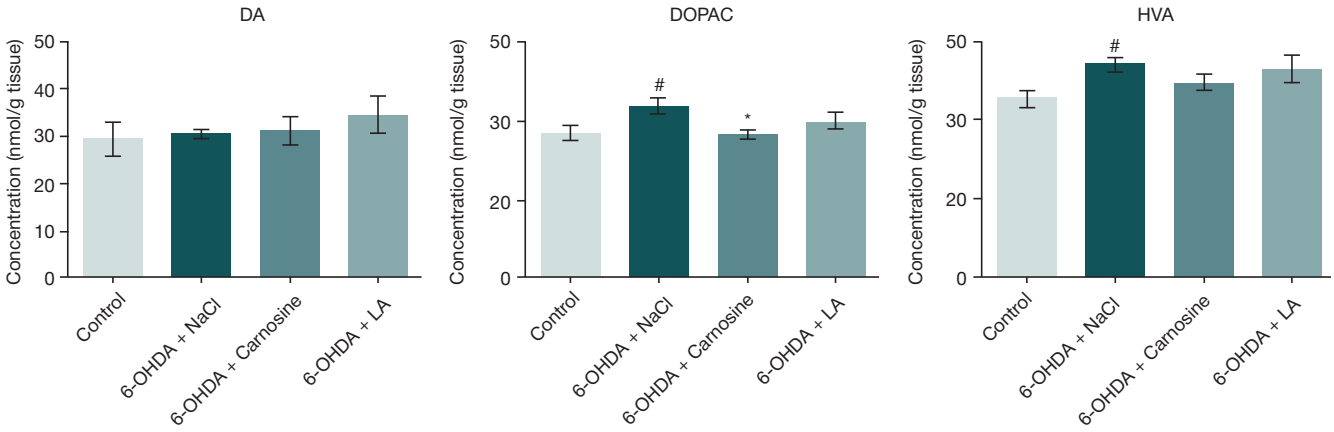

Fig. 2. Effects of carnosine and lipoic acid (LA) on the levels of dopamine (DA), 3,4-dihydroxyphenylacetic acid (DOPAC) and homovanillic acid (HVA) in the left striatum. # — difference from the control group is significant, $p < 0.05$; * — difference from the 6-OHDA+NaCl group is significant, $p < 0.05$

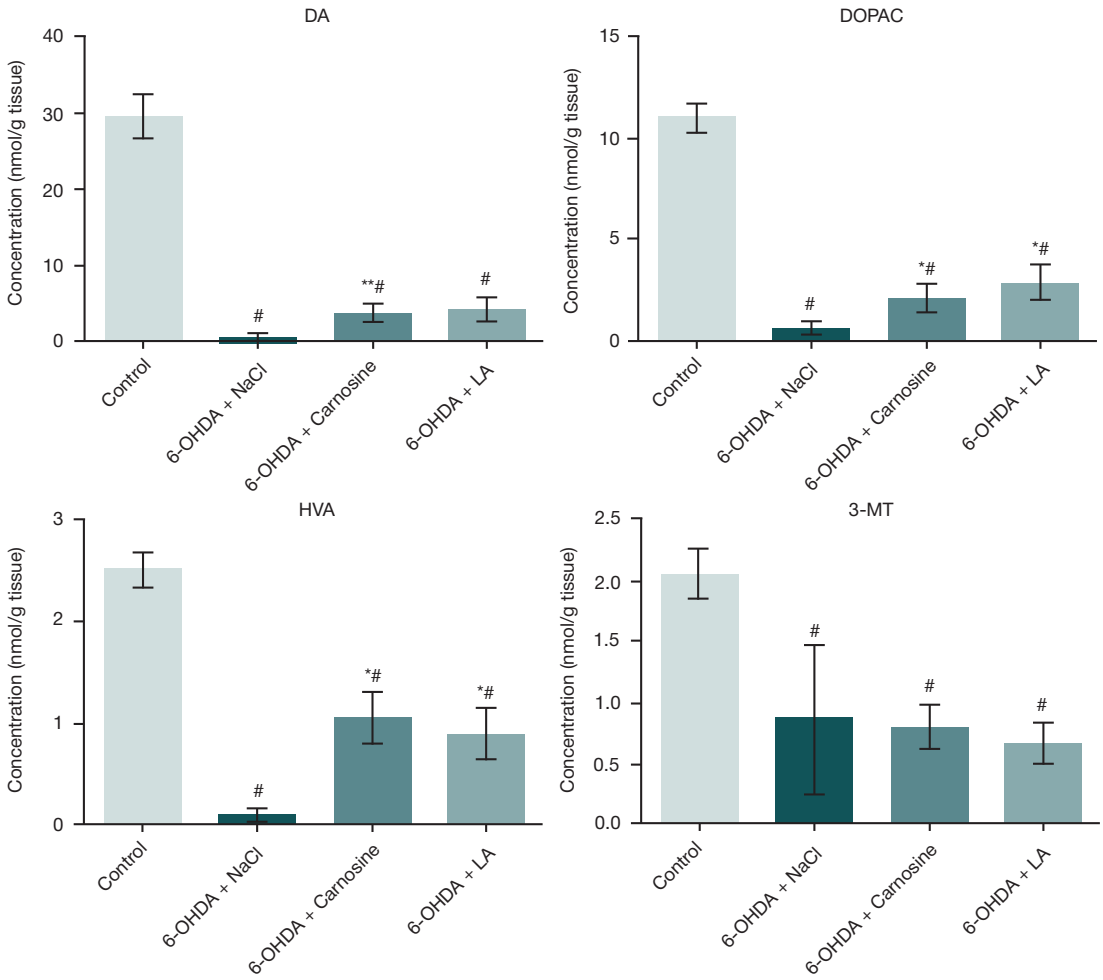

Fig. 3. Effects of carnosine and lipoic acid (LA) on the levels of dopamine (DA), 3,4-dihydroxyphenylacetic acid (DOPAC), homovanillic acid (HVA), and 3-methoxytyramine (3-MT) in the right striatum. # — difference from the control group is significant, $p < 0.05$; * — difference from the 6-OHDA+NaCl group is significant, $p < 0.05$; ** — $p < 0.01$

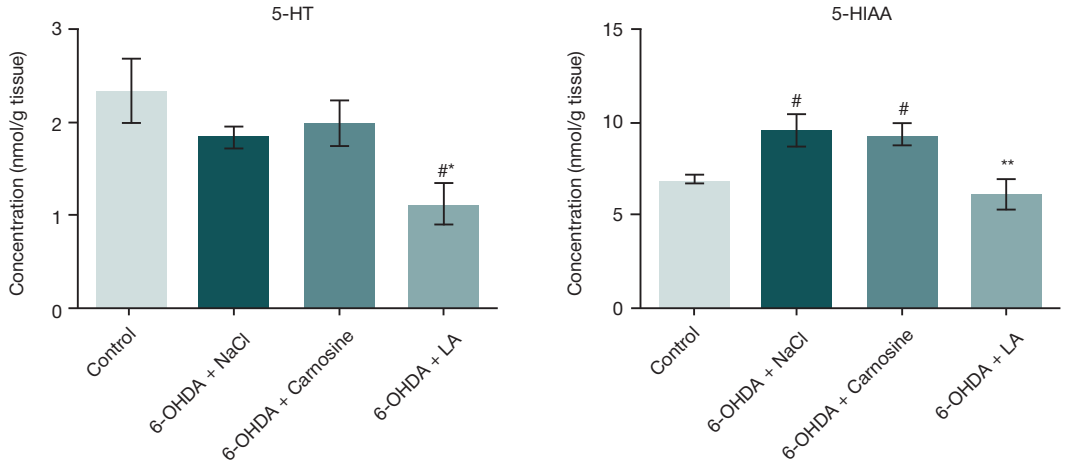

Fig. 4. Effects of carnosine and lipoic acid (LA) on the levels of serotonin (5-HT) and 5-hydroxyindoleacetic acid (5-HIAA) in the right striatum. # — difference from the control group is significant, $p < 0.05$; * — difference from the 6-OHDA+NaCl group is significant, $p < 0.05$; ** — $p < 0.01$

the mechanisms of action of these compounds. Our study provides evidence of symptomatic relief produced by the tested drugs in the late stage of induced parkinsonism.

On the whole, our findings suggest that the tested antioxidants could be used as an adjunctive component to conventional antiparkinsonian therapy. Previously, lipoic acid was proposed for use in combination with levodopa [14], and the combination regimen of carnosine and levodopa was reported to be effective [15].

CONCLUSOINS

Although carnosine and LA did not have a direct neuroprotective effect, they attenuated parkinsonian symptoms due to a compensatory increase in the levels of DA and its metabolites and a simultaneous decrease in serotonin concentrations. Our findings suggest that the tested antioxidants could be used in combination with conventional antiparkinsonian drugs and provide a symptomatic relief.

References

1. Sarkar S, Raymick J, Imam S. Neuroprotective and Therapeutic Strategies against Parkinson's Disease: Recent Perspectives. Int J Mol Sci. 2016; 17 (6): E904. DOI: 10.3390/ijms17060904. PMID: 27338353.
2. Illarioshkin SN, Slominsky PA, Shadrina MI, Bagyeva GKh, Zagorovskaya TB, Markova ED, et al. The heterogeneity of sporadic Parkinson's disease: a molecular approach to solving a problem. Annaly Klinicheskoy I Experimental`noy Nevrologii. 2007; 1 (1): 23–31. Russian.
3. Mazzio EA, Reams RR, Soliman KF. The role of oxidative stress, impaired glycolysis and mitochondrial respiratory redox failure in the cytotoxic effects of 6-hydroxydopamine in vitro. Brain Research. 2004; 1004 (1): 29–44.
4. Jeon BS, Jackson-Lewis V, Burke RE. 6-Hydroxydopamine lesion of the rat substantia nigra: time course and morphology of cell death. Neurodegeneration. 1995: 4 (2): 131–7.
5. Zbarsky V, Datla KP, Parkar S, Rai DK, Aruoma OI, Dexter DT. Neuroprotective properties of the natural phenolic antioxidants curcumin and naringenin but not quercetin and fisetin in a 6-OHDA model of Parkinson's disease. Free Radic Res. 2005; 39 (10): 1119–25. PMID: 7583676.
6. Soto-Otero R, Mendez-Alvarez E, Hermida-Ameijeiras A, Muñoz-Patiño AM, Labandeira-Garcia JL. Autoxidation and neurotoxicity of 6-hydroxydopamine in the presence of some antioxidants: potential implication in relation to the pathogenesis of Parkinson's disease. J Neurochem. 2000; 74 (4): 1605–12. DOI: 10.1046/j.1471-4159.2000.0741605.x. PMID: 10737618.
7. Kulikova OI, Berezhnoy DS, Stvolinsky SL, Lopachev AV, Orlova VS, Fedorova TN. Neuroprotective effect of the carnosine — alpha-lipoic acid nanomicellar complex in a model of early-stage Parkinson's disease. Regul Toxicol Pharmacol. 2018; 95: 254–9. DOI: 10.1016/j.yrtph.2018.03.025. PMID: 2960191.
8. Paxinos G, Watson C. The Rat Brain in Stereotaxic Coordinates. 6th Edition. San Diego: Academic Press, 2006. 456 p.
9. Bolotova VTs, Krauz VA, Shustov EB. Biological model of experimental neurosis in laboratory animals. Biomedicina. 2015; (1): 66–80. Russian.
10. Khudoerkov RM, Voronkov DN, Dikalova YuV. Quantitative morphochemical characteristics of the neurons of the rat brain's substantia nigra and its volume reconstruction. Bull experiment biol and medicine. 2013; 156 (6): 861–4. Russian.
11. Kryzhanovsky GN, Magaeva SV, Trekova HA, Vetrila LA, Basharova LA, Atadzhanov MA. Participation of the serotonergic apparatus of the striatum in the Parkinsonian syndrome. Bull experiment biol and medicine. 1993; (5): 466–9. Russian.
12. Zhao J, Shi L, Zhang LR. Neuroprotective effect of carnosine against salsolinol-induced Parkinson's disease. Exp Ther Med. 2017; 14 (1): 664–70.
13. de Araujo DP, De Sousa CN, Araujo PV, Menezes CE, Sousa Rodrigues FT, Escudeiro S S, et al. Behavioral and neurochemical effects of alpha-lipoic Acid in the model of Parkinson's disease induced by unilateral stereotaxic injection of 6-OHDA in rat. Evid Based Complement Alternat Med. 2013; (1): 571–8.
14. Di Stefano A, Sozio P, Cocco A, Iannitelli A, Santucci E, Costa M, et al. L-dopa- and dopamine-(R)-alpha-lipoic acid conjugates as multifunctional codrugs with antioxidant properties. J Med Chem. 2006; 49 (4): 1486–93.
15. Fedorova TN, Bagieva GH, Stepanova MS, Dobrotvorskaya MS, Ivanova-Smolenskaya IA, Polevaya EV, et al. Effectivity of carnosine in Parkinson's disease. Neurological bull. 2009; 41 (1): 24–9. Russian.

Литература

1. Sarkar S, Raymick J, Imam S. Neuroprotective and Therapeutic Strategies against Parkinson's Disease: Recent Perspectives. Int J Mol Sci. 2016; 17 (6): E904. DOI: 10.3390/ijms17060904. PMID: 27338353.
2. Иллариошкин С. Н., Сломинский П. А., Шадрина М. И., Багыева Г. Х., Загоровская Т. Б., Маркова Е. Д. и др. Гетерогенность спорадической болезни паркинсона: молекулярный подход к решению проблемы. Анналы клинической и экспериментальной неврологии. 2007; 1 (1): 23–31.
3. Mazzio EA, Reams RR, Soliman KF. The role of oxidative stress, impaired glycolysis and mitochondrial respiratory redox failure in the cytotoxic effects of 6-hydroxydopamine in vitro. Brain Research. 2004; 1004 (1): 29–44.
4. Jeon BS, Jackson-Lewis V, Burke RE. 6-Hydroxydopamine lesion of the rat substantia nigra: time course and morphology of cell death. Neurodegeneration. 1995: 4 (2): 131–7.
5. Zbarsky V, Datla KP, Parkar S, Rai DK, Aruoma OI, Dexter DT. Neuroprotective properties of the natural phenolic antioxidants curcumin and naringenin but not quercetin and fisetin in a 6-OHDA model of Parkinson's disease. Free Radic Res. 2005; 39 (10): 1119–25. PMID: 7583676.
6. Soto-Otero R, Mendez-Alvarez E, Hermida-Ameijeiras A, Muñoz-Patiño AM, Labandeira-Garcia JL. Autoxidation and neurotoxicity of 6-hydroxydopamine in the presence of some antioxidants: potential implication in relation to the pathogenesis of Parkinson's disease. J Neurochem. 2000; 74 (4): 1605–12. DOI: 10.1046/j.1471-4159.2000.0741605.x. PMID: 10737618.
7. Kulikova OI, Berezhnoy DS, Stvolinsky SL, Lopachev AV, Orlova VS, Fedorova TN. Neuroprotective effect of the carnosine — alpha-lipoic acid nanomicellar complex in a model of early-stage Parkinson's disease. Regul Toxicol Pharmacol. 2018; 95: 254–9. DOI: 10.1016/j.yrtph.2018.03.025. PMID: 2960191.
8. Paxinos G, Watson C. The Rat Brain in Stereotaxic Coordinates. 6th Edition. San Diego: Academic Press, 2006. 456 p.
9. Болотова В. Ц., Крауз В. А., Шустов Е. Б. Биологическая модель экспериментального невроза у лабораторных животных. Биомедицина. 2015; (1): 66–80.
10. Худоерков Р. М., Воронков Д. Н., Дикалова Ю. В. Количественная морфохимическая характеристика нейронов черной субстанции мозга крысы и ее объемная реконструкция. Бюллетень экспериментальной биологии и медицины. 2013; 156 (6): 861–4.
11. Крыжановский Г. Н., Магаева С. В., Трекова Н. А., Ветрилэ Л. А., Башарова Л. А., Атаджанов М. А. Участие серотонинергического аппарата стриатума в паркинсоническом синдроме. Бюлл. эксперим. биол. и медицины. 1993; (5): 466–9.
12. Zhao J, Shi L, Zhang LR. Neuroprotective effect of carnosine against salsolinol-induced Parkinson's disease. Exp Ther Med. 2017; 14 (1): 664–70.
13. de Araujo DP, De Sousa CN, Araujo PV, Menezes CE, Sousa Rodrigues FT, Escudeiro S S, et al. Behavioral and neurochemical effects of alpha-lipoic Acid in the model of Parkinson's disease induced by unilateral stereotaxic injection of 6-OHDA in rat. Evid Based Complement Alternat Med. 2013; (1): 571–8.
14. Di Stefano A, Sozio P, Cocco A, Iannitelli A, Santucci E, Costa M, et al. L-dopa- and dopamine-(R)-alpha-lipoic acid conjugates as multifunctional codrugs with antioxidant properties. J Med Chem. 2006; 49 (4): 1486–93.
15. Федорова Т. Н., Багыева Г. Х., Степанова М. С., Добротворская И. С., Иванова-Смоленская И. А., Полевая Е. В. и др. Эффективность карнозина при болезни Паркинсона. Неврологический вестник. 2009; 41 (1): 24–9.

BRAIN CONNECTIVITY CHANGES IN PATIENTS WITH WORKING MEMORY IMPAIRMENTS WITH CHRONIC ISCHEMIC CEREBROVASCULAR DISEASE

Fokin VF ✉, Ponomareva NV, Konovalov RN, Krotenkova MV, Medvedev RB, Lagoda OV, Tanashyan MM

Research Center of Neurology, Moscow, Russia

One of the methods of assessment of cognitive functions in patients with chronic ischemic cerebrovascular disease — CICD (dyscirculatory encephalopathy) implies studying connectivity of neural networks through the analysis of rest functional magnetic resonance imaging (rest fMRI) data. The main objective of this study was to assess the relationship between working memory (WM) characteristics and connectivity of various parts of the brain in patients diagnosed with CICD. The study involved 22 female CICD patients; they were divided into two groups, one with satisfactory level of WM and the other with compromised WM. We assessed intra-brain connectivity with the help of rest fMRI, using the SPM-12 and CONN18b software applications in Matlab platform. The other aspects evaluated were the gray to white matter ratio and the association of this indicator with WM. Significant differences in the intra-brain connectivity were registered in both the satisfactory WM group and the compromised WM group. The brain parts where those differences were found are left parahippocampal area and right supramarginal gyrus; right cerebellar hemisphere and left parietal, as well as left frontal areas; right cingular and left lingual gyri. In addition, we detected significant differences in the ratio in the gray and white matter volumes in both groups (p = 0.007). The results obtained indicate that memory deterioration in CICD patients is concomitant with deteriorating connectivity between the cortical areas, as well as between cerebellum and cortex, which may be associated with a more significant loss of the white matter.

Keywords: neuroimaging, rest fMRI, working memory, connectivity, cognitive functions, gray and white matter of the brain, chronic ischemic cerebrovascular disease

Funding: the study was ordered by the Research Center of Neurology (Federal Research Institution).

Author contribution: Fokin VF — data analysis, article authoring; Ponomareva NV — psychometric and neuroimaging data collection and analysis, participation in authoring the article; Konovalov RN — neuroimaging, processing of the results; Krotenkova MV — neuroimaging, analysis of the results; Medvedev RB — clinical examinations, analysis of the literature; Lagoda OV — analysis of the clinical data; Tanashyan MM — generalization of the clinical material in the context of the results obtained.

Compliance with ethical standards: the study was approved by the Research Center of Neurology Ethics Committee (Protocol № 11/14 dated November 19, 2014); all participants signed the voluntary informed consent.

✉ **Correspondence should be addressed:** Vitaly F. Fokin
Volokolamskoye shosse, 80, Moscow, 125367; fvf@mail.ru

Received: 19.08.2019 **Accepted:** 13.09.2019 **Published online:** 22.09.2019

DOI: 10.24075/brsmu.2019.061

ИЗМЕНЕНИЯ КОННЕКТИВНОСТИ ГОЛОВНОГО МОЗГА У БОЛЬНЫХ С НАРУШЕНИЯМИ ВЕРБАЛЬНОЙ ОПЕРАТИВНОЙ ПАМЯТИ ПРИ ДИСЦИРКУЛЯТОРНОЙ ЭНЦЕФАЛОПАТИИ

В. Ф. Фокин ✉, Н. В. Пономарева, Р. Н. Коновалов, М. В. Кротенкова, Р. Б. Медведев, О. В. Лагода, М. М. Танашян

Научный центр неврологии, Москва, Россия

Один из методов оценки когнитивных функций у пациентов с хроническими цереброваскулярными заболеваниями — исследование коннективности нейросетей с помощью анализа показателей функциональной магнитно-резонансной томографии (фМРТ) покоя. Основной целью исследования было оценить взаимосвязь коннективности различных отделов мозга с характеристиками вербальной оперативной памяти (ВОП) у больных с дисциркуляторной энцефалопатией (ДЭ). В исследовании участвовали 22 женщины с ДЭ, разделенные на две группы: с удовлетворительной и сниженной ВОП. У всех пациенток определяли коннективность между различными областями мозга с помощью анализа фМРТ покоя с использованием программных приложений SPM-12 и CONN18b в среде Matlab, а также оценивали отношение объемов серого вещества к белому и сопряженность этого показателя с ВОП. У больных в группе с удовлетворительной ВОП и в группе со сниженной ВОП статистически значимые различия коннективности обнаружены между следующими областями: левой парагиппокампальной областью и правой супрамаргинальной извилиной; правым полушарием мозжечка и левой теменной, а также левой лобной областями; правой поясной и левой язычной извилинами. Кроме того, в обеих группах выявлены статистически значимые различия в отношениях между объемами серого и белого вещества (p = 0,007). Полученные результаты указывают, что снижение памяти у больных с ДЭ сопровождается сокращением коннективности между областями коры, а также между мозжечком и корой, что может быть связано с более значительной утратой белого вещества.

Ключевые слова: дисциркуляторная энцефалопатия, нейровизуализация, фМРТ покоя, вербальная оперативная память, коннективность, когнитивные функции, серое и белое вещество мозга

Финансирование: работа была выполнена в рамках государственного задания ФГБНУ НЦН.

Информация о вкладе авторов: В. Ф. Фокин — анализ данных, написание статьи; Н. В. Пономарева — сбор и анализ психометрических и нейровизуалиционных данных, участие в написании статьи; Р. Н. Коновалов — нейровизуалиционные исследования, обработка результатов; М. В. Кротенкова — нейровизуалиционные исследования, анализ результатов; Р. Б. Медведев — клинические обследования, анализ литературы; О. В. Лагода — анализ клинических данных; М. М. Танашян — обобщение клинического материала в контексте полученных результатов.

Соблюдение этических стандартов: исследование одобрено этическим комитетом Научного центра неврологии (протокол № 11/14 от 19 ноября 2014 г.); все участники подписали информированное согласие на участие в исследовании.

✉ **Для корреспонденции:** Виталий Федорович Фокин
Волоколамское ш., д. 80, г. Москва, 125367; fvf@mail.ru

Статья получена: 19.08.2019 **Статья принята к печати:** 13.09.2019 **Опубликована онлайн:** 22.09.2019

DOI: 10.24075/vrgmu.2019.061

Vascular brain damage in the elderly is an important problem from both the medical and the socio-economic viewpoints. According to a number of researchers, 5 to 22% of the senior citizens are diagnosed with cognitive impairments of vascular origin [1, 2]. In the Russian scientific literature, such disorders are traditionally considered through the lens of chronic ischemic cerebrovascular disease — CICD (dyscirculatory encephalopathy). Mnestic disorders, including working memory (WM) deterioration, occupy a certain place in the clinical picture of CICD [3–5]. From the pathomorphological point of view, CICD-conditioned cognitive impairments result from diffusive and multiple lacunar local changes in the subcortical white matter and cerebral cortex. The most common subcortical disorders are associated with atherosclerotic lesions or lipohyalinosis of the small penetrating arteries delivering blood to the deep parts of the brain [4]. Numerous studies show that from the neurochemical point of view vascular cognitive impairments result from acetylcholinergic deficiency. With CICD in the background, it is brought by the periventricular white matter ischemia, since acetylcholinergic axons pass through the white matter [6]. There is no doubt it is necessary to detect cognitive impairments at an early stage since timely therapy prescribed early yields best results and improves the prognosis. Cognitive activity runs against the background of coordinated processing of information in different areas of the brain. Neural network communication disruptions affect the contiguity of information coming from various areas of the brain, which leads to the cognitive dysfunction. Incomplete synchronization of neocortex with paleocortex and archicortex, subcortex and cerebellum is one of the reasons behind diminution of the higher mental functions, including memory. Aging is one of the factors promoting such processes, especially when there are vascular and neurodegenerative brain diseases in the background; often, they are caused by the diminishing volume of white matter that is a communication medium for the various parts of the brain [7, 8].

Connectivity is the term used to describe the unity of the various components of the system that makes it a single whole, and it is applicable to the brain. The data delivered by rest fMRI that allows evaluating connectivity is the BOLD (blood oxygen level-dependent) signal synchronization in various parts of the brain. According to the rest fMRI and the background electroencephalography data, connectivity is related to the cognitive functions, including memory. In general, deterioration of connectivity between different regions of the brain leads to cognitive dysfunction [9, 10].

Normal functioning of the nerve networks depends on the adequacy of blood supply to metabolic needs. With CICD, connectivity in the neural networks worsens, which is to be expected, as do the cognitive functions. The process is the results of death of neurons and their axons in various parts of the brain. MRI scans of the brain of elder people often exhibit damaged white matter, the lesions actively contributing to the cognitive decline and dementia pathogenesis. Vascular risk factors are connected to the white matter damage, which hinders synchronization between various parts of the brain, especially those remote to each other. In practice, the gray to white matter ratio is a common indicator allowing assessment of damage to the gray or white matter [11, 12].

This study aimed to use rest fMRI data to assess the contingency between WM and connectivity alterations, as well as the gray to white matter ratio, in CICD patients.

METHODS

The study was conducted at the Research Center of Neurology (Federal Research Institution) in 2017–2019. There were 22 patients aged 50–85 years (mean age 64 years) participating in the study, all female. The inclusion criteria were: chronic cerebrovascular diseases (CICD, stage 1–2, the diagnosis complying with the brain and spinal cord vascular trauma classification developed by the RAMS Research Institute of Neurology in 1985); underlying vascular disease and disseminated local neurological symptoms concomitant with cerebral symptoms: headache, dizziness, tinnitus, compromised memory, working ability and intelligence; registered arterial hypertension; cognitive impairment (impaired memory, working ability, irritability) [13]; all patients were right-handed. The exclusion criteria were: mild, moderate or severe dementia under the Clinical Dementia Rating Scale [14] (scores 1 up), as well as a history of acute cerebrovascular accidents; traumatic brain injury; severe cardiac, metabolic (type 2 diabetes mellitus) pathology; renal failure, uncompensated dysfunction of the thyroid gland; MRI contraindications.

The patients did a number of tests before being split into two groups. Psychometric examination implied a Luria test [15] modified for patients with this kind of vascular pathology; the registered outcome was the sum of words remembered by the patients after 5 repetitions (sets of 10 words). The immediate reproduction of the words in the context of this test allowed dividing the patients into two equal groups with the memorized words indicator lower and higher than the median: 27.7 ± 1.4 and 35.8 ± 0.8, respectively. The difference in the immediate words reproduction capability was highly significant between the formed groups ($p = 0.000006$). Agewise, the groups were not statistically different from each other ($p = 0.26$), therefore, they were called the compromised WM group and the satisfactory WM group. The groups also showed different results in the delayed words reproduction part of the test ($p = 0.0008$).

The fluency test (FT) [16] results yielded no differences between the groups (summed fluency; $p = 0.57$).

The correction test results revealed no differences between the groups, too ($p = 0.77$); the test was based on the n-back test (Kirchner, 1958), which describes attention stability and concentration capacity [16].

All participants had their cognitive function assessed using the Montreal Cognitive Assessment (MoCa), a cognitive impairment screening tool. This test also returned no differences between the groups ($p = 0.68$); the average values for both groups were 25.6 ± 1.2 and 25.0 ± 0.9, meaning that cognitive impairments in the patients participating in the study were fairly mild (norm — 26–30 points) [17].

According to the results of the sequential counting test (subtracting sevens from hundred down [15]), the patients were not significantly different.

The rest fMRI the participants underwent followed the BOLD method, sequence T2*; we used the Magnetom Verio MRI system (Siemens; Germany), 3T. The participants were instructed to fully relax, lie calmly with eyes closed (to exclude stimulation of the visual analyzer) and not think about anything specific. We used the SPM12 (Functional Imaging Laboratory at University College London; UK) application in the MATLAB (MathWorks; USA) environment to process the MRI data. As for the connectivity study, our software of choice was the CONN-18b application (McGovern Institute for Brain Research, Massachusetts Institute of Technology; USA) in the SPM-12 toolbox [18]. We assessed connectivity in various neural networks of the brain, including the default mode network (DMN).

We compared connectivity between the two groups defined earlier according to the WM specifics; CONN-18b software (McGovern Institute for Brain Research, Massachusetts Institute of Technology; USA) allowed assessing the significance

of differences using the standardized regression coefficient adjusted for multiple comparisons.

The same CONN 18b application enabled volumetric studies that yielded general assessments of the gray and white matter volume and that of the cerebrospinal fluid (CSF). The CSF volume was the same in both groups (p = 0.58), which signals of the approximately equal level of atrophy in all the participants. We analyzed the gray to white matter ratio.

We used the Statistica-12 package (Dell; USA) for ANOVA and other variance analyses; connectivity assessment was done with the help of SPM-12 and CONN-18b applications in the MATLAB platform. The assessments of connectivity proper and group differences in connectivity were adjusted for multiple comparisons while accounting for the false discovery rate (FDR).

RESULTS

In the compromised WM group of CICD patients, the connectivity of the left frontal parahippocampal area was limited mainly by the subcortical structures (Fig. 1A). In the satisfactory WM group, we registered negative connectivity between left frontal parahippocampal area and right supramarginal gyrus in addition to the subcortex links, which probably signal of the inhibitory nature of these links (Fig. 1B). The intergroup comparison of connectivity revealed significant differences in the quality of the link between left frontal parahippocampal area and right supramarginal gyrus (Fig. 1B).

Significant intergroup differences in connectivity were also observed between the right cerebellar hemisphere (segments 4 and 5) and the neocortex. There were no negative contingency registered between the cortex and the right cerebellar hemisphere in the compromised WM group (Fig. 2). The differences between the groups were significant ($p < 0.05$) (Fig. 2C).

The cingulate gyrus (part of DMN) correlation links were also different in the compared groups (Fig. 3). Satisfactory WM group exhibited higher connectivity between the right cingulate gyrus and the left lingual gyrus than the compromised WM group (Fig. 3C).

The table below shows statistical indicators of all the intergroup differences discovered that are significant with the multiple comparisons factored in.

Since CICD typically translates into damage to white matter, it is possible that the deterioration of connectivity and memory is associated with the decreasing volume of white matter. We have registered significant differences in gray to white matter ratio between the satisfactory and compromised WM groups. The latter has it significantly higher than the former (p = 0.007) (Fig. 4). This fact signals of a relatively large loss of white matter in patients with compromised memory.

DISCUSSION

CICD patients suffer from progressive memory impairment that mainly affects reproduction of the memorized material [6]. At the early stages of cognitive decline, some CICD patients exhibit WM of the same level as healthy individuals, but it naturally deteriorates with time [19]. In this work, we attempted to study the pathogenetic mechanisms behind deterioration of the verbal operative memory in CICD patients, specifically those related to the changes in functional connectivity of the brain's neural networks. Memory impairment is usually associated with the damage to hippocampus and entorhinal cortex. We registered no significant differences in hippocampus connectivity between satisfactory WM and compromised WM groups; however, such differences were found in the parahippocampal area, where neocortex connects with allocortex. This area receives cognitive and sensory information from the association cortex and passes it to the hippocampus for transition to the long-term memory. Supramarginal gyrus participates in the working memory functions: it helps integrate auditory and visual information. Therefore, the higher connectivity of the parahippocampal area and the supramarginal gyrus registered in the satisfactory WM group were to be expected [19].

Cognitive decline is also associated with the cerebellum. The satisfactory WM group exhibited a significant negative connectivity between cerebellum's right hemisphere (segments 4 and 5), cortex and subcortex. CICD-conditioned operative memory deterioration results from the significant diminution of connectivity between cortex and cerebellum while maintaining connectivity at the subcortex level. The cerebellum is associated mainly with various motor functions. However, in the second half of the past century researchers started to point to the non-motor functions, including cognitive, that the cerebellum partakes in. Interestingly, motor impairments in CICD patients often go in parallel with the cognitive function deterioration. Primarily, the functions in question are those governing speech, learning and memory [20, 21]. In the cerebellum, these functions employ spatially separated areas; the memory is associated with segments of 4, 5, and 6 [22]. There is a growing body of data revealing involvement of the cerebellum in regulation of sensorimotor, vestibular and cognitive functions [23]. In our studies, WM was also associated with the 4th and 5th segments of the cerebellum. Investigation of the cerebellum's functional topography revealed connections between its frontal part, sensorimotor functions and, what is more, cognitive functions, as well as a number of neural networks, including DMN, frontoparietal networks, etc. It is likely that the neocortex-cerebellum discord evidenced by the deteriorating connectivity

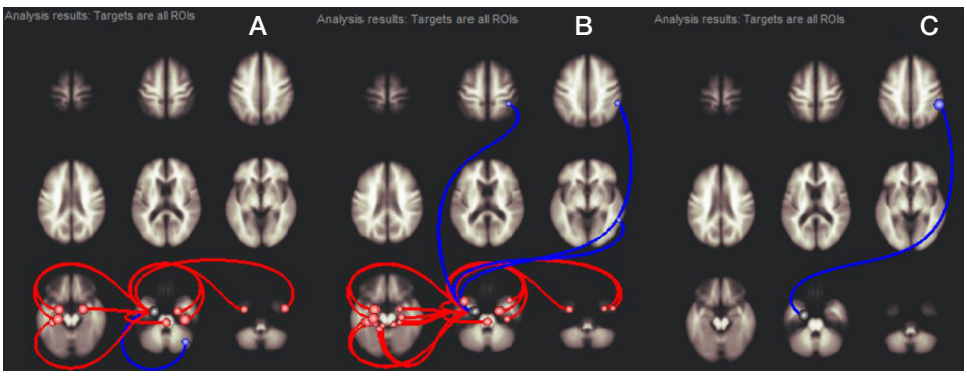

Fig. 1. Left frontal parahippocampal area connectivity to various brain structures; compromised WM group (**A**) and satisfactory WM group (**B**). **C**. Intergroup connectivity comparison (**B**–**A**). Red lines show positive correlation; blue lines show negative correlation. Blue lines in the Figure **B** indicate significant differences in patients with satisfactory WM compared to patients with compromised WM. Only statistically significant relationships are given, FDR-adjusted for multiple comparisons ($p < 0.05$)

against the background of a developing CICD also contributes to the motor and cognitive function impairments.

DMN also plays a significant role in the memory processes [24]. The lingual gyrus aides visual information processing; it is significantly better connected to the DMN in individuals with satisfactory level of WM.

It can be assumed that the decreasing volume of white matter, which is peculiar to normal aging and aging conditioned by a vascular disease, is one of the reasons behind connectivity and memory deterioration. CICD development translates into damage to the white matter, and it often leads to violations of the gray to white matter ratio, which integratively reflects the predominant loss of gray or white matter. As the diffusion tensor tomography examinations undertaken in the context of longitudinal studies show, maturation of neural connections and development of the fine structure of white matter contribute to growth of the working memory volume [12, 25]. The loss of the white matter volume peculiar to Alzheimer's and Kreutzfeldt–Jacob neurodegenerative diseases directly correlates with the working memory deflation [26, 27]. Almost every case of CICD has concomitant arterial hypertension. The blood pressure spikes registered in the elder people complaining about memory deterioration occurred against the background of degenerative changes of not only gray but also white matter, the changes closely resembling those peculiar to the early stages of the Alzheimer's [28]. Overall, white matter lesions (leukoaraiosis) in the presence of CICD correlates with the cognitive decline [29]. It is clear that the decrease in the volume of white matter is directly proportional to the loss of long-axon neurons, including those that participate in the interaction of neocortex, subcortex, and cerebellum, as well as cortex-to-cortex integration.

Thus, it seems likely that the operative memory deterioration in CICD patients is largely associated with the loss of the white matter.

CONCLUSIONS

1. WM impairments in CICD patients are more significant with the decreasing functional connectivity in the brain neural networks, as registered with fMRI. 2. Significant differences

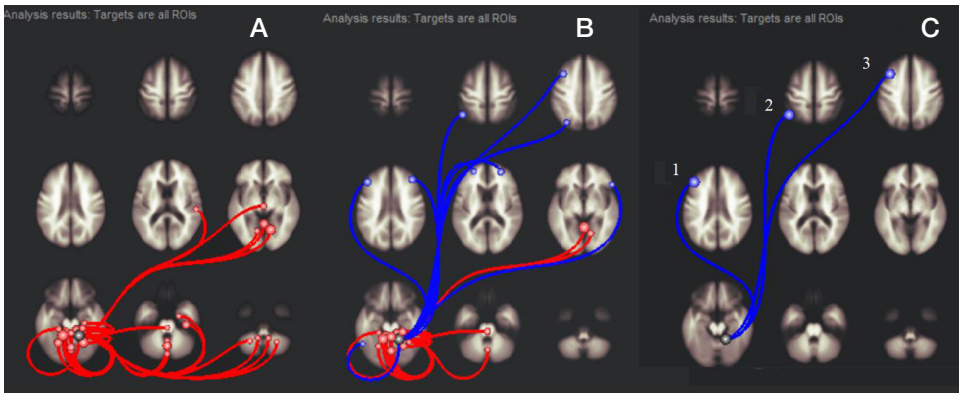

Fig. 2. Connectivity of segments 4 and 5 of the right cerebellum hemisphere to the various brain structures, compromised WM group and satisfactory WM group. Segments 4–5 belong to the frontal cerebellum. **A**. Compromised WM group. **B**. Satisfactory WM group. **C**. Difference in connectivity (**B**–**A**). 1, 2 — areas of interest are in the left frontoparietal network (FPN); 3 — middle frontal gyrus

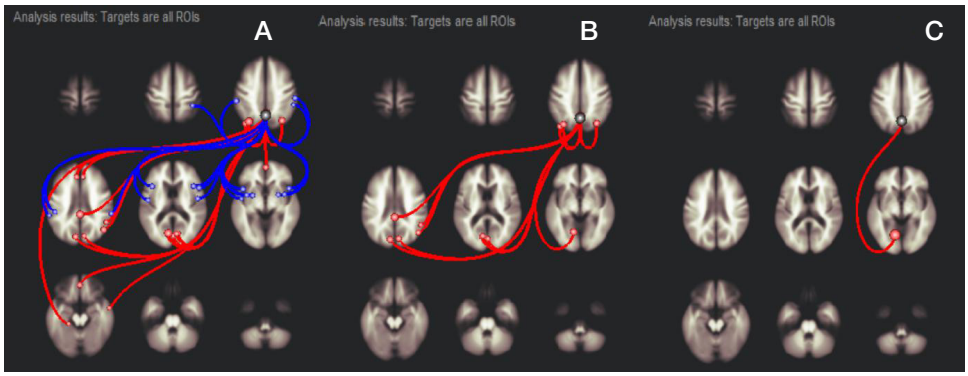

Fig. 3. Connectivity of the right cingulate gyrus posterior (part of DMN), compromised WM group and satisfactory WM group. (See Figures 1 and 2 for designations.) Intergroup differences in connectivity found between the right cingulate gyrus and the left lingual gyrus

Table. Statistical indicators of intergroup differences, satisfactory WM group and compromised WM group

Areas of interest	Beta	T-test	Unadjusted significance level	FDR-adjusted *p*-value
L-FPN, frontal region — cerebellum	–0.18	–4.46	0.000242	0.02196
L-FPN, parietal region — cerebellum	–0.23	–4.41	0.000268	0.02196
MFG — cerebellum	–0.21	–4.05	0.000622	0.03401
L-PHA — R-SMG	–0.30	–5.33	0.000032	0.00524
DMN — L-LG	0.25	4.43	0.000259	0.04240

Note: beta — standardized regression coefficient; FDR — false discovery rate; negative beta and T-test mean negative connectivity; L — left; R — right; FPN — frontoparietal network; MFG — middle frontal gyrus; PHA — parahippocampal area; SMG — supramarginal gyrus; DMN — default mode network; LG — lingual gyrus.

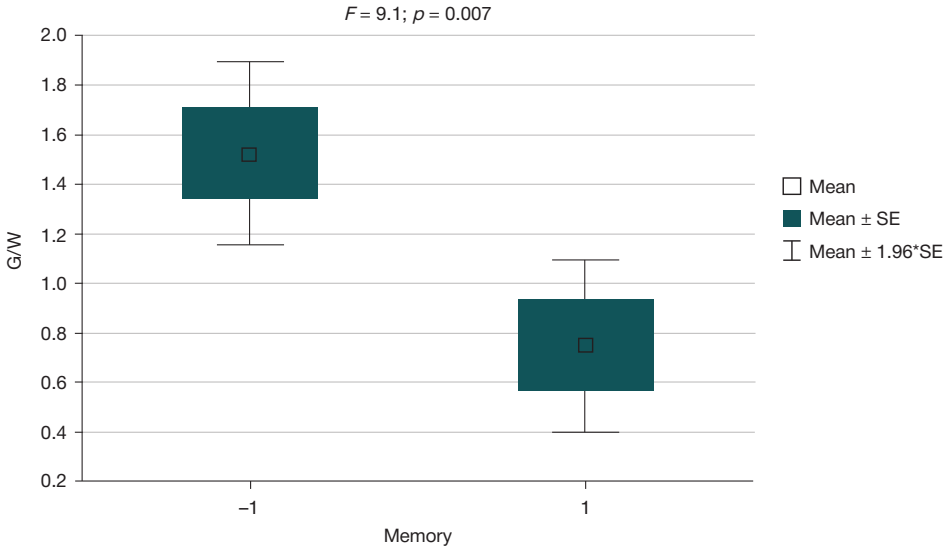

Fig. 4. WM and the relationship between the volume of gray and white matter (G/W). "–1" and "1" — compromised and satisfactory WM groups of CICD patients, respectively. Gray (G) to white (W) matter volume ratio (Y-axis). Statistical indicators of differences between groups: *F* — Fisher's test, *p* — level of significance (*above*)

in the intra-brain connectivity were registered in both the satisfactory WM group and the compromised WM group. The brain parts where those differences were found are right cerebellar hemisphere and left parietal, as well as left frontal areas; left parahippocampal area and right supramarginal gyrus; right cingulate and left lingual gyri. 3. There are significant differences between gray to white matter ratios in patients with satisfactory and compromised memory; memory deterioration is concomitant with the greater loss of white matter. 4. Connectivity alteration reflects pathophysiological mechanisms of the WM disorders that mainly depend on the loss of white matter. Further research would allow evaluating prognostic significance of the revealed decrease in the WM-related connectivity in CICD patients.

References

1. Levin OS. Discirkuljatornaja jencefalopatija: sovremennye predstavlenija o mehanizmah razvitija i lechenii. Consilium medicum. 2007; (8): 72–9.
2. Yahno NN, Zaharov VV, Lokshina AB, Koberskaya NN, Mhitaryan EA. Demencii: rukovodstvo dlja vrachej. M.: MEDpress-inform, 2013; 264 s.
3. Jahno NN. Kognitivnye narushenija v nevrologicheskoj praktike. Nevrologicheskij zhurnal. 2006; 11 (1): 4–12.
4. Tanashyan MM, Medvedev RB, Evdokimenko AN, Gemdzhyan EG, Ckrylev SI, Lagoda OV, i dr. Prognozirovanie ishemicheskih povrezhdenij golovnogo mozga pri rekonstruktivnyh operacijah na vnutrennih sonnyh arterijah. Angiologija i sosudistaja hirurgija. 2017; 23 (1): 59–65.
5. Levin OS, Anikina MA, Vasenina EE. Kognitivnye i nejropsihiatricheskie rasstrojstva pri jekstrapiramidnyh zabolevanijah. Nevrologija, nejropsihiatrija, psihosomatika. 2012; 4 (2S): 22–30.
6. Zaharov VV. Lokshina AB. Kognitivnye narushenija pri discirkuljatornoj jencefalopatii. RMZh. 2009; (20): 1325–31.
7. Bennett IJ, Madden DJ. Disconnected Aging: Cerebral White Matter Integrity and Age-Related Differences in Cognition. Neuroscience. 2014; r. 187–205. Published online 2013 Nov 23. DOI: 10.1016/j.neuroscience.2013.11.026.
8. van Kesteren MTR, Fernández G, Norris DG, Hermans EJ. Persistent schema-dependent hippocampal-neocortical connectivity during memory encoding and postencoding rest in humans. PNAS. 2010; 107 (16): 7550–5; Available from: https://doi.org/10.1073/pnas.0914892107.
9. Piradov MA, Suponeva NA, Seliverstov YuA, i dr. Vozmozhnosti sovremennyh metodov nejrovizualizacii v izuchenii spontannoj aktivnosti golovnogo mozga v sostojanii pokoja. Nevrologicheskij zhurnal. 2016; 21 (1): 4–12. DOI: 10.18821/1560-9545-2016-21-1-4-12.
10. Ponomareva NV, Fokin VF, Rogaev EI, Illarioshkin SN. Vlijanie geneticheskih faktorov na nejrofiziologicheskie mehanizmy nejrodegenerativnyh zabolevanij. Annaly klinicheskoj i jeksperimental'noj nevrologii. 2018: 12 (special'nyj vypusk): 46–54. DOI: 10.25692/ACEN.2018.5.6.
11. Andreone BJ, Lacoste B, Gu Ch. Neuronal and vascular interactions. Annu Rev Neurosci. 2015; (38): 25–46. DOI: 10.1146/annurev-neuro-071714-033835.
12. de Leeuw FE, de Groot JC, Oudkerk M, Witteman JC, Hofman A, et al. Hypertension and cerebral white matter lesions in a prospective cohort study. Brain. 2002; 125 (4): 765–72.
13. Tanashjan MM, Maksimova MYu, Domashenko MA. Discirkuljatornaja jencefalopatija. Putevoditel' vrachebnyh naznachenij. Terapevticheskij spravochnik. 2015; (2): 1–25.
14. Hughes CP, Berg L, Danziger WL, Coben LA, Martin RL. A new clinical scale for the staging of dementia. Br J Psychiatry. 1982; (140): 566–72.
15. Luriya AR, Simernickaya YeG. O funkcional'nom vzaimodejstvii polusharij golovnogo mozga v organizacii verbal'no-mnesticheskih funkcij. Fiziologija cheloveka. 1975; 1 (3): 411–7.
16. Fokin VF, Shabalina AA, Ponomareva NV, Medvedev RB, Lagoda OV, Tanashyan MM. Soprjazhennost' pokazatelej jenergeticheskogo obmena i urovnja gormona stressa kortizola s kognitivnymi harakteristikami bol'nyh discirkuljatornoj jencefalopatiej. Annaly klinicheskoj i jeksperimental'noj nevrologii. 2018; 4 (12): 47–51.
17. Kasten M, Bruggemann N, Schmidt A, Klein Ch. Validity of the MoCA and MMSE in the detection of MCI and dementia in Parkinson disease. Neurology. 2010; 75 (5): 478–9. DOI:10.1212/WNL.0b013e3181e7948a.
18. Whitfield-Gabrieli S, Nieto-Castanon A. Conn: A Functional Connectivity Toolbox for Correlated and Anticorrelated Brain Networks. Brain Connect. 2012; 2 (3): 125–41. DOI: 10.1089/brain.2012.0073.
19. Eichenbaum H, Lipton PA. Towards a Functional Organization of the Medial Temporal Lobe Memory System: Role of the Parahippocampal and Medial Entorhinal Cortical Areas. Hippocampus. 2008; (1) 8: 1314–24.

20. Desmond JE, Fiez JA. Neuroimaging studies of the cerebellum: language, learning and memory. Trend in Cognivity Sciences 1998; 2 (9): 355–61.
21. Larsell O, Jansen J. The human cerebellum, cerebellar connections, and cerebellar cortex. Univerity of Minnesota Press, 1972; 201 p.
22. Habas Ch, Kamdar N, Nguyen D, Prater R, Beckmann ChF, et al. Distinct cerebellar contributions to intrinsic connectivity networks. The Journal of Neuroscience. 2009; 29 (26): 8586–94.
23. Schmahmann JD, The cerebellum and cognition. Neuroscience Letters. 2018; Available from: https://DOI.org/10.1016/j.neulet.2018.07.005.
24. Beason-Held LL, Hohman TJ, Venkatraman VAJ, Resnick SM. Brain Network Changes and Memory Decline in Aging. Brain Imaging Behav. 2017; 11 (3): 859–73. DOI: 10.1007/s11682-016-9560-3.
25. Krogsrud SK, Fjell AM, Tamnes ChK. Development of white matter microstructure in relation to verbal and visuospatial working memory — A longitudinal study. PLoS One. 2018; 13 (4): e0195540. Published online 2018. DOI: 10.1371/journal.pone.0195540.
26. Caverzasi E, Mandelli ML, DeArmond SJ, et al. White matter involvement in sporadic Creutzfeldt-Jakob disease. Brain. 2014; 137 (12): 3339–54. Published online 2014 Nov 3. DOI: 10.1093/brain/awu298.
27. Caballero MAA, Suárez-Calvet M, Duering M. White matter diffusion alterations precede symptom onset in autosomal dominant Alzheimer's disease. Brain. 2018; 141 (10): 3065–80. Published online 2018. DOI: 10.1093/brain/awy229.
28. Chetouani A, Chawki MB, Hossu G. Cross-sectional variations of white and grey matter in older hypertensive patients with subjective memory complaints. Neuroimage Clin. 2018; (17): 804–10. Published online 2017. DOI:10.1016/j.nicl.2017.12.024.
29. Levin OS. Patologija belogo veshhestva pri discirkuljatornoj jencefalopatii: diagnosticheskie i terapevticheskie aspekty. Trudnyj pacient. 2011; (12): 16–24.

Литература

1. Левин О. С. Дисциркуляторная энцефалопатия: современные представления о механизмах развития и лечении. Consilium medicum. 2007; (8): 72–9.
2. Яхно Н. Н., Захаров В. В., Локшина А. Б., Коберская Н. Н., Мхитарян Э. А. Деменции: руководство для врачей. М.: МЕДпресс-информ, 2013; 264 с.
3. Яхно Н. Н. Когнитивные нарушения в неврологической практике. Неврологический журнал. 2006; 11 (1): 4–12.
4. Танашян М. М., Медведев Р. Б., Евдокименко А. Н., Гемджян Э. Г., Скрылев С. И., Лагода О. В. и др. Прогнозирование ишемических повреждений головного мозга при реконструктивных операциях на внутренних сонных артериях. Ангиология и сосудистая хирургия. 2017; 23 (1): 59–65.
5. Левин О. С., Аникина М. А., Васенина Е. Е. Когнитивные и нейропсихиатрические расстройства при экстрапирамидных заболеваниях. Неврология, нейропсихиатрия, психосоматика. 2012; 4 (2S): 22–30.
6. Захаров В. В. Локшина А. Б. Когнитивные нарушения при дисциркуляторной энцефалопатии. РМЖ. 2009; (20): 1325–31.
7. Bennett IJ, Madden DJ. Disconnected Aging: Cerebral White Matter Integrity and Age-Related Differences in Cognition. Neuroscience. 2014; p. 187–205. Published online 2013 Nov 23. DOI: 10.1016/j.neuroscience.2013.11.026.
8. van Kesteren MTR, Fernández G, Norris DG, Hermans EJ. Persistent schema-dependent hippocampal-neocortical connectivity during memory encoding and postencoding rest in humans. PNAS. 2010; 107 (16): 7550–5; Available from: https://doi.org/10.1073/pnas.0914892107.
9. Пирадов М. А., Супонева Н. А., Селиверстов Ю. А. и др. Возможности современных методов нейровизуализации в изучении спонтанной активности головного мозга в состоянии покоя. Неврологический журнал. 2016; 21 (1): 4–12. DOI: 10.18821/1560-9545-2016-21-1-4-12.
10. Пономарева Н. В., Фокин В. Ф., Рогаев Е. И., Иллариошкин С. Н. Влияние генетических факторов на нейрофизиологические механизмы нейродегенеративных заболеваний. Анналы клинической и экспериментальной неврологии. 2018: 12 (специальный выпуск): 46–54. DOI: 10.25692/ACEN.2018.5.6.
11. Andreone BJ, Lacoste B, Gu Ch. Neuronal and vascular interactions. Annu Rev Neurosci. 2015; (38): 25–46. DOI: 10.1146/annurev-neuro-071714-033835.
12. de Leeuw FE, de Groot JC, Oudkerk M, Witteman JC, Hofman A, et al. Hypertension and cerebral white matter lesions in a prospective cohort study. Brain. 2002; 125 (4): 765–72.
13. Танашян М. М., Максимова М. Ю., Домашенко М. А. Дисциркуляторная энцефалопатия. Путеводитель врачебных назначений. Терапевтический справочник. 2015; (2): 1–25.
14. Hughes CP, Berg L, Danziger WL, Coben LA, Martin RL. A new clinical scale for the staging of dementia. Br J Psychiatry. 1982; (140): 566–72.
15. Лурия А. Р., Симерницкая Э. Г. О функциональном взаимодействии полушарий головного мозга в организации вербально-мнестических функций. Физиология человека. 1975; 1 (3): 411–7.
16. Фокин В. Ф., Шабалина А. А., Пономарева Н. В., Медведев Р. Б., Лагода О. В., Танашян М. М. Сопряженность показателей энергетического обмена и уровня гормона стресса кортизола с когнитивными характеристиками больных дисциркуляторной энцефалопатией. Анналы клинической и экспериментальной неврологии. 2018; 4 (12): 47–51.
17. Kasten M, Bruggemann N, Schmidt A, Klein Ch. Validity of the MoCA and MMSE in the detection of MCI and dementia in Parkinson disease. Neurology. 2010; 75 (5): 478–9. DOI:10.1212/WNL.0b013e3181e7948a.
18. Whitfield-Gabrieli S, Nieto-Castanon A. Conn: A Functional Connectivity Toolbox for Correlated and Anticorrelated Brain Networks. Brain Connect. 2012; 2 (3): 125–41. DOI: 10.1089/brain.2012.0073.
19. Eichenbaum H, Lipton PA. Towards a Functional Organization of the Medial Temporal Lobe Memory System: Role of the Parahippocampal and Medial Entorhinal Cortical Areas. Hippocampus. 2008; (1) 8: 1314–24.
20. Desmond JE, Fiez JA. Neuroimaging studies of the cerebellum: language, learning and memory. Trend in Cognivity Sciences 1998; 2 (9): 355–61.
21. Larsell O, Jansen J. The human cerebellum, cerebellar connections, and cerebellar cortex. Univerity of Minnesota Press, 1972; 201 p.
22. Habas Ch, Kamdar N, Nguyen D, Prater R, Beckmann ChF, et al. Distinct cerebellar contributions to intrinsic connectivity networks. The Journal of Neuroscience. 2009; 29 (26): 8586–94.
23. Schmahmann JD, The cerebellum and cognition. Neuroscience Letters. 2018; Available from: https://DOI.org/10.1016/j.neulet.2018.07.005.
24. Beason-Held LL, Hohman TJ, Venkatraman VAJ, Resnick SM. Brain Network Changes and Memory Decline in Aging. Brain Imaging Behav. 2017; 11 (3): 859–73. DOI: 10.1007/s11682-016-9560-3.
25. Krogsrud SK, Fjell AM, Tamnes ChK. Development of white matter microstructure in relation to verbal and visuospatial working memory — A longitudinal study. PLoS One. 2018; 13 (4): e0195540. Published online 2018. DOI: 10.1371/journal.pone.0195540.
26. Caverzasi E, Mandelli ML, DeArmond SJ, et al. White matter involvement in sporadic Creutzfeldt-Jakob disease. Brain. 2014; 137 (12): 3339–54. Published online 2014 Nov 3. DOI: 10.1093/brain/awu298.
27. Caballero MAA, Suárez-Calvet M, Duering M. White matter

diffusion alterations precede symptom onset in autosomal dominant Alzheimer's disease. Brain. 2018; 141 (10): 3065–80. Published online 2018. DOI: 10.1093/brain/awy229.
28. Chetouani A, Chawki MB, Hossu G. Cross-sectional variations of white and grey matter in older hypertensive patients with subjective memory complaints. Neuroimage Clin. 2018; (17): 804–10. Published online 2017. DOI:10.1016/j.nicl.2017.12.024.
29. Левин О. С. Патология белого вещества при дисциркуляторной энцефалопатии: диагностические и терапевтические аспекты. Трудный пациент. 2011; (12): 16–24.

PARAQUAT-INDUCED MODEL OF PARKINSON'S DISEASE AND DETECTION OF PHOSPHORYLATED α-SYNUCLEIN IN THE ENTERIC NERVOUS SYSTEM OF RATS

Stavrovskaya AV ✉, Voronkov DN, Kutukova KA, Ivanov MV, Gushchina AS, Illarioshkin SN

Research Center of Neurology, Moscow, Russia

Parkinson's disease (PD) is a common neurodegenerative disorder with a variety of motor and non-motor features. Non-motor symptoms, such as gastrointestinal dysfunction, usually set in 5 to 15 years earlier than motor manifestations. Cytoplasmic aggregates of phosphorylated α-synuclein are a typical marker of PD. They are observed not only in cerebral neurons but also in intramural plexuses of the intestine. Therefore, it is essential to investigate the peripheral component of the molecular pathogenesis of the disease using PD models, including those involving the use of parkinsonian neurotoxins, such as the well-known herbicide paraquat. The aim of this study was to identify a complex of early α-synuclein-related changes induced by long-term systemic administration of paraquat to rats at doses of 6 mg/kg. The open-field test revealed a decline in the motor activity of the experimental animals; the tapered beam walking test demonstrated a two-fold increase (p = 0.044) in the number of left paw slips. Besides, the intensity of staining for tyrosine hydroxylase (TH) in the substantia nigra and myenteric plexus fibers was 50% (p = 0.033) and 20% (p = 0.01) lower, respectively, in the main group than in the controls. Phosphorylated α-synuclein content was increased in the cell bodies of myenteric neurons and in TH-positive nervous fibers of the experimental animals. Changes indicating the development of peripheral α-synuclein pathology in the early stage of induced PD are similar to the changes observed in patients with PD at the onset of the disease. The proposed paraquat regimen could be very promising for PD modeling.

Keywords: Parkinson's disease, animal models, α-synuclein, paraquat, behavior, tyrosine hydroxylase

Funding: this work supported by the Russian Science Foundation (Grant 19-15-00320).

Acknowledgement: the authors thank their colleagues, Olshansky AS and Yamshchikova NG (the Laboratory of Experimental Pathology of the Nervous System), for their valuable contribution.

Author contribution: Stavrovskaya AV planned the study, analyzed the literature, collected, analyzed and interpreted the obtained data, conducted behavioral tests, administered drugs to the animals, and prepared the draft of the manuscript; Voronkov DN analyzed the literature, analyzed and interpreted the obtained data, prepared brain slides, conducted the histopathologic examination, and prepared the draft of the manuscript; Kutukova KA analyzed the literature, analyzed the obtained data, prepared jejunum slides, carried out the histopathologic examination, and prepared the draft of the manuscript; Ivanov MV prepared jejunum slides and carried out the histopathologic examination; Gushchina AS collected data, administered drugs to the rats, carried out behavioral tests, and monitored the animals' health as a vet; Illarioshkin SN supervised the study and prepared the draft of the manuscript.

Compliance with ethical standards: the animals were treated and the experiments were conducted in full compliance with the Guide for the Care and Use of Laboratory Animals; the study was approved by the Ethics Committee of Research Center of Neurology (Protocol № 2–5/19 dated February 20, 2019).

✉ **Correspondence should be addressed:** Alla V. Stavrovskaya
per. Obukha 5, Moscow, 103064; alla_stav@mail.ru

Received: 12.08.2019 **Accepted:** 26.08.2019 **Published online:** 13.09.2019

DOI: 10.24075/brsmu.2019.058

ПАРАКВАТНАЯ МОДЕЛЬ ПАРКИНСОНИЗМА И ВЫЯВЛЕНИЕ ФОСФОРИЛИРОВАННОГО α-СИНУКЛЕИНА В ЭНТЕРАЛЬНОЙ НЕРВНОЙ СИСТЕМЕ У КРЫС

А. В. Ставровская ✉, Д. Н. Воронков, К. А. Кутукова, М. В. Иванов, А. С. Гущина, С. Н. Иллариошкин

Научный центр неврологии, Москва, Россия

Болезнь Паркинсона (БП) — распространенное нейродегенеративное заболевание с широким спектром моторных и немоторных нарушений. Немоторные симптомы (в частности, нарушения функций желудочно-кишечного тракта) обычно опережают манифестацию нарушений моторики на 5–15 лет. Характерный признак БП, цитоплазматические агрегаты фосфорилированного белка α-синуклеина, обнаруживают не только в церебральных нейронах, но и в интрамуральных вегетативных сплетениях кишечника. В связи с этим большое значение имеет оценка периферического звена молекулярного патогенеза БП на экспериментальных моделях, в том числе при воздействии специфических «паркинсонических» нейротоксинов, таких как гербицид паракват. Целью работы было выявить комплекс ранних патологических изменений, вовлекающих α-синуклеин, при системном многократном введении крысам параквата в дозе 6 мг/кг. У экспериментальных животных было показано снижение двигательной активности в открытом поле, двукратное (p = 0,044) одностороннее увеличение числа случаев соскальзывания в тесте «сужающаяся дорожка», снижение интенсивности окрашивания на тирозингидроксилазу (ТирГд) структур черной субстанции среднего мозга и нервных волокон миентерального сплетения кишечника крысы на 50% (p = 0,033) и на 20% (p = 0,01) соответственно, а также увеличение содержания фосфорилированного α-синуклеина в телах миентеральных нейронов и в ТирГд-позитивных волокнах. Полученные изменения, свидетельствующие о развитии периферической α-синуклеинопатии на ранней стадии экспериментального паркинсонизма, сходны с таковыми у пациентов в дебюте БП. Предложенный режим введения параквата может быть чрезвычайно перспективным в моделировании БП.

Ключевые слова: болезнь Паркинсона, моделирование на животных, α-синуклеин, паракват, поведение, тирозингидроксилаза

Финансирование: работа поддержана грантом РНФ № 19-15-00320.

Благодарности: авторы благодарят сотрудников лаборатории экспериментальной патологии нервной системы А. С. Ольшанского и Н. Г. Ямщикову за вклад в работу.

Информация о вкладе авторов: А. В. Ставровская — планирование исследования, анализ литературы, сбор, анализ и интерпретация данных, введение препаратов, проведение поведенческих тестов, подготовка черновика рукописи; Д. Н. Воронков — анализ литературы, анализ и интерпретация данных, подготовка и проведение морфохимического исследования образцов мозга экспериментальных крыс, подготовка черновика рукописи; К. А. Кутукова — анализ литературы, анализ данных, подготовка и проведение морфохимического исследования образцов тонкого кишечника экспериментальных крыс, подготовка черновика рукописи; М. В. Иванов — подготовка и проведение морфохимического исследования образцов тонкого кишечника экспериментальных крыс; А. С. Гущина — сбор данных, введение препаратов, проведение поведенческих тестов, ветеринарное сопровождение исследования; С. Н. Иллариошкин — общее руководство исследованием, подготовка черновика рукописи.

Соблюдение этических стандартов: содержание животных и проведение экспериментов с ними осуществляли в соответствии с международными правилами «Guide for the Care and Use of Laboratory Animals»; исследование одобрено этическим комитетом ФГБНУ НЦН (протокол № 2–5/19 от 20 февраля 2019 г.).

✉ **Для корреспонденции:** Алла Вадимовна Ставровская
пер. Обуха, д. 5, г. Москва, 103064; alla_stav@mail.ru

Статья получена: 12.08.2019 **Статья принята к печати:** 26.08.2019 **Опубликована онлайн:** 13.09.2019

DOI: 10.24075/vrgmu.2019.058

Parkinson's disease (PD) is a widespread neurological disorder most common in people over > 60 years of age. It is estimated that at least 4 million individuals are affected worldwide. Today, the world's population is aging, and PD prevalence is expected to double by 2040 [1]. In the absence of curative treatment, the focus should be placed on researching the underlying molecular mechanisms of PD in animal models.

Typical motor symptoms of PD (bradykinesia, rigidity, resting tremors) are linked to the loss of dopaminergic neurons in *substantia nigra pars compacta*, nigrostriatal pathway degeneration and progressive neurotransmitter imbalance in the central nervous system (CNS) [2]. Non-motor features commonly include, but are not limited to, gastrointestinal disorders (constipation, etc.) striking long before the first motor symptoms are manifested [3]. Although the peripheral nervous system (PNS) is thought to be implicated in PD-related gastrointestinal dysfunction, its trigger mechanisms and patterns of interaction between the CNS and PNS contributors to PD pathogenesis have not been completely elucidated.

The most significant molecular event leading to the loss of CNS neurons in patients with PD is misfolding of a small synaptic protein known as α-synuclein [4]. Phosphorylated α-synuclein aggregates observed in the neuronal cytoplasm are the primary constituents of Lewy bodies — the classic histopathological hallmarks of PD [2]. Interestingly, α-synuclein pathology is not confined to cerebral neurons and is also seen in biopsy and autopsy specimens of the intramural intestinal plexus obtained from patients with PD. This inspired a hypothesis that the disease begins in enteric plexuses and then spreads to other CNS structures via the vagus nerve [5]. Some findings suggest that the α-synuclein cascade is triggered by certain environmental neurotoxins, such as heavy metals, pesticides and fungicides [6, 7]. For example, abnormal deposition of α-synuclein can be induced by the powerful non-selective herbicide paraquat (1,1-dimethyl-4,4-bipyridinium dichloride). Paraquat is widely used for controlling noxious weeds that invade orchards, agricultural lands, coffee, tea and cocoa plantations, as well as for desiccating crops [6, 8, 9]. It bears structural resemblance to 1-methyl-4-phenylpyridinium (MPP^+), the toxic metabolite of the well-known neurotoxin 1-methyl-4-phenyl-1,2,3,6-tetrahydropyridine (MPTP). This makes paraquat suitable for modeling PD in animals. The toxic effect of paraquat is linked to the production of superoxide radicals; at the same time, the herbicide has low affinity for complex I of the mitochondrial electron transport chain.

Studies exploiting animal models of PD usually involve long-term exposure to paraquat administered systemically at 10 mg/ kg. Such regimens result in pronounced motor impairment in the animals and cause significant degeneration of dopamine-producing neurons in the substantia nigra [10]. This approach cannot be applied to obtain information about the early stages of PD or to assess non-motor symptoms that precede the onset of motor impairment. This study aimed to identify a complex of prodromal α-synuclein-related pathological changes in rats exposed to small doses of paraquat and to compare it to the symptoms observed in the experimental animals in the early stage of induced PD.

METHODS

The study was conducted in male Wistar rats (n = 18) aged 3–3.5 months. The animals were kept under standard housing conditions (the 12/12 light/dark cycle) and had free access to food and water.

The animals were stratified into the main (paraquat) group (n = 10) and the control group (n = 8). Paraquat was dissolved in normal saline; 0.5 ml (6 mg/kg) of the obtained solution were administered to the animals from the main group on alternate days over the course of 4 weeks. The control group received an equal amount of normal saline. The next day after the last injection, the open field test (OPT) and the tapered beam walking test (BWT) were conducted to assess locomotor activity in the animals. The initial level of motor activity was measured in intact rats before the experiment. The open field arena was fabricated in the workshop of Research Institute of Neurology. It was a cube-shaped 75 x 75 x 40 cm box; its floor was divided into 25 equal squares. During the open-field test, we measured the distance each rat covered within 3 minutes. The beam-walking apparatus (Open science; Russia) was made of 2 overlaying 165-cm long beams; the bottom beam was 10 to 5.5 cm in width; the lower beam, 6 to 1.5 cm; the height was 2 cm for both beams. The enclosure at the narrow end of the walking bridge had a removable lid and a hole in the front panel to allow the animal inside. The apparatus was installed 70 cm above the floor. The rat traveled along the top beam from its far end towards the safe enclosure. For each animal, we counted the number of slips from the top beam throughout the entire route and the total number of steps made by each paw. The experiment was recorded using the Any-maze video-tracking system (Stoelting Inc.; USA).

Four brain tissue samples were selected from each group for further histopathologic examination. Briefly, the brain was removed and fixed in 4% formalin. The samples were soaked in O.C.T. compound (TissueTek; USA); a series of 10-μm frontal sections was prepared in a Tissue-Tek Cryo3 Flex cryostat (Sakura Finetek; USA). The slides were immunofluorescently stained in order to determine tyrosine hydroxylase (TH) and glial fibrillary acidic protein (GFAP) content in the tissue. TH is a protein marker for dopaminergic neurons, whereas GFAP levels are indicative of neurodegeneration in the nigrostriatal system. Cell nuclei were stained with DAPI. TH content was determined using polyclonal rabbit antibodies (1 : 500, Sigma; Germany) and CF488-conjugated goat secondary antirabbit antibodies (1 : 500, Sigma; Germany). GFAP levels were estimated using Cys3-conjugated antibodies (1 : 80; Sigma). We examined 5 to 10 slides of each brain sample prepared from the tissue along the rostrocaudal axis at the level of the caudate nuclei and substantia nigra. The slides were studied under the Eclipse NiU fluorescence microscope (Nikon; Japan). The density of TH-positive fibers was estimated in manually delineated regions at ×40 magnification in ImageJ (Wayne Rasband (NIH); USA); the mean fluorescence intensity of striatal tissue was corrected to background fluorescence.

Five to seven cm-long regions of the jejunum were excised and dissected in the longitudinal plane following the mesentery course, washed in normal saline and spread out on the paraffin-coated bottom of Petri dishes. The specimens were fixed in 4% buffered formalin for 3 h and then washed in a phosphate buffer (pH = 7.4). After that, the mucosal lining and the underlying submucosal layer were removed with ophthalmic forceps; the procedure was carried out under the Wild M7A stereomicroscope (Wild Heerbrugg; Germany). Fluorescence assays were performed on the obtained samples of the jejunum constituted of circular and longitudinal muscle fibers and the myenteric plexus. Primary antibodies to class III β-tubulin, TH and serin-129-phosphorylated α-synuclein (α-Syn-p129) taken at 1 : 250 dilutions were used to identify nervous fibers in the myenteric plexus. Visualization of binding reactions was aided by secondary CF448-conjugated antibodies (Sigma; Germany) taken at a 1 : 100 dilution. The samples were examined and photographed using Nikon Eclipse NiU (Nikon; Japan)

equipped with a Nikon DS-Qi digital camera (Nikon; Japan). Morphometric measurements were done in NIS Elements (Nikon; Japan) using images obtained at ×10 magnification in at least 30–40 fields of view per animal. The mean fluorescence intensity and brightness (corrected to background staining) of the myenteric plexus fibers positive for class III β-tubulin and TH were measured in the NIS Elements software.

The obtained data were analyzed in Statistica 12 (StatSoft; USA); one-way ANOVA was followed by Fisher's exact test and Mann-Whitney U test for post-hoc comparisons. The differences were considered significant at $p < 0.05$.

RESULTS

Each experimental animal received a total of 12 paraquat injections. The initial distance travelled by the intact rats in the open field was 4.96 ± 0.7 m. The next day after the last injection, OFT revealed a decline in motor activity in the rats who had been exposed to paraquat, but the differences between the groups were insignificant (Fig. 1).

BWT demonstrated poor motor coordination in the rats from the main group manifesting itself as a statistically significant increase in the number of slips from the top beam made by left paws (Fig. 2). The number of slips was expressed as percentage from the total number of steps made by the corresponding limb.

The intensity of staining for TH was decreased in the substantia nigra of the animals who had been receiving paraquat injections; the histopathologic examination revealed damage to dopaminergic neurons. The most pronounced changes were observed in the striatum. The intensity of TH-positive staining in striatal tissue was significantly lower in the main group than in the controls (Fig. 3). Low density of the detected dopaminergic fibers was predominantly observed in the dorsal aspect of the striatum. Another important finding was moderate gliosis (hypertrophy of GFAP-positive astrocyte projections).

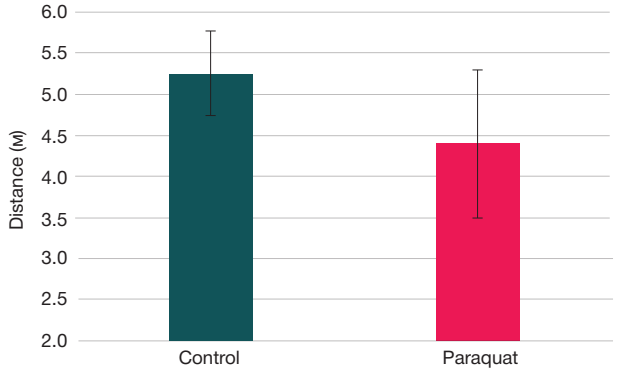

Fig. 1. The distance covered by the rats from the main and control groups in the open field test

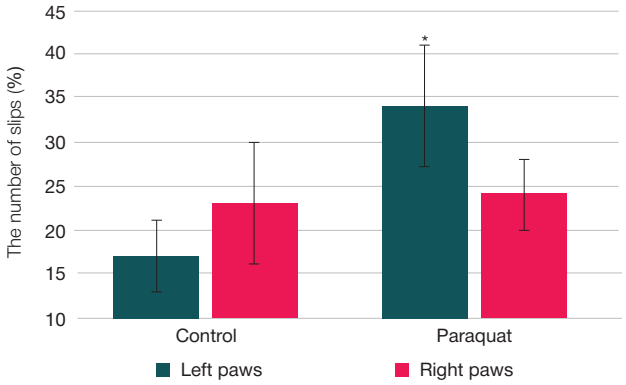

Fig. 2. The number of slips made by the animals in the main and control groups during the tapered beam walking test expressed as % from the total number of steps (* — $p = 0.0445$)

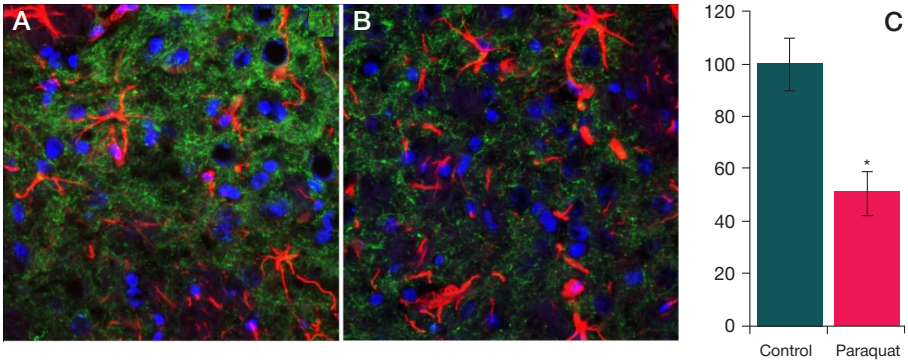

Fig. 3. Changes in the striatum of the experimental animals following long-term exposure to paraquat. Reduced density of TH-positive fibers and astrocyte hypertrophy in the striatum of the control (**A**) and the main (**B**) groups. Staining for TH is shown in *green*; staining for GFAP, in *red*; DAPI staining, in *blue* (immunofluorescent staining; magnification ×40). **C**. Changes in the intensity of TH-positive staining expressed as % from the staining intensity observed in the intact controls (* — $p = 0.033$; Mann-Whitney U)

The intensities of staining for class III β-tubulin and TH were low in the myenteric plexus of the rat jejunum (Fig. 4). The levels of phosphorylated α-synuclein (α-Syn-p129) were elevated in the cell bodies of myenteric neurons and in TH-positive fibers (Fig. 5).

DISCUSSION

Paraquat holds great promise for PD modeling: some of its properties make paraquat-induced PD models suitable for exploring hypotheses of PD pathogenesis and testing novel drugs [11]. According to the literature, paraquat induces neuronal stress, stimulates production of free radicals *in vitro* and *in vivo*, causes elevation of α-synuclein and tau, and promotes deposition of these proteins [8, 12, 13]. Despite the structural similarity between paraquat and MPP^+ [14], the two neurotoxins enter the brain via different pathways and have different mechanisms of action. Both of them are charged molecules; however, unlike MPP^+, paraquat is delivered to the brain by a neutral amino acid transporter [15, 16]. Reports of paraquat effects on dopaminergic neurons are controversial. Some authors describe motor dysfunction and death of dopaminergic neurons in rats and mice following systemic administration of paraquat [14, 10, 17]. Others report that experimental animals show no signs of motor deterioration in spite of nigrostriatal pathway degeneration [18, 14]. Although paraquat induces aggregation of α-synuclein and other damage to dopamine-producing neurons of the substantia nigra, it does not have a pronounced effect on dopamine levels in the striatum, which might be due to the compensatory increase in TH activity in tis brain region [19].

In rats, paraquat-induced PD is usually modeled by exposing the animals to 10 mg/kg doses of the herbicide dissolved in normal saline. When administered intraperitoneally for 3 weeks, such doses cause selective death of dopaminergic neurons in the substantia nigra, poor motor coordination, reduced muscle tone and contractility [10]. Higher paraquat doses (20–25 mg/kg) are used to model severe damage to internal organs, such as kidneys or lungs [20]. However, our previous experience of exposing Wistar rats to 10 mg/kg paraquat doses for modeling PD was negative: by the time of the 5th injection, all experimental animals (n = 10) had been already dead. Necropsy revealed

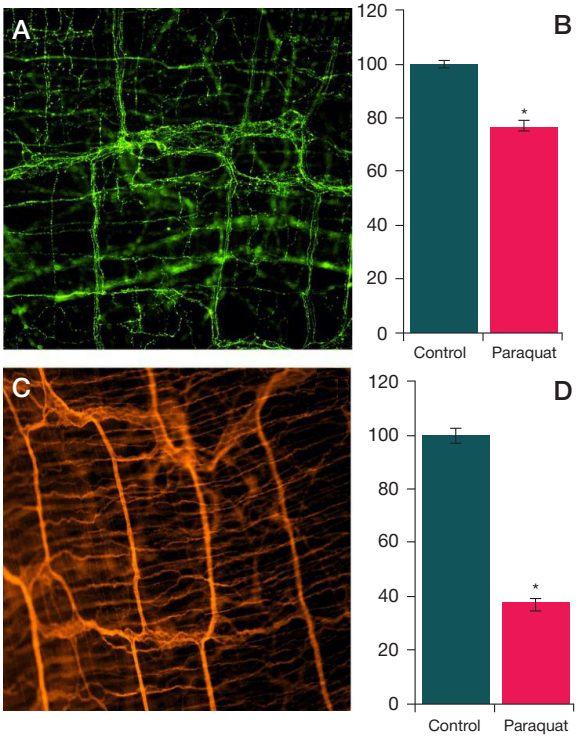

Fig. 4. Nervous fibers in the myenteric plexus of the rat jejunum containing TH (**A**) and class III β-tubulin (**C**) and changes in the fluorescence intensity of TH-positive (**B**) and class III β-tubulin-positive (**D**) fibers in the rats exposed to paraquat (% from the intensity observed in the control group; magnification ×10; * — p = 0.01)

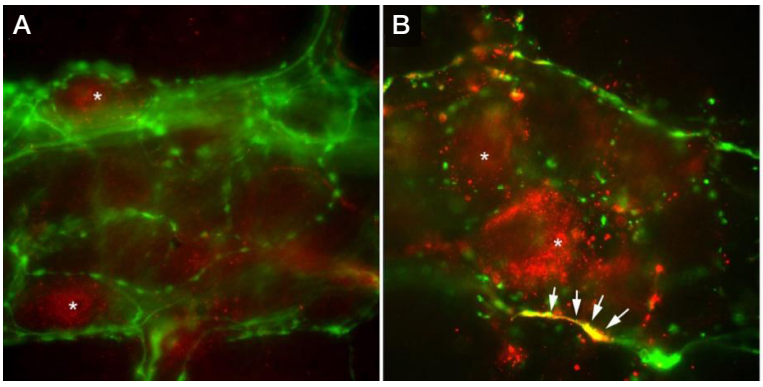

Fig. 5. Location of α-Syn-p129 (shown in *red*) and TH (shown in *green*) in the myenteric plexus of the control group (**A**) and the rats exposed to paraquat (**B**). Synuclein-positive inclusions in TH-positive nervous fibers are marked by arrows; neuronal bodies are marked by *asterisks* (*) (magnification ×40)

typical paraquat-induced changes in the lungs, kidneys and other visceral organs [20]. In this study, we used 6 mg/kg paraquat doses, which allowed us to avoid animal death and to reproduce behavioral and morphological changes imitating the early manifestations of PD, including motor asymmetry. Asymmetry of motor symptoms (hypokinesia, resting tremors, etc.) is observed at the onset of the disease, but can become less pronounced over time as the disease progresses [21]. Motor asymmetry is instrumental in differentiating PD from other parkinsonian syndromes. At the same time, there have been few reports of asymmetrical damage to substantia nigra neurons in patients with PD [22, 21]. There is also only a scarce description of PD models that recreate motor asymmetry following systemic administration of neurotoxins. Our study fills this gap.

The intensity of staining in the myenteric fibers positive for class III β-tubulin was lower in the main group than in the controls. Although paraquat-induced disruption of microtubule assembly was described previously [23], our data on decreased staining intensity in the fibers positive for class III β-tubulin are inconsistent with the results obtained by some other researchers [6]. Perhaps, our findings do not so much indicate a decline in the absolute number of tubulin-positive nervous fibers, but instead point to a changed morphology of the enteric innervation, i.e. its exhaustion.

The studied brain samples were devoid of TH-containing neuronal bodies; this suggests that TH-positive nervous fibers found in the intermuscular plexus are sympathetic afferents, which is consistent with the reports by other researchers [24, 25]. The intensity of staining for TH was lower in the paraquat group than in the controls, which may indicate damage to sympathetic innervation in the small intestine and low TH content. Besides, weak staining intensity may reflect changes in fiber density or the functional state of the neurons.

Alpha-synuclein was detected in the peripheral nervous tissue fibers of both experimental and control groups. Under normal conditions, some α-synuclein is present in neurons in the phosphorylated state [26]. In our study, the protein was diffusely distributed in the cell bodies of some myenteric plexus neurons. At the same time, the intensity of neuronal body staining was increased and TH-containing fibers immunopositive for phosphorylated α-synclein (α-Syn-p129) were thicker in the animals from the paraquat group. Morphological changes observed in nervous fibers and α-Syn-p129 accumulation may be indicative of paraquat-induced production of protein aggregates typically seen in PD. Our findings coupled with previous reports of paraquat-induced α-synuclein overexpression in the substantia nigra [6] emphasize the similarity of molecular pathogenesis of our PD model to the mechanisms of the actual disease.

The possible causes underlying paraquat-induced α-synuclein accumulation in the enteric nervous system include production of reactive oxygen species and inflammation [27]. It was shown previously that inflammatory disorders of the intestine trigger accumulation of phosphorylated α-synuclein in the myenteric plexus neurons of primates [28]. Imbalance between the phosphorylated and non-phosphorylated α-synuclein pools is accompanied by the production of toxic protein fibrils and formation of its insoluble aggregates [29]. Pathologic accumulation of α-synuclein in the fibers innervating the gastrointestinal tract and in the enteric plexus is typical of early PD stages and is regarded as a potential biomarker of the disease [30].

CONCLUSIONS

Systemic administration of 6 mg/kg doses of paraquat to rats induces behavioral and morphological changes similar to those seen in patients with early stages of PD, one of them being α-synuclein pathology in the peripheral nervous system that plays a key role in the pathogenesis of the disease. The proposed regimen is very promising for PD modeling and plays an important role in broadening our understanding of PD pathogenesis and developing novel therapeutic strategies.

References

1. Pringsheim T, Jette N, Frolkis A, Steeves TD. The prevalence of Parkinson's disease: a systematic review and meta-analysis. Mov Disord. 2014; (29): 1583–90.
2. Poewe W, Seppi K, Tanner CM, Halliday GM, Brundin P, Volkmann J, et al. Parkinson disease. Nat Rev Dis Primers. 2017; (3): 17013.
3. Chaudhuri K Ray, Titova N, editors. Nonmotor Parkinson's: The hidden face. International Review of Neurology. Vol. 133. Academic Press, 2017; 794 p.
4. Illarioshkin SN. Sovremennye predstavleniya ob etiologii bolezni Parkinsona. Nevrologicheskiy zhurnal. 2015; (4): 4–13.
5. Jellinger KA. Synuclein deposition and non-motor symptoms in Parkinson disease. J Neurol Sci. 2011; (310): 107–11.
6. Manning-Bog A, Mccormack A, Li J, Uversky V, Fink A, Di Monte D. The herbicide paraquat causes up-regulation and aggregation of alpha-synuclein in mice: paraquat and alpha-synuclein. J Biol Chem. 2002; (277): 1641–4.
7. Moretto A, Colosio C. Biochemical and toxicological evidence of neurological effects of pesticides: the example of Parkinson's disease. Neurotoxicology. 2011; (32): 383–91.
8. Fernagut PO, Hutson CB, Fleming SM, Tetreaut NA, Salcedo J, Masliah E, et al. Behavioral and histopathological consequences of paraquat intoxication in mice: Effects of alpha-synuclein over-expression. Synapse. 2007; (61): 991–1001.
9. Mak SK, McCormack AL, Manning-Bog AB, Cuervo AM, Di Monte DA. Lysosomal degradation of alpha-synuclein in vivo. J Biol Chem. 2010; (285): 13621–9.
10. Fahimi MA. Shechab S, Nemmar A, Adem A, Dhanasekaran S, Hasan MY. Daily Subacute Paraquat Exposure Decreases Muscle Function and Substantia Nigra Dopamine Level Physiol Res. 2013; (62): 313–21.
11. Tieu K. A Guide to Neurotoxic Animal Models of Parkinson's Disease Cold Spring Harb Perspect Med. 2011; (1): a009316.
12. Bus JS, Gibson JE. Paraquat: Model for Oxidant-Initiated Toxicity. Environ Health Perspect. 1984; (55): 37–46.
13. Wills J, Credle J, Oaks AW, Duka V, Lee JH, Jones J, et al. Paraquat, but Not Maneb, Induces Synucleinopathy and Tauopathy in Striata of Mice through Inhibition of Proteasomal and Autophagic Pathways. PLoS ONE. 2012; 7(1): 1–12. DOI: 10.1371/journal.pone.0030745.
14. McCormack AL, Thiruchelvam M, Manning-Bog AB, Thiffault C, Langston JW, Cory-Slechta DA, et al. Environmental risk factors and Parkinson's disease: Selective degeneration of nigral dopaminergic neurons caused by the herbicide paraquat. Neurobiol Dis. 2002; 10: 119–27.
15. Shimizu K, Ohtaki K, Matsubara K, Aoyama K, Uezono T, Saito O, et al. Carrier-mediated processes in blood — brain barrier penetration and neural uptake of paraquat. Brain Res. 2001; (906): 135–42.
16. McCormack AL, Di Monte DA. Effects of L-dopa and other amino acids against paraquat-induced nigrostriatal degeneration. J Neurochem. 2003; (85): 82–6.

17. Izumi Y, Ezumi M, Takada-Takatori Y, Akaike A, Kume T. Endogenous Dopamine Is Involved in the Herbicide Paraquat-Induced Dopaminergic Cell Death Toxicological Sciences. 2014; 139 (2): 466–78.
18. Thiruchelvam M, Brockel BJ, Richfield EK, Baggs RB, Cory-Slechta DA. Potentiated and preferential effects of combined paraquat and maneb on nigrostriatal dopamine systems: Environmental risk factors for Parkinson's disease? Brain Res. 2000; (873): 225–34.
19. Ossowska K, Wardas J, Smialowska M, Kuter K, Lenda T, Wieronska JM, et al. A slowly developing dysfunction of dopaminergic nigrostriatal neurons induced by long-term paraquat administration in rats: An animal model of pre-clinical stages of Parkinson's disease? Eur J Neurosci. 2005; (22): 1294–304.
20. Junboa Z, Yongtaob Y, Hongboa Li, Fenshuanga Z, Ruyuna L, Chun'aia Y. Experimental study of sucralfate intervention for paraquat poisoning in rats. Environmental Toxicology and Pharmacology. 2017; (53): 57–63.
21. Riederer P, Jellinger KA, Kolber P, Hipp G, Sian-Hulsmann J, Kruger R. Lateralisation in Parkinson disease. Cell Tissue Res. 2018; (373): 297. https://doi.org/10.1007/s00441-018-2832-z.
22. Djaldetti R, Ziv I, Melamed E. The mystery of motor asymmetry in Parkinson's disease. The Lancet Neurology. 2006; 5 (9): 796–802. DOI: 10.1016/s1474-4422(06)70549-x
23. Li WD, Zhao YZ, Chou IN. Paraquat-induced cytoskeletal injury in cultured cells. Toxicol Appl Pharmacol. 1987; 91 (1): 96–106.
24. Phillips RJ, Pairitz JC, Powley TL. Age-related neuronal loss in the submucosal plexus of the colon of Fischer 344 rats. Neurobiol Aging. 2007; 28 (7): 1124–37.
25. Phillips RJ, Hudson CN, Powley TL. Sympathetic axonopathies and hyperinnervation in the small intestine smooth muscle of aged Fischer 344 rats. Auton Neurosci. 2013; 179 (1–2): 108–121. DOI: 10.1016/j.autneu.2013.09.002.
26. Muntané G, Ferrer I, Martinez-Vicente M. α-Synuclein phosphorylation and truncation are normal events in the adult human brain. Neuroscience. 2012; (200): 106–19. DOI: 10.1016/j.neuroscience.2011.10.042.
27. Toygar M, Aydin I, Agilli M, Aydin FN, Oztosun M, Gul H, et al. The relation between oxidative stress, inflammation, and neopterin in the paraquat-induced lung toxicity. Hum Exp Toxicol. 2015; 34 (2): 198–204. DOI: 10.1177/0960327114533808.
28. Resnikoff H, Metzger JM, Lopez M, Bondarenko V, Mejia A, Simmons HA, et al. Colonic inflammation affects myenteric alpha-synuclein in nonhuman primates. J Inflamm Res. 2019; (12): 113–26. DOI: 10.2147/JIR.S196552.
29. Zhang J, Li X, Li JD. The Roles of Post-translational Modifications on α-Synuclein in the Pathogenesis of Parkinson's Diseases. Front Neurosci. 2019; (13): 381. DOI: 10.3389/fnins.2019.00381.
30. Yan F, Chen Y, Li M, Wang Y, Zhang W, Chen X, et al. Gastrointestinal nervous system α-synuclein as a potential biomarker of Parkinson disease. Medicine (Baltimore). 2018; 97 (28): e11337. DOI:10.1097/MD.0000000000011337.

Литература

1. Pringsheim T, Jette N, Frolkis A, Steeves TD. The prevalence of Parkinson's disease: a systematic review and meta-analysis. Mov Disord. 2014; (29): 1583–90.
2. Poewe W, Seppi K, Tanner CM, Halliday GM, Brundin P, Volkmann J, et al. Parkinson disease. Nat Rev Dis Primers. 2017; (3): 17013.
3. Chaudhuri K Ray, Titova N, editors. Nonmotor Parkinson's: The hidden face. International Review of Neurology. Vol. 133. Academic Press, 2017; 794 p.
4. Иллариошкин С. Н. Современные представления об этиологии болезни Паркинсона. Неврологический журнал. 2015; (4): 4–13.
5. Jellinger KA. Synuclein deposition and non-motor symptoms in Parkinson disease. J Neurol Sci. 2011; (310): 107–11.
6. Manning-Bog A, Mccormack A, Li J, Uversky V, Fink A, Di Monte D. The herbicide paraquat causes up-regulation and aggregation of alpha-synuclein in mice: paraquat and alpha-synuclein. J Biol Chem. 2002; (277): 1641–4.
7. Moretto A, Colosio C. Biochemical and toxicological evidence of neurological effects of pesticides: the example of Parkinson's disease. Neurotoxicology. 2011; (32): 383–91.
8. Fernagut PO, Hutson CB, Fleming SM, Tetreaut NA, Salcedo J, Masliah E, et al. Behavioral and histopathological consequences of paraquat intoxication in mice: Effects of alpha-synuclein over-expression. Synapse. 2007; (61): 991–1001.
9. Mak SK, McCormack AL, Manning-Bog AB, Cuervo AM, Di Monte DA. Lysosomal degradation of alpha-synuclein in vivo. J Biol Chem. 2010; (285): 13621–9.
10. Fahimi MA. Shechab S, Nemmar A, Adem A, Dhanasekaran S, Hasan MY. Daily Subacute Paraquat Exposure Decreases Muscle Function and Substantia Nigra Dopamine Level Physiol Res. 2013; (62): 313–21.
11. Tieu K. A Guide to Neurotoxic Animal Models of Parkinson's Disease Cold Spring Harb Perspect Med. 2011; (1): a009316.
12. Bus JS, Gibson JE. Paraquat: Model for Oxidant-Initiated Toxicity. Environ Health Perspect. 1984; (55): 37–46.
13. Wills J, Credle J, Oaks AW, Duka V, Lee JH, Jones J. et al. Paraquat, but Not Maneb, Induces Synucleinopathy and Tauopathy in Striata of Mice through Inhibition of Proteasomal and Autophagic Pathways. PLoS ONE. 2012; 7(1): 1–12. DOI: 10.1371/journal.pone.0030745.
14. McCormack AL, Thiruchelvam M, Manning-Bog AB, Thiffault C, Langston JW, Cory-Slechta DA, et al. Environmental risk factors and Parkinson's disease: Selective degeneration of nigral dopaminergic neurons caused by the herbicide paraquat. Neurobiol Dis. 2002; (10): 119–27.
15. Shimizu K, Ohtaki K, Matsubara K, Aoyama K, Uezono T, Saito O, et al. Carrier-mediated processes in blood — brain barrier penetration and neural uptake of paraquat. Brain Res. 2001; (906): 135–42.
16. McCormack AL, Di Monte DA. Effects of L-dopa and other amino acids against paraquat-induced nigrostriatal degeneration. J Neurochem. 2003; (85): 82–6.
17. Izumi Y, Ezumi M, Takada-Takatori Y, Akaike A, Kume T. Endogenous Dopamine Is Involved in the Herbicide Paraquat-Induced Dopaminergic Cell Death Toxicological Sciences. 2014; 139 (2): 466–78.
18. Thiruchelvam M, Brockel BJ, Richfield EK, Baggs RB, Cory-Slechta DA. Potentiated and preferential effects of combined paraquat and maneb on nigrostriatal dopamine systems: Environmental risk factors for Parkinson's disease? Brain Res. 2000; (873): 225–34.
19. Ossowska K, Wardas J, Smialowska M, Kuter K, Lenda T, Wieronska JM, et al. A slowly developing dysfunction of dopaminergic nigrostriatal neurons induced by long-term paraquat administration in rats: An animal model of pre-clinical stages of Parkinson's disease? Eur J Neurosci. 2005; (22): 1294–304.
20. Junboa Z, Yongtaob Y, Hongboa Li, Fenshuanga Z, Ruyuna L, Chun'aia Y. Experimental study of sucralfate intervention for paraquat poisoning in rats. Environmental Toxicology and Pharmacology. 2017; (53): 57–63.
21. Riederer P, Jellinger KA, Kolber P, Hipp G, Sian-Hulsmann J, Kruger R. Lateralisation in Parkinson disease. Cell Tissue Res. 2018; (373): 297. https://doi.org/10.1007/s00441-018-2832-z.
22. Djaldetti R, Ziv I, Melamed E. The mystery of motor asymmetry in Parkinson's disease. The Lancet Neurology. 2006; 5 (9): 796–802. DOI: 10.1016/s1474-4422(06)70549-x
23. Li WD, Zhao YZ, Chou IN. Paraquat-induced cytoskeletal injury in cultured cells. Toxicol Appl Pharmacol. 1987; 91 (1): 96–106.
24. Phillips RJ, Pairitz JC, Powley TL. Age-related neuronal loss in the submucosal plexus of the colon of Fischer 344 rats. Neurobiol Aging. 2007; 28 (7): 1124–37.
25. Phillips RJ, Hudson CN, Powley TL. Sympathetic axonopathies and hyperinnervation in the small intestine smooth muscle of aged Fischer 344 rats. Auton Neurosci. 2013; 179 (1–2): 108–121. DOI: 10.1016/j.autneu.2013.09.002.
26. Muntané G, Ferrer I, Martinez-Vicente M. α-Synuclein phosphorylation and truncation are normal events in the adult human brain. Neuroscience. 2012; (200): 106–19. DOI: 10.1016/j.

neuroscience.2011.10.042.
27. Toygar M, Aydin I, Agilli M, Aydin FN, Oztosun M, Gul H, et al. The relation between oxidative stress, inflammation, and neopterin in the paraquat-induced lung toxicity. Hum Exp Toxicol. 2015; 34 (2): 198–204. DOI: 10.1177/0960327114533808.
28. Resnikoff H, Metzger JM, Lopez M, Bondarenko V, Mejia A, Simmons HA, et al. Colonic inflammation affects myenteric alpha-synuclein in nonhuman primates. J Inflamm Res. 2019; (12): 113–26. DOI: 10.2147/JIR.S196552.
29. Zhang J, Li X, Li JD. The Roles of Post-translational Modifications on α-Synuclein in the Pathogenesis of Parkinson's Diseases. Front Neurosci. 2019; (13): 381. DOI: 10.3389/fnins.2019.00381.
30. Yan F, Chen Y, Li M, Wang Y, Zhang W, Chen X, et al. Gastrointestinal nervous system α-synuclein as a potential biomarker of Parkinson disease. Medicine (Baltimore). 2018; 97 (28): e11337. DOI:10.1097/MD.0000000000011337.

THE STATE OF COGNITIVE FUNCTIONS AFTER ANGIORECONSTRUCTIVE OPERATIONS ON THE CAROTID ARTERIES

Tanashyan MM[1], Medvedev RB[1] ✉, Lagoda OV[1], Berdnikovich ES[1], Skrylev SI[1], Gemdzhian EG[2], Krotenkova MV[1]

[1] Research Centre of Neurology, Moscow, Russia

[2] National Research Center for Hematology, Moscow, Russia

Carotid artery stenosis is a risk factor for ischemic stroke. Surgical treatment is often used to improve cerebral perfusion and prevent the development of cerebrovascular pathology and related cognitive impairment. The aim of this prospective pilot study was to evaluate the cognitive functions (CF) of patients after surgery (open or endovascular intervention) on the internal carotid artery. The study included 90 patients (mean age 62 years, 71% of men) with atherosclerotic lesions of the carotid arteries. The CF was evaluated at four time points (before the intervention, 3, 6, and 9 months after) using cognitive scales and measuring cognitive evoked potentials. The state of the brain substance before and after the intervention was evaluated by the results of diffusion-weighted magnetic resonance imaging (DW-MRI). Three and six months after the operation, the patients demonstrated minor and varied CF alterations by the MMSE scale, but by the end of the observation period (9 months) the participants had their CF at the level close to that registered before the operation (p = 0.43). Thus, the intervention-associated changes in CF, regardless of the surgical approach, were primarily transient in nature. The rare cases of CF deterioration, as registered by the postoperative DW-MRI scans, were linked to the acute brain ischemia, both symptomatic and asymptomatic, and a perioperative stroke (1 case). Advanced age and altered cerebral arteries may be listed as the risk factors for the probable CF deterioration. Evaluation of the connections between CF alterations and multiple cases of intraoperative cerebral vascular embolism requires a longer observation period.

Keywords: carotid artery, stenosis, stent, endarterectomy, emboli, cognitive function, analysis of variance

Funding: the study was ordered by the Research Center of Neurology (Federal Research Institution).

Author contribution: Tanashyan MM — study design development, manuscript editing; Medvedev RB — literature analysis, study design development, data collection, analysis and interpretation, manuscript authoring; Lagoda OV and Berdnikovich ES — literature analysis, study design development, data collection and interpretation, manuscript editing; Skrylev SI — angiosurgery, manuscript editing; Gemdzhian EG — study concept and design, data analysis, statistical analysis, manuscript compilation and editing; Krotenkova MV — image data analysis and interpretation, manuscript editing.

Compliance with ethical standards: the study was approved by the Research Center of Neurology Ethics Committee (protocol № 11/14 of November 19, 2014). All patients or their legally authorized representatives have signed the informed consent for surgery; the study followed the ethical principles of the Declaration of Helsinki (1975).

✉ **Correspondence should be addressed:** Roman B. Medvedev
Volokolamskoye shosse, 80, Moscow, 125367; medvedev-roman@yandex.ru

Received: 15.08.2019 **Accepted:** 29.08.2019 **Published online:** 16.09.2019

DOI: 10.24075/brsmu.2019.059

СОСТОЯНИЕ КОГНИТИВНЫХ ФУНКЦИЙ ПОСЛЕ АНГИОРЕКОНСТРУКТИВНЫХ ОПЕРАЦИЙ НА СОННЫХ АРТЕРИЯХ

М. М. Танашян[1], Р. Б. Медведев[1] ✉, О. В. Лагода[1], Е. С. Бердникович[1], С. И. Скрылев[1], Э. Г. Гемджян[2], М. В. Кротенкова[1]

[1] Научный центр неврологии, Москва, Россия

[2] Национальный медицинский исследовательский центр гематологии, Москва, Россия

Атеросклероз сонных артерий является фактором риска ишемического инсульта. Для улучшения мозговой перфузии и предотвращения развития цереброваскулярной патологии и связанных с ней когнитивных нарушений нередко используют хирургическое лечение. Целью данного проспективного поискового исследования было оценить когнитивные функции (КФ) пациентов после операции (открытого или эндоваскулярного вмешательства) на внутренней сонной артерии. В исследование было включено 90 пациентов (средний возраст — 62 года, 71% мужчин) с атеросклеротическим поражением сонных артерий. КФ оценивали в четырех временных точках (до вмешательства, через 3, 6 и 9 месяцев после него) с использованием когнитивных шкал и измерением когнитивных вызванных потенциалов. Состояние вещества головного мозга до и после вмешательства оценивали по результатам диффузионно-взвешенной магнитно-резонансной томографии (ДВ-МРТ). Через 3 и 6 месяцев после операции у пациентов наблюдали небольшие разнонаправленные изменения КФ (по шкале MMSE), но к концу срока наблюдения (9 месяцам) распределение оценок КФ у пациентов приблизилось к дооперационному (p = 0,43). Таким образом, ассоциированные с вмешательством (независимо от его вида) изменения КФ носили преимущественно транзиторный характер. Единичные случаи ухудшения (по данным ДВ-МРТ после операции) КФ были ассоциированы с острыми очагами ишемии (как симптомными, так и бессимптомными) в веществе мозга, а также с периоперационным инсультом (1 случай). К факторам риска неблагоприятного прогноза для КФ можно отнести: пожилой возраст и изменения в церебральных артериях. Для оценки связи КФ с множественными интраоперационными эмболиями сосудов мозга требуется более длительное наблюдение.

Ключевые слова: сонная артерия, стеноз, стент, эндартерэктомия, эмболия, когнитивные функции, дисперсионный анализ

Финансирование: работа выполнена в рамках государственного задания ФГБНУ НЦН.

Информация о вкладе авторов: М. М. Танашян — разработка дизайна исследования, редактирование рукописи; Р. Б. Медведев — анализ литературы, разработка дизайна исследования, сбор, анализ и интерпретация данных, написание рукописи; О. В. Лагода и Е. С. Бердникович — анализ литературы, разработка дизайна исследования, сбор и интерпретация данных, редактирование рукописи; С. И. Скрылев — проведение ангиохирургических операций, редактирование рукописи; Э. Г. Гемджян — концепция и дизайн исследования, анализ данных, статистический анализ, составление и редактирование рукописи; М. В. Кротенкова — анализ и интерпретация данных изображения, редактирование рукописи.

Соблюдение этических стандартов: исследование одобрено этическим комитетом Научного центра неврологии (протокол № 11/14 от 19 ноября 2014 г.). Все пациенты (или их законно уполномоченные представители) подписали добровольное информированное согласие на проведение оперативного лечения; исследование проведено в соответствии с этическими принципами Хельсинкской декларации 1975 г.

✉ **Для корреспонденции:** Роман Борисович Медведев
Волоколамское шоссе, д. 80, г. Москва, 125367; medvedev-roman@yandex.ru

Статья получена: 15.08.2019 **Статья принята к печати:** 29.08.2019 **Опубликована онлайн:** 16.09.2019

DOI: 10.24075/vrgmu.2019.059

Vascular diseases are some of the leading causes of mortality and permanent disability, which makes their prevention and treatment an extremely urgent task from both medical and social viewpoints [1]. Average life expectancy is growing, as does the number of diagnosed vascular diseases and cognitive disorders associated with them. These factors call for further investigation of cerebrovascular pathology.

Cognitive dysfunction hinders social adaptation of the patients. It degrades their quality of life and, moreover, does the same to their ability to control the core disease and its comorbidities: arterial hypertension, atherosclerosis, diabetes mellitus.

The most important cause of the ischemic stroke is atherosclerotic stenosis of brachiocephalic arteries (BCA) and the internal carotid artery (ICA) in particular. The atherothrombotic subtype cerebral circulation failures cause over 30% of ischemic strokes, and up to 80% of them occur in the absence of preceding symptoms, which underlines the importance of thorough examination of atherosclerosis patients.

Embolism and cerebral hypoperfusion are the two major mechanisms distinguished in the pathogenesis of cognitive impairment (CI) associated with an ICA atherosclerosis [2]. Regardless of the presence or absence of signs of white matter lesions on the MRI scans, ICA stenosis is an independent marker of CI. A study that recruited over 4000 patients with asymptomatic ICA stenosis revealed CI in the group that had the disease in the pronounced form [3]. There is evidence of direct correlation between ICA intima-media thickness, which is the earliest atherosclerosis marker, and lower neuropsychological testing scores [4].

The current medical care doctrine prescribes shifting the focus from disease treatment to active health preservation pursued by each individual. In this context, guaranteeing adequate perfusion of the brain is the key preventive measure against development of a cerebrovascular pathology and CI.

Alongside antithrombotic therapy, surgery offers effective ways to normalize cerebral circulation. The methods are carotid endarterectomy (CEE) and transluminal balloon angioplasty with carotid artery stenting (CAS) [5–8]. Vascular bed correction undoubtedly improves cerebral circulation on the whole; however, with accumulation of practical clinical experience, some drawbacks peculiar to the surgery techniques were revealed. One of such drawbacks is the risk of intraoperative embolism and hemodynamic instability (up to a stagnation) and subsequent development of cerebral ischemia [9]. According to a randomized CREST study, the incidence of perioperative stroke after CEE and CAS was 2.3 and 4.1%, respectively [10]. DW-MRI scans reveal acute ischemia foci (AIF) in 21% of patients that underwent open surgery and 50% of those who had an endovascular intervention [11].

What links carotid revascularization and cognitive functions (CF) is still not entirely clear due to the large number of factors: 1) patients heterogeneity in stenosis clinical manifestations, localization and severity, initial status of cerebral perfusion, time between appearance of the symptoms and revascularization [12]; 2) types of neuropsychological tests used and timing of such assessments; 3) variability of surgical techniques and postoperative changes classification criteria [13]. In this study we aimed to identify and evaluate cognitive changes in surgery patients that had their ICA atherosclerosis operated on.

METHODS

The study included 90 patients (64 male and 26 female, age 47–83 years, average age 61 years) who were observed at the Department of General Angioneurology of the Research Center of Neurology (Moscow). The inclusion criteria were: any gender; an active chronic ischemic cerebrovascular disease (discirculatory encephalopathy, stage 1 or 2); ICA surgery performed from May 2015 to December 2018 at the Department of Vascular and Endovascular Surgery (27 patients underwent carotid endarterectomy (CEE), 63 patients underwent carotid angioplasty with stenting). The exclusion criteria were: a pronounced cardiac and somatic pathology; severe stroke; mental disorders; hemianopsia as a result of posterior cerebral artery circulation disorders; pronounced CI (MMSE score < 24 points) making neuropsychological testing impossible.

The carotid artery atherosclerosis diagnosis was confirmed with the help of the Viamo ultrasound examination system (Toshiba; Japan); we applied the NASCET (North American Symptomatic Carotid Endarterectomy Trial) examination algorithm [14].

All patients had their cognitive status assessed before surgery and 3, 6, and 9 months afterwards. We used the following CF assessment tools and methods: MMSE (Mini-Mental State Examination) [15]; 10 word memory trial, frontal assessment battery (FAB), clock-drawing test, digit span test (subtest of Wechsler Adult Intelligence Scale and Wechsler Memory Scales), conceptualization test, Schulte table and dynamic praxis [16]. The CF assessment tools and methods were selected based on their functional compatibility with the cognitive evoked potentials (CEP) examination.

We used the Neuro-MVP (Neurosoft; Russia) device and relied on the P300 wave to examine CEP; the results of the examination allowed objectification of changes in the participants' CF. 25 healthy individuals of the appropriate age provided baseline P300 potential data. We measured the P300 amplitude from the previous negative peak to the P300 peak.

Considering selection of the surgical treatment method, patients that had CEE contraindications according to the SAPPHIRE (Stenting and Angioplasty With Protection in Patients at High Risk for Endarterectomy) [17] trial results and CAS indications according to the CREST [10] trial underwent endovascular surgery. Twenty-four hours after open or endovascular surgery, we initiated neurological examination that implied deficit assessment using the National Institutes of Health (NIH) stroke scale [18].

DW-MRI scans were used to evaluate the condition of the brain substance before and 24 hours after the intervention. We used a Siemens Magnetom Symphony 1.5T MRI system (1.5 Tesla magnet) to obtain the scans. The foci were predominantly small, therefore we relied on the diffusion-weighted scan images (b1000 diffusion coefficient) to assess damage to the brain substance [19].

At least 5 days before the surgery all patients received corrective antithrombotic, hypolipidemic, antihypertensive and antianginal therapy. After the surgery, all patients received basic drug therapy (antithrombotic, antihypertensive and lipid-lowering drugs). No nootropic drugs were prescribed.

Statistical analysis was performed using repeated measures ANOVA and analysis of contingency tables.

RESULTS

All patients participating in the study were diagnosed with arterial hypertension; every second patient exhibited two or more risk factors for vascular diseases. Sixty (67%) patients had cerebral circulation disturbances (ischemic) registered in their medical histories. Having analyzed the initial data, we

learned that 33% of the patients scored 28-30 points on the MMSE scale, which indicates normal cognition, and 67% scored 25–27 points, which signals of mild CI. Analysis of the CF dynamics (MMSE scale) 3, 6 and 9 months after surgery revealed no notable deterioration: at 3 and 6 months, we detected multidirectional changes in CF (greater variety of scores, isolated cases of pronounced CF alterations), but at the 9-month time point, when the observation period ended, the said changes practically disappeared and all patients scored close to the pre-surgery values, the difference between pre- and post-surgery scores being insignificant ($p = 0.43$) (Fig. 1, 2). Thus, the post-surgery CF changes registered were primarily transient in nature.

Additional neuropsychological testing revealed baseline moderate impairments of verbal thinking, attention and short-term memory in some patients (Table 1). The development of CI was associated with the severity of BCA atherosclerosis, advanced age, arterial hypertension, coronary heart disease, diabetes mellitus, previous cerebral circulation failures.

Thorough post-surgery examination of these patients revealed a perioperative stroke (embolism of the middle cerebral artery) on the intervention side in one patient: the neurological deficit reached 6 points on the NIH stroke scale; the stroke manifested itself in the form of motor disorders. Further observation of this patient and verbal thinking and speech fluency tests revealed semantic memory deterioration that persisted throughout the study.

Positive changes were mainly observed in such neurodynamic processes as attention, fluency, operative and short-term memory (Fig. 3).

We found no correlation between the type of surgery performed and CF scores of the examined patients. Throughout the entire observation period, some patients older than 60 years exhibited more pronounced CI. Most patients younger than 60 years (86%) had their CF changing positively (MMSE scores) by the 6th month of the observation; by the 9-month time point, we registered a growing share of patients whose attention and short-term scores returned to norm, which was further confirmed by the P300 peak amplitude changes ($p = 0.05$). Previous ischemic strokes had no detectable effect on the post-surgery CF alterations.

The analysis of DW-MRI scans taken shortly after surgery revealed asymptomatic AIF embolic origin visualizing in 30 (33%) patients. The detected brain substance alterations were predominantly localized in the cortex (16 (53%)) on the intervention side (22 (73%)); the spots measured up to 5 mm. A separate analysis of DW-MRI scans and CEP data showed that the positive dynamics registered in patients without AIF at the 3- and 6-month time points and lack of such in patients with AIF allow considering the foci a factor preventing CF restoration post-surgery (Fig. 4).

Neuropsychological tests have also detected minor positive changes in the CF of patients without AIF 3, 6 and 9 months post-surgery.

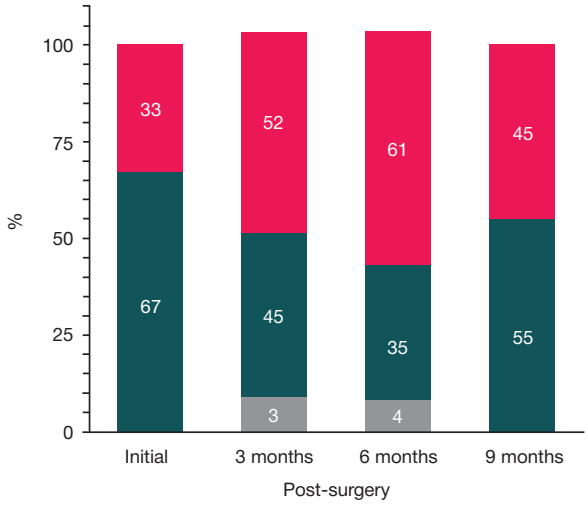

Fig. 1. Dynamics of the proportion of patients (Y axis, %) with different MMSE scores: no cognitive impairment (28–30 score) — upper fields, mild impairment (25–27 score) — middle fields, severe impairment (< 25 score) — two lower fields

Table 1. Patient CF assessment scores (based on screening tests)*

Neuropsychological tests	Screening tests			
	Before treatment	After 3 months	After 6 months	After 9 months
MMSE	27.1 ± 0.2	28.3 ± 0.1	28.2 ± 0.1	27.2 ± 0.1
FAB	13.1 ± 0.3	17.4 ± 0.1	18.1 ± 0.2	18.7 ± 0.3
Schulte table	57.3 ± 8.5	53.4 ± 13.1	47.7 ± 9.6	46.2 ± 10.3
Digit span test (direct)	5.1 ± 1.1	5.9 ± 1.1	6.1 ± 1.1	6.5 ± 1.2
Digit span test (reverse)	2.5 ± 1.1	3.7 ± 1.0	3.8 ± 1.1	3.8 ± 1.1
Dynamic praxis	1.6 ± 0.6	2.1 ± 0.7	2.2 ± 0.8	2.3 ± 0.6
Clock-drawing test	4.6 ± 2.2	5.7 ± 0.2	5.9 ± 1.1	5.8 ± 1.0
Conceptualization	2.3 ± 0.7	2.3 ± 0.1	2.2 ± 0.4	2.3 ± 0.3

Note: * — test results are presented as mean values with standard errors of mean (test result histograms are close to normal distribution).

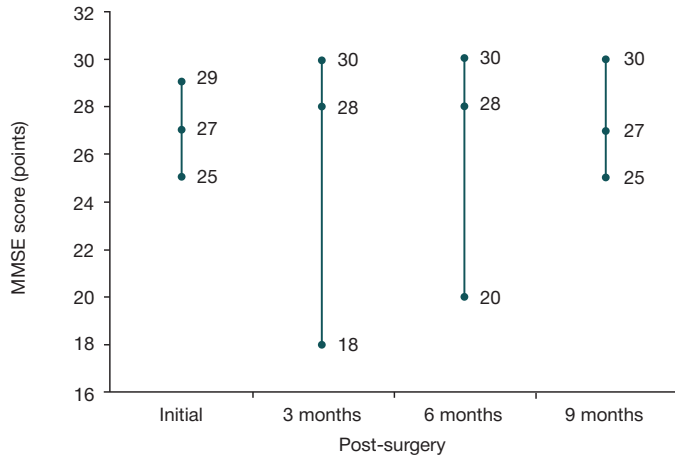

Fig. 2. Dynamics of MMSE scores describing cognitive functions (pre- and post-surgery at different time points); mean values (with minimum and maximum) are presented

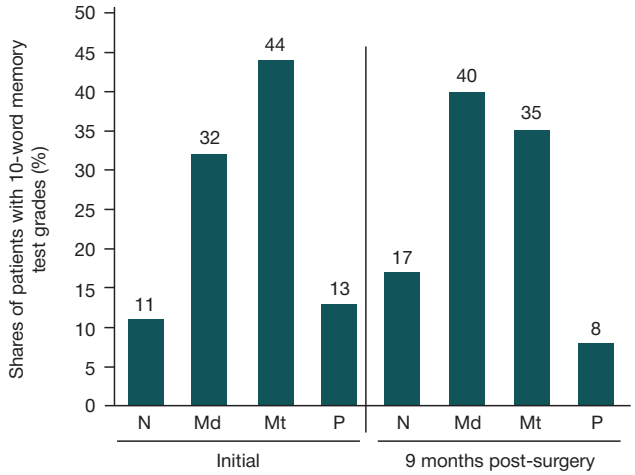

Fig. 3. Operative memory scores (10-word test) compared, pre-surgery (initial) and post-surgery (by the end of the observation period); N — norm (10 words); Md — mild impairments (8–9); Mt — moderate (6–7); S — severe (< 6). By the end of the observation period (9 months) all patients generally exhibited improvements of their operative memory

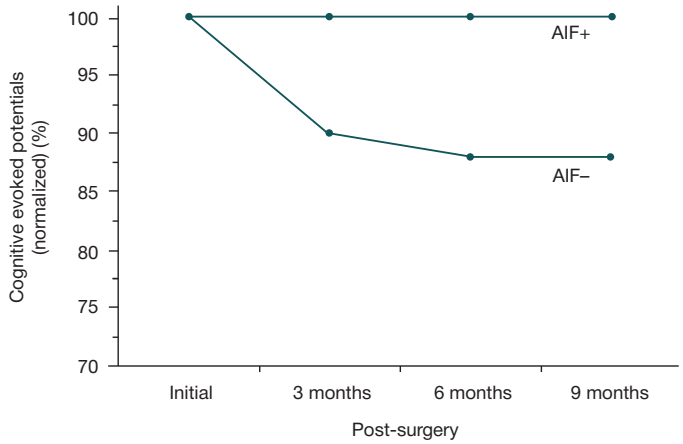

Fig. 4. CEP dynamics in patients with intraoperative acute ischemia foci (AIF+) and in patients without intraoperative acute ischemia foci (AIF–): during the observation period, the CEP level in the AIF+ group (n = 30) did not change, but in the AIF– group (n = 60) it decreased by 15% (p = 0.05). Normalized (divided by the initial levels) main CEP values (%) are given

There were no independent and significant predictors registered that were associated with the patient's condition 9 months after surgery.

The results of the P300 CEP study acquire particular importance in the context of studying CF. Initial testing of 90 patients showed that 22 (25%) of them had no changes in the features considered, while 68 (75%) patients exhibited the following deviations from the norm: 24 had no P300 peak, 25 had the peak latent, 19 had the P300 amplitude reduced. It should be noted here that the features of P300 (we give average values with standard deviations) registered in patients with arterial hypertension and without it were not significantly different from each other: 366.4 ± 29.6 versus 360.9 ± 51.1 ms (latency) and 5.4 ± 2.6 versus 5.4 ± 3.2 μV (amplitude). The P300 features revealed neither hemispheric asymmetry nor a correlation with the number of affected extracranial arteries (from one to four).

In the postoperative period, the average P300 latency and amplitude did not differ from the initial values. In the longer

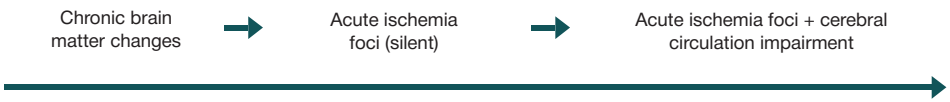

Fig. 5. Possible changes in the brain matter and post-surgery cognitive functions deterioration vector

term (9 months), P300 peak latency decrease and a slight response amplitude increase were registered in 55 (61%) patients. The average P300 potential latency values (with standard deviations) pre-surgery were 364.5 ± 37.5 ms, response amplitude — 5.4 ± 2.7 μV; post-surgery, the values were 349.5 ± 42.7 ms and 6.4 ± 3.3 μV, respectively.

DISCUSSION

The internal carotid artery system supplies about 2/3 of all the blood delivered to the namesake brain hemisphere. Atherosclerotic lesions in the extracranial arteries significantly hinder cerebral blood flow. The hemodynamic effect ICA stenosis has on cerebral circulation can lead to the development of a stroke with a clear neurological deficit or brain substance diffusion manifested in the form of diffused neurological symptoms. Post-surgery CF changes have been of interest to researchers for some time now. One of the early studies dedicated to psychopathological disorders following cardiac surgery reports the participants' impaired ability to focus attention, impaired delayed and fast memory, slowed psychomotor processes. The authors of this study concluded that it is advanced age and hypertension that are the risk factors for the development of postoperative cognitive complications [20].

The first research reports covering CI after carotid artery surgery were published in mid-1990s. The degree of intraoperative ischemia was assessed by monitoring somatosensory cortical evoked potentials during surgery. The alterations of neuropsychological indicators that depended on the degree of intraoperative ischemia were detected in patients that survived a stroke previously and had a more pronounced degree of damage to the arteries [21].

Further research efforts addressed the link between the stage of carotid stenosis and CI in patients showing no clinical signs of dementia. It was shown that CF deteriorate in patients that do not suffer from dementia but have stenosis at an advanced stage, while at the initial stages the disease does not affect the said functions. According to the psychometric tests, the revealed mild CI correlated with a change in latency of the P300 potential. The altered P300 potentials associated with mild CI were found in ICA stenosis patients, both asymptomatic and exhibiting symptoms locally [22]. In contrast to psychometric tests, CEP do not depend on the patient's motivation.

Given that the results of some studies indicate a significant improvement in CF after carotid artery interventions [23] while other papers provide evidence to the contrary [24, 25], the issue of identifying the factors driving change in cognitive abilities following surgery remains open.

We also studied CF after ICA surgery; in our work, we learned that the MMSE scores describing the state of CF in patients were most varied in the first 3 months post-surgery, which may have been a result of the patients' psychoemotional reaction to the operation [26]. The changes were mainly observed in such neurodynamic processes as attention, fluency, operative and short-term memory. After 9 months, CF have on average returned to the initial (pre-surgery) level. We can make an assumption that the long-term factors affecting the CF post-surgery are the initial status of the said functions and the adequacy of the secondary prevention measures aimed at vascular diseases. In addition, it is probable that restoration of perfusion and improvement of brain metabolism also cause a gradual recovery from the CI [27, 28].

The lack of connection between CF and the type of surgery performed (CEE or CAS) we have registered in our study is consistent with the findings reported by other researchers [29, 30].

At the 6-month time point, we detected a link between the patient's age (below 60 years) and the positive dynamics in CF restoration; moreover, at the 9-month time point we witnessed a growing number of patients whose short-term memory and attention indicators returned to norm, a finding consistent with other such findings published earlier [31, 32].

A feature of our work was the comparison of changes in the brain substance (as seen on DW-MRI scan) with the CF status at various time points post-surgery. We have detected some form of AIF in 33% of patients shortly after surgery. However, there was only one case of an acute ischemic stroke with hemiparesis on the contralateral side; the remaining AIF cases diagnosed were clinically asymptomatic.

Only a few studies [33, 34] did the DW-MRI-assisted correlation of acute ischemic lesions and neuropsychological outcome parameters, which is why there is still insufficient data to enable assessment of the forecast effect of detected lesions on cognitive status.

The clinical neuroimaging, neuropsychological and neurophysiological study we conducted allowed formulating a single CF component and establishing that the presence of AIF worsens the prognosis for cognitive functions. The dynamics of this single combined measure of CF in the remaining periods of observation depends on their clinical manifestations. In this connection, it is possible to suggest CF deterioration after CA stenosis surgery (Fig. 5).

The limitation of this study is the relatively short observation period (9 months). Continuation of the study would allow verifying the results.

CONCLUSIONS

1. One of the most important symptoms of chronic cerebrovascular disease in most patients with atherosclerotic pathology of the carotid arteries is cognitive dysfunction, which requires mandatory neuropsychological, neuroimaging and neurophysiological testing when planning angioreconstructive surgery. 2. Cognitive impairments in patients after angioreconstructive surgery on carotid artery are associated with the possible changes (symptomatic or asymptomatic) in the state of the brain substance.

References

1. Tanashyan MM, Medvedev RB, Evdokimenko AN, Gemdzhian EG, Skrylev SI, Lagoda OV, et al. Prediction of ischaemic lesions of the brain in reconstructive operations on internal carotid arteries. Angiol Sosud Khir. 2017; 23 (1): 59–65.
2. Bossema ER, Brand N, Moll FL, Ackerstaff RG, de Haan EH, van Doornen LJ. Cognitive functions in carotid artery disease before endarterectomy. J Clin Exp Neuropsychol. 2006; (28): 357–69.
3. Johnston SC, O'Meara ES, Manolio TA, Lefkowitz D, O'Leary DH, Goldstein S, et al. Cognitive impairment and decline are associated with carotid artery disease in patients without clinically evident cerebrovascular disease. Ann Intern Med. 2004; 140 (4): 237–47.
4. Romero JR, Beiser A, Seshadri S, Benjamin EJ, Polak JF, Vasan RS, et al. Carotid artery atherosclerosis, MRI indices of brain ischemia, aging, and cognitive impairment: the Framingham study. Stroke. 2009; 40 (5): 1590–6.
5. Kuntsevich GI, Tanashyan MM, Skrylev SI, Krotenkova MV, Shchipakin VL, Koshcheev Alu, et al. Intraoperative monitoring of cerebral blood-flow and condition of cerebral at open and endovascular interventions in carotid system. Angiol Sosud Khir. 2011; 17 (3): 43–8.
6. Barnett HJM, Taylor DW, Haynes RB, Sackett DL, Peerless SJ, Ferguson GG, et al. North American Symptomatic Carotid Endarterectomy Trial Collaborators. Beneficial effect of carotid endarterectomy in symptomatic patients with high grade carotid stenosis. N Engl J Med. 1991; 325 (7): 445–53.
7. Endarterectomy for asymptomatic carotid artery stenosis. Executive Committee for the Asymptomatic Carotid Atherosclerosis Study. JAMA. 1995; 273 (18): 1421.
8. Endovascular versus surgical treatment in patients with carotid stenosis in the Carotid and Vertebral Artery Transluminal Angioplasty Study (CAVATAS): a randomised trial. Lancet. 2001; 357 (9270): 1729–37.
9. Mas JL, Trinquart L, Leys D, Albucher JF, Rousseau H, Viguier A, et al. Endarterectomy Versus Angioplasty in Patients with Symptomatic Severe Carotid Stenosis (EVA-3S) trial: results up to 4 years from a randomised, multicentre trial. Lancet Neurol. 2008; 7 (10): 885–92.
10. Brott TG, Hobson RW, Howard G, Roubin GS, Clark WM, Brooks W, et al. Stenting versus endarterectomy for treatment of carotid-artery stenosis. N Engl J Med. 2010; 363 (1): 11–23.
11. Medvedev RB, Tanashyan MM, Skrylev SI, Gemdzhian EG, Gulevskaya TS, Anufriev PL. Relation between ultrasonographic and morphological characteristics of atherosclerotic plaques of carotid sinus. Angiol Sosud Khir. 2018; 24 (4): 43–9.
12. Altinbas A, van Zandvoort MJ, van den Berg E, Jongen LM, Algra A, Moll FL, et al. Cognition after carotid endarterectomy or stenting a randomized comparison. Neurology. 2011; 77 (11): 1084–90.
13. Zhou W, Hitchner E, Gillis K, Sun L, Floyd R, Lane B, et al. Prospective neurocognitive evaluation of patients undergoing carotid interventions. J Vasc Surg. 2012; 56 (6): 1571–8.
14. Barnett HJ, Taylor DW, Eliasziw M, Fox AJ, Ferguson GG, Haynes RB, et al. Benefit of carotid endarterectomy in patients with symptomatic moderate or severe stenosis. North American Symptomatic Carotid Endarterectomy Trial Collaborators. N Engl J Med. 1998; 339 (20): 1415–25.
15. Folstein MF, Folstein SE, McHugh PR. "Mini-mental state". A practical method for grading the cognitive state of patients for the clinician. J Psychiatr Res. 1975; 12 (3): 189–98.
16. Yakhno NN. Cognitive impairment in neurological practice. Nevrologicheskii Zhurnal. 2006; 11 (1): 4–12.
17. Yadav JS, Wholey MH, Kuntz RE, Fayad P, Katzen BT, Mishkel GJ, et al. Protected carotid-artery stenting versus endarterectomy in high-risk patients. N Engl J Med. 2004; 351 (15): 1493–501.
18. Brott T, Adams HP Jr, Olinger CP, Marler JR, Barsan WG, Biller J, et al. Measurements of acute cerebral infarction: a clinical examination scale. Stroke. 1989; 20 (7): 864–70.
19. Medvedev RB, Tanashian MM, Kuntsevich GI, Lagoda OV, Skrylev SI, Krotenkova MV, et al. Ischaemic lesions of cerebral after carotid stenting. Angiol Sosud Khir. 2015; 21 (1): 65–71.
20. Fox HM, Rizzo ND, Gifford S. Psychological observations of patients undergoing mitral surgery; a study of stress. Psychosom Med. 1954; 16 (3): 186–208.
21. Kügler CF, Vlajic P, Funk H, Raithel D, Platt D, et al. The event-related P300 potential approach to cognitive functions of nondemented patients with cerebral and peripheral arteriosclerosis. J Am Geriatr Soc. 1995; 43 (11): 1228–36.
22. Inoue T, Ohwaki K, Tamura A, Tsutsumi K, Saito I, Saito N. Subclinical ischemia verified by somatosensory evoked potential amplitude reduction during carotid endarterectomy: negative effects on cognitive performance clinical article. J Neurosurg. 2013; 118 (5): 1023–9.
23. Xu G, Liu X, Meyer JS, Yin Q, Zhang R. Cognitive performance after carotid angioplasty and stenting with brain protection devices. Neurol Res. 2007; (29): 251–55.
24. Witt K, Borsch K, Daniels C, Walluscheck K, Alfke K. Neuropsychological consequences of endarterectomy and endovascular angioplasty with stent placement for treatment of symptomatic carotid stenosis: a prospective randomised study. J Neurol. 2007; (254): 1524–32.
25. Lal BK, Younes M, Cruz G, Kapadia I, Jamil Z, Pappas PJ. Cognitive changes after surgery vs stenting for carotid artery stenosis. J Vasc Surg. 2011; 54 (3): 691–8.
26. Vybornykh DE, Fedorova SYu, Khrushchev SO, Drokov MYu, Gemdzhian EG, Kuzmina LA, Parovichnikova EN. Cognitive impairments in patients with hematological malignancies prior and after allogeneic hematopoietic stem cells transplantation. Obozrenie psihiatrii i medicinskoj psihologii im VM Behtereva. 2019; (2): 18–26.
27. Shimada Y, Kobayashi M, Yoshida K, Terasaki K, Fujiwara S, Kubo Y, et al. Reduced Hypoxic Tissue and Cognitive Improvement after Revascularization Surgery for Chronic Cerebral Ischemia. Cerebrovasc Dis. 2019; 47 (1–2): 57–64.
28. List J, Hertel-Zens S, Kübke JC, Lesemann A, Schreiber SJ, Flöel A. Cortical reorganization due to impaired cerebral autoregulation in individuals with occlusive processes of the internal carotid artery. Brain Stimul. 2014; 7 (3): 381–7.
29. Kuo-Lun Huang, Ting-Yu Chang, Meng-Yang Ho, Wei-Hao Chen, Mei-Yu Yeh, Yeu-JhyChang, et al. The correlation of asymmetrical functional connectivity with cognition and reperfusion in carotid stenosis patients. Neuro Image Clinical. 2018; (20): 476–84.
30. Crawley F, Stygall J, Lunn S, Harrison M, Brown MM. Comparison of microembolism detected by transcranial Doppler and neuropsychological sequelae of carotid surgery and percutaneous transluminal angioplasty. Stroke. 2000; (31): 1329–34.
31. Ortega G, Alvarez B, Quintana M, Yugueros X, Alvarez-Sabin J, Matas M. Asymptomatic carotid stenosis and cognitive improvement using transcervical stenting with protective flow reversal technique. Eur J Vasc Endovasc Surg. 2014; 47 (6): 585–92.
32. Turan TN, Smock A, Cotsonis G, Bachman D, Al Kasab S, Lynn MJ, et al. SAMMPRIS Investigators. Is There Benefit from Stenting on Cognitive Function in Intracranial Atherosclerosis? Cerebrovasc Dis. 2017; 43 (1–2): 31–5.
33. Tanashyan MM, Medvedev RB, Gemdzhian EG, Skrylev SI, Krotenkova MV, Shchipakin VL, et al. Predictors of acute cerebral embolic lesions during carotid artery stenting. Angiol Sosud Khir. 2019; 25 (4). (In Print)
34. Barber PA, Hach S, Tippett LJ, Ross L, Merry AF. Cerebral ischemic lesions on diffusion-weighted imaging are associated with neurocognitive decline after cardiac surgery. Stroke. 2008; (39): 1427–33.

Литература

1. Танашян М. М., Медведев Р. Б., Евдокименко А. Н., Гемджян Э. Г., Скрылев С. И., Лагода О. В., и др. Прогнозирование ишемических повреждений головного мозга при реконструктивных операциях на внутренних сонных артериях. Ангиология и сосудистая хирургия. 2017; 23 (1): 59–65.
2. Bossema ER, Brand N, Moll FL, Ackerstaff RG, de Haan EH, van Doornen LJ. Cognitive functions in carotid artery disease before endarterectomy. J Clin Exp Neuropsychol. 2006; (28): 357–69.
3. Johnston SC, O'Meara ES, Manolio TA, Lefkowitz D, O'Leary DH, Goldstein S, et al. Cognitive impairment and decline are associated with carotid artery disease in patients without clinically evident cerebrovascular disease. Ann Intern Med. 2004;140 (4): 237–47.
4. Romero JR, Beiser A, Seshadri S, Benjamin EJ, Polak JF, Vasan RS, et al. Carotid artery atherosclerosis, MRI indices of brain ischemia, aging, and cognitive impairment: the Framingham study. Stroke. 2009; 40 (5): 1590–6.
5. Кунцевич Г. И., Танашян М. М., Скрылев С. И., Кротенкова М. В., Щипакин В. Л., Кощеев А. Ю., и др. Интраоперационное мониторирование мозгового кровотока и состояние вещества головного мозга при открытых и эндоваскулярных вмешательствах в каротидной системе. Ангиология и сосудистая хирургия. 2011; 17 (3): 43–8.
6. Barnett HJM, Taylor DW, Haynes RB, Sackett DL, Peerless SJ, Ferguson GG, et al. North American Symptomatic Carotid Endarterectomy Trial Collaborators. Beneficial effect of carotid endarterectomy in symptomatic patients with high grade carotid stenosis. N Engl J Med. 1991; 325 (7): 445–53.
7. Endarterectomy for asymptomatic carotid artery stenosis. Executive Committee for the Asymptomatic Carotid Atherosclerosis Study. JAMA. 1995; 273 (18): 1421.
8. Endovascular versus surgical treatment in patients with carotid stenosis in the Carotid and Vertebral Artery Transluminal Angioplasty Study (CAVATAS): a randomised trial. Lancet. 2001; 357 (9270): 1729–37.
9. Mas JL, Trinquart L, Leys D, Albucher JF, Rousseau H, Viguier A, et al. Endarterectomy Versus Angioplasty in Patients with Symptomatic Severe Carotid Stenosis (EVA-3S) trial: results up to 4 years from a randomised, multicentre trial. Lancet Neurol. 2008; 7 (10): 885–92.
10. Brott TG, Hobson RW, Howard G, Roubin GS, Clark WM, Brooks W, et al. Stenting versus endarterectomy for treatment of carotid-artery stenosis. N Engl J Med. 2010; 363 (1): 11–23.
11. Медведев Р. Б., Танашян М. М., Скрылев С. И., Гемджян Э. Г., Гулевская Т. С., Ануфриев П. Л. Связь ультразвуковых и морфологических характеристик атеросклеротических бляшек каротидного синуса. Ангиология и сосудистая хирургия. 2018; 24 (4): 43–9.
12. Altinbas A, van Zandvoort MJ, van den Berg E, Jongen LM, Algra A, Moll FL, et al. Cognition after carotid endarterectomy or stenting a randomized comparison. Neurology. 2011; 77 (11): 1084–90.
13. Zhou W, Hitchner E, Gillis K, Sun L, Floyd R, Lane B, et al. Prospective neurocognitive evaluation of patients undergoing carotid interventions. J Vasc Surg. 2012; 56 (6): 1571–8.
14. Barnett HJ, Taylor DW, Eliasziw M, Fox AJ, Ferguson GG, Haynes RB, et al. Benefit of carotid endarterectomy in patients with symptomatic moderate or severe stenosis. North American Symptomatic Carotid Endarterectomy Trial Collaborators. N Engl J Med. 1998; 339 (20): 1415–25.
15. Folstein MF, Folstein SE, McHugh PR. "Mini-mental state". A practical method for grading the cognitive state of patients for the clinician. J Psychiatr Res. 1975; 12 (3): 189–98.
16. Яхно Н. Н. Когнитивные нарушения в неврологической практике. Неврологический журнал. 2006; 11 (1): 4–12.
17. Yadav JS, Wholey MH, Kuntz RE, Fayad P, Katzen BT, Mishkel GJ, et al. Protected carotid-artery stenting versus endarterectomy in high-risk patients. N Engl J Med. 2004; 351 (15): 1493–501.
18. Brott T, Adams HP Jr, Olinger CP, Marler JR, Barsan WG, Biller J, et al. Measurements of acute cerebral infarction: a clinical examination scale. Stroke. 1989; 20 (7): 864–70.
19. Медведев Р. Б., Танашян М. М., Кунцевич Г. И., Лагода О. В., Скрылев С. И., Кротенкова М. В., и др. Ишемические повреждения головного мозга после каротидного стентирования. Ангиология и сосудистая хирургия. 2015; 21 (1): 65–71.
20. Fox HM, Rizzo ND, Gifford S. Psychological observations of patients undergoing mitral surgery; a study of stress. Psychosom Med. 1954; 16 (3): 186–208.
21. Kügler CF, Vlajic P, Funk H, Raithel D, Platt D, et al. The event-related P300 potential approach to cognitive functions of nondemented patients with cerebral and peripheral arteriosclerosis. J Am Geriatr Soc. 1995; 43 (11): 1228–36.
22. Inoue T, Ohwaki K, Tamura A, Tsutsumi K, Saito I, Saito N. Subclinical ischemia verified by somatosensory evoked potential amplitude reduction during carotid endarterectomy: negative effects on cognitive performance clinical article. J Neurosurg. 2013; 118 (5): 1023–9.
23. Xu G, Liu X, Meyer JS, Yin Q, Zhang R. Cognitive performance after carotid angioplasty and stenting with brain protection devices. Neurol Res. 2007; (29): 251–55.
24. Witt K, Borsch K, Daniels C, Walluscheck K, Alfke K. Neuropsychological consequences of endarterectomy and endovascular angioplasty with stent placement for treatment of symptomatic carotid stenosis: a prospective randomised study. J Neurol. 2007; (254): 1524–32.
25. Lal BK, Younes M, Cruz G, Kapadia I, Jamil Z, Pappas PJ. Cognitive changes after surgery vs stenting for carotid artery stenosis. J Vasc Surg. 2011; 54 (3): 691–8.
26. Выборных Д. Э., Федорова С. Ю., Хрущев С. О., Дроков М. Ю., Гемджян Э. Г., Кузьмина Л.А., и др. Когнитивные нарушения у пациентов с заболеваниями системы крови, перенесших трансплантацию аллогенных гемопоэтических стволовых клеток. Обозрение психиатрии и медицинской психологии им. В. М. Бехтерева. 2019; (2): 18–26.
27. Shimada Y, Kobayashi M, Yoshida K, Terasaki K, Fujiwara S, Kubo Y, et al. Reduced Hypoxic Tissue and Cognitive Improvement after Revascularization Surgery for Chronic Cerebral Ischemia. Cerebrovasc Dis. 2019; 47 (1–2): 57–64.
28. List J, Hertel-Zens S, Kübke JC, Lesemann A, Schreiber SJ, Flöel A. Cortical reorganization due to impaired cerebral autoregulation in individuals with occlusive processes of the internal carotid artery. Brain Stimul. 2014; 7 (3): 381–7.
29. Kuo-Lun Huang, Ting-Yu Chang, Meng-Yang Ho, Wei-Hao Chen, Mei-Yu Yeh, Yeu-JhyChang, et al. The correlation of asymmetrical functional connectivity with cognition and reperfusion in carotid stenosis patients. Neuro Image Clinical. 2018; (20): 476–84.
30. Crawley F, Stygall J, Lunn S, Harrison M, Brown MM. Comparison of microembolism detected by transcranial Doppler and neuropsychological sequelae of carotid surgery and percutaneous transluminal angioplasty. Stroke. 2000; (31): 1329–34.
31. Ortega G, Alvarez B, Quintana M, Yugueros X, Alvarez-Sabin J, Matas M. Asymptomatic carotid stenosis and cognitive improvement using transcervical stenting with protective flow reversal technique. Eur J Vasc Endovasc Surg. 2014; 47 (6): 585–92.
32. Turan TN, Smock A, Cotsonis G, Bachman D, Al Kasab S, Lynn MJ, et al. SAMMPRIS Investigators. Is There Benefit from Stenting on Cognitive Function in Intracranial Atherosclerosis? Cerebrovasc Dis. 2017; 43 (1–2): 31–5.
33. Танашян М. М., Медведев Р. Б., Гемджян Э. Г., Скрылев С. И., Кротенкова М. В., Щипакин В. Л., и др. Предикторы острых церебральных эмболических повреждений при стентировании сонной артерии. Ангиология и сосудистая хирургия. 2019; 25 (4). (В печати)
34. Barber PA, Hach S, Tippett LJ, Ross L, Merry AF. Cerebral ischemic lesions on diffusion-weighted imaging are associated with neurocognitive decline after cardiac surgery. Stroke. 2008; (39): 1427–33.

INTERNAL CAROTID AND VERTEBRAL ARTERY DISSECTION: MORPHOLOGY, PATHOPHYSIOLOGY AND PROVOKING FACTORS

Kalashnikova LA ✉, Gulevskaya TS, Sakharova AV, Chaykovskaya RP, Gubanova MV, Danilova MS, Dobrynina LA, Shabalina AA

Research Center of Neurology, Moscow, Russia

The causes of internal carotid artery (ICA) and vertebral artery (VA) dissection, as well as its provoking factors, remain understudied. The aim of this paper was to explore morphological changes in the ICA/VA walls, factors provoking dissection, clinical signs and biomarkers of connective tissue (CT) damage. A total of 271 patients were examined, of whom 54% were women. The mean age of the participants was 37.0 ± 10 years. Clinical signs and biomarkers of CT damage (matrix metalloproteinase 9, tissue inhibitor of metalloproteinase 1, hydroxyproline, sulphated glycosaminoglycans) were analyzed in 82 patients and 40 healthy volunteers. Histologic examination of dissected and seemingly intact arteries conducted in 5 cases revealed signs of arterial wall dysplasia similar to those characteristics of fibromuscular dysplasia: thinning and splitting of the internal elastic membrane, areas of fibrosis, irregular orientation of myocytes, and their necrosis in the tunica media. Clinical signs and biomarkers of CT dysplasia (CTD) were more pronounced in patients with arterial dissection than in the controls. The major provoking factors were head turns and physical activity (42%), minor head injury (10%), and acute respiratory infection in the month preceding arterial dissection (14%). We conclude that arterial wall dysplasia is a predisposing factor for ICA/VA dissection, both spontaneous and provoked. The analysis of CTD biomarkers and clinical signs suggests connective tissue pathology in patients with ICA/VA dissection.

Keywords: internal carotid artery dissection, vertebral artery dissection, morphological changes in the arterial wall, clinical signs of connective tissue dysplasia, biomarkers of connective tissue damage, factors provoking dissection

Funding: this study was part of the state assignment for Research Center of Neurology.

Author contribution: Kalashnikova LA, Gubanova MV — literature analysis, data acquisition, processing of the obtained data, manuscript preparation; Gulveskaya TS, Sakharova AV, Chaykovskaya RP, Shabalina AA — data acquisition, analysis and interpretation; Danilova MS — recruitment of participants; Dobrynina LA — processing of the obtained data, manuscript preparation.

Compliance with ethical standards: the study was approved by the Ethics Committee of Research Center of Neurology (Protocol 12/14 dated December 10, 2014). All study participants consented to participate in the study and to have the results published.

✉ **Correspondence should be addressed:** Ludmila A. Kalashnikova
Volokolamskoe shosse, 80, Moscow, 125367; kalashnikovancn@yandex.ru

Received: 03.09.2019 **Accepted:** 19.09.2019 **Published online:** 03.10.2019

DOI: 10.24075/brsmu.2019.064

ДИССЕКЦИЯ ВНУТРЕННЕЙ СОННОЙ И ПОЗВОНОЧНОЙ АРТЕРИЙ: МОРФОЛОГИЯ, ПАТОФИЗИОЛОГИЯ, ПРОВОЦИРУЮЩИЕ ФАКТОРЫ

Л. А. Калашникова ✉, Т. С. Гулевская, А. В. Сахарова, Р. П. Чайковская, М. В. Губанова, М. С. Данилова, А. А. Шабалина, Л. А. Добрынина

Научный центр неврологии, Москва, Россия

Причина и провоцирующие факторы диссекции внутренней сонной и позвоночной (ВСА/ПА) артерий остаются малоизученными. Целью работы было изучить морфологические изменения стенок ВСА/ПА при диссекции, провоцирующие факторы диссекции, клинические признаки и биомаркеры повреждения соединительной ткани (СТ). Обследован 271 больной (средний возраст — 37,0 ± 10 лет, женщины — 54%) с диссекцией ВСА/ПА. Провоцирующие факторы диссекции проанализированы у всех больных. Клинические признаки и биомаркеры повреждения СТ (матриксная металлопротеиназа 9, тканевой ингибитор металлопротеиназы, гидроксипролин, сульфатированные гликозаминогликаны) исследованы у 82 больных и 40 здоровых добровольцев. Гистологическое исследование расслоенных и не расслоенных артерий, проведенное в 5 случаях, обнаружило признаки дисплазии артериальной стенки, сходные с таковыми при фибромышечной дисплазии: истончение, расщепление внутренней эластической мембраны, участки фиброза, неправильной ориентировки и некроза миоцитов в медии. Клинические признаки и биомаркеры дисплазии соединительной ткани (ДСТ) были более выражены при диссекции, чем в контроле. Основными провоцирующими факторами диссекции были повороты головы/физическая нагрузка (42%), травма головы, как правило, легкая (10%), острая респираторная инфекция, перенесенная в течение предшествующего месяца (14%). Заключение: дисплазия артериальной стенки служит причиной диссекции ВСА/ПА, которая развивается спонтанно или под действием провоцирующих факторов. Исследование биомаркеров и клинических признаков ДСТ указывает на наличие распространенного дефекта СТ у больных с диссекцией ВСА/ПА.

Ключевые слова: диссекция внутренней сонной и позвоночной артерий, морфологические изменения артериальной стенки, клинические признаки дисплазии соединительной ткани, биомаркеры повреждения соединительной ткани, провоцирующие факторы диссекции

Финансирование: работа выполнена в рамках государственного задания ФГБНУ НЦН.

Информация о вкладе авторов: Л. А. Калашникова, М. В. Губанова — анализ литературы, сбор и обработка материала, обработка полученных данных, написание текста статьи; Т. С. Гулевская, А. В. Сахарова, Р. П. Чайковская, А. А. Шабалина — сбор, анализ и интерпретация данных; М. С. Данилова — подбор участников исследования; Л. А. Добрынина — обработка полученных данных, редактирование текста статьи.

Соблюдение этических стандартов: исследование одобрено этическим комитетом ФГБНУ НЦН (протокол № 12/14 от 10 декабря 2014 г.). Все участники исследования подписали добровольное информированное согласие на участие в исследовании и публикацию результатов.

✉ **Для корреспонденции:** Людмила Андреевна Калашникова
Волоколамское шоссе, д. 80, г. Москва, 125367; kalashnikovancn@yandex.ru

Статья получена: 03.09.2019 **Статья принята к печати:** 19.09.2019 **Опубликована онлайн:** 03.10.2019

DOI: 10.24075/vrgmu.2019.064

Cervical artery dissection (CeAD) (internal carotid artery — ICA, vertebral artery — VA) occurs when blood enters the arterial wall through an intimal tear and spreads between its layers. This leads to the formation of an intramural hematoma (IMH), less often — to a double lumen or a dissecting aneurysm [1]. The narrowing or occlusion of the arterial lumen by IMH is the main cause of cerebral ischemia. Another cause of cerebral ischemia is arterio-arterial embolism by blood clots formed at

the site of the intimal tear. In the absence of hemodynamically significant ICA/VA stenosis, neck pain and headache can be the only clinical manifestation of CeAD dissection [1, 2].

Until the late 20th century, ICA/VA dissection was thought to be extremely rare because it was mainly verified on autopsy in cases of fatal stroke. The latter rarely occurs in CeAD, which led to a misconception about the rarity of CeAD. After neuroimaging techniques, such as magnetic resonance angiography (MRA), computed tomography angiography (CTA) and MRI of neck arteries, were introduced into routine clinical practice, it became clear that ICA/VA dissection was the main cause of ischemic stroke in young adults and that it could be manifested as isolated neck pain and headache [1, 3–7].

In Russia, research of brain-supplying arteries dissection was pioneered by the Research Center of Neurology in the late 1990s, almost simultaneously with the studies conducted abroad. Despite the advancements in the study of clinical and neuroimaging features of arterial dissection, its cause remains poorly understood. Researchers often point to arterial wall weakness in brain-supplying arteries. But because autopsy studies are rare, the nature of arterial wall weakness remains unclear, although some authors report connective tissue disorders in the affected individuals [8, 9]. So far, no mutations have been detected in the collagen gene that could explain the weakness of the arterial wall in CeAD patients [10, 11].

The aim of this study was to analyze the following aspects of CeAD: 1) morphological changes in the ICA/VA wall; 2) clinical signs of connective tissue weakness and biomarkers of connective tissue damage; 3) the main provoking factors for CeAD.

METHODS

Between 2000 and 2018, we examined 271 patents with CeAD (mean age — 37.0 ± 10 years, 54% women). The inclusion criteria were as follows: the presence of IMH and/or characteristic angiographic CeAD signs on neuroimaging. Patients with traumatic CeAD and patients with a typical clinical picture of CeAD not verified by neuroimaging were excluded from the study. Before developing CeAD, all patients considered themselves practically healthy. Clinical manifestations of CeAD included ischemic stroke (63%), a transient ischemic attack (9%), isolated neck pain /headache (27%), or isolated caudal nerve palsy (1%). Localization of CeAD was as follows: ICA — 139 patients (51%), VA — 116 patients (43%), ICA + VA — 16 patients (6%). Fifty-nine patients (22%) had multiple dissections involving both VA, both ICA or their combination. Four patients with ICA dissection developed a massive cerebral infarction and died. Their brain-supplying arteries, both dissected and non-dissected, were subjected to a histopathologic examination (Laboratory of Pathological Anatomy, Research Center of Neurology). An ICA fragment was obtained from one patient during reconstructive ICA surgery complicated by its dissection and stroke and subjected to a histopathologic examination. Staining of histological preparations was performed using hematoxylin and eosin, fuchselin (Weigert's method), von Kossa's method for calcium salts detection, and van Gieson's method.

A total of 48 clinical signs of connective tissue dysplasia (CTD) selected from the diagnostic criteria for inherited connective tissue diseases were analyzed in 82 CeAD patients. Every sign was classified as present (1 point) or absent (0 points). In addition, the presence of past history headaches was assessed in all patients. The control group included 40 healthy volunteers (mean age 38.5 ± 6.6 years; 62.5% of them were women.). The serological biomarkers of CTD, including matrix metalloproteinase 9 (MMP-9), tissue inhibitor of metalloproteinase 1 (TIMP-1), hydroxyproline, sulphated glycosaminoglycans, as well as fibroblast growth factor 21 (FGF-21), were measured once using ELISA. Orosomucoid levels were determined in 82 patients using an automated Konelab 30IPrime chemistry analyzer (Thermo Fisher Scientific Oy; Finland). The control subgroup included 25 healthy volunteers (mean age — 36.9 ± 6.6 years; 60.1% of them were women). Provoking factors, the frequency of CeAD recurrence and its seasonal variability were analyzed in all patients.

The IBM SPSS 23.0 (IBM; USA) statistics software package was used for statistical analysis. In this study, quantitative variables are presented as a mean and a standard deviation from the mean; qualitative and ordered categorical variables are presented as frequency and percentage. The normality of qualitative data distribution was tested with the Shapiro–Wilk test. Differences between the groups were assessed by the chi-squared test or Fisher's exact test for categorical variables and one-way ANOVA for continuous variables. Homoskedasticity of the residuals was tested using the Goldfeld–Quandt test. Differences were considered significant at $p < 0.05$. CTD signs relevant to dissection were identified using binary statistical regression: significant signs were selected stepwise from the entire set of all features by applying the Wald test method. Considering the significance of differences in CTD signs between the affected patients and the controls (the chi-squared test), additional signs were introduced in order to improve the quality of our model. This algorithm allowed us to identify CTD signs also typical of ICA and VA dissection. The model demonstrated its best predictive performance with 4 main and 2 additional signs; such combination of clinical signs was considered diagnostically relevant to ICA and VA dissection.

RESULTS

Morphological changes in brain-supplying arteries

On the macroscopic examination, dissected arteries appeared dilated and thickened, looking similar to thrombosed blood vessels. The histopathologic examination of extra- and intracranial arteries revealed changes in the internal elastic membrane: thinning, splitting, lack of physiological tortuosity, and calcifications. Some arterial segments were totally devoid of the internal elastic membrane. Changes in the tunica media were represented by its uneven thickness with areas of severe thinning, a decrease in the number of myocytes, their incorrect orientation, necrosis, areas of fibrosis and sclerosis, a decrease in the number of elastic fibers. These pathologic changes were found in both dissected and non-dissected ICA and VA (see the Figure).

Clinical signs of connective tissue dysplasia and its biomarkers in patients with CeAD

Clinical signs of CTD were more pronounced in the patients with CeAD (the average total score was 7.9 ± 3.6 points) than in the controls (6 ± 2.5; $p = 0.0039$). Besides, they were more pronounced in females (8.73 ± 3.0) than in males (6.4 ± 2.5; $p = 0.05$). The following 8 clinical signs were observed more frequently in CeAD patients than in the controls: arterial hypotension (51% vs 20%; $p < 0.012$), extensive bruising (40% vs 10%; $p = 0.011$); widened atrophic scars on skin (22.5% vs 0%; $p = 0.019$); translucent skin (28.75% vs 5%; $p = 0.034$); high-arched palate (20% vs 0%; $p = 0.034$); propensity to constipation (30% vs 10%; $p = 0.05$); nasal bleeding (33.75% vs 15%; $p = 0.043$); blue sclera (20% vs 5%; $p = 0.05$). In

addition, CeAD patients suffered from headache in the past history more often than the controls (60% vs 35%; $p = 0.02$). Based on statistical significance, 8 CTD signs listed above and past history headache were divided into main (hypotension, extensive bruising, widened atrophic scars on skin, past history headache) and additional (translucent skin, nasal bleeding, propensity to constipation, blue sclera, high-arched palate) features.

According to the regression model, the maximum predictive ability for arterial dissection (77%) was observed in the presence of 4 main and 2 additional clinical signs of CTD. In the presence of 4 main signs only, the predictive accuracy of the model was 75%.

Biological markers of connective tissue damage

Patients with CeAD had elevated MMP-9 (384 ± 69.3 ng/ml vs 203.1 ± 60.5 ng/ml in the controls; $p < 0.0005$), TIMP-1 (393.9 ± 63.4 ng/ml vs 134.4 ± 30.8 ng/ml in the controls; $p < 0.0005$), sulphated glycosaminoglycans (6.2 ± 1.4 μg/ml vs 4.5 ± 0.8 μg/ml in the controls; $p < 0.0005$), and orosomucoid (121.6 ± 27.8 mg/dl vs 88.8±17.4 mg/dl in the controls; $p < 0.0005$). Hydroxyproline levels were decreased in CeAD patients (604.9 ± 350.9 ng/ml vs 1293.6 ± 214.5 ng/ml in the controls; $p < 0.0005$) (Table 1). MMP-9 was higher in the patients with multiple dissections (400.5 ± 71.5 ng/ml) than in those with one dissected ICA (375.5 ± 71.55 ng/ml; $p < 0.03$) or one dissected VA (369.3 ± 68.6 ng/ml; $p < 0.08$). TIMP-1 was also higher in the patients with multiple dissections (422.2 ± 53.8 ng/ml) than in those who had only one dissected ICA (378.5 ± 62.3 ng/ml; $p < 0.024$) or one dissected VA (373.6 ± 60.6 ng/ml; $p < 0.008$). In the patients with multiple dissections, sulphated glycosaminoglycans were as high as 6.8 ± 1.2 μg/ml, while in the patients with one dissected ICA or one dissected VA their concentrations were lower (5.8 ± 1.3 μg/ml and 5.7 ± 1.5 μg/ml, $p < 0.029$ and < 0.016, respectively). Orosomucoid levels were higher in the patients with multiple dissections (129.7 ± 34 mg/dl) than in those with one dissected artery: ICA (118.6 ± 25.3; $p < 0.039$) or VA (112.6 ± 20.6 mg/dl; $p < 0.011$) (Table 2). In the first 3 months of CeAD, orosomucoid and hydroxyproline levels were higher than in the late stage of the disease. By contrast, TIMP-1concentrations were higher in later stages. FGF-21, which is the biomarker of mitochondrial pathology [12], was increased in CeAD patients (536 ± 250 pg/ml), as compared to the controls (204 ± 50 pg/ml; $p < 0.0005$).

Factors provoking arterial dissection

The most common provoking factors for CeAD responsible for 42% of the studied cases were neck movements and physical exertion; they were observed more often in VA dissection (61%) than in ICA dissection (27%; $p < 0.0009$). A minor preceding head trauma was observed in 10% of the patients (ICA — 14%, VA — 5%; $p < 0.05$). Acute respiratory infection in the month preceding CeAD was reported by 14% of the patients. Twelve percent of women were on contraceptive pills before dissection.

No significant differences were observed in the incidence of dissections between the months of the year. The frequency of dissection occurrence was 9.6%, 9.3%, 8.1%, 4.2%, 8%, 9.6%, 5.9%, 10%, 9.6%, 8.5%, 7.0%, 10.4% for January through December, respectively. No associations were found with acute respiratory infection occurring in the month preceding CeAD.

Recurrences

Twelve percent of our patients developed a recurrent dissection usually involving the opposite eponymous artery. All recurrences were verified by neuroimaging. In most cases, they occurred in the first 35 days of dissection (7.3%), in the months that followed (within a year), their frequency was 1.5%. Further relapses developed 3.3% of the patients 5 to 10 years later.

DISCUSSION

Clinical, laboratory and morphological examinations of CeAD patients revealed the presence of connective tissue pathology; these findings were consistent with the literature reports

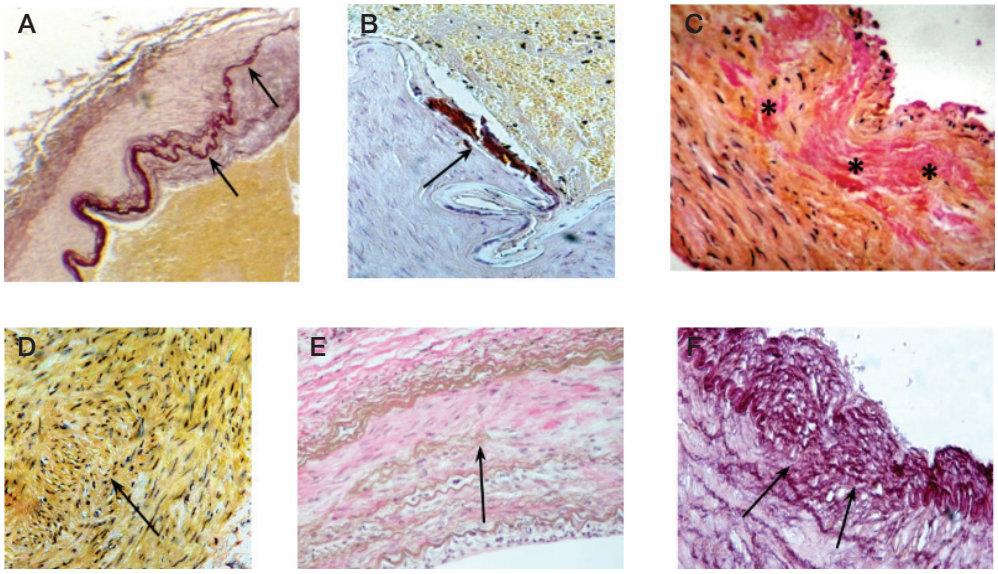

Figure. Arterial wall dysplasia in the internal carotid and vertebral arteries. **A**. Thinning and splitting of the internal elastic membrane in the dissected ICA siphon (*shown by arrows*). Staining: Weigert's elastic stain (*fuchselin*); x100 magnification. **B**. Calcium deposits on the internal elastic membrane in the dissected ICA siphon (shown by an arrow). Staining: von Kossa method; x200 magnification. **C**. Areas of fibrosis (*marked by an asterisk*) in the tunica media of the extracranial segment of the dissected ICA. Staining: van Gieson's stain; x200 magnification. **D**. An area of the tunica media in the dissected ICA siphon containing irregularly oriented myocyts (*marked by an arrow*). Staining: van Gieson's stain; x200 magnification. **E**. Areas of fibrosis and the decreased number of elastic fibers in the tunica media of the intact internal carotid artery (*shown by an arrow*). Staining: van Gieson's stain; x200 magnification. **F**. A fragment of the internal elastic membrane is missing (*shown by an arrow*) in the intact vertebral artery. Staining: Weigert's elastic stain (*fuchselin*); x200 magnification

[8, 9]. The detected abnormalities were not characteristic of well-known inherited connective tissue disorders, such as Ehlers–Danlos, Marfan or joint hypermobility syndromes, and, in our opinion, could be classified as undifferentiated. The morphological examination of both dissected and non-dissected brain-supplying arteries revealed pronounced dysplastic changes, which underlay arterial wall weakness and predisposed it to dissection [13–16]. In our opinion, the changes found on microscopic examination of brain-suppling arteries are similar to those in fibromuscular dysplasia (FMD) [13, 16]. Of note, FMD, whose international diagnostic criteria were published in 2019 [17], bears many similarities to CeAD dissection. FMD patients often develop dissections of various arteries, including ICA/VA, have cerebral aneurysms and tortuosity of the arteries [17], which are also typically seen in CeAD patients [18]. Many FMD patients [17], as well as CeAD patients [18], suffer from headaches. The incidence of hereditary burden in FMD (1.9–7.3%) [17] and CeAD (2%) [19] is similar. A genome-wide association study of FMD patients identified a common genetic risk variant: a single nucleotide polymorphism (SNP) rs9349379-A in the PHACTR1 locus (6p24) [20] also detected in CeAD patients during a multicenter international study conducted in 1,393 individuals, including our cohort of patients [21]. The adverse effect of contraceptive pills was observed in both patients with CeAD [1, 5, 22] and FMD [17]. Despite the similarity between patients with FMD and CeAD, the latter do not have the key diagnostic angiographic feature of FMD: alternating areas of stenosis and dilation (the so-called 'string of beads'). Therefore, the presence of FMD in the absence of typical angiography findings requires further investigation. The possibility of FMD can be indirectly confirmed by a case of our patient who had 3 dissection recurrences involving both ICA and the right VA plus left kidney infarction over the course of 10 years. CT-angiography of his renal arteries revealed alternating areas of narrowing and dilation — changes typically seen in FMD; those changes were not detected in the patient's ICA and VA. According to the contemporary diagnostic criteria for FMD, if a patient has typical FMD changes in at least one artery, then dissection, tortuosity or aneurysms in other arteries should be considered as manifestations of FMD. This was the case with our patient.

The cause of arterial wall dysplasia similar to that observed in CeAD patients is not completely clear [23]. According to our hypothesis, dysplasia may be associated with mitochondrial disorders [24]. Elevated FGF-21, a biomarker of mitochondrial pathology [12], found in our CeAD patients indirectly confirms this assumption. The pathogenesis of FMD also remains unknown; some authors pinpoint the significance of elevated transforming growth factors β1 and β2 (TGF-β1 and TGF-β2) produced by fibroblasts [25].

Clinical signs of CTD were more pronounced in CeAD patients than in the controls, which is consistent with the literature reports [9]. This indicates the widespread nature of connective tissue damage, which agrees with electron microscopy findings in skin biopsies [8, 24]. The higher incidence of CTD signs in women, as compared to men, suggests that female sex hormones play a role in the development of dysplasia. Along with clinical CTD signs, we analyzed the presence of past history headaches in CeAD patients, since our previous studies revealed that headache might be associated with arterial wall dysplasia [22]; in the literature, such headache is usually interpreted as migraine [5]. The analysis of CTD signs in young patients with stroke can help to clarify the cause of stroke in cases when neuroimaging examination is not available. Statistical analysis showed that in the presence of four main and two additional CTD signs, the probability of dissection as a cause of ischemic stroke in young adults is as high as 77% [22].

Connective tissue damage in CeAD patients was confirmed by the elevated levels of CDT biomarkers (MMP-9 and sulfated glycosaminoglycans). Increased orosomucoid levels were suggestive of inflammation in the arterial wall. Laboratory signs of inflammation are also reported by other authors, who link them to a previous infection seen as a provoking factor

Table 1. CTD biomarkers in the patients with ICA/VA dissections in the controls (one-way ANOVA)

Biomarkers (mean ± SD)	Arterial dissection *n* = 82	Control *n* = 25	*p*
MMP-9, ng/ml	384 ± 69.3	203.1 ± 60.5	< 0.0005
TIMP-1, ng/ml	393.9 ± 63.4	134.4 ± 30.8	< 0.0005
Orosomucoid, mg/dl	121.6 ± 27.8	88.8 ±17.4	< 0.0005
Sulphated glycosaminoglycans, μg/ml	6.2 ± 1.4	4.5 ± 0.8	< 0.0005
Hydroxyproline, ng/ml	604.9 ± 350.9	1293.6 ± 214.5	< 0.0005

Note: *p* — statistical significance; SD — standard deviation.

Table 2. CTD biomarkers in patients with different localization of arterial dissection (one-way ANOVA and post-hoc tests + Scheffe's procedure)

Biomarker (mean ± SD)	Group 1 ICA dissection *n* = 28	Group 2 VA dissection *n* = 27	Group 3 Dissection of more than 1 artery *n* = 27	*p*
MMP-9, ng/ml	375.5 ± 71.5	369.3 ± 68.6	400.5 ± 71.5	Groups 1 and 3 0.03
				Groups 2 and 3 0.008
TIMP-1, ng/ml	378.5 ± 62.3	373.6 ± 60.6	422.2 ± 53.8	Groups 1 and 3 0.024
				Groups 2 and 3 0.008
Sulphated glycosaminoglycans, μg/ml	5.8 ± 1.3	5.7 ± 1.5	6.8 ± 1.2	Groups 1 and 3 0.029
				Groups 2 and 3 0.016
Orosomucoid, mg/dl	118.6 ± 25.3	112.6 ± 20.6	129.7 ± 34	Groups 1 and 3 0.039
				Groups 2 and 3 0.011

Note: *p* — statistical significance; ICA — internal carotid artery; VA — vertebral artery; SD — standard deviation.

of dissection [26]. Higher levels of orosomucoid (a marker of inflammation) during the first 3 months of CeAD are also evident of inflammatory response induced by dissection. In our study, the levels of CTD biomarkers were higher in the patients with multiple dissections than in the individuals with one dissected artery, indicating more pronounced connective tissue damage in the former that led to multiple dissections. TIMP-1, an enzyme that blocks matrix proteinases, was higher in the patients examined after 3 months into dissection than in those examined in the first 3 months, which apparently was indicative of the reparative stage.

In patients with arterial wall dysplasia, ICA/VA dissection can be provoked by a number of factors, including head movements, minor head injury, physical exertion, acute respiratory infection in the month preceding dissection, birth pills, elevated blood pressure, alcohol consumption immediately before dissection, weight loss pills, long and frequent plane journeys [1, 5, 22]. In our patients, neck movements and physical exertion were the most frequent provoking factors (42%), occurring more often in the individuals with VA dissection (61%) than in those with ICA dissection (27%). Some researchers suggest the provoking role of manual therapy [5], which some of our patients had received immediately before dissection, as well as the role of neck injuries [6, 7]. VA is especially vulnerable at the moment of neck movement because of its fixation inside the vertebral canal. Because of low elasticity of the dysplastic arterial wall, artery stretching during neck/head movement leads to intimal tears at the sites where the artery is attached to the surrounding structures. In our patients, minor head injury preceded ICA dissection more often (14%) than VA dissection (5%); this finding is consistent with the reports of other researchers [5]. Head injury causes brain displacement relative to the skull, which is accompanied by tension of the intracranial ICA segment and causes an intimal tear at the level where ICA enters the scull and fixed to the bones. This is a common site of IMH formation.

Recent infection (most commonly, acute respiratory infection), which is considered to be a provoking CeAD factor, was found in 14% of our patients. In young patients with ischemic stroke unrelated to dissection recent infection is not so frequent, which confirms its provoking role in CeAD [27]. Infection is accompanied by elevated leukocyte proteolytic enzymes and increased concentrations of matrix metalloproteinases that induce protein degradation in the extracellular matrix of the arterial wall and cause endothelial damage [26, 27]. Elevated levels of MMT-9 and orosomucoid revealed in our patients confirm this mechanism of provoking action of infection.

Contraceptive pills as a factor provoking dissection was detected in 12% of female participants, which is less common than in European studies [6, 7]. The mechanism underlying the effect of contraceptives on the arterial wall is unknown; perhaps they aggravate dysplastic changes in the arterial wall, predisposing it to dissection.

Some authors point to the role of seasonal weather changes because CeAD occurs in cold periods more often. It is hypothesized that elevated arterial pulse pressure and frequent respiratory infections at the cold time of the year may provoke arterial dissection [28, 29]. In our study we did not find any significant differences in the CeAD incidence between the months of the year and did not detect any associations with infections. Atmospheric instability in general and air pressure fluctuations in particular are common to all seasons in the middle part of Russia, where the majority of our patients were residing. Perhaps, low atmospheric pressure is a pathogenically important environmental factor since it causes arteries to dilate. In this case, an intimal tear can occur at the site of more severe morphological changes (defects of the internal elastic membrane, a thin tunica media with few elastic fibers, areas of fibrosis, myocyte necrosis).

Although the mechanism of action is clear for most provoking factors, there is still no explanation as to why CeAD recurrences are rare, given that these factors are very common in everyday life (head turns, physical exercise, respiratory infections, etc.) and that, according to our morphological data, dysplasia involves all brain suppling arteries. Recurrences verified by neuroimaging occurred in 12.1% of our patients, usually in the first 35 days of CeAD (7.3%); in the few months that followed (within a year) their frequency was 1.5%. Further relapses developed in 3.3% of patients within 5 to 10 years. The true recurrence rate in the first month of CeAD seems to be higher, since the first neuroimaging examination carried out in this period revealed multiple dissections in 22% of our patients. According to other authors, relapses occur more often in the first weeks of the disease, and their frequency is less than 3%. The late-term recurrence rate among 200 patients observed for 7.4 years was 7% [30].

The highest recurrence rate in the first month after dissection and the low recurrence frequency in later follow-up periods allowed us to hypothesize the existence of critical periods when the arterial wall weakens and becomes susceptible to dissection. Along with infection and hormonal changes seen in a number of our patients, some endogenous metabolic disorders leading to degradation of the extracellular matrix, necrosis of myocytes in media, and impairment of fibroblast function, seem to be important [13]. From the standpoint of our concept that sees mitochondrial cytopathy as a cause of arterial wall dysplasia [24], a parallel can be drawn to an energy crisis characteristic of mitochondrial diseases, which could explain the low rate of late and the high rate of early dissection recurrences.

CONCLUSIONS

Arterial wall weakness due to its dysplasia predisposes patients to CeAD; the morphological changes in the arterial wall in CeAD are similar to those in FMD. 2. Endogenous and exogenous factors can severely aggravate dysplasia, which at a critical point can lead to spontaneous or provoked arterial dissection. 3. The critical period lasts about a month; this is when recurrences are most likely to happen. In order to prevent them, it is important to avoid abrupt head movements and wear a neck orthosis. 4. A repeated MRI scan of cervical arteries is recommended at the end of the first month to catch a possible clinically asymptomatic recurrence. 5. Further research into the pathogenesis of arterial wall dysplasia in CeAD will help to develop a pathogenetically based preventive treatment.

References

1. Kalashnikova LA, Dobrynina LA. Dissekcija arterij golovnogo mozga: ishemicheskij insul't i drugie klinicheskie projavlenija. M.: Izd-vo «Vako», 2013; 208 s. Russian.
2. Robertson JJ, Koyfman A. Cervical artery dissection: a review. J

Emerg Med. 2016; 51 (5): 508–18. PubMed PMID: 27634674.
3. Hakimi R, Sivakumar S. Imaging of Carotid Dissection. Curr Pain Headache Rep. 2019; 23 (1): 2. PubMed PMID: 30661121.
4. Kalashnikova LA, Dobrynina LA, Dreval MV, Doronina EV, Nazarova MA. Shejnaya i golovnaja bol' kak edinstvennoe projavlenie dissekcii vnutrennej sonnoj i pozvonochnoj arterij. Zhurnal nevrologii i psihiatrii im. Korsakova. 2015; (3): 9–16. PubMed PMID: 24300790. Russian.
5. Débette S. Pathophysiology and risk factors for cervical artery dissection: what have we learned from large hospital-based cohorts? Curr Opin Neurol. 2014; (1): 20–8. PubMed PMID: 24300790.
6. von Babo M, De Marchis GM, Sarikaya H, Stapf C, Buffon F, Fischer U, et al. Differences and similarities between spontaneous dissections of the internal carotid artery and the vertebral artery. Stroke. 2013; 44 (6): 1537–42. PubMed PMID: 23632978.
7. Debette S, Grond-Ginsbach C, Bodenant M, Kloss M, Engelter S, Metso, et al. Differential features of carotid and vertebral artery dissections: the CADISP study. Neurology. 2011; 77 (12): 1174–81. PubMed PMID: 21900632.
8. Brandt T, Hausser I, Orberk E, Grau A, Hartschuh W, Anton-Lamprecht I, et al. Ultrastructural connective tissue abnormalities in patients with spontaneous cervicocerebral artery dissections. Ann Neurol. 1998; (44): 281–285. PubMed PMID: 9708556.
9. Giossi A, Ritelli M, Costa P, Morotti A, Poli L, Del Zotto E, et al. Connective tissue anomalies in patients with spontaneous cervical artery dissection. Neurology. 2014; 83 (22): 2032–7. PubMed PMID: 25355826.
10. Grond-Ginsbach C, Thomas-Feles C, Werner I, Weber R, Wigger F, Hausser I, et al. Mutations in the tropoelastin gene (ELN) were not found in patients with spontaneous cervical artery dissections. Stroke. 2000; 31 (8): 1935–8. PubMed PMID: 10926960.
11. Grond-Ginsbach C, Weber R, Haas J, Orberk E, Kunz S., Busse O, et al. Mutations in the COL5A1 coding sequence are not common in patients with spontaneous cervical artery dissections. Stroke. 1999; 30 (9):1887–90. PubMed PMID: 10471441.
12. Lehtonen JM, Forsström S, Bottani E, Viscomi C, Baris OR, Isoniemi H, et al. FGF 21 is a biomarker for mitochondrial translation and mtDNA maintenance disorders. Neurology. 2016; 87 (22): 2290–9. PubMed PMID: 27794108.
13. Kalashnikova LA, Gulevskaya TS, Anufriev PL, Gnedovskaja EV, Konovalov RN, Piradov MA. Ischemic stroke in young age due to dissection of intracranial carotid artery and its branches (clinical and morphological study). Annals of Clinical and Experimental Neurology. 2009; 3 (1): 18–24. Russian.
14. Anderson RM, Schechter MM. A case of spontaneous dissecting aneurysm of the internal carotid artery. J Neurol Neurosurg Psychiatry. 1959; (22): 195–201. PMID: 13793447.
15. Southerland AM, Meschia JF, Worrall BB. Shared associations of nonatherosclerotic, large-vessel, cerebrovascular arteriopathies: considering intracranial aneurysms, cervical artery dissection, moyamoya disease and fibromuscular dysplasia. Curr Opin Neurol. 2013; (26): 13–28. PubMed PMID: 23302803.
16. Kalashnikova LA, Chaykovskaya RP, Gulevskaya TS, Dobrynina LA, Gubanova MV, Dreval MV, et al. Intimal rupture of the displastic middle cerebral artery wall complicated by thrombosis and fatal ischemic stroke. Zh Nevrol Psikhiatr Im S S Korsakova. 2018; 118 (3): 9–14. PubMed PMID: 29798974. Russian.
17. Gornik HL, Persu A, Adlam D, Aparicio LS, Azizi M, Boulanger M, et al. First International Consensus on the diagnosis and management of fibromuscular dysplasia. Vascular Medicine. 2019; 24 (2): 164–89. PubMed PMID: 306448921.
18. De Giuli V, Grassi M, Lodigiani C, Patella R, Zedde M, Gandolfo C, et al. Association between migraine and cervical artery dissection: the Italian project on stroke in young adults. JAMA Neurol. 2017; 74 (5) 512–18. PubMed PMID: 28264095.
19. Schievink WI, Mokri B, Piepgras DG, Kuiper JD. Recurrent spontaneous artery dissections. Risk in familial versus nonfamilial disease. Stroke. 1996; 27 (4): 622–4. PubMed PMID: 8614918.
20. Kiando SR, Tucker NR, Castro-Vega LJ, Katz A, D'Escamard V, Tréard C, et al. PHACTR1 is a genetic susceptibility locus for fibromuscular dysplasia supporting its complex genetic pattern of inheritance. PLOS Genet. 2016; 12 (10): e1006367. PubMed PMID: 27792790.
21. Debette S, Kamatani Y, Metso TM, Kloss M, Chauhan G, Engelter ST, et al. Common variation in PHACTR1 is associated with susceptibility to cervical artery dissection. Nat Genet. 2015; 47 (1): 78–83. PubMed PMID: 25420145.
22. Gubanova MV, Kalashnikova LA, Dobrynina LA, Shamtieva KV, Berdalin AB. Markery displazii soedinitel'noj tkani pri dissekcii magistral'nyh arterij golovy i provocirujushhie faktory dissekcii. Annaly klinicheskoj i jeksperimental'noj nevrologii. 2017; 11 (4): 19–28. DOI: 10.18454/ACEN.2017.4.2. Russian.
23. Hausser I, Muller U, Engelter S, Lyrer P, Pezzini A, Padovani A, et al. Different types of connective tissue alterations associated with cervical artery dissections. Acta Neuropathol. 2004; 107 (6): 509–14. PubMed PMID: 15067552.
24. Sakharova AV, Kalashnikova LA, Dobrynina LA, Chaykovskaya RP, Mir-Kasimov MF, Nazarova MA, et al. Morphological signs of mitochondrial cytopathy in skeletal muscles and micro-vessels in a patient with cerebral artery dissection associated with MELAS syndrome. Arkhiv patologii. 2010; 74 (2): 51–6. Russian.
25. Ganesh SK, Morissette R, Xu Z, Schoenhoff F, Griswold BF, Yang J, et al. Clinical and biochemical profiles suggest fibromuscular dysplasia is a systemic disease with altered TGF-β expression and connective tissue features. FASEB J. 2014; 28 (8): 3313–24. PubMed PMID: 24732132.
26. Grond-Ginsbach C, Giossi A, Aksay SS, Engelter ST, Lyrer PA, Metso TM, et al. Elevated peripheral leukocyte counts in acute cervical artery dissection. Eur J Neurol. 2013; 20 (10):1405–10. PubMed PMID: 23879551.
27. Guillon B, Berthet K, Benslamia L, Bertrand M, Bousser MG, Tzourio C. Infection and the risk of spontaneous cervical artery dissection: a case-control study. Stroke. 2003; 34 (7): 79–81. PubMed PMID: 12805497.
28. Schievink WI, Wijdicks EF, Kuiper JD. Seasonal pattern of spontaneous cervical artery dissection. J Neurosurg. 1998; 89 (1): 101–3. PubMed PMID: 9647179.
29. Kloss M, Metso A, Pezzini A, Leys D, Giroud M, Metso TM, et al. Towards understanding seasonal variability in cervical artery dissection (CeAD). J Neurol. 2012; 259 (8):1662–7. PubMed PMID: 22286657.
30. Schievink WI, Mokri B, O'Fallon WM. Recurrent spontaneous cervical-artery dissection. N Engl J Med. 1994; 330 (6): 393–7. PubMed PMID: 8284004.

Литература

1. Калашникова Л. А., Добрынина Л. А. Диссекция артерий головного мозга: ишемический инсульт и другие клинические проявления. М.: Изд-во «Вако», 2013; 208 с.
2. Robertson JJ, Koyfman A. Cervical artery dissection: a review. J Emerg Med. 2016; 51 (5): 508–18. PubMed PMID: 27634674.
3. Hakimi R, Sivakumar S. Imaging of Carotid Dissection. Curr Pain Headache Rep. 2019; 23 (1): 2. PubMed PMID: 30661121.
4. Калашникова Л. А., Добрынина Л. А., Древаль М. В., Доронина Е. В., Назарова М. А. Шейная и головная боль как единственное проявление диссекции внутренней сонной и позвоночной артерий. Журнал неврологии и психиатрии им. Корсакова. 2015; (3): 9–16. PubMed PMID: 24300790.
5. Débette S. Pathophysiology and risk factors for cervical artery dissection: what have we learned from large hospital-based cohorts? Curr Opin Neurol 2014; (1): 20–8. PubMed PMID: 24300790.
6. von Babo M, De Marchis GM, Sarikaya H, Stapf C, Buffon F, Fischer U, et al. Differences and similarities between spontaneous dissections of the internal carotid artery and the vertebral artery. Stroke. 2013; 44 (6): 1537–42. PubMed PMID: 23632978.
7. Debette S, Grond-Ginsbach C, Bodenant M, Kloss M, Engelter S, Metso, et al. Differential features of carotid and vertebral artery dissections: the CADISP study. Neurology. 2011; 77 (12): 1174–81. PubMed PMID: 21900632.

8. Brandt T, Hausser I, Orberk E, Grau A, Hartschuh W, Anton-Lamprecht I, et al. Ultrastructural connective tissue abnormalities in patients with spontaneous cervicocerebral artery dissections. Ann Neurol. 1998; (44): 281–285. PubMed PMID: 9708556.
9. Giossi A, Ritelli M, Costa P, Morotti A, Poli L, Del Zotto E, et al. Connective tissue anomalies in patients with spontaneous cervical artery dissection. Neurology. 2014; 83 (22): 2032–7. PubMed PMID: 25355826.
10. Grond-Ginsbach C, Thomas-Feles C, Werner I, Weber R, Wigger F, Hausser I, et al. Mutations in the tropoelastin gene (ELN) were not found in patients with spontaneous cervical artery dissections. Stroke. 2000; 31 (8): 1935–8. PubMed PMID: 10926960.
11. Grond-Ginsbach C, Weber R, Haas J, Orberk E, Kunz S., Busse O, et al. Mutations in the COL5A1 coding sequence are not common in patients with spontaneous cervical artery dissections. Stroke. 1999; 30 (9):1887–90. PubMed PMID: 10471441.
12. Lehtonen JM, Forsström S, Bottani E, Viscomi C, Baris OR, Isoniemi H, et al. FGF 21 is a biomarker for mitochondrial translation and mtDNA maintenance disorders. Neurology. 2016; 87 (22): 2290–9. PubMed PMID: 27794108.
13. Калашникова Л. А., Гулевская Т. С., Ануфриев П. Л., Гнедовская Е. В., Коновалов Р. Н., Пирадов М. А. Ишемический инсульт в молодом возрасте, обусловленный стенозирующим расслоением (диссекцией) интракраниального отдела внутренней сонной артерии и ее ветвей (клинико-морфологическое наблюдение). Анналы клинической и экспериментальной неврологии. 2009; 3 (1): 18–24.
14. Anderson RM, Schechter MM. A case of spontaneous dissecting aneurysm of the internal carotid artery. J Neurol Neurosurg Psychiatry. 1959; (22): 195–201. PMID: 13793447.
15. Southerland AM, Meschia JF, Worrall BB. Shared associations of nonatherosclerotic, large-vessel, cerebrovascular arteriopathies: considering intracranial aneurysms, cervical artery dissection, moyamoya disease and fibromuscular dysplasia. Curr Opin Neurol. 2013; (26): 13–28. PubMed PMID: 23302803.
16. Калашникова Л. А., Чайковская Р. П., Гулевская Т. С., Добрынина Л. А., Губанова М. В., Древаль М. В., Максимова М. Ю. Разрыв интимы при дисплазии стенки средней мозговой артерии, осложнившийся тромбозом и развитием тяжелого ишемического инсульта (клинико-морфологическое наблюдение). Журнал неврологии и психиатрии им. С. С. Корсакова. 2018; 118 (3): 9–14. PubMed PMID: 29798974.
17. Gornik HL, Persu A, Adlam D, Aparicio LS, Azizi M, Boulanger M, et al. First International Consensus on the diagnosis and management of fibromuscular dysplasia. Vascular Medicine. 2019; 24 (2): 164–89. PubMed PMID: 306448921.
18. De Giuli V, Grassi M, Lodigiani C, Patella R, Zedde M, Gandolfo C, et al. Association between migraine and cervical artery dissection: the Italian project on stroke in young adults. JAMA Neurol. 2017; 74 (5) 512–18. PubMed PMID: 28264095.
19. Schievink WI, Mokri B, Piepgras DG, Kuiper JD. Recurrent spontaneous artery dissections. Risk in familial versus nonfamilial disease. Stroke. 1996; 27 (4): 622–4. PubMed PMID: 8614918.
20. Kiando SR, Tucker NR, Castro-Vega LJ, Katz A, D'Escamard V, Tréard C, et al. PHACTR1 is a genetic susceptibility locus for fibromuscular dysplasia supporting its complex genetic pattern of inheritance. PLOS Genet. 2016; 12 (10): e1006367. PubMed PMID: 27792790.
21. Debette S, Kamatani Y, Metso TM, Kloss M, Chauhan G, Engelter ST, et al. Common variation in PHACTR1 is associated with susceptibility to cervical artery dissection. Nat Genet. 2015; 47 (1): 78–83. PubMed PMID: 25420145.
22. Губанова М. В., Калашникова Л. А., Добрынина Л. А., Шамтиева К. В., Бердалин А. Б. Маркеры дисплазии соединительной ткани при диссекции магистральных артерий головы и провоцирующие факторы диссекции. Анналы клинической и экспериментальной неврологии. 2017; 11 (4): 19–28. DOI: 10.18454/ACEN.2017.4.2.
23. Hausser I, Muller U, Engelter S, Lyrer P, Pezzini A, Padovani A, et al. Different types of connective tissue alterations associated with cervical artery dissections. Acta Neuropathol. 2004; 107 (6): 509–14. PubMed PMID: 15067552.
24. Сахарова А. В., Калашникова Л. А., Чайковская Р. П., Добрынина Л. А., Мир-Касимов М. Ф. Назарова М. А. и др. Морфологические и ультраструктурные признаки митохондриальной цитопатии в скелетных мышцах и микрососудах мышц и кожи при диссекции церебральных артерий, ассоциированной с мутацией A3243G в митохондриальной ДНК. Архив патологии. 2012; 74 (2): 51–6.
25. Ganesh SK, Morissette R, Xu Z, Schoenhoff F, Griswold BF, Yang J, et al. Clinical and biochemical profiles suggest fibromuscular dysplasia is a systemic disease with altered TGF-β expression and connective tissue features. FASEB J. 2014; 28 (8): 3313–24. PubMed PMID: 24732132.
26. Grond-Ginsbach C, Giossi A, Aksay SS, Engelter ST, Lyrer PA, Metso TM, et al. Elevated peripheral leukocyte counts in acute cervical artery dissection. Eur J Neurol. 2013; 20 (10):1405–10. PubMed PMID: 23879551.
27. Guillon B, Berthet K, Benslamia L, Bertrand M, Bousser MG, Tzourio C. Infection and the risk of spontaneous cervical artery dissection: a case-control study. Stroke. 2003; 34 (7): 79–81. PubMed PMID: 12805497.
28. Schievink WI, Wijdicks EF, Kuiper JD. Seasonal pattern of spontaneous cervical artery dissection. J Neurosurg. 1998; 89 (1): 101–3. PubMed PMID: 9647179.
29. Kloss M, Metso A, Pezzini A, Leys D, Giroud M, Metso TM, et al. Towards understanding seasonal variability in cervical artery dissection (CeAD). J Neurol. 2012; 259 (8):1662–7. PubMed PMID: 22286657.
30. Schievink WI, Mokri B, O'Fallon WM. Recurrent spontaneous cervical-artery dissection. N Engl J Med. 1994; 330 (6): 393–7. PubMed PMID: 8284004.

PROTHROMBOGENIC POLYMORPHIC VARIANTS OF HEMOSTATIC AND FOLATE METABOLISM GENES IN PATIENTS WITH ASEPTIC CEREBRAL VENOUS THROMBOSIS

Maksimova MYu ✉, Dubovitskaya YuI, Krotenkova MV, Shabalina AA

Research Center of Neurology, Moscow, Russia

Cerebral venous sinus thrombosis (CVT) becomes the cause of stroke in less than 1% of patients. In 20-30% of patients, the cause of thrombosis remains unclear, and thrombosis is considered idiopathic. Inherited hypercoagulable conditions significantly increase the risk of CVT. The aim of the study was to evaluate the frequency of prothrombogenic polymorphic variants of hemostatic and methionine-homocysteine metabolism genes alleles and genotypes in patients with aseptic CVT. Fifty one patients aged 18–75 with aseptic CVT were examined. The control group included 36 healthy volunteers. Neuroimaging methods included brain MRI in standard modes (T1, T2, T2 d-f (FLAIR), DWI) and MR venosinusography. All patients were surveyed to identify carriers of prothrombogenic polymorphic variants of hemostatic and folate metabolism genes alleles and genotypes. Prothrombogenic polymorphic variants of hemostatic genes were detected in 94% of patients, and the variants of the methionine-homocysteine metabolism genes were observed in 86% of patients. The differences between distributions of alleles and genotypes 5G6754G of the *PAI-1* gene, G103T of the *FXIIIA1* gene, A66G of the *MTRR* gene, A2756G of the *MTR* gene in the group of patients with CVT and in the control group were significant. Allele 4G, genotypes 4G/4G and 5G/4G of 5G6754G polymorphism of the *PAI-1* gene; allele T of G103T polymorphism of the *FXIIIA1* gene; allele G and genotype A/G of A66G polymorphism of the *MTRR* gene; allele G and genotype A/G of A2756G polymorphism of the *MTR* gene correlated with aseptic CVT. It was concluded that the gene polymorphisms 5G6754G (*PAI-1*), G103T (*FXIIIA1*), A66G (*MTRR*) and A2756G (*MTR*) carriage increased the risk of aseptic CVT and did not affect the thrombosis clinical manifestations.

Keywords: aseptic cerebral venous sinus thrombosis, prothrombogenic polymorphic variants of hemostatic and folate metabolism genes

Funding: the study was performed as a part of the public assignment of the Research Center of Neurology.

Author contribution: Maksimova MYu — concept development and study arrangement, clinical and laboratory data analysis, statistical analysis, manuscript writing; Dubovitskaya YuI — clinical examination of patients, data aquisition and primary analysis of the results; Krotenkova MV — brain MRI, MR venography and neuroimaging diagnosis of cerebral venous sinus thrombosis; Shabalina AA — laboratory analysis of prothrombogenic polymorphic variants of hemostatic and folate metabolism genes.

Compliance with ethical standards: the study was approved by the Ethics Committee of the Research Center of Neurology (protocol № 12–8/16 dated December 14, 2016). All patients submitted the informed consent to participation in the study.

✉ **Correspondence should be addressed:** Marina Yu. Maximova
Volokolamskoye Shosse, 80, Moscow, 125367; ncnmaximova@mail.ru

Received: 19.08.2019 **Accepted:** 06.10.2019 **Published online:** 16.10.2019

DOI: 10.24075/brsmu.2019.065

ПРОТРОМБОГЕННЫЕ ПОЛИМОРФНЫЕ ВАРИАНТЫ ГЕНОВ СИСТЕМЫ ГЕМОСТАЗА И ФОЛАТНОГО ОБМЕНА ПРИ АСЕПТИЧЕСКОМ ТРОМБОЗЕ ЦЕРЕБРАЛЬНЫХ ВЕНОЗНЫХ СИНУСОВ

М. Ю. Максимова ✉, Ю. И. Дубовицкая, М. В. Кротенкова, А. А. Шабалина

Научный центр неврологии, Москва, Россия

Тромбоз церебральных венозных синусов (ТЦВС) составляет менее 1% всех случаев инсульта. В 20–30% случаев причина тромбоза остается неясной и его расценивают как идиопатический. Врожденные гиперкоагуляционные состояния значительно увеличивают риск развития ТЦВС. Целью исследования было оценить частоту аллелей и генотипов протромбогенных полиморфных вариантов генов гемостаза и метионин-гомоцистеинового обмена при асептическом ТЦВС. Обследован 51 пациент с асептическим ТЦВС в возрасте от 18 до 75 лет. Контрольную группу составили 36 здоровых добровольцев. Нейровизуализационные методы включали МРТ головного мозга в стандартных режимах (T1, T2, T2 d-f (FLAIR), ДВИ) и МР-веносинусографию. Всем пациентам проводили исследование на носительство аллелей и генотипов протромбогенных полиморфных вариантов генов системы гемостаза и фолатного обмена. Протромбогенные полиморфные варианты генов системы гемостаза были выявлены в 94% случаев, генов метионин-гомоцистеинового обмена — в 86% случаев. Получены достоверные различия при исследовании распределения аллелей и генотипов 5G6754G гена *PAI-1*, G103T гена *FXIIIA1*, A66G гена *MTRR*, A2756G гена *MTR* в группе больных ТЦВС по сравнению с группой здоровых добровольцев. Аллель 4G, генотипы 4G/4G и 5G/4G полиморфизма 5G6754G гена *PAI-1*; аллель T полиморфизма G103T гена *FXIIIA1*; аллель G и генотип A/G полиморфизма A66G гена *MTRR*; аллель G и генотип A/G полиморфизма A2756G гена *MTR* связаны с развитием асептического ТЦВС. Сделан вывод, что носительство полиморфизма генов *PAI-1* (5G6754G), *FXIIIA1* (G103T), *MTRR* (A66G) и *MTR* (A2756G) повышает риск развития асептического ТЦВС и не влияет на клинические проявления тромбоза.

Ключевые слова: асептический тромбоз церебральных венозных синусов, протромбогенные полиморфные варианты генов гемостаза и фолатного обмена

Финансирование: работа выполнена в рамках государственного задания ФГБНУ НЦН.

Информация о вкладе авторов: М. Ю. Максимова — разработка концепции и организация исследования, обобщающий анализ клинических и лабораторных данных, статистическая обработка, написание статьи; Ю. И. Дубовицкая — проведение клинического обследования пациентов, сбор и первичный анализ полученных результатов; М. В. Кротенкова — проведение МРТ головного мозга, МР-веносинусографии и нейровизуализационной диагностики тромбоза церебральных венозных синусов; А. А. Шабалина — проведение лабораторного исследования протромбогенных полиморфных вариантов генов гемостаза и фолатного обмена.

Соблюдение этических стандартов: исследование одобрено этическим комитетом ФГБНУ «Научный центр неврологии» (протокол № 12–8/16 от 14 декабря 2016 г.). Все пациенты подписали добровольное информированное согласие на участие в исследовании.

✉ **Для корреспонденции:** Марина Юрьевна Максимова
Волоколамское ш., д. 80, г. Москва, 125367; ncnmaximova@mail.ru

Статья получена: 19.08.2019 **Статья принята к печати:** 06.10.2019 **Опубликована онлайн:** 16.10.2019

DOI: 10.24075/vrgmu.2019.065

Cerebral venous sinus thrombosis (CVT) becomes the cause of stroke in less than 1% of patients [1, 2]. In 20–30% of patients, the cause of thrombosis remains unclear, and thrombosis is considered idiopathic [3]. Inherited hypercoagulable conditions significantly increase the risk of CVT [4, 5].

The incidence of cerebral venous sinus thrombosis (CVT) is 1.3 per 100,000 adults per year. Onset may occur at any age, but the highest incidence is noted in people aged 31–50 [6]. Among patients, the women prevail [7]. Despite the improvement of diagnostic and treatment methods, the CVT patients' mortality remains high and reaches 30% [8].

CVT can be either septic (as a result of complications of purulent otitis media, mastoiditis, sinusitis) or aseptic (occurs as a complication of numerous diseases that increase the tendency to form a blood clot).

Many factors are involved in the development of aseptic CVT: severe dehydration, cardiac disorders (congenital heart defects, heart failure, artificial cardiac pacemaker), cancer, pregnancy, diabetes mellitus, hormonal drugs usage (contraceptive pills, hormone replacement therapy), nephrotic syndrome, polycythemia, essential thrombocytosis, antiphospholipid syndrome, connective tissue disorders and vasculitis (systemic lupus erythematosus, granulomatosis with polyangiitis, temporal arteritis, Behcet's disease), inflammatory bowel disease (Crohn's disease, ulcerative colitis), brain injury, congenital or acquired hemostasis alterations [9–12].

Hereditary thrombophilia is a significant risk factor for aseptic CVT. The most studied are polymorphic variants of factor V (Leiden) and prothrombin genes [13]. Thus, correlation was observed between the risk of CVT and the clotting factor V (OR 4.3; 95% CI — 1.5–12.3) and prothrombin genes (OR 3,6; 95% CI — 1,0–13,1) polymorphisms [14]. In another study, prothrombin gene polymorphism (A replaced with G at position 20210) was found in 19% of patients with CVT [15]. Correlation between the presence of the Leiden mutation and a 5-fold increase in the risk of CVT was confirmed [13]. Analysis of 26 case-control type studies demonstrated that the occurrence of the clotting factor V gene polymorphism (Leiden/G1691A) leaded to 2.4 fold increase of the risk of CVT (95% CI — 1.75–3.30; $p < 0.00001$), and the occurrence of the prothrombin gene polymorphism (G20210A) leaded to 5.48 fold increase of the CVT risk (95% CI — 3.88–7.74; $p < 0.00001$) [16].

Significant polymorphism of clinical manifestations, the absence of pathognomonic symptoms, as well as a variety of options for the onset, course, and localization of thrombosis make the clinical recognition of CVT difficult. Possibilities of CVT early diagnosis significantly expanded due to the neuroimaging methods (CT and MRI) [2, 17, 18]. Currently, MR venosinusography is one of the most reliable methods for the CVT diagnosis [19]. In up to 63% of patients, CVT is complicated by cerebral edema and the formation of necrosis foci with the addition of hemorrhagic component (37.57% of patients) [20]. In such a situation, these foci of necrosis are not infarcts, but arise as a result of the venous outflow slowdown, edema, hypoxia of brain tissue followed by diapedesis of red blood cells and leukocytes through necrotic walls of capillaries and microvessels. The factors predisposing to development of necrosis foci and hematomas in patients with CVT include the female sex, epileptic seizure, impaired consciousness, rapidly spreading thrombosis involving two or more venous sinuses [2, 8, 20].

Often, CVT is suppressed, it is detected unexpectedly by physician during CT or MRI of the brain. For most patients with CVT, a mismatch between the general condition of the patient and the neuroimaging manifestations of the disease is typical [17, 21].

Early diagnosis and well-organized treatment of aseptic CVT in the vast majority of patients leads to clinical recovery. Later, a decrease in the frequency of recurrent thrombosis depends on the timely identification of the thrombosis causes. Almost all researchers agree that recurrent CVT is more severe than the first diagnosed, and its prognosis is much worse.

The aim of the study was to evaluate the frequency of the prothrombogenic polymorphic variants of hemostatic and methionine-homocysteine metabolism genes alleles and genotypes in patients with aseptic CVT.

METHODS

In 2016–2019, 51 patients with aseptic CVT were examined in the 2nd Department of Neurology of the Research Center of Neurology (20 men and 31 women, the average age of the patients was 42.2 ± 13.1). Twenty eight patients were hospitalized in the acute phase of the disease. In 23 patients, the duration of thrombosis was 1–10 months. Control group included 36 healthy volunteers (14 men and 22 women, their average age was 44.7 ± 10.4). The groups under study were comparable by gender and age. Inclusion criteria: 1) acute aseptic CVT confirmed by neuroimaging data; 2) pre-existing aseptic CVT confirmed by neuroimaging data; 3) patients aged 18–75. Exclusion criteria: 1) septic CVT; 2) lower-extremity deep vein thrombosis (DVT) and pulmonary embolism (PE); 3) atherothrombosis involving cerebral arteries, lower limb arteries; 4) other (nonvascular) nervous system diseases; 5) decompensated comorbidities.

In all CVT patients, a detailed study of complaints, general and family history data, the clinical picture of the disease and medical documentation was performed, somatic and neurological statuses were evaluated.

For CVT diagnosis, each patient underwent brain MRI using the Magnetom Verio (Siemens; Germany) and Magnetom Symphony (Siemens; Germany) systems with 3T (Tesla) and 1.5T magnetic field strength respectively. MRI of the brain was performed in the sagittal, axial and coronal planes in T1, T2, T2 d-f (FLAIR), DWI modes with a slice thickness of 1, 3 and 5 mm. Later the images of the cerebral veins and venous sinuses were obtained using MRI in the venosinusography mode. Only after a comprehensive evaluation and a detailed study of the neuroimaging results obtained using standard modes and venosinusography, the CVT diagnosis was considered confirmed. Standard modes, T2, T2-FLAIR, were used for assessment of brain tissue focal lesions and for exclusion of other possible pathologies. Image evaluation was performed using the eFilm Workstation software (Merge Healthcare; USA).

Measurement of the hemostasis parameters (fibrinogen level, fibrinolytic activity level, partial thromboplastin time (PTT)) was performed using the ACL-9000 Coagulation Analyzer (Instrumentation Laboratory; USA).

Quantitative determination of D-dimer was carried out by the specific antigen–antibody reaction based immunochemical method using the immunoturbidimetric latex-agglutination assay (Instrumentation Laboratory; USA).

The level of homocysteine in the blood was determined by enzyme immunoassay using the diagnostic kits (AXIS; Norway) and the Immulite 2000 Immunoassay System (Siemens; USA).

DNA diagnostics of prothrombotic polymorphic gene variants was performed using polymerase chain reaction (PCR).

Detection of mutations (polymorphisms) in the human genome was carried out using the DNA-Technology kit (Russia). The patient's genomic DNA was isolated from whole blood

(EDTA tube) using NC sample, the DNA extraction reagent kit (DNA-Technology; Russia).

Two amplification reactions were simultaneously carried out with a sample of isolated DNA using two pairs of allele-specific primers. Real-time PCR was used for simultaneous amplification and for measuring of the studied DNA molecule amount (DTlite Real-Time PCR System; DNA-Technology; Russia). The DNA-Technology (Russia) commercial kits were used. The analysis results were represented by three types of decisions: a) allele 1 homozygote; b) heterozygote; c) allele 2 homozygote.

Studied prothrombogenic polymorphic variants of hemostatic and folate metabolism genes list:

- prothrombin gene, *FII* (c.G20210A);
- coagulation factor V gene, *FV* (c.G1691A);
- coagulation factor VII gene, *FVII* (c.G10976A);
- activated factor XIII (fibrinase) gene, *FXIIIA1* (c.G103T);
- fibrinogen beta gene, *FGB* (c.G455A);
- plasminogen activator inhibitor gene, *PAI-1* (c.5G6754G);
- Integrin alpha (Gp1a glycoprotein) gene, *ITGA2* (c.C807T);
- Platelet fibrinogen receptor (Gp3a glycoprotein) gene, *ITGB3* (c.T1565C);
- methylenetetrahydrofolate reductase gene, *MTHFR* (c.C677T);
- methylenetetrahydrofolate reductase gene, *MTHFR* (c.A1298C);
- methionine synthase gene, *MTR* (c.A2756G);
- methionine synthase reductase gene, *MTRR* (c.A66G).

Statistical analysis was performed using the IBM SPSS Statistics software, v.23 (IBM Corporation; Russia). Nominal data were described with absolute values and percentages. For categorical data analysis the contingency tables were used. The significance level was taken equal to 0.05 in all comparisons.

Frequency of allele and genotype variants (*f*) was calculated by the following formula:

$$f = \frac{n}{2N} \text{ — allele frequency,}$$

$$f = \frac{n}{N} \text{ — genotype frequency,}$$

where *n* was the variant (allele or genotype) occurrence, *N* was the sample size.

The significance of differences in the allele and genotype frequencies between the studied groups was evaluated using the χ^2 criterion.

To assess the relative risk, the odds ratio (OR) and its confidence interval (CI) calculations were used at a confidence level of 95%.

$$OR = \frac{(a + d)}{(b + c)},$$

where *a* was the frequency of the studied allele (genotype) in the treatment group; *b* was the frequency of the allele in the control group; *c* was the sum of other alleles (genotypes) frequencies in the treatment group; *d* was the sum of other alleles (genotypes) frequencies in the control group.

RESULTS

Isolated CVT was observed in 14 patients (27.5%). In other 37 patients (72.5%) multiple thrombosis was detected involving two or more venous sinuses.

Left transverse sinus thrombosis was detected in 28 patients (54.9%), left sigmoid sinus thrombosis in 26 patients (51%), right transverse sinus thrombosis in 21 patient (41.2%), right sigmoid sinus thrombosis in 14 patients (27.5%), superior sagittal sinus thrombosis in 11 patients (21.6%), inferior sagittal sinus thrombosis in 4 patients (7.8%), tentorial sinus in 3 patients (5.9%), and left cavernous sinus thrombosis in 1 patient.

Among patients with thrombosis of individual venous sinuses, 5 patients (35.7%) were diagnosed with thrombosis of the left transverse sinus, 5 patients (35.7%) were diagnosed with thrombosis of the left sigmoid sinus, 3 patients (21.4%) were diagnosed with thrombosis of the right transverse sinus, and 1 patient was diagnosed with thrombosis of the superior sagittal sinus.

In 4 women, CVT occurred after abortion, in 1 woman onset took place 9 days after delivery, in 7 women (22.6%) CVT developed while taking hormonal drugs (contraceptives). A history of inflammatory diseases of the paranasal sinuses was observed in 3 women and 1 man. Aseptic CVT was confirmed by the absence of systemic inflammatory reactions and inflammatory changes of the laboratory blood parameters.

Among all CVT patients, the focal necrosis in brain tissue caused by thrombosis was observed in 14 patients (27.5%).

Diffuse headache was the chief complaint, which was observed in 45 patients (88.2%). A typical feature of the headache was its worsening after being in a horizontal position. Unsystematic dizziness was noted in 27.5% of patients; it was constant, independent of body position. Nausea occurred in 23.5% of patients. In 7 patients (13.7%), thrombosis began with impaired consciousness. Convulsive seizures were observed in 5 patients (9.8%): focal motor seizures in 2 patients and generalized tonic-clonic seizures in 3 patients. In 9.8% of patients, the meningitis symptoms were noted. Impaired motor function was detected in 3 patients (5.9%): hemiplegia in 1 patient, mild or moderate decrease in muscle strength in the limbs in 2 patients. Speech problems were represented by mild motor aphasia in 4 patients (7.8%).

When calculating the correlation coefficients, a relationship was found between brain tissue focal lesions and the development of convulsive seizures (correlation coefficient $r = 0.4$; $p < 0.01$), motor function impairment (correlation coefficient $r = 0.5$; $p < 0.01$), speech problems (correlation coefficient $r = 0.5$; $p < 0.01$), and depression of consciousness (correlation coefficient $r = 0.5$; $p < 0.01$).

Statistical analysis revealed correlation of superior sagittal sinus thrombosis with the development of a convulsive seizure (correlation coefficient $r = 0.4$; $p < 0.01$), as well as impaired venous outflow (correlation coefficient $r = 0.5$; $p < 0.01$). It also revealed correlation of tentorial sinus thrombosis with the depression of consciousness (correlation coefficient $r = 0.3$; $p < 0.01$).

Hemostasis parameters

In the group of patients with CVT the fibrinogen level was 3.7 g/l [2.2; 6.8] (in the control group it was 3.8 g/l [2.9; 5.0]); activated partial thromboplastin time was 29.5 s [22.5; 36.2] (in the control group it was 28.7 s [26.5; 29.9]); antithrombin III level was 112 [98; 119] (in the control group it was 115 [107; 126]); C protein level was 134% [125; 148] (in the control group it was 143% [125; 165]); D-dimer level did not exceed 0.5 μg/ml. The fibrinogen level increase over 5.5 mmol/l was detected in one patient. Hemostasis parameters of the CVT patients did not differ significantly from the hemostasis parameters of the control group patients.

Homocysteine level in the blood plasma of CVT patients was 16.2 μmol/l [14.6; 17.7] (in the control group it was 7.7 [5.6; 10.9]; $p < 0.05$).

Prothrombogenic polymorphic variants of hemostasis and folate metabolism genes

Molecular genetic testing for detection of prothrombogenic polymorphic variants of hemostatic genes (Table 1) and methionine-homocysteine metabolism genes (Table 2) was carried out in 51 patients with aseptic CVT.

Homozygous (4G/4G) allele 4G at the –675 position of the *PAI-1* gene was detected in 11 patients (22.4%). Homozygous allele 103T of the *FXIIIA1* gene was detected in 3 patients, homozygous allele 807T of the *ITGA2* gene was present in 3 patients. Two patients were the 455A allele of the *FGB* gene homozygous carriers, 1 patient was the 10976A allele of the *FVII* gene carrier, and 1 patient was the 1565C allele of the *ITGB3* gene carrier. Combination of two alleles in a homozygous state was detected in 2 patients. In the first of them the combination of homozygous 10976A allele of the *FVII* gene and 6754G allele of plasminogen activator inhibitor gene *PAI-1* was observed. In the other of them the combination of homozygous 103T allele of the *FXIIIA1* gene and 6754G allele of the plasminogen activator inhibitor gene *PAI-1* was present. No patients with homozygous 1691A allele of the *FV Leiden* and 20210A allele of the *FII* gene were revealed.

Heterozygous allele 4G at the –675 position of the *PAI-1* gene was detected in 28 patients (57.1%). Isolated polymorphic variant of the *PAI-1* gene (c. 5G6754G) in the heterozygous state was present in 9 patients (19%). Seventeen patients (34.7%) were heterozygous carriers of 455A of the *FGB* gene. Thirteen patients (26.5%) were carriers of 10976A allele of the *FVII* gene, 103T allele of the *FXIIIA1* gene, and 1565C allele of the *ITGB3* gene. Polymorhic variant 807T of the *ITGA2* gene in the heterozygous state was observed in 9 patients (18.4%). Polymorhic variant 1691A of the *FV Leiden* gene in the heterozygous state was present in 3 patients (5.9%). Two patients (4%) were heterozygous carriers of 20210A allele of the *FII* gene.

The frequency distribution of hemostasis genes prothrombogenic polymorphic variants alleles and genotypes could be found in Table 1.

Alleles 5G and 4G of the *PAI-1* gene frequency was 48 (49%) and 50 (51%) in the treatment group, in the control group it was 59 (82%) and 13 (18%). According to the calculated odds ratio, 4G allele increases the risk of CVT by more than 4 times ($\chi^2 = 19.337$; $p < 0.001$; OR = 4.728; 95% CI — 2.303–9.706). Homozygous 4G/4G polymorphism increases the risk of CVT by 10.1 times ($\chi^2 = 6.623$; $p = 0.011$; OR = 10.132 + 1.070; 95% CI — 1.243–82.573), and heterozygous 5G/4G polymorphism increases the risk of the disease by 3.03 times ($\chi^2 = 5.908$; $p = 0.016$; OR = 3.030 + 0.463; 95% CI — 1.223–7.507).

Comparative analysis of the alleles of *FXIIIA1* gene G103T polymorphism frequencies in patients of the treatment group and control group revealed statistically significant differences. Alleles G and T of the *FXIIIA1* gene occurrence was 79 (80.6%) and 19 (19,4%) in the CVT patients group, and 67 (93%) and 5 (7%) in the control group. Thus, the frequency of 103T allele of the *FXIIIA1* gene in patients with CVT significantly exceeds the frequency of the allele in the group of healthy people ($\chi^2 = 5.3$; $p = 0.022$). According to the calculated odds ratio, the presence of T allele in the *FXIIIA1* gene increases the risk of CVT by more than 3 times (OR = 3.223; 95% CI — 1.142–9.095).

There were no differences in the allele and genotype frequencies distribution of the *FII* (c.G20210A), *FV* (c.G1691A), *FVII* (c.G10976A), *FGB* (c.G455A), *ITGA2* (c.C807T), *ITGB3* (c.T1565C), *MTHFR* (c.C677T), *MTHFR* (c.A1298C) genes between patients with CVT and healthy volunteers.

Among patients with polymorphic variants of methionine-homocysteine metabolism genes, 66G allele of the *MTRR* gene in a homozygous state was detected in 5 patients (10.9%). Three patients (6.8%) were homozygous carriers of 677T allele of the *MTHFR* gene, and 2 patients (4.2%) were carriers of 1298C allele of the *MTHFR* gene. In one patient, the combination of the homozygous 1298C allele of the *MTHFR* gene and 66G allele of the *MTRR* gene was observed. No patients were homozygous carriers of 2756G allele of the *MTR* gene.

Sixteen patients (36.4%) were identified as heterozygous carriers of 677T allele of the *MTHFR* gene, 19 patients (41.3%) as carriers of 66G allele of the *MTRR* gene, 18 patients (39.1%) as carriers of 2756G allele of the *MTR* gene, and 9 patients (18.8%) as carriers of 1298C allele of the *MTHFR* gene.

Isolated polymorphic variant of the *MTRR* gene (c.A66G) in heterozygous state was present in 7 patients (17%).

In 3 patients (7%), the isolated polymorphic variant of the *MTR* gene (c.A2756G) in heterozygous state was identified.

Among 19 patients who were identified as heterozygous carriers of 66G allele of the *MTRR* gene, in 9 patients (47%), the heterozygous variant of 1298C allele of the *MTHFR* gene was also detected.

The frequency values for individual polymorphic variants of methionine-homocysteine metabolism genes are presented in Table 2.

According to data obtained, the frequency of alleles A and G of the *MTRR* gene (c.A66G) in the treatment group was 63 (68.5%) and 29 (31.5%). The frequency of these alleles in the control group was 64 (89%) and 8 (11%) respectively. The G allele frequency differences between the group of patients with CVT and the group of healthy people were significant ($\chi^2 = 9.631$; $p = 0.002$; OR = 3.683; 95% CI — 1.564–8.672). Allele G increased the risk of CVT by 3.68 times ($\chi^2 = 9.631$; $p = 0.002$; OR = 3.683 ± 0.437; 95% CI — 1.564–8.672). The presence of A/G polymorphism increased the risk of CVT by 3.5 times ($\chi^2 = 5.784$; $p = 0.017$; OR = 3.519 + 0.538; 95% CI — 1.225–10.104).

Allele G of A2756G polymorphism of the *MTR* gene frequency in the group of patients with CVT was significantly higher than in the control group (18 (19.6%) against 6 (8%); $\chi^2 = 4.079$; $p = 0.044$), and the frequency of allele A was significantly lower (74 (80,4%) against 66 (92%); $\chi^2 = 4.079$; $p = 0.044$). The odds ratio calculation demonstrated that allele G of A2756G polymorphism correlated with CVT (OR = 2.676 ± 0.501; 95% CI — 1.002–7.142). In patients with CVT, the frequency of A/G heterozygous genotypes was significantly higher than in the control group ($\chi^2 = 4.923$; $p = 0.027$; OR = = 3.214 ± 0.540; 95% CI — 1.116–9.257).

When performing the clinical molecular analysis, no significant correlation between the CVT clinical features and the identified prothrombogenic polymorphic gene variants was revealed.

Isolated CVT without any *PAI-1* gene polymorphisms (c.5G6754G) was diagnosed in 1 patient, and isolated CVT with PAI-1 polymorphisms in the homozygous or heterozygous state was diagnosed in 13 patients (33%). Multiple CVT without any *PAI-1* gene polymorphisms was detected in 9 patients (90%), and multiple CVT with *PAI-1* polymorphisms in the homozygous or heterozygous state was identified in 26 (67%) patients ($p = 0.244$).

Table 1. Frequency of alleles and genotypes of the hemostasis genes prothrombogenic polymorphic variants

Prothrombin gene *FII* (c.G20210A)						
	n	Allele frequency		Genotype frequency		
		G	A	G/G	G/A	A/A
CVT patients	50	98 (98%)	2 (2%)	48 (96%)	2 (4%)	0 (0%)
Control group	36	71 (99%)	1 (1%)	35 (97.2%)	1 (2.8%)	0 (0%)
Coagulation factor V gene, *FV* (c.G1691A)						
	n	Allele frequency		Genotype frequency		
		G	A	G/G	G/A	A/A
CVT patients	51	99 (97.1%)	3 (2.9%)	48 (94.1%)	3 (5.9%)	0 (0%)
Control group	36	72 (100%)	0 (0%)	36 (100%)	0 (0%)	0 (0%)
Coagulation factor VII gene, *FVII* (c.G10976A)						
	n	Allele frequency		Genotype frequency		
		G	A	G/G	G/A	A/A
CVT patients	49	83 (84.7%)	15 (15.3%)	35 (71.4%)	13 (26.5%)	1 (2%)
Control group	36	66 (92%)	6 (8%)	30 (83.3%)	6 (16.7%)	0 (0%)
Activated factor XIII (fibrinase) gene, *FXIIIA1* (c.G103T)						
	n	Allele frequency		Genotype frequency		
		G*	T**	G/G	G/T	T/T
CVT patients	49	79 (80.6%)	19 (19.4%)	33 (67.3%)	13 (26.5%)	3 (6.1%)
Control group	36	67 (93%)	5 (7%)	31 (86.1%)	5 (13.9%)	0 (0%)

Note: * — χ^2 = 5.3; p = 0.022; OR = 0.310; 95% CI 0.110–0.876
**— χ^2 = 5.3; p = 0.022; OR = 3.223 + 0.529; 95% CI 1.142–9.095

Plasminogen activator inhibitor gene, *PAI-1* (c.5G6754G)						
	n	Allele frequency		Genotype frequency		
		5G*	4G**	5G/5G***	5G/4G****	4G/4G*****
CVT patients	49	48 (49%)	50 (51%)	10 (20.4%)	28 (57.1%)	11 (22.4%)
Control group	36	59 (82%)	13 (18%)	24 (66.7%)	11 (30.6%)	1 (2.8%)

Note: * — χ^2 = 19.337; p < 0.001; OR = 0.212; 95% CI 0.103–0.434;
** — χ^2 = 19.337; p < 0.001; OR = 4.728 + 0.367; 95% CI 2.303–9.706;
*** — χ^2 = 18.503; p < 0.001; OR = 0.128; 95% CI 0.048–0.302;
**** — χ^2 = 5.908; p = 0.016; OR = 3.030 + 0.463; 95% CI 1.223–7.507;
***** — χ^2 = 6.623; p = 0.011; OR = 10.132 + 1.070; 95% CI 1.243–82.573.

Fibrinogen beta gene, *FGB* (c.G455A)						
	n	Allele frequency		Genotype frequency		
		G	A	G/G	G/A	A/A
CVT patients	49	77 (78.6%)	21 (21.4%)	30 (61.2%)	17 (34.7%)	2 (4.1%)
Control group	36	62 (86%)	10 (14%)	26 (72.2%)	10 (27.8%)	0 (0%)
Integrin alpha (Gp1a glycoprotein) gene, *ITGA2* (c.C807T)						
	n	Allele frequency		Genotype frequency		
		C	T	C/C	C/T	T/T
CVT patients	49	83 (84.7%)	15 (15.3%)	37 (75.5%)	9 (18.4%)	3 (6.1%)
Control group	36	61 (85%)	11 (15%)	26 (72.2%)	9 (25%)	1 (2.8%)
Platelet fibrinogen receptor (Gp3a glycoprotein) gene, *ITGB3* (c.T1565C)						
	n	Allele frequency		Genotype frequency		
		T	C	T/T	T/C	C/C
CVT patients	49	83 (84.7%)	15 (15.3%)	35 (71.4%)	13 (26.5%)	1 (2%)
Control group	36	67 (93%)	5 (7%)	31 (86.1%)	5 (13.9%)	0 (0%)

Isolated CVT with polymorphic variants of the *FXIIIA1* gene (c.G103T) in the homozygous or heterozygous state was observed in 5 patients (31%), and the isolated CVT without any *FXIIIA1* polymorphisms was present in 9 patients (27%). Multiple CVT was diagnosed in 11 patients (69%) with polymorphic variants of the *FXIIIA1* gene (c.G103T) in the homozygous or heterozygous state, and in 24 patients (73%) with no *FXIIIA1* polymorphisms (p = 1.000).

Among patients with polymorphic variant of the *MTR* 2756 gene in heterozygous state, isolated CVT was observed in 10 patients (56%), and multiple thrombosis was observed in 8 patients (44%). In the absence of polymorphisms of the *MTR*

Table 2. Frequency of alleles and genotypes of the folate metabolism genes pro-thrombogenic polymorphic variants

Methylenetetrahydrofolate reductase gene, *MTHFR* (c.C677T)						
	n	Allele frequency		Genotype frequency		
		C	T	C/C	C/T	T/T
CVT patients	44	66 (75%)	22 (25%)	25 (56.8%)	16 (36.4%)	3 (6.8%)
Control group	36	60 (83%)	12 (17%)	26 (72.2%)	8 (22.2%)	2 (5.6%)
Methylenetetrahydrofolate reductase gene, *MTHFR* (c.A1298C)						
	n	Allele frequency		Genotype frequency		
		A	C	A/A	A/C	C/C
CVT patients	48	83 (86.5%)	13 (13.5%)	37 (77.1%)	9 (18.8%)	2 (4.2%)
Control group	36	64 (89%)	8 (11%)	29 (80.6%)	6 (16.7%)	1 (2.8%)
Methionine synthase reductase gene, *MTRR* (c.A66G)						
	n	Allele frequency		Genotype frequency		
		A*	G**	A/A***	A/G****	G/G
CVT patients	46	63 (68.5%)	29 (31.5%)	22 (47.8%)	19 (41.3%)	5 (10.9%)
Control group	36	64 (89%)	8 (11%)	29 (80.6%)	6 (16.7%)	1 (2.8%)

Note: * — $\chi^2 = 9.631$; $p = 0.002$; OR = 0.272; 95% CI 0.115–0.640;
** — $\chi^2 = 9.631$; $p = 0.002$; OR = 3.683 + 0.437; 95% CI 1.564–8.672;
*** — $\chi^2 = 9.201$; $p = 0.003$; OR = 0.221; 95% CI 0.081–0.606;
**** — $\chi^2 = 5.784$; $p = 0.017$; OR = 3.519 + 0.538; 95% CI 1.225–10.104.

Methionine synthase gene, *MTR* (c.A2756G)						
	n	Allele frequency		Genotype frequency		
		A*	G**	A/A***	A/G****	G/G
CVT patients	46	74 (80.4%)	18 (19.6%)	28 (69.9%)	18 (39.1%)	0 (0%)
Control group	36	66 (92%)	6 (8%)	30 (83.3%)	6 (16.7%)	0 (0%)

Note: * — $\chi^2 = 4.079$; $p = 0.044$; OR = 0.374; 95% CI 0.140–0.998;
** — $\chi^2 = 4.079$; $p = 0.044$; OR = 2.676 + 0.501; 95% CI 1.002–7.142;
*** — $\chi^2 = 4.923$; $p = 0.027$; OR = 0.311; 95% CI 0.108–0.896;
**** — $\chi^2 = 4.923$; $p = 0.027$; OR = 3.214 + 0.540; 95% CI 1.116–9.257.

gene (c.A2756G), isolated CVT was diagnosed in 7 patients (25%), and multiple CVT was diagnosed in 21 (75%) patients ($p = 0.06$).

In homozygous and heterozygous carriers of 677T allele of the *MTRR* gene, isolated CVT was detected in 5 patients (21%), multiple CVT was detected in 19 patients (79%). Among patients with no *MTRR* gene polymorphism isolated CVT was diagnosed in 8 patients (38%), and multiple CVT was diagnosed in 13 (62%) patients ($p = 0.323$).

DISCUSSION

During our study, CVT was diagnosed in 24 patients (47.1%) aged under 40. The ratio between males and females was 1 : 1.2. Slight prevalence of thrombosis among women of childbearing age could be explained by such risk factors as pregnancy, the use of contraceptives and hormone replacement therapy [22].

Prothrombogenic polymorphic variants of hemostatic genes were diagnosed in 94% of patients. Most often, polymorphic variants of the *PAI-1* gene (c.5G6754G) were observed, the product of which was involved in the fibrinolysis regulation. The presence of a polymorphic variant of such gene leads to an increase in the plasminogen activator inhibitor protein functional activity, which in turn contributes to an increased risk of thrombosis [23]. The frequency of heterozygous 4G allele at the –675 position of the *PAI-1* gene in the population is 50%, and the frequency of the homozygous allele is 26% [24]. In our study, 4G allele at the –675 position of the *PAI-1* gene in heterozygous state (5G/4G) was detected in 57.1% of patients, and in the homozygous state (4G/4G) it was detected in 22.4% of patients.

For the *PAI-1* gene, significant differences between the group of patients with CVT and the group of healthy people were observed in the distribution of both alleles and genotypes. In patients with the 4G/4G genotype, the risk of CVT increased by 10.1 times (OR = 10.132; 95% CI — 1.243–82.573), and in patients with the 5G/4G genotype it increased by 3.03 times (OR = 3.030; 95% CI — 1.223–7.507).

The effect of factor *FXIIIA1* on CVT still remains unclear [25]. It is possible that G103T polymorphism of the *FXIIIA1* gene is associated with the fibrin structure alterations. At a low concentration of fibrinogen, the blood clot density in patient with G103T polymorphism is high, while with an increase in the level of fibrinogen, the density of the blood clot, and therefore its stability, decrease. In the presence of 4G/4G polymorphism of the *PAI-1* gene the protective effect of G103T polymorphism of the *FXIIIA1* gene decreases drastically [26].

Some authors note correlation of C677T polymorphism of the *MTHFR* gene and the risk of CVT [27, 28]. During our study, the prothrombogenic polymorphic variants of the methionine-homocysteine metabolism genes were detected in 86% of patients. Polimorphic variants of the *MTRR* (c.A66G) and *MTR* (A2756G) genes were most common. According to literature data, 66G allele of the *MTRR* gene frequency in the European population reaches 54%. In our study the frequency of the allele was 31.5%. Allelle G of A66G polymorphism of the *MTRR* gene increases the risk of CVT by 3.68 times (OR = 3.683; 95% CI — 1.564–8.672), allele G of A2756G polymorphism of the *MTR* gene increases the risk by 2.676 times (OR = 2.676; 95% CI — 1.002–7.142)

The presence of A/G polymorphism of the *MTRR* gene increases the risk of CVT by 3.5 times (OR = 3.519; 95% CI — 1.225–10.104), and the presence of A/G polymorphism of the *MTR* increases the risk by 3.2 times (OR = 3.214; 95% CI — 1.116–9.257).

CONCLUSION

Gene polymorphisms 5G6754G (*PAI-1*), G103T (*FXIIIA1*), A66G (*MTRR*) and A2756G (*MTR*) carriage increases the risk of aseptic CVT and do not affect the thrombosis clinical manifestations.

References

1. Behrouzi R, Punter M. Diagnosis and management of cerebral venous thrombosis. Clin Med (Lond). 2018; 18 (1): 75–9. DOI: 10.7861/clinmedicine.18-1-75.
2. Maali L, Khan S, Qeadan F, Ismail M, Ramaswamy D, Hedna VS. Cerebral venous thrombosis: continental disparities. Neurol Sci. 2017; 38 (11): 1963–8. PubMed PMID: 28808795. DOI: 10.1007/s10072-017-3082-7.
3. Lee DJ, Ahmadpour A, Binyamin T, Dahlin BC, Shahlaie K, Waldau B. Management and outcome of spontaneous cerebral venous sinus thrombosis in a 5-year consecutive single-institution cohort. J Neurointerv Surg. 2017; 9 (1): 34–8. DOI: 10.1136/neurintsurg-2015-012237.
4. Agrawal K, Burger K, Rothrock JF. Cerebral sinus thrombosis. Headache. 2016; 56 (8): 1380–9. DOI: 10.1111/head.12873.
5. Capecchi M, Abbattista M, Martinelli I. Cerebral venous sinus thrombosis. J Thromb Haemost. 2018;16 (10):1918–31. DOI: 10.1111/jth.14210.
6. Coutinho JM, Zuurbier SM, Aramideh M, Stam J. The incidence of cerebral venous thrombosis: a cross-sectional study. Stroke. 2012; 43 (12): 3375–7. PubMed PMID: 22996960. DOI: 10.1161/STROKEAHA.112.671453.
7. Janghorbani M, Zare M, Saadatnia M, Mousavi SA, Mojarrad M, Asgari E. Cerebral vein and dural sinus thrombosis in adults in Isfahan, Iran: frequency and seasonal variation. Acta Neurol Scand. 2008; 117 (2): 117–21. PubMed PMID: 18184347. DOI: 10.1111/j.1600-0404.2007.00915.x.
8. Coutinho JM, Zuurbier SM, Stam J. Declining mortality in cerebral venous thrombosis: a systematic review. Stroke. 2014; 45 (5): 1338–41. DOI: 10.1161/STROKEAHA.113.004666.
9. de Freitas GR, Bogousslavsky J. Risk factors of cerebral vein and sinus thrombosis. Front Neurol Neurosci. 2008; (23): 23–54.
10. Kashkoush AI, Ma H, Agarwal N, Panczykowski D, Tonetti D, Weiner GM, et al. Cerebral venous sinus thrombosis in pregnancy and puerperium: A pooled, systematic review. J Clin Neurosci. 2017; (39): 9–15. DOI: 10.1016/j.jocn.2017.02.046.
11. Bushnell C, McCullough LD, Awad IA, Chireau MV, Fedder WN, Furie KL, et al. Guidelines for the prevention of stroke in women: a statement for healthcare professionals from the American Heart Association/American Stroke Association. Stroke. 2014; 45 (5): 1545–88. DOI: 10.1161/01.str.0000442009.06663.48.
12. Ilyas A, Chen CJ, Raper DM, Ding D, Buell T, Mastorakos P, et al. Endovascular mechanical thrombectomy for cerebral venous sinus thrombosis: a systematic review. J Neurointerv Surg. 2017; 9 (11):1086–92. DOI: 10.1136/neurintsurg-2016-012938.
13. McBane RD, Tafur A, Wysokinski WE. Acquired and congenital risk factors associated with cerebral venous sinus thrombosis. Thromb Res. 2010; 126 (2): 81–7. DOI: 10.1016/j.thromres.2010.04.015.
14. Martinelli I, Cattaneo M, Taioli E, De Stefano V, Chiusolo P, Mannucci PM. Genetic risk factors for superficial vein thrombosis. Thromb Haemost. 1999; 82 (4): 1215–7. PMID: 10544900.
15. Bushnell C, Saposnik G. Evaluation and management of cerebral venous thrombosis. Continuum (Minneap Minn). 2014; 20 (2 Cerebrovascular Disease): 335–51. DOI: 10.1212/01.CON.0000446105.67173.a8.
16. Marjot T, Yadav S, Hasan N, Bentley P, Sharma P. Genes associated with adult cerebral venous thrombosis. Stroke. 2011; 42 (4): 913–8. DOI: 10.1161/STROKEAHA.110.602672.
17. Ferro JM, Bousser MG, Canhão P, Coutinho JM, Crassard I, Dentali F, et al. European Stroke Organization guideline for the diagnosis and treatment of cerebral venous thrombosis — Endorsed by the European Academy of Neurology. Eur Stroke J. 2017; 2 (3): 195–221. DOI: 10.1177/2396987317719364.
18. Alshoabi SA. Cerebral venous sinus thrombosis: a diagnostic challenge in a rare presentation. Brain Circ. 2017; 3 (4): 227–230. DOI: 10.4103/bc.bc_27_17.
19. Gao L, Xu W, Li T, Yu X, Cao S, Xu H, et al. Accuracy of magnetic resonance venography in diagnosing cerebral venous sinus thrombosis. Thromb Res. 2018; (167): 64–73. DOI: 10.1016/j.thromres.2018.05.012.
20. Goyal G, Charan A, Singh R. Clinical Presentation, Neuroimaging Findings, and Predictors of Brain Parenchymal Lesions in Cerebral Vein and Dural Sinus Thrombosis: A Retrospective Study. Ann Indian Acad Neurol. 2018; 21 (3): 203–8. DOI: 10.4103/aian.AIAN_470_17.
21. Cai H, Ye X, Zheng W, Ma L, Hu X, Jin X. Pitfalls in the diagnosis and initial management of acute cerebral venous thrombosis. Rev Cardiovasc Med. 2018; 19 (4): 129–33. DOI: 10.31083/j.rcm.2018.04.4081.
22. Ferro JM, Canhão P, Aguiar de Sousa D. Cerebral Venous Thrombosis. Presse Med. 2016; 45 (12 Pt 2): e429–e450. PubMed PMID: 27816347. DOI: 10.1016/j.lpm.2016.10.007.
23. Schneider S, Kapelushnik J, Kraus M, El Saied S, Levi I, Kaplan DM. The association between otogenic lateral sinus thrombosis and thrombophilia — A long-term follow-up. Am J Otolaryngol. 2018; 39 (3): 299–302. PubMed PMID: 29530427. DOI: 10.1016/j.amjoto.2018.03.013.
24. Lichy C, Dong–Si T, Reuner K, Genius J, Rickmann H, Hampe T, et al. Risk of cerebral venous thrombosis and novel gene polymorphisms of the coagulation and fibrinolytic systems. J Neurol. 2006; 253 (3): 316–20. PubMed PMID: 16155788. DOI: 10.1007/s00415-005-0988-4.
25. Li B, Heldner MR, Arnold M, Coutinho JM, Zuurbier SM, Meijers JCM, et al. Coagulation Factor XIII in Cerebral Venous Thrombosis. TH Open. 2019; 3 (3): e227–e229. DOI: 10.1055/s-0039-1693487.
26. Bagoly Z, Muszbek L. Factor XIII: What does it look like? J Thromb Haemost. 2019; 17 (5): 714–6. DOI: 10.1111/jth.14431.
27. Ali Z, Troncoso JC, Fowler DR. Recurrent cerebral venous thrombosis associated with heterozygote methylenetetrahydrofolate reductase C677T mutation and sickle cell trait without homocysteinemia: an autopsy case report and review of literature. Forensic Sci Int. 2014; (242): e52–e55. DOI: 10.1016/j.forsciint.2014.07.007.
28. Ghaznavi H, Soheili Z, Samiei S, Soltanpour MS. Association study of methylenetetrahydrofolate reductase C677T mutation with cerebral venous thrombosis in an Iranian population. Blood Coagul Fibrinolysis. 2015; 26 (8): 869–73. DOI: 10.1097/MBC.0000000000000292.

Литература

1. Behrouzi R, Punter M. Diagnosis and management of cerebral venous thrombosis. Clin Med (Lond). 2018; 18 (1): 75–9. DOI: 10.7861/clinmedicine.18-1-75.
2. Maali L, Khan S, Qeadan F, Ismail M, Ramaswamy D, Hedna VS. Cerebral venous thrombosis: continental disparities. Neurol Sci. 2017; 38 (11): 1963–8. PubMed PMID: 28808795. DOI: 10.1007/s10072-017-3082-7.

3. Lee DJ, Ahmadpour A, Binyamin T, Dahlin BC, Shahlaie K, Waldau B. Management and outcome of spontaneous cerebral venous sinus thrombosis in a 5-year consecutive single-institution cohort. J Neurointerv Surg. 2017; 9 (1): 34–8. DOI: 10.1136/neurintsurg-2015-012237.
4. Agrawal K, Burger K, Rothrock JF. Cerebral sinus thrombosis. Headache. 2016; 56 (8): 1380–9. DOI: 10.1111/head.12873.
5. Capecchi M, Abbattista M, Martinelli I. Cerebral venous sinus thrombosis. J Thromb Haemost. 2018;16 (10):1918–31. DOI: 10.1111/jth.14210.
6. Coutinho JM, Zuurbier SM, Aramideh M, Stam J. The incidence of cerebral venous thrombosis: a cross-sectional study. Stroke. 2012; 43 (12): 3375–7. PubMed PMID: 22996960. DOI: 10.1161/STROKEAHA.112.671453.
7. Janghorbani M, Zare M, Saadatnia M, Mousavi SA, Mojarrad M, Asgari E. Cerebral vein and dural sinus thrombosis in adults in Isfahan, Iran: frequency and seasonal variation. Acta Neurol Scand. 2008; 117 (2): 117–21. PubMed PMID: 18184347. DOI: 10.1111/j.1600-0404.2007.00915.x.
8. Coutinho JM, Zuurbier SM, Stam J. Declining mortality in cerebral venous thrombosis: a systematic review. Stroke. 2014; 45 (5): 1338–41. DOI: 10.1161/STROKEAHA.113.004666.
9. de Freitas GR, Bogousslavsky J. Risk factors of cerebral vein and sinus thrombosis. Front Neurol Neurosci. 2008; (23): 23–54.
10. Kashkoush AI, Ma H, Agarwal N, Panczykowski D, Tonetti D, Weiner GM, et al. Cerebral venous sinus thrombosis in pregnancy and puerperium: A pooled, systematic review. J Clin Neurosci. 2017; (39): 9–15. DOI: 10.1016/j.jocn.2017.02.046.
11. Bushnell C, McCullough LD, Awad IA, Chireau MV, Fedder WN, Furie KL, et al. Guidelines for the prevention of stroke in women: a statement for healthcare professionals from the American Heart Association/American Stroke Association. Stroke. 2014; 45 (5): 1545–88. DOI: 10.1161/01.str.0000442009.06663.48.
12. Ilyas A, Chen CJ, Raper DM, Ding D, Buell T, Mastorakos P, et al. Endovascular mechanical thrombectomy for cerebral venous sinus thrombosis: a systematic review. J Neurointerv Surg. 2017; 9 (11):1086–92. DOI: 10.1136/neurintsurg-2016-012938.
13. McBane RD, Tafur A, Wysokinski WE. Acquired and congenital risk factors associated with cerebral venous sinus thrombosis. Thromb Res. 2010; 126 (2): 81–7. DOI: 10.1016/j.thromres.2010.04.015.
14. Martinelli I, Cattaneo M, Taioli E, De Stefano V, Chiusolo P, Mannucci PM. Genetic risk factors for superficial vein thrombosis. Thromb Haemost. 1999; 82 (4): 1215–7. PMID: 10544900.
15. Bushnell C, Saposnik G. Evaluation and management of cerebral venous thrombosis. Continuum (Minneap Minn). 2014; 20 (2 Cerebrovascular Disease): 335–51. DOI: 10.1212/01.CON.0000446105.67173.a8.
16. Marjot T, Yadav S, Hasan N, Bentley P, Sharma P. Genes associated with adult cerebral venous thrombosis. Stroke. 2011; 42 (4): 913–8. DOI: 10.1161/STROKEAHA.110.602672.
17. Ferro JM, Bousser MG, Canhão P, Coutinho JM, Crassard I, Dentali F, et al. European Stroke Organization guideline for the diagnosis and treatment of cerebral venous thrombosis — Endorsed by the European Academy of Neurology. Eur Stroke J. 2017; 2 (3): 195–221. DOI: 10.1177/2396987317719364.
18. Alshoabi SA. Cerebral venous sinus thrombosis: a diagnostic challenge in a rare presentation. Brain Circ. 2017; 3 (4): 227–230. DOI: 10.4103/bc.bc_27_17.
19. Gao L, Xu W, Li T, Yu X, Cao S, Xu H, et al. Accuracy of magnetic resonance venography in diagnosing cerebral venous sinus thrombosis. Thromb Res. 2018; (167): 64–73. DOI: 10.1016/j.thromres.2018.05.012.
20. Goyal G, Charan A, Singh R. Clinical Presentation, Neuroimaging Findings, and Predictors of Brain Parenchymal Lesions in Cerebral Vein and Dural Sinus Thrombosis: A Retrospective Study. Ann Indian Acad Neurol. 2018; 21 (3): 203–8. DOI: 10.4103/aian.AIAN_470_17.
21. Cai H, Ye X, Zheng W, Ma L, Hu X, Jin X. Pitfalls in the diagnosis and initial management of acute cerebral venous thrombosis. Rev Cardiovasc Med. 2018; 19 (4): 129–33. DOI: 10.31083/j.rcm.2018.04.4081.
22. Ferro JM, Canhão P, Aguiar de Sousa D. Cerebral Venous Thrombosis. Presse Med. 2016; 45 (12 Pt 2): e429–e450. PubMed PMID: 27816347. DOI: 10.1016/j.lpm.2016.10.007.
23. Schneider S, Kapelushnik J, Kraus M, El Saied S, Levi I, Kaplan DM. The association between otogenic lateral sinus thrombosis and thrombophilia — A long-term follow-up. Am J Otolaryngol. 2018; 39 (3): 299–302. PubMed PMID: 29530427. DOI: 10.1016/j.amjoto.2018.03.013.
24. Lichy C, Dong–Si T, Reuner K, Genius J, Rickmann H, Hampe T, et al. Risk of cerebral venous thrombosis and novel gene polymorphisms of the coagulation and fibrinolytic systems. J Neurol. 2006; 253 (3): 316–20. PubMed PMID: 16155788. DOI: 10.1007/s00415-005-0988-4.
25. Li B, Heldner MR, Arnold M, Coutinho JM, Zuurbier SM, Meijers JCM, et al. Coagulation Factor XIII in Cerebral Venous Thrombosis. TH Open. 2019; 3 (3): e227–e229. DOI: 10.1055/s-0039-1693487.
26. Bagoly Z, Muszbek L. Factor XIII: What does it look like? J Thromb Haemost. 2019; 17 (5): 714–6. DOI: 10.1111/jth.14431.
27. Ali Z, Troncoso JC, Fowler DR. Recurrent cerebral venous thrombosis associated with heterozygote methylenetetrahydrofolate reductase C677T mutation and sickle cell trait without homocysteinemia: an autopsy case report and review of literature. Forensic Sci Int. 2014; (242): e52–e55. DOI: 10.1016/j.forsciint.2014.07.007.
28. Ghaznavi H, Soheili Z, Samiei S, Soltanpour MS. Association study of methylenetetrahydrofolate reductase C677T mutation with cerebral venous thrombosis in an Iranian population. Blood Coagul Fibrinolysis. 2015; 26 (8): 869–73. DOI: 10.1097/MBC.0000000000000292.

ANALYSIS OF ASSOCIATIONS OF POLYMORPHISMS IN THE GENES CODING FOR L4, IL10, IL13 WITH THE DEVELOPMENT OF ATOPIC BRONCHIAL ASTHMA AND ITS REMISSION

Zhorina YuV[1]✉, Abramovskikh OS[1], Ignatova GL[1], Ploshchanskay OG[2]

[1] South Ural State Medical University, Chelyabinsk, Russia

[2] DNA Clinic LLC, Chelyabinsk, Russia

Bronchial asthma is a multifactorial disease underpinned by chronic inflammation. The atopic phenotype of BA implies the presence of similar molecular mechanisms of pathogenesis between the patients. The aim of this study was to analyze the associations between the development of atopic BA/its remission and the following polymorphisms of interleukin genes: IL4 (*rs2243250; C-589T*), IL10 (*rs1800896; G-1082A; rs1800872; C-592A*), and IL13 (*rs20541; Arg130Gln*). Using allele-specific polymerase chain reaction (PCR), we studied the listed SNPs in the mixed urban sample of patients with BA (n = 53) and the controls (n = 30) residing in South Ural. The analysis revealed that genotype AA of IL10 (*rs1800872*) occurred more frequently in the control group (23.3%) than in the patients with atopic BA (5.7%) (OR = 0.197; 95% CI [0.047–0.832]; p = 0.031). No differences in genotype frequencies were observed between the patients with atopic BA and the controls for other studied polymorphisms. Our study failed to demonstrate the association of the listed polymorphisms and BA remission.

Keywords: bronchial asthma in adults, atopy, remission, gene polymorphism, cytokines

Author contribution: Zhorina YuV — conceived and planned the study, collected, processed and interpreted the data, performed statistical analysis, participated in writing the manuscript; Abramovskikh OS — proposed the method and supervised the study, analyzed and interpreted the data, participated in writing the manuscript; Ignatova GL — analyzed the clinical data, supervised the study, interpreted the data, participated in writing the manuscript; Ploshchanskay OG — collected the data, conducted laboratory tests, interpreted the data and participated in writing the manuscript.

Compliance with ethical standards: the study was approved by the Ethics Committee of South Ural State Medical University (Protocol № 10 dated November 17, 2016). The patients gave informed consent to participate in the study.

✉ **Correspondence should be addressed:** Yulia Yu. Zhorina
Vorovskogo, 64, Chelyabinsk, 454092; juliamart24@mail.ru

Received: 25.09.2019 **Accepted:** 11.10.2019 **Published online:** 21.10.2019

DOI: 10.24075/brsmu.2019.067

АНАЛИЗ СВЯЗИ ПОЛИМОРФНЫХ ВАРИАНТОВ ГЕНОВ IL4, IL10, IL13 С РАЗВИТИЕМ АТОПИЧЕСКОЙ БРОНХИАЛЬНОЙ АСТМЫ И РЕМИССИЕЙ

Ю. В. Жорина[1]✉, О. С. Абрамовских[1], Г. Л. Игнатова[1], О. Г. Площанская[2]

[1] Южно-Уральский государственный медицинский университет, Челябинск, Россия

[2] ООО «ДНК Клиника», Челябинск, Россия

Бронхиальная астма (БА) является многофакторным заболеванием, в основе которого лежит хроническое воспаление. Атопический фенотип предполагает наличие у пациентов сходных молекулярных механизмов патогенеза. Целью работы было провести анализ ассоциации полиморфных локусов генов IL4 (*rs2243250; C-589T*), IL10 (*rs1800896; G-1082A; rs1800872; C-592A*), IL13 (*rs20541; Arg130Gln*) с развитием атопической БА и ремиссией. С помощью аллель-специфичной полимеразной цепной реакции (ПЦР) проведено исследование полиморфных локусов генов больных БА (n = 53) и группы сравнения (n = 30), смешанной городской выборки, проживающих на Южном Урале. Анализ ассоциации полиморфных вариантов генов интерлейкинов с развитием БА показал, что генотип АА IL10 (*rs1800872*) встречается чаще в группе сравнения (23,3%), чем в группе атопической БА (5,7%) (ОШ = 0,197; 95% ДИ [0,047–0,832]; p = 0,031). Для остальных исследованных полиморфных локусов генов интерлейкинов отличий в частотах генотипов между больными атопической БА и группой сравнения не обнаружено. Не удалось показать влияние изученных полиморфных локусов на развитие ремиссии заболевания.

Ключевые слова: бронхиальная астма у взрослых, атопия, ремиссия, полиморфизм генов, цитокины

Информация о вкладе авторов: Ю. В. Жорина — общая идея и методология исследования, сбор, обработка и интерпретация данных, статистический анализ, написание и оформление статьи; О. С. Абрамовских — методика и курирование исследования, анализ и интерпретация данных, написание и оформление статьи; Г. Л. Игнатова — анализ клинической части данных, курирование исследования, интерпретация данных, написание статьи; О. Г. Площанская — сбор данных, осуществление лабораторного этапа обследования, интерпретация данных, написание статьи.

Соблюдение этических стандартов: исследование одобрено этическим комитетом ФГБОУ ВО «ЮУГМУ Минздрава» (протокол № 10 от 17 ноября 2016 г.). Все участники подписали добровольное информированное согласие на участие в исследовании.

✉ **Для корреспонденции:** Юлия Владимировна Жорина
ул. Воровского, д. 64, г. Челябинск, 454092; juliamart24@mail.ru

Статья получена: 25.09.2019 **Статья принята к печати:** 11.10.2019 **Опубликована онлайн:** 21.10.2019

DOI: 10.24075/vrgmu.2019.067

Bronchial asthma (BA) is a complex disease arising from a random combination of both allergic and non-allergic factors. BA presents with a diversity of phenotypes. According to epidemiological surveillance reports, the atopic phenotype prevails in the adult population, occurring in 40 to 80% of adult asthmatic individuals. In Russia, atopic BA is diagnosed in 68–78% of adult cases [1].

Genetic predisposition is a significant contributor to asthma development. Familial aggregation of asthma was demonstrated as early as the first half of the 20th century. Twin studies conducted in the second half of the 20th century estimated the heritability of the disease in the range between 36 and 95% [2]. In the past few years, the focus has been on conducting genetic studies of BA in large clnically heterogeneous populations [3]. The analysis of candidate susceptibility genes in phenotypically homogenous cohorts allows identifying groups with similar molecular-genetic origin of the disease. A small homogeneous sample can be sufficient to detect the genetic effect of the analyzed gene [4].

Atopic disorders are regarded as immune response (type I hypersensitivity) caused and/or mediated by class IgE

antibodies against environmental antigens. Immunological reactions underlying atopic disorders can be broken down into few major categories; some of them are implicated in the epidermal barrier dysfunction, while others regulate innate and adaptive immune responses, including IgE sensitization [5].

The list of genes reliably and positively associated with allergies and asthma includes candidate genes coding for cytokines IL4, IL10 and IL13 involved in regulating persistent allergic inflammation [6]. Russian researchers also report an association between the polymorphisms of the aforementioned genes and BA [7, 8].

Most research works on BA genetics focus on the genetic predisposition to this disease [9]. Few studies have looked at its course and progression. Moreover, there is evidence that genetic risk factors for BA identified so far cannot accurately predict the development of the disease or its course [10].

In the literature, the remission rate ranges from 5% in late-onset patients [11] to 65% in children and teenagers [12]. According to our estimates, the remission rate in the adults with atopic BA residing in Chelyabinsk is 22.7%. A positive association with remission is observed in patients with normal BMI, undergoing allergen-specific therapy and eliminating exposure to allergens. Other factors, such as sex, age of onset, disease duration, familial background, co-morbid seasonal or perennial rhinitis, and smoking, do not differ significantly between patients with and without remission [13].

The aim of this study was to analyze the associations between the SNPs in the genes coding for IL4 (*rs2243250; C -589T*), IL10 (*rs1800896; G -1082A; rs1800872; C -592A*), IL13 (*rs20541; Arg130Gln*) and the development of atopic BA /its remission in the mixed sample of Chelyabinsk (South Ural) residents.

METHODS

We conducted a telephone survey of 181 individuals with atopic BA who had been patients of the allergy unit of Chelyabinsk City Clinic № 7 between 1992 and 2018. The diagnosis was established or confirmed by an allergist/immunologist based on clinical, laboratory, instrumental, and skin tests, as recommended by the Guidelines for the Diagnosis and Management of Asthma [14]. The median follow-up period was 8 years [5; 15 years].

The study included patients of both sexes aged 18 to 70 years diagnosed with mild or moderate atopic BA, with confirmed sensitivity to noninfectious allergens, who had been followed up for at least 3 years and gave consent to participate in the study. Patients with comorbid chronic obstructive lung disease, silicosis, tuberculosis, sarcoidosis, bronchiectasis or a history of previous lung surgery were excluded from the study.

Fifty-three patients aged 23–70 years underwent a physical examination; their medical history was taken, including complaints and symptoms of asthma, possible allergies and comorbidities. The patients also took the asthma control test (AST) and the bronchial reversibility test (spirometry). Screening for SNPs in interleukin genes was done using allele-specific polymerase chain reaction (PCR).

The molecular-genetic analysis was conducted at the laboratory of DNA Clinic LLC (Chelyabinsk). Genomic DNA of the patients and controls was isolated from whole-blood lymphocytes using a DNA-Express-Blood reagent kit (DNA-Technology; Russia). Single nucleotide polymorphisms (SNPs) in the genes coding for IL4 (*rs2243250; C-589T*), IL10 (*rs1800896; G-1082A; rs1800872; C-592 A*), and IL13 (*rs20541; Arg130Gln*) were identified using an SNP-express test system (Litech; Russia) and allele-specific PCR.

Spirometry criteria for normal lung function were as follows: the absence of bronchial obstruction defined as the ratio of forced expiratory volume in 1 s (FEV1) to forced vital capacity (FVC) of less than 0.7 before inhalation of a bronchodilator. The bronchodilator test was considered positive if an increase in FEV1 was 12% or more after inhalation of 4 salbutamol doses and an absolute FEV1 increase was over 200 ml [15].

There are a few definitions of asthma remission in the literature varying in length between 1 and 6 years. Some criteria for remission are based on the resolution of clinical symptoms, whereas others require rely on the objective assessment of pulmonary function [16].

Because there is no consensus as to what should be considered BA remission, we defined it as the absence of symptoms (cough, shortness of breath, sensation of suffocation, wheezing) for 1 year in the absence of baseline therapy and short-acting β_2 agonist therapy and the presence of normal pulmonary function observed in a negative spirometry test. Based on this definition, we stratified the patients into 2 groups: with remission of atopic BA (n = 17; 14 men and 3 women) and without remission of atopic BA (n = 36; 14 men and 22 women). The control group consisted of 30 individuals aged 23–73 years (11 men and 19 women) who had no respiratory complaints, no allergies and no family history of allergies.

The obtained data were processed in SPSS Statistics 17.0.1 (SPSS Inc; USA). The analysis was performed using descriptive statstics. Categorical variables were described as absolute and relative frequencies. A median (Me) and an interquartile range [IQR, 25% : 75%] were calculated for quantitative variables. The analysis of quantitative data distribution was done using the Shapiro-Wilk test. In order to compare two means in independent samples, the Mann–Whitney U test was applied. Differences were considered significant at $p < 0.05$.

Allele and genotype frequencies were calculated for the studied SNPs in the candidate genes and compared to the frequencies predicted by the Hardy-Weinberg equation (χ^2 at $p < 0.05$). The two-tailed Fisher exact test was applied to run pairwise comparison of allele and genotype frequencies in the patients and the controls. Associations were analyzed using the odds ratio (OR) and the 95% confidence interval (CI).

RESULTS

The clinical characteristics of patients with atopic BA (n = 53) were as follows: 36 (68%) had polysensitization to indoor,

Table 1. Spirometry test results in patients with atopic BA remission, without remission and in the controls

Parameter	Patients with BA remission, n = 17 (group 1)	Patients without BA remission, (controlled, partially controlled/uncontrolled asthma) (group 2), n = 36	Controls (group 3), n = 30	p (groups 1–3)	p (groups 1–2)
FEV1 %, Me [Q1; Q3]	99 [89.5; 107.8]	84 [74; 97]	104 [95.5; 110]	0.4	0.001
FEV1 increase (ml) after inhalation of salbutamol (400 μg), Me [Q1; Q3]	155 [0; 247.5]	240 [107.5; 445]	167.5 [82.25; 228.75]	0.72	0.013
FEV1 /FVC %, Me [Q1; Q3]	81.5 [76.3; 88.5]	74 [67; 79.75]	83 [80.5; 85.5]	0.69	0.001

Table 2. Genotype frequency distribution for SNPs in the interleukin genes in patients with atopic BA and the controls

Genotype	Patients with atopic BA (*n* = 53), % (*n*)	Control (*n* = 30), % (*n*)	OR (95% CI)	*p*
IL4 (*rs2243250*)				
CC	52.8 (28)	53.3 (16)	0.98 (0.39–2.4)	1.000
CT	43.3 (23)	46.6 (14)	0.876 (0.35–2.15)	0.821
TT	3.8 (2)	0 (0)	0.63 (0.53–0.74)	0.533
IL10 (*rs1800896*)				
GG	37.7 (20)	43.3 (13)	0.79 (0.31–1.97)	0.647
GA	45.3 (24)	30 (9)	1.93 (0.74–4.93)	0.243
AA	17 (9)	26.6 (8)	0.56 (0.19–1.65)	0.397
IL10 (*rs1800872*)				
CC	56.6 (30)	46.6 (14)	1.49 (0.60–3.66)	0.493
CA	37.7 (20)	30 (9)	1.41 (0.54–3.68)	0.632
AA	5.7 (3)	23.3 (7)	0.197 (0.047–.832)	0.031
IL13 (*rs20541*)				
GG	55 (29)	56.6 (17)	0.924 (0.37–2.27)	1.000
GA	34 (18)	30 (9)	1.2 (0.45–3.15)	0.810
AA	11 (6)	13.3 (4)	0.83 (0.21–3.21)	1.000

Table 3. Frequency of SNP genotypes of interleukin genes in patients with atopic BA remission and without it

Genotype	Patients with BA remission (group 1) *n* = 17, % (*n*)	Patients without BA remission (group 2) *n* = 36, % (*n*)	Control (group 3) *n* = 30, % (*n*)	OR (95%CI) for all groups	*p*
IL4 (*rs2243250*)					
CC	52.9 (9)	52.7 (19)	53.3 (16)	1–3 = 1.01 (0.30–3.34) 2–3 = 0.97 (0.37–2.58)	1–3 = 1.000 2–3 = 1.000
CT	47.1 (8)	41.7 (15)	46.6 (14)	1–3 = 0.98 (0.29–3.24) 2–3 = 0.81 (0.31–2.16)	1–3 = 1.000 2–3 = 0.804
TT	0 (0)	5.6 (2)	0 (0)	1–3 = – 2–3 = 0.53 (0.42–0.7)	1–3 = – 2–3 = 0.497
IL10 (*rs1800896*)					
GG	47.1(8)	33.3 (12)	43.3 (13)	1–3 = 0.86 (0.26–2.84) 2–3 = 0.65 (0.24–1.77)	1–3 = 1.000 2–3 = 0.452
GA	35.3 (6)	50 (18)	30 (9)	1–3 = 0.78 (0.22–2.78) 2–3 = 2.3 (0.84–6.45)	1–3 = 0.753 2–3 = 0.133
AA	17.6 (3)	16.7 (6)	26.6 (8)	1–3 = 1.69 (0.38–7.5) 2–3 = 0.55 (0.16–1.8)	1–3 = 0.722 2–3 = 0.375
IL10 (*rs1800872*)					
CC	47.1 (8)	61.1 (22)	46.6 (14)	1–3 = 0.98 (0.29–3.24) 2–3 = 1.79 (0.67–4.79)	1–3 = 1.000 2–3 = 0.322
CA	41.1 (7)	36.1 (13)	26.6 (8)	1–3 = 0.61 (0.17–2.12) 2–3 = 1.31 (0.46–3.71)	1–3 = 0.528 2–3 = 0.794
AA	11.7 (2)	2.8 (1)	23.3 (7)	1–3 = 2.28 (0.41–12.5) 2–3 = 0.094 (0.011–0.814)	1–3 = 0.455 2–3 = 0.019
IL13 Arg130 Gln (*rs20541*)					
GG	52.9 (9)	55.6 (20)	56.6 (17)	1–3 = 1.16 (0.35–3.8) 2–3 = 0.95 (0.36–2.53)	1–3 = 1.000 2–3 = 1.000
GA	29.4 (5)	36.1 (13)	30 (9)	1–3 = 1.02 (0.28–3.28) 2–3 = 1.31 (0.47–3.7)	1–3 = 1.000 2–3 = 0.794
AA	17.7 (3)	8.3 (3)	13.3 (4)	1–3 = 0.71 (0.14–3.6) 2–3 = 0.59 (0.12–2.87)	1–3 = 0.692 2–3 = 0.693

epidermal and plant allergens; 25 (47%) had a family history of allergies; 22 (42%) had early-onset BA (before 18 years of age); 41 (78%) had comorbid allergic rhinitis; 38 (72%) had mild BA, and 15 (28%) had moderate BA. Lung function was normal in the group of patients with remission of atopic BA; no statistical difference in the results of the bronchodilator test was detected between this group of patients and the controls (Table 1). In patients without remission the bronchodilator test was positive, FEV1% and FEV/FVC% were lower than in the controls.

Genotype frequencies were calculated for the total sample of patients with atopic BA relative to the control group and for the subgroups of patients with and without remission. Linkage disequilibrium was detected for all studied loci in the control group; the studied loci were in the Hardy–Weinberg equilibrium for the group of patients with atopic BA.

The analysis of associations between the polymorphisms of interleukin genes and BA development (Table 2) revealed a statistically significant difference in the frequencies of IL10

(*rs1800872*) genotypes: genotype AA was more frequent in the control group (23.3%) than in the group of patients with atopic BA (5.7%) (OR = 0.197; 95% CI [0.047–0.832]; $p = 0.031$) and perhaps had a protective role. No difference in frequencies were detected for other studied SNP between the patients with atopic BA and the controls.

Intergroup comparison revealed a difference in the frequency of IL10 genotypes (*rs1800872*) between the patients without BA remission and the control group: the frequency of AA genotype was 2.8% vs 23.3% (OR= 0.094; 95% CI [0.011–0.814]; $p = 0.019$). Integral assessment of clinical and molecular-genetic data did not reveal any significant associations with BA remission (Table 3).

DISCUSSION

Previous studies of the polymorphic *C-592A* locus of the IL10 gene produced controversial results: some authors reported no association with predisposition to asthma [17], while others observed significant correlations [18, 19]. Previous metanalyses demonstrated an association between the polymorphism *C-589T* of the IL4 gene and the risk for BA in the European population [20] and another association between the polymorphism *Arg130Gln* of the IL13 gene and an increased risk for BA in children and adults [21–23]. According to the literature, the *G-1082A* polymorphism of the IL10 gene predisposes to asthma [24].

It is hypothesized that factors increasing the risk of BA may differ from those affecting its progression [25]. Perhaps, the SNPs studied in this work are not associated with the clinical prognosis of patients with BA. This question needs further investigation in larger patient samples.

CONCLUSIONS

This study presents the first data on the distribution of genotypes of the polymorphic loci *C-589T* (IL4), *G-1082A* (IL10), *C-592A* (IL10), and *Arg130Gln* (IL13) in the mixed sample of urban patients with atopic BA residing in South Ural. Considering the small sample size, the results should be interpreted with caution. So far, many genetic aspects of BA have been studied that contribute to the understanding of the pathogenesis of this multifactorial disease. Further research in this field is needed in order to adapt genetic diagnostic techniques to the clinical setting. The study of SNPs in interleukin genes can become an auxiliary tool for predicting the prognosis of the disease and encouraging patients to adhere to therapeutic regimens.

References

1. Nenasheva NM. Atopicheskaya bronhial'naya astma: rol' allergen-specificheskoj immunoterapii. Rossijskij allergologicheskij zhurnal. 2015; (6): 54–67. Russian.
2. Mathias RA. Introduction to genetics and genomics in asthma: genetics of asthma. Adv Exp Med Biol. 2014; (795): 125–55. DOI: 10.1007/978-1-4614-8603-9_9.
3. Baye TM, Martin LJ, Khurana Hershey GK. Application of genetic/genomic approaches to allergic disorders. J Allergy Clin Immunol. 2010; 126 (3): 425–36. DOI: 10.1016/j.jaci.2010.05.025.
4. Gupta J, Johansson E, Bernstein JA, Chakraborty R, Khurana Hershey GK, Rothenberg ME, et al. Resolving the etiology of atopic disorders by genetic analysis of racial ancestry. J Allergy Clin Immunol. 2016; 138 (3): 676–99. DOI: 10.1016/j.jaci.2016.02.045.
5. Halapi E, Hakonarson H. Recent development in genomic and proteomic research for asthma. Curr Opin Pulm Med. 2004; 10 (1): 22–30. DOI: 10.1097/00063198-200401000-00005.
6. Ober C, Hoffja S. Asthma genetics 2006: the long and winding road to gene discovery. Genes Immun. 2006; 7 (2): 95–100. DOI:10.1038/sj.gene.6364284.
7. Smolnikova MV, Freidin MB, Smirnova SV. Cytokine genes as genetic markers of controlled and uncontrolled atopic bronchial asthma. Medical Immunology (in Russia)/Meditsinskaya Immunologiya. 2017; 19 (5): 605–14. DOI: 10.15789/1563-0625-2017-5-605-614. Russian.
8. Karunas AS, Fedorova YY, Ramazanova NN, Galimova ES, Gimalova GF, Guryeva LL, et al. Evaluation of a role of cytokine gene polymorphisms in development of bronchial asthma in the Republic of Bashkortostan. Russian Pulmonology. 2012; (5): 37–40. Russian.
9. Marenholz I, Esparza-Gordillo J, Rüschendorf F, Bauerfeind A, Strachan DP, Spycher BD, et al. Meta-analysis identifies seven susceptibility loci involved in the atopic march. Nat Commun. 2015; (6): 8804. DOI: 10.1038/ncomms9804.
10. Belsky DW, Sears MR, Hancox RJ, Harrington H, Houts R, Moffitt TE, et al. Polygenic risk and the development and course of asthma: Evidence from a 4-decade longitudinal study. Lancet Respir Med. 2013; 1 (6): 453–61. DOI: 10.1016/S2213-2600(13)70101-2.
11. Tiomisto LE, Ilmarinen P, Kankaanranta H. Prognosis of new-onset asthma diagnosed in adult age. Respir Med. 2015; 109 (8): 944–54. DOI: 10.1016/j.rmed.2015.05.001.
12. Javed A, Yoo KH, Agarwal K, Jacobson RM, Li X, Juhn YJ, et al. Characteristics of children with asthma who achieved remission of asthma. J Asthma. 2013; 50 (5): 472–9. DOI: 10.3109/02770903.2013.787625.
13. Ignatova GL, Zhorina YV, Abramovskikh OS, Zherebtsova IA. Clinical course and remission rate in adult patients with atopic asthma in Chelyabinsk. Russian Pulmonology. 2019; 29 (3): 263–8. DOI: 10.18093/0869-0189-2019-29-3-263-268. Russian.
14. Global Initiative for asthma — NHLBI/WHO Workshop Report/National Heart Lung Blood Institute Updated 2016. https://ginasthma.org/ (дата обращения: 19.09.2018).
15. Chuchalin AG, Aysanov ZR, Chikina SY, Chernyak AV, Kalmanova EN. Federal guidelines of Russian Respiratory Society on spirometry. Russian Pulmonology. 2014; (6): 11–23. Russian.
16. Koh YY, Kang H, Nah KM, Kim CK. Absence of association of peripheral blood eosinophilia or increased eosinophil cationic protein with bronchial hyperresponsiveness during asthma remission. Ann Allergy Asthma Immunol. 2003; 91 (3): 297–302. DOI: 10.1016/S1081-1206(10)63533-8.
17. Karjalainen J, Hulkkonen J, Nieminen MM, Huhtala H, Aromaa A, Klaukka T, et al. Interleukin-10 gene promoter region polymorphism is associated with eosinophil count and circulating immunoglobulin E in adult asthma. Clin Exp Allergy. 2003; 33 (1): 78–83. DOI: 10.1046/j.1365-2222.2003.01577.x
18. Huang ZY, Cheng BJ, Wan Y, Zhou C. Meta-analysis of the IL10 promoter polymorphisms and pediatric asthma susceptibility. Genet Mol Res. 2016; 15 (2): gmr.15028320 DOI: 10.4238/gmr.15028320.
19. Nie W, Fang Z, Li B, Xiu QY. Interleukin-10 promoter polymorphisms and asthma risk: a meta-analysis. Cytokine. 2012; 60 (3): 849–55. DOI: 10.1016/j.cyto.2012.08.023.
20. Tang L, Lin HG, Chen BF. Association of IL4 promoter polymorphisms with asthma: a meta-analysis. Genet Mol Res. 2014; 13 (1): 1383–94.
21. Heinzmann A, Mao X-Q, Akaiwa M, Kreomer RT, Gao PS, Ohshima K, et al. Genetic variants of IL13 signalling and human asthma and atopy. Human Molecular Genetics. 2000; 9 (4): 549–59. DOI: 10.1093/hmg/9.4.549.
22. Liu Z, Li P, Wang J, Fan Q, Yan P, Zhang X, et al. A meta-analysis of IL13 polymorphisms and pediatric asthma risk. Med Sci Monit. 2014; (20): 2617–23. DOI: 10.12659/MSM.891017.

23. Mei Q, Qu J. Interleukin-13 +2044 G/A and +1923C/T polymorphisms are associated with asthma susceptibility in Asians: A meta-analysis. Medicine (Baltimore). 2017; 96 (51): e9203. DOI: 10.1097/MD.0000000000009203.
24. Zheng XY, Guan WJ, Mao C, Chen HF, Ding H, Zheng JP, et al. Interleukin-10 promoter 1082/2819/2592 polymorphisms are associated with asthma susceptibility in Asians and atopic asthma: a meta-analysis. Lung. 2014; 192 (1): 65–73.
25. Guerra S. Clinical remission of asthma: what lies beyond? Thorax. 2005; 60 (1): 5–6. DOI: 10.1136/thx.2004.033480.

Литература

1. Ненашева Н. М. Атопическая бронхиальная астма: роль аллерген-специфической иммунотерапии. Российский аллергологический журнал. 2015; (6): 54–67.
2. Mathias RA. Introduction to genetics and genomics in asthma: genetics of asthma. Adv Exp Med Biol. 2014; (795): 125–55. DOI: 10.1007/978-1-4614-8603-9_9.
3. Baye TM, Martin LJ, Khurana Hershey GK. Application of genetic/genomic approaches to allergic disorders. J Allergy Clin Immunol. 2010; 126 (3): 425–36. DOI: 10.1016/j.jaci.2010.05.025.
4. Gupta J, Johansson E, Bernstein JA, Chakraborty R, Khurana Hershey GK, Rothenberg ME, et al. Resolving the etiology of atopic disorders by genetic analysis of racial ancestry. J Allergy Clin Immunol. 2016; 138 (3): 676–99. DOI: 10.1016/j.jaci.2016.02.045.
5. Halapi E, Hakonarson H. Recent development in genomic and proteomic research for asthma. Curr Opin Pulm Med. 2004; 10 (1): 22–30. DOI: 10.1097/00063198-200401000-00005.
6. Ober C, Hoffja S. Asthma genetics 2006: the long and winding road to gene discovery. Genes Immun. 2006; 7 (2): 95–100. DOI:10.1038/sj.gene.6364284.
7. Смольникова М. В., Фрейдин М. Б., Смирнова С. В. Гены цитокинов как генетические маркеры атопической бронхиальной астмы с контролируемым и неконтролируемым течением. Медицинская иммунология. 2017; 19 (5): 605–14. DOI: 10.15789/1563-0625-2017-5-605-614.
8. Карунас А. С., Федорова Ю. Ю., Рамазанова Н. Н., Галимова Е. С., Гималова Г. Ф., Гурьева Л. Л. и др. Исследование роли полиморфных вариантов генов цитокинов в развитии бронхиальной астмы в Республике Башкортостан. Пульмонология. 2012; (5): 37–40.
9. Marenholz I, Esparza-Gordillo J, Rüschendorf F, Bauerfeind A, Strachan DP, Spycher BD, et al. Meta-analysis identifies seven susceptibility loci involved in the atopic march. Nat Commun. 2015; (6): 8804. DOI: 10.1038/ncomms9804.
10. Belsky DW, Sears MR, Hancox RJ, Harrington H, Houts R, Moffitt TE, et al. Polygenic risk and the development and course of asthma: Evidence from a 4-decade longitudinal study. Lancet Respir Med. 2013; 1 (6): 453–61. DOI: 10.1016/S2213-2600(13)70101-2.
11. Tiomisto LE, Ilmarinen P, Kankaanranta H. Prognosis of new-onset asthma diagnosed in adult age. Respir Med. 2015; 109 (8): 944–54. DOI: 10.1016/j.rmed.2015.05.001.
12. Javed A, Yoo KH, Agarwal K, Jacobson RM, Li X, Juhn YJ, et al. Characteristics of children with asthma who achieved remission of asthma. J Asthma. 2013; 50 (5): 472–9. DOI: 10.3109/02770903.2013.787625.
13. Игнатова Г. Л., Жорина Ю. В., Абрамовских О. С., Жеребцова И. А. Особенности течения и частота ремиссии атопической бронхиальной астмы у взрослых пациентов в Челябинске. Пульмонология. 2019; 29 (3): 263–8. DOI: 10.18093/0869-0189-2019-29-3-263-268.
14. Global Initiative for asthma — NHLBI/WHO Workshop Report/National Heart Lung Blood Institute Updated 2016. https://ginasthma.org/ (дата обращения: 19.09.2018).
15. Чучалин А. Г., Айсанов З. Р., Чикина С. Ю., Черняк А. В., Калманова Е. Н. Федеральные клинические рекомендации Российского респираторного общества по использованию метода спирометрии. Пульмонология. 2014; (6): 11–23.
16. Koh YY, Kang H, Nah KM, Kim CK. Absence of association of peripheral blood eosinophilia or increased eosinophil cationic protein with bronchial hyperresponsiveness during asthma remission. Ann Allergy Asthma Immunol. 2003; 91 (3): 297–302. DOI: 10.1016/S1081-1206(10)63533-8.
17. Karjalainen J, Hulkkonen J, Nieminen MM, Huhtala H, Aromaa A, Klaukka T, et al. Interleukin-10 gene promoter region polymorphism is associated with eosinophil count and circulating immunoglobulin E in adult asthma. Clin Exp Allergy. 2003; 33 (1): 78–83. DOI: 10.1046/j.1365-2222.2003.01577.x
18. Huang ZY, Cheng BJ, Wan Y, Zhou C. Meta-analysis of the IL10 promoter polymorphisms and pediatric asthma susceptibility. Genet Mol Res. 2016; 15 (2): gmr.15028320 DOI: 10.4238/gmr.15028320.
19. Nie W, Fang Z, Li B, Xiu QY. Interleukin-10 promoter polymorphisms and asthma risk: a meta-analysis. Cytokine. 2012; 60 (3): 849–55. DOI: 10.1016/j.cyto.2012.08.023.
20. Tang L, Lin HG, Chen BF. Association of IL4 promoter polymorphisms with asthma: a meta-analysis. Genet Mol Res. 2014; 13 (1): 1383–94.
21. Heinzmann A, Mao X-Q, Akaiwa M, Kreomer RT, Gao PS, Ohshima K, et al. Genetic variants of IL13 signalling and human asthma and atopy. Human Molecular Genetics. 2000; 9 (4): 549–59. DOI: 10.1093/hmg/9.4.549.
22. Liu Z, Li P, Wang J, Fan Q, Yan P, Zhang X, et al. A meta-analysis of IL13 polymorphisms and pediatric asthma risk. Med Sci Monit. 2014; (20): 2617–23. DOI: 10.12659/MSM.891017.
23. Mei Q, Qu J. Interleukin-13 +2044 G/A and +1923C/T polymorphisms are associated with asthma susceptibility in Asians: A meta-analysis. Medicine (Baltimore). 2017; 96 (51): e9203. DOI: 10.1097/MD.0000000000009203.
24. Zheng XY, Guan WJ, Mao C, Chen HF, Ding H, Zheng JP, et al. Interleukin-10 promoter 1082/2819/2592 polymorphisms are associated with asthma susceptibility in Asians and atopic asthma: a meta-analysis. Lung. 2014; 192 (1): 65–73.
25. Guerra S. Clinical remission of asthma: what lies beyond? Thorax. 2005; 60 (1): 5–6. DOI: 10.1136/thx.2004.033480.

CYCLODIALYSIS *AB EXTERNO* WITH IMPLANTATION OF A COLLAGEN IMPLANT IN SURGICAL MANAGEMENT OF GLAUCOMA

Shradqa AS[1]✉, Kumar V[2], Frolov MA[1], Dushina GN[2], Bezzabotnov AI[2,3], Abu Zaalan KA[1]

[1] People's Friendship University of Russia, Moscow, Russia

[2] Eye microsurgery center «Pro zrenie», Moscow province, Russia

[3] Ophthalmic unit of Skhodnya City Hospital, Khimki, Moscow province, Russia

Glaucoma is one of the main causes of irreversible blindness in the Russian Federation and it is the leading cause of visual impairments among working age population. The primary goal of glaucoma therapy is to preserve the visual function, which is mainly achieved through persistent normalization of IOP by instillation of hypotensive drugs, laser therapy and/or surgery/ In this clinical study safety and efficacy of a glaucoma surgical technique implying valve cyclodialysis *ab externo* with implantation of a non-absorbable collagen implant (NACl) (Xenoplast, Dubna-Biofarm, Russia) in the supraciliary space were evaluated. All patients exhibited moderate and severe primary open-angle glaucoma (POAG). The efficacy assessment criterias were intraocular pressure (IOP) dynamics, use of hypotensive medications, need for repeat surgical intervention and complications. A total of 26 patients (26 eyes) were operated upon and under observation. Twelve months after surgery, 34% IOP decrease from the baseline level was observed: from 29.5 ± 6.8 to 18.8 ± 4.3 mmHg. The amount of hypotensive medications used reduced from 2.8 ± 0.9 to 0.6 ± 0.9. Applying the criteria recommended by the World Glaucoma Association, complete success was registered in 73.1% of patients and partial success — in 26.9% patients. No surgery ended in a failure through the follow-up period. Post-operatively, one patient developed hyphema, 2 patients had some blood elements in aqueous humor and 1 patient had shallow anterior chamber (AC). The suggested surgical technique proved to be an efficient and safe way to decrease IOP and reduce the number of hypotensive medications and had a minimal number of complications associated with the surgery, therefore it can be recommended as a method of choice in patients with advanced stage POAG.

Keywords: glaucoma, glaucoma surgery, intraocular pressure, cyclodialysis *ab externo*, uveoscleral outflow

Author contribution: Shradqa AS — study concept and design, data collection and processing, statistical processing, article authoring, design of graphs and drawings; Kumar V — study concept and design, data collection and processing, statistical processing, article authoring and editing, overall responsibility; Frolov MA — editing and overall responsibility; Dushina GN — study concept and design, data collection and processing, article editing; Bezzabotnov AI — study concept and design; data collection and processing; Abu Zaalan KA — data collection and processing.

Compliance with ethical standards: the study was approved by the Peoples' Friendship University of Russia Medical University Ethics Committee (protocol №16 of November 17, 2016); the patients gave informed consent to participate in the study.

✉ **Correspondence should be addressed:** Ahmad S. Shradqa
proezd Shokalskogo, 13, bl. 1, Moscow, 127221; sh1988moscow@gmail.com

Received: 16.08.2019 **Accepted:** 08.10.2019 **Published online:** 23.10.2019

DOI: 10.24075/brsmu.2019.068

ЦИКЛОДИАЛИЗ *AB EXTERNO* С ИМПЛАНТАЦИЕЙ КОЛЛАГЕНОВОГО ДРЕНАЖА В ХИРУРГИЧЕСКОМ ЛЕЧЕНИИ ГЛАУКОМЫ

А. С. Шрадка[1]✉, В. Кумар[2], М. А. Фролов[1], Г. Н. Душина[2], А. И. Беззаботнов[2,3], К. А. Абу Заалан[1]

[1] Российский университет дружбы народов, Москва, Россия

[2] ООО Центр микрохирургии глаза «Про зрение», Химки, Московская область, Россия

[3] Офтальмологическое отделение ГБУЗ МО «Сходненская городская больница», Химки, Московская область, Россия

Глаукома является актуальнейшей проблемой офтальмологии. Будучи одной из главных причин необратимой слепоты на территории Российской Федерации, она занимает лидирующее место в нозологической структуре инвалидности по зрению среди трудоспособного населения. Хирургическое вмешательство зачастую является единственным методом лечения рефрактерной глаукомы. Целью данного исследования было оценить безопасность и эффективность гипотензивной операции (ГО) клапанного циклодиализа *ab externo* с имплантацией в супрацилиарное пространство нерассасывающегося коллагенового дренажа (НКД) у пациентов с продвинутыми стадиями развития первичной открытоугольной глаукомы (ПОУГ). Критериями оценки безопасности и эффективности были: динамика внутриглазного давления (ВГД), количество используемых гипотензивных средств, потребность в повторном хирургическом вмешательстве и наличие осложнений. В результате наблюдения за 26 пациентами (26 глаз) с продвинутыми стадиями ПОУГ через 12 месяцев после оперативного вмешательства было зарегистрировано снижение ВГД на 34% от исходного уровня (с 29,5 ± 6,8 до 18,8 ± 4,3 мм рт. ст.). Количество используемых гипотензивных средств сократилось с 2,8 ± 0,9 до 0,6 ± 0,9. Успешность проведенной ГО оценивали согласно рекомендациям Всемирной глаукомной ассоциации: полный успех был достигнут в 73,1% случаев, а признанный — в 26,9% случаев. Неудачных исходов от оперативного лечения не наблюдали. Предложенное хирургическое лечение показало высокую эффективность и безопасность снижения ВГД, сокращение числа используемых гипотензивных средств и минимальное количество осложнений у пациентов с продвинутыми стадиями ПОУГ. Таким образом, метод клапанного циклодиализа *ab externo* с имплантацией в супрацилиарное пространство НКД можно рекомендовать в качестве терапии пациентов с ПОУГ в связи с его высокой эффективностью и безопасностью.

Ключевые слова: глаукома, хирургическое лечение, внутриглазное давление, циклодиализ *ab externo*, увеасклеральный отток внутриглазной жидкости

Информация о вкладе авторов: А. С. Шрадка — концепция и дизайн исследования, сбор и обработка материала, статистическая обработка, написание текста статьи, оформление графиков и рисунков; В. Кумар — концепция и дизайн исследования, сбор и обработка материала, статистическая обработка, написание и редактирование текста статьи; М. А. Фролов — концепция и дизайн исследования, редактирования; Г. Н. Душина — концепция и дизайн исследования; сбор и обработка материала, редактирование текста статьи; А. И. Беззаботнов — концепция и дизайн исследования, сбор и обработка материала; К. А. Абу Заалан — сбор и обработка материала.

Соблюдение этических стандартов: исследование одобрено этическим комитетом медицинского института Российского университета дружбы народов, (протокол № 16 от 17 ноября 2016 г.); все пациенты подписали добровольное информированное согласие на участие в исследовании.

✉ **Для корреспонденции:** Ахмад Салех Солиман Шрадка
проезд Шокальского, д. 13, корп. 1, г. Москва, 127221; sh1988moscow@gmail.com

Статья получена: 16.08.2019 **Статья принята к печати:** 08.10.2019 **Опубликована онлайн:** 23.10.2019

DOI: 10.24075/vrgmu.2019.068

Glaucoma is one of the main causes of irreversible blindness in the Russian Federation and it is the leading cause of visual impairment among working age population. [1,2]. In 2013, there were 1,180,708 patients registered with this diagnosis in Russian Federation. According to the World Health Organization, there are 60.5 to 105 million people worldwide suffering from glaucoma. The disease turns blind 1 adult person every minute and 1 child every 10 minutes [1].

Glaucoma is a multifactorial disease. Today, there is no consensus as to its etiology and pathogenesis. The primary goal of glaucoma therapy is to preserve the visual function, which is mainly achieved through persistent normalization of IOP by instillation of hypotensive drugs, laser therapy and/or surgery [3, 4]. Some researchers report that in 62 to 82% of patients' glaucoma is at its advanced stages when it is diagnosed for the first time; in such cases local instillation of hypotensive medications are effective only for a short term [5].

Activation of the aqueous humor outflow through natural pathway is probably the most promising surgery aimed to treat POAG [6–9]. These paths are trabecular and uveoscleral outflow pathways (UOP). From the point of view of surgery, UP boasts great potential because of its anatomical and physiological features. Some ophthalmologists believe that there is a link between the uveoscleral outflow path and the eyeball and orbit's lymphatic system [10]. Current glaucoma surgical techniques aimed at activating the UOP imply cyclodialysis with implantation of various types of drainage devices in the supraciliary space. In Russia, the most common implants selected for such surgeries are auto sclera strips [9]. In other countries, surgeons opt for CyPass Micro-Stent (Transcend Medical; USA), iStent Supra (Glaukos; USA), Gold Shunt (SOLX; USA), STARFlo (iSTAR Medical; Belgium), and Aquashunt (OPKO Health Inc.; USA) [11–13].

A surgical UOP activation technique implying cyclodialysis *ab externo* with implantation of NACI in the supraciliary and suprachoroidal spaces has been developed. The implant is usually used to prolong the hypotensive effect after non-penetrating deep sclerectomy.

Purpose. To evaluate the effectiveness and safety of a novice glaucoma surgical technique implying valve cyclodialysis ab externo with implantation of NACI supraciliary space in moderate and severe POAG patients.

METHODS

A total of 26 patients (26 eyes) aged 54 to 87 years (mean age 73.0 ± 8.3; 12 male and 14 female), exhibiting severe POAG were operated upon and under observation. Seventeen patients (65.4%) exhibited severe POAG and 9 (34.6%) — terminal stage of glaucoma.

The inclusion criteria were: POAG; concomitant pathology (POAG and cataract); medically uncontrolled IOP informed consent to participate in the study. The exclusion criteria were narrow-angle glaucoma, secondary glaucoma, patients exhibiting acute attack of glaucoma, and congenital glaucoma. Neither previous cataract surgery nor previous glaucoma surgery substantiated exclusion of participants from the study. The post-surgery follow-up period was 12 months.

Eighteen patients (69.2%) had undergone simultaneous surgery for concomitant pathology. Thirteen patients (50%) were suffering from pseudoexfoliation syndrome. Eleven (42.3%) patients had previously undergone glaucoma surgery. The mean number of previous surgeries associated with glaucoma was 1.6.

Before surgery, all glaucoma patients were instilling one or a combination of two or more hypotensive drugs. Two (7.7%) patients were instilling 1 drug, 5 (19.2%) patients — a combination of 2 hypotensive drugs, 15 (57.7%) patients — 3 drugs and 4 (15.4%) patients — a combination of 4 drugs. Despite the local hypotensive therapy, the average IOP level before surgery was 29.5 ± 6.8 mmHg.

All patients underwent the following standard ophthalmological examination before surgery: visual acuity checkup, tonometry (used Maklakov method with 10.0 g), biomicroscopy, ophthalmoscopy, gonioscopy, ultrasound biomicroscopy (UBM), B-scanning and optical coherence tomography (OCT). The cyclodialysis cleft (CC) was monitored with the help of a single-mirror goniolens, B-scanning and UBM (Marvel B-scan with UBM, Appasamy medical equipment (P) ltd; India) with the sensor operating at 50 MHz and 30 MHz and up to 30 dB, and OCT (Visante OCT, Zeiss; Germany).

The patients were examined on 1st day, 1 week, 1, 3 and 6 months and 1 year after surgery. Each examination included gonioscopy, tonometry, visual acuity testing. The anterior chamber angle (ACA), CC condition and position of the implant were registered with the AIA 11 slit lamp (Appasamy associates, India) and its built-in Canon digital camera (Canon; China).

The main efficacy criteria were IOP dynamics, number of hypotensive drugs used, number of intra- and postoperative complications, and need for a repeat surgery. Descriptive statistical methods were applied to analyze the results of the study: mean, 95% confidence interval (CI) and standard deviation were calculated; Student's test was used to determine the significance (*P*). Statistical processing of the digital data was performed with the help of SPSS Statistics (IBM) 22.0 (USA) for Windows 10.

Nesterov–Vurgaft–Kiselev–Tanyashina's table [14] was used to convert tonometry IOP data into true IOP (P°).

Surgical outcomes were evaluated as per World Glaucoma Association recommendations [15]. It was considered a complete success if P° was ≤15 for moderate glaucoma patients and ≤12 mmHg for severe glaucoma patients or when the IOP decrease was by more than 30% against baseline, and P° was >6 mmHg.

Further, a complete success was registered when the target pressure was achieved without hypotensive medication; in case additional hypotensive medications were required to achieve the target IOP, the success was considered as partial. Criteria for a failure were inability to achieve the target pressure even with additional hypotensive medications and the need for a repeat surgical intervention.

Surgery technique

The surgical field was prepared with 0.5% chlorhexidine (ethanol) solution and 5% aqueous povidone-iodine solution (Betadine, EGIS; Hungary), followed by instillation of local anesthetic (proxymethacaine 0.5% solution, Alcaine) (Alcon; USA) in conjunctival sac. A fixation suture was placed at 6 o'clock at the limbus (7–0 polypropylene). Two paracenteses were made at 7–8 hours or 4–5 hours. The AC was irrigated with 0.2 ml of 0.01% carbachol solution to constrict pupil followed by irrigation with 1.4% hyaluronic acid to maintain AC depth during surgery and, to avoid post-operative hypotony and hyphema. A conjunctivotomy was performed parallel to the limbus running from 10 to 13 hours. A 5 mm long conjunctival flap was dissected. Minimal diathermocoagulation of the superficial scleral vessels was performed when needed. Five mm away from the limbus, a ½ thickness rectangular scleral flap measuring 3 × 2 mm, was dissected with its base to the limbus (Fig. 1A). In the next step, 4.0 mm away from the posterior

border of the surgical limbus and parallel to it an incision up to the ciliary body was made through remaining deep layers of sclera. (Fig. 1B). At the extreme points of this incision, 2 vertical cuts (1mm long) were made towards limbus on either side to create a valve. (Fig. 1C). A spatula was inserted through paracentesis into the AC and cyclodialysis ab interno under visual control was performed till its distal end appeared in the incision (Fig. 1D). The spatula was withdrawn and cyclodialysis was completed ab externo through the scleral incision (Fig. 1E). The thus created cyclodialysis tunnel (CT) was filled with 0.1–0.2 ml of cohesive viscoelastic (1.4% hyaluronic acid). Through the scleral incision an angled long suture tying forceps with closed tying platforms was inserted through the tunnel until its ends were visible in the anterior chamber angle. At this stage the arms of the forceps were released to widen the cleft as wide as the incision in the sclera (Fig. 1F). Cyclodialysis was further advanced under the back lip of the incision in the sclera to expand it towards the suprachoroidal space. Next, using the same angled forceps the NACI (pre-moistened in a balanced salt solution) was captured between the tying platforms in such a way that distal 0.5mm of tying platforms remained free (Fig. 1G). Under visual control, the forceps with NACI was inserted through the incision in the sclera and pushed forward until the distal ends of the forceps and the NACI appeared in the AC's angle. After this, the forceps was opened and withdrawn carefully leaving the implant in the tunnel. The posterior end of the implant was inserted under the back lip of the incision into the suprachoroidal space (Fig. 1H). The NACI's position in the tunnel was checked (Fig. 1I). Once satisfied, the superficial scleral flap was put back in its place and sutured with 2 interrupted sutures (10–0 nylon). Conjunctiva was sutured to the limbus using the same suture material. The corneal incisions were sealed with corneal stromal hydration. At the end of the operation, 0.2 ml of dexamethasone solution was injected under the conjunctiva. Antibacterial ointment in the conjunctival cavity and a sterile aseptic dressing were applied to the eye. Conjunctival sutures were removed on 7th day after surgery.

Thus, the technique allowed to create a CT of sufficient width to enable reliable communication between AC and the supraciliary space that, in turn, communicates with the suprachoroidal space, which is the key to the aqueous humor outflow via UP.

The Xenoplast implants used in this study were customized as per needs. Its dimensions were changed to 6.0 × 1.0 × 0.5 mm instead of the standard 4.0 × 1.0 × 0.5 mm. This length was necessary to have the implant reaching the suprachoroidal space with 1 mm being left behind in the AC angle.

RESULTS

The mean baseline IOP was 29.5 ± 6.8 mmHg. (95% CI 26.6–32.3). Twelve months after surgery, the mean IOP was 18.8 ± 4.3 mmHg. (95% CI 16.9–20.6; $p \leq 0.01$). The decrease in IOP was by 33.8 ± 18.8% against the baseline. Figure 2 shows the IOP dynamics at different follow-up visits.

A significant decrease in IOP was registered in postoperative period. As compared to baseline IOP, at 1, 3, 6 and 12 months after surgery the decrease was by 37.6 ± 16.4%, 33.6 ± 10.7%, 32.1 ± 13.0% and 33.8 ± 18.8%, respectively.

The mean number of hypotensive medications used before the surgery was 2.8 ± 0.9 (95% CI 2.5–3.2). Twelve months after surgery this reduced to 0.6 ± 0.9 (95% CI 0.2–0.9) ($p \leq 0.01$), a reduction by more than 80%. Figure 3 shows use of hypotensive medications at different follow-up visits.

Complete success was registered in 84.6% of cases (22 patients) at 1 and 3 months after surgery, in 80.8% of cases (21 patients) — at 6 months and in 73.1% of cases (19 patients) — at 12 months. Partial success was in 15.4% (4 patients), 15.4% (4 patients), 19.2% (5 patients) and 26.9% (7 patients) of cases at 1, 3, 6 and 12 months, respectively. There were no failures

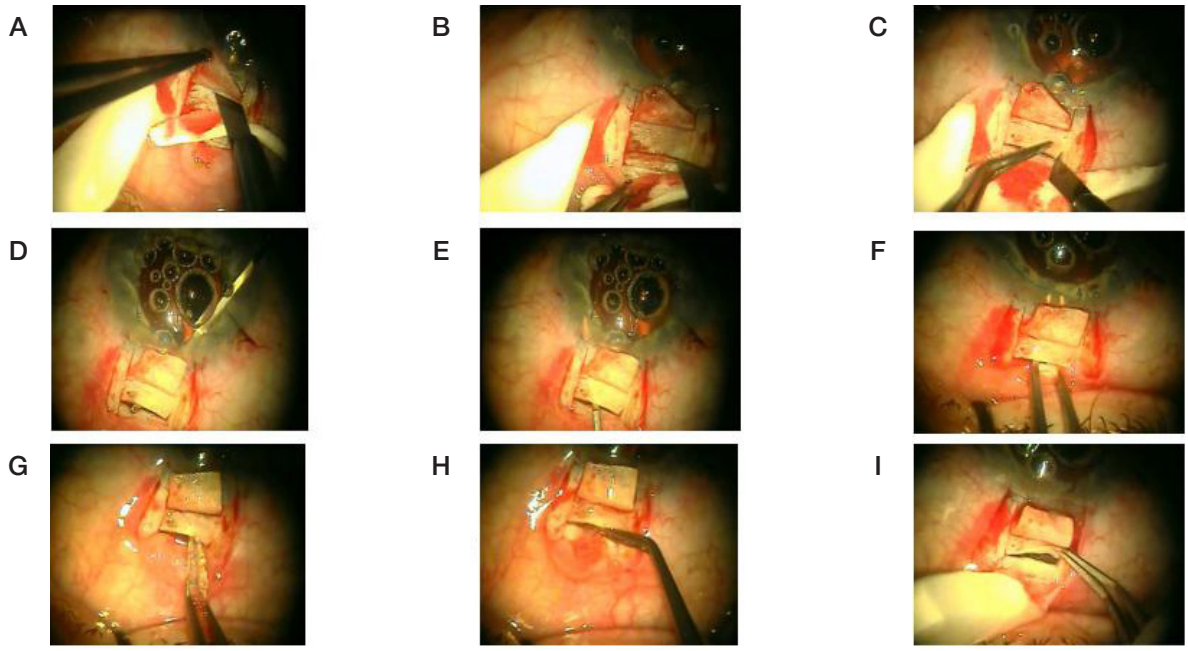

Fig. 1. A. Dissection of limbal based superficial scleral flap (3 × 2 mm). **B**. Horizontal incision of the sclera's deep layers up to the ciliary body. **C**. Formation of the valve by making 2 vertical incisions 1.0 mm long at both ends of the incision. **D**. Cyclodialysis ab interno step. Using a spatula inserted into AC through the paracentesis the ciliary body was separated from the scleral spur, spatula's distal end exiting through the incision in the sclera. **E**. Completion of tunnel formation *ab externo*. The spatula was inserted through the scleral incision, its end entered the AC; the ciliary body was detached from sclera along the entire length of the incision. **F**. CT expansion with the help of suture tying forceps. **G**. NACI implantation into the supraciliary space. Pre-moistened in the balanced salt solution NACI was captured between tying platforms of the forceps and was inserted into the tunnel through the incision in the sclera and was pushed forward till it appeared in the AC angle. **H**. NACI implantation in the suprachoroidal space. Posterior end of the implant was captured with toothed forceps and inserted under the back lip of the scleral incision into the suprachoroidal space. **I**. NACI position checkup

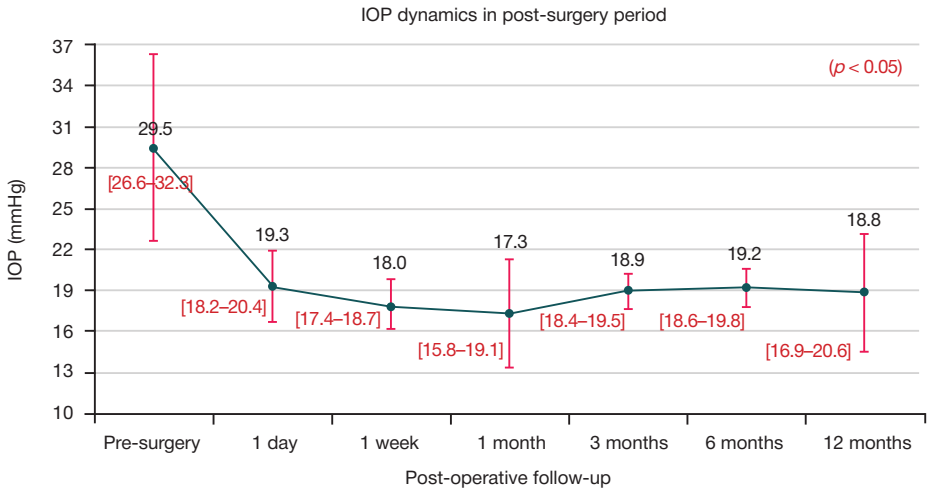

Fig. 2. Graph showing IOP dynamics after cyclodialysis *ab externo* with implantation of NACI at different follow-up visits

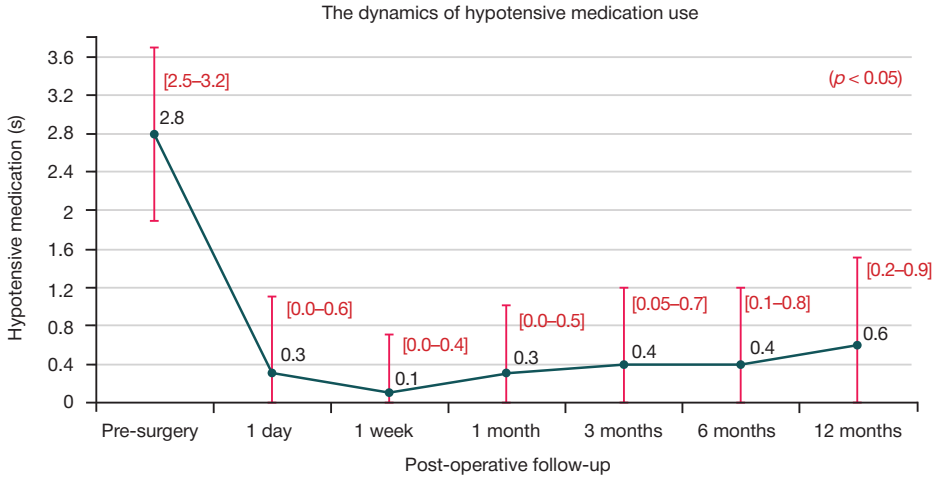

Fig. 3. Use of hypotensive medication by POAG patients at different follow-up visits

registered in this clinical study: up to 1 year after the surgery all the participating patients had their IOP normalized.

In patients with partial success hypotensive drugs were prescribed (1% and 2% pilocarpine, 0.5% timolol, 0.005% latanoprost, 2% dorzolamide and their combinations), which brought the IOP down to the target values and below.

In most of the cases, during surgery there was intraoperative mild hemorrhage in the area of cyclodialysis. To prevent further possible complications, the AC was irrigated with balanced salt solution before hydrating the corneal incisions.

Post-operative follow-up

Early postoperative period. Filtration bleb. A flat bleb was registered in 7 (27%) patients on the first day after surgery, in 4 (15%) patients it developed during the 1st week. In 1 patient (4%) the bleb lasted for a period of 1 month. After 3 months there were no filtering blebs noticed in any of the patients.

Hyphema. Through the entire follow-up period there was only one case of hyphema. Its level measured less than 1 mm; it self-resorbed within 3–5 days without any additional medication. There were another 2 cases with some blood elements in aqueous humour. In both cases it resolved without interventions.

Hypotension and shallow AC. P° below 6 mmHg was considered hypotension; this value corresponds to 14.5 mmHg IOP value measured with a tonometer following the Maklakov method with a weight of 10.0 g. The minimum IOP value registered after surgery was 15 mmHg, i.e. there were no cases of hypotension. One patient had shallow AC; in this case, a combined surgery was performed for a concomitant pathology. An iris-claw intraocular lens (Appasamy associates, India) was implanted in the retro pupillary space. The patient had a pupillary block that needed laser iridectomy. After iridectomy the block was resolved, and AC deepened.

There were no complications registered in the late post-operative period. Gonioscopically, NACI was stable and maintained its position in CT, no shift or total dislocation was observed (Fig. 4). Also, there were no obvious signs of inflammation observed.

Imaging of the formed outflow paths. To assess state of the created CT and position of the implant in the tunnel ultrasound B-scanning and UBM of the surgery zone, as well as longitudinal and transverse OCT of the anterior segment of the eye, were done (Fig. 5), (Fig. 6). Integrity of the CT at 12 months post-operatively was confirmed. The NACI was in the supraciliary and suprachoroidal spaces, which were expanded.

DISCUSSION

Today, there are many surgical techniques aimed at activating aqueous humor outflow through natural paths [6–9, 11, 13]. The most interesting of them imply activation of the UOP [6, 9, 11, 13]. The majority of UOP activation surgeries include elements of cyclodialysis [16–18]. Some Russian

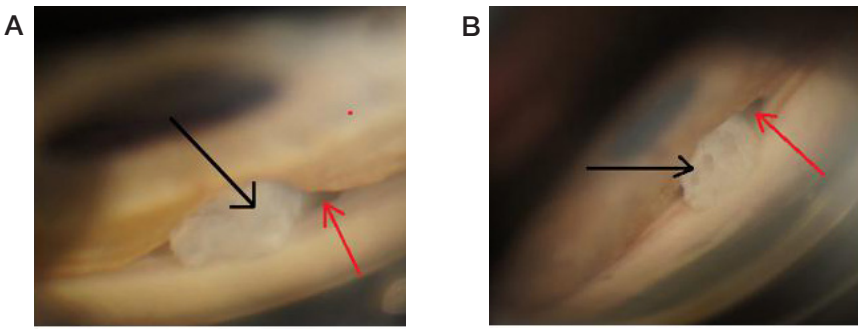

Fig. 4. Gonioscopy view of the AC angle. **A**. 1 month after surgery. **B**. 12 months after surgery. NACI (*black arrow*) is in the CT; CC is clearly visible (*red arrow*)

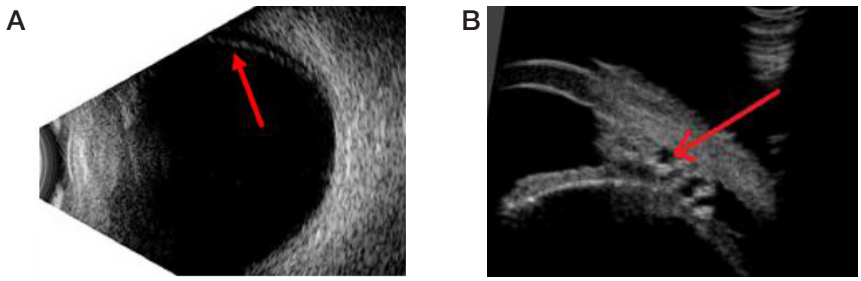

Fig. 5. Ultrasound examination of the surgical area. Post-operative follow-up — 12 months. **A**. Ultrasonic B-scan. The cyclodialysis tunnel is clearly visible. **B**. Ultrasonic biomicroscopy. The NACI is in the created tunnel. No dislocation was observed. Implants porous structure is clearly visible

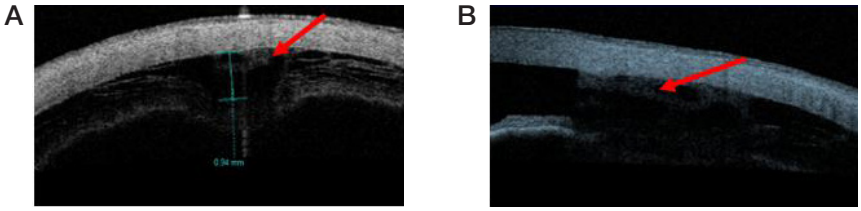

Fig. 6. OCT of the anterior segment of the eye. Post-operative follow-up — 12 months. **A**. Transverse section. **B**. longitudinal section. The NACI in the supraciliary and suprachoroidal spaces is clearly visible. The spaces are expanded

ophthalmologists suggested using autologous sclera as drainage device in the context of the UOP outflow surgery [19].

Two-year observation of 55 refractory glaucoma patients that underwent cyclodialysis ab externo and had Gold Shunt drainage device implanted revealed that the IOP level stabilized in 67.3% of cases aided by additional hypotensive medication. Only 3 patients (5.5%) did not need supplementary therapy to have the IOP level reach the target values. The registered post-surgery complications were ciliochoroidal detachment, corneal edema, and excessive filtering. The main factor that makes Gold Shunt implants inefficient is formation of a thin fibrous membrane that obliterates the front end of the drainage device [20].

There is a report [21] that states Gold Shunt inefficiency in patients with advanced stages of glaucoma: 77% of cases required repeat hypotensive surgery due to high IOP. Examination of the 5 explanted Gold Shunt implants revealed that the reason of their failure is the fibrous tissue that prevented aqueous humor outflow through the CC and the implant's slits [22].

In case of well-known CyPass Micro-Stent, which was implanted in the supraciliary space ab interno while treating a concomitant pathology secured, only a 14% reduction of IOP at 12 months post-surgery [23]. The surgery lead to complications, such as temporary hypotension, transient IOP increase and microshunt slit obstruction. Other researchers also reported CyPass Micro-Stent slit obstruction and CC obliteration as the main cause of IOP decompensation [24]. Some ophthalmic surgeons used a YAG laser to reopen the drainage; the procedure allowed restoring of fluid outflow through the microshunt and normalizing IOP [25]. Recently, Alcon discontinued its CyPass microshunt due to significant loss of endothelial cells 5 years after implantation.

To date, there are few studies investigating Aquashunt and iStent Supra systems in the context of glaucoma surgery [11, 26]. It should be noted that Aquashunt is implanted into the CC *ab externo*, and iStent Supra — *ab interno*.

There are also reports describing the effect of phacoemulsification on IOP in the early and late postoperative periods in patients with POAC [27, 28]. Some authors noted a 3–3.5 mmHg increase in IOP in the early post-operative period (up to 2 weeks). By the end of the first month after surgery the IOP level returned to its pre-surgery values. At 3 months authors noted a mean decrease in IOP by 3.1 mmHg from the baseline [27]. Another study reported a decrease in IOP level by 1.7 ± 3.1 mmHg from the baseline at 12 months after surgery [28]. In our study, 18 (69.2%) patients presented concomitant pathologies that were treated simultaneously with the main disease. The IOP level decreased by 11 ± 7.3 mmHg from the baseline at 12 months after surgery. The significant IOP decrease at 12 months after surgery proves more marked hypotensive effect by our technique than by phacoemulsification alone.

In this study cyclodialysis ab externo with implantation of NACI has been advocated for severe glaucoma patients. The surgery aims to activate outflow through UOP by forming a CT connecting AC to the supraciliary and suprachoroidal spaces. Implantation of the NACI in the CT ensures lasting and effective opening of the tunnel, thus activating aqueous outflow through UOP and secures persistence of the hypotensive effect. Watertight closure of scleral incisions helps avoiding filtration under the conjunctiva, which is unnatural. The surgery is

minimally traumatic. Sclera was sectioned between two rectus muscles so that the eyeball's mobility remained undisturbed. Cyclodialysis ab interno was necessary to avoid any descemet's membrane detachment, while detaching the ciliary body from the scleral spur. This is a common complication occurred if the approach is *ab externo*. In our ab interno — *ab externo* combined approach, a limited amount of ciliary body is detached from the scleral spur ab interno, thus creating a shallow cleft, which is then enlarged by *ab externo* approach. The scleral valve facilitates insertion of instruments through the scleral incision into supraciliary space, thus reduces trauma to the ciliary body. The valve is also an eyeball anchor point, which facilitates manipulations in the supraciliary space.

The NACI "Xenoplast" implanted into supraciliary and suprachoroidal spaces was selected because of its high biocompatibility with the eye tissues and lack of a pronounced inflammation after implantation due to the material being non-toxic and non-immunogenic [29]. The implant is available in dry form; when wetted, it swells no more than 0.1%. Its porous structure (pore size 200–700 μm) allows the fluid flow through the entire structure. A large number of studies implying non-penetrating deep sclerectomy with NACI implantation in the intrascleral space demonstrate the high efficiency of this implant. The authors reported a persistent decrease of the IOP level 1.5 years after surgery in patients with advanced glaucoma: the IOP reached 13.0 ± 0.5 mmHg without hypotensive medication [30].

In this series over the entire follow-up period not a single failure case was registered. Obvious signs of inflammation, hypotension, reactive syndrome, NACI dislocation was not observed, which confirm safety of the suggested surgical technique. There was only one case of hyphema, which resolved within 5 days.

Twelve months after valve cyclodialysis ab externo with NACI implantation the mean IOP decreased by 33.8 ± 8.8% from the baseline and equaled to 18.8 ± 4.4 mmHg ($p \leq 0.01$), which proves the high hypotensive efficacy of the suggested modality. Another proof thereof is the 80.1% reduction in the use of hypotensive medication (from 2.8 ± 0.9 to 0.6 ± 0.9) ($p \leq 0.01$) at 12 months after surgery, which improves the patients' quality of life and significantly reduces their expenses on medicine purchase. It should be noted that through the follow-up period all cases ended in a overall success: complete success in 73.1% of cases (19 patients), partial — in 29.9% of cases (7 patients).

CONCLUSION

Valve cyclodialysis *ab externo* with implantation of the Xenoplast NACI in the supraciliary space proved to be a highly effective and safe way to decrease IOP and the amount of hypotensive medications used in the advanced stage POAG patients; the number of complications associated with the surgery is minimal.

Thus, the suggested valve cyclodialysis *ab externo* with implantation of Xenoplast NACI is a highly effective and safe surgery for advanced staged POAG.

References

1. Egorov EA, Astakhov YuS, Erichev VP. Natsional'noe rukovodstvo po glaukome. M.: GEOTAR-Media, 2015; 457 p.
2. Liebman ES. Present-day positions of the clinical-and-social ophthalmology. Vestnik oftal'mologii. 2004; 120 (1): 10–2.
3. Lovpache JN, Arakelyan MA, Ramazanova KA. Hypotinsive effect, tolerance and safety of the preparations Timolol 0,5%, Dorzolamide and combination of these preparations in treatment of patients with primary open-angle glaucoma. Ros. oftal'mol. zhurnal. 2011; (1): 40–5.
4. Svetozarskiy SN, Maslennikova YA, Anikeeva MV. Modern Technologies of Open-Angle Glaucoma Surgery. STM. 2014; 6 (1): 102–9.
5. 5–de Moraes CG, Liebmann JM, Medeiros FA, Weinreb RN. Management of advanced glaucoma: Characterization and monitoring. Surv Ophthalmol. 2016; 61 (5): 597–615.
6. Kumar V, Frolov MA, Dushina GN, Shradqa AS, Bezzabotnov AI. Reverse meridional cyclodialysis ab interno with implantation of metallic implant in patientswith glaucoma of different etiology. Vestnik oftal'mologii. 2019; 135 (3): 10–9.
7. Johnson M, Mclaren JW, Overby DR. Unconventional aqueous humor outflow: A review. Exp Eye Res. 2017; (158): 94–111.
8. Carreon T, van der Merwe E, Fellman RL, Johnstone M, Bhattacharya SK. Aqueous outflow — A continuum from trabecular meshwork to episcleral veins. Prog Retin Eye Res. 2017; (57): 108–33.
9. Frolov MA, Frolov AM, Kazakova KA. Combination treatment for cataract and glaucoma. Vestnik oftal'mologii. 2017; 133 (4): 42–6.
10. Yucel Y, Gupta N. Lymphatic drainage from the eye: A new target for therapy. Prog Brain Res. 2015; (220):185–98.
11. Kammer JA, Mundy KM. Suprachoroidal Devices in Glaucoma Surgery. Middle East Afr Ophthalmol. 2015; 22 (1): 45–52.
12. Tanito M, Chihara E. safety and effectiveness of gold glaucoma micro shunt for reducing intraocular pressure in Japanese patients with open angle glaucoma. Jpn J Ophthalmol. 2017; 61 (5): 388–94.
13. Grisanti S, Grisanti S, Garcia-Feijoo J, Dick HB, Munoz-Negrete FJ, Arrondo E., et al. Supraciliary microstent implantation for open-angle glaucoma: multicentre 3-year outcomes. BMJ Open Ophthalmol. 2018; 22 (1): e000183.
14. Krasnov MM. Mikrokhirurgiya glaukom, 2-eizdanie. M.: Meditsina, 1980; 248 c.
15. Shaarawy TM, Grehn F, Sherwood MB, editors. Guidelines on design and reporting of glaucoma surgical trials. World Glaucoma Association. Amsterdam: Kugler publications, 2008; 2009.
16. Kolesnikova LH, Pantsireva LP, Svirin AB. Dilation of suprachoroidal space in combination with cyclodialysis. Vestnik oftal'mologii. 1976; (4): 18–20.
17. Demeler U. Direct cyclopexy following operative and traumatic cyclodialysis. Fortschr Ophthalmol. 1984; (81): 466–8.
18. Kumar V, Frolov MA, Dushina GN, Shradqa AS, Bezzabotnov AI. Reverse meridional cyclodialysis ab interno in surgical management of different types of glaucoma: Long-term results. Natsional'nyy zhurnal glaukoma. 2018; 17 (4): 63–73.
19. Frolov MA, Ryabey AV, Frolov AM, Al' Khatib NS. Rezul'taty modifitsirovannoy sinustrabekulektomii s bazal'noy iridektomiey, drenirovaniem peredney kamery i suprakhorioidal'nogo prostranstva autoskleroy pri pervichnoy otkrytougol'noy glaukome. Tochka zreniya. Vostok — zapad, nauchno-prakticheskiy zhurnal. 2018; (3): 23–6.
20. Figus M, Lazzeri S, Fogagnolo P, Laster M, Martinelli P, Nardi M. Supraciliary shunt in refractory glaucoma. Br J Ophthalmol. 2011; 95 (11): 1537–41.
21. Hueber A, Roters S, Jordan JF, Konen W. Retrospective analysis of the success and safety of Gold Micro Shunt Implantation in glaucoma. BMC Ophthalmol. 2013; (13): 35.
22. Agnifili L, Costagliola C, Figus M, Lezzi G, Piattelli A, Carpineto, et al. Histological findings of failed gold micro shunts in primary open-angle glaucoma. Graefes Arch Clin Exp Ophthalmol. 2012; 250 (1): 143–9.
23. Hoeh H, Vold SD, Ahmed IK, Anton A, Rau M, Singh K, et al.

Initial Clinical Experience with the CyPass Micro-Stent: Safety and Surgical Outcomes of a Novel Supraciliary Microstent. J Glaucoma. 2016; 25 (1): 106–12.
24. Grisanti S, Margolina E, Hoeh H, Rau M, Erb C, Kersten-Gomez, et al. Supraciliary microstent for open-angle glaucoma: clinical results of a prospective multicenter study. Ophthalmologe. 2014; 111 (6): 548–52.
25. Perez CI, Chansangpetch S, Hsia YC, Lin SC. Use of Nd:YAG laser to recanalize occluded Cypass Micro-Stent in the early post-operative period. Am J Ophthalmol Case Rep. 2018; (10): 114–6.
26. Gigon A, Shaarawy T. The Suprachoroidal Route in Glaucoma Surgery. J Curr Glaucoma Pract. 2016; 10 (1): 13–20.
27. Rjabceva AA, Jugaj MP. Izmenenie vnutriglaznogo davlenija v rannie sroki posle fakojemul'sifikacii katarakty. Tochka zrenija. Vostok — zapad, nauchno-prakticheskij zhurnal. 2014; (1): 84.
28. DeVience E., Chaudhry S., Saeedi OJ. Effect of intraoperative factors on IOP reduction after phacoemulsification. Int Ophthalmol. 2017; 37 (1): 63–70.
29. Anisimov SI, Anisimova SYu, Drozdova GA, Larionov EV, Rogacheva IV. Patofiziologicheskie aspekty ispol'zovaniya novogo biologicheskogo materiala ksenoplast v khirurgicheskom lechenii glaukomy. Natsional'nyy zhurnal glaukoma. 2008; (2): 40–5.
30. Anisimova SYu, Anisimov SI, Rogacheva IV. khirurgicheskoe lechenie rafrakternoy glaukomy s ispol'zovaniem novogo, stoykogo k biodestruktsii kollagenovogo drenazha. Natsional'nyy zhurnal glaukoma. 2006; (2): 51–6.

Литература

1. Егоров Е. А., Астахов Ю. С., Еричев В. П. Национальное руководство по глаукоме. М.: ГЭОТАР-Медиа, 2015; 457 с.
2. Либман Е. С. Современные позиции клинико-социальной офтальмологии. Вестник офтальмологии. 2004; 120 (1): 10–2.
3. Ловпаче Дж. Н., Аракелян М. А., Рамазанова К. А. Гипотензивная эффективность, переносимость и безопасность препаратов Тимолол 0,5%, Дорзопт 2%, комбинации Тимолол 0,5% и Дорзопт 2% в лечении пациентов с первичной открытоугольной глаукомой. Рос. офтальмол. журнал. 2011; (1): 40–5.
4. Светозарский С. Н., Масленникова Ю. А., Аникеева М. В. Современные технологии хирургического лечения открытоугольной глаукомы. СТМ. 2014; 6 (1): 102–9.
5. de Moraes CG, Liebmann JM, Medeiros FA, Weinreb RN. Management of advanced glaucoma: Characterization and monitoring. Surv Ophthalmol. 2016; 61 (5): 597–615.
6. Кумар В., Фролов М. А., Душина Г. Н., Шрадка А. С., Беззаботнов А. И. Обратный меридиональный циклодиализ ab interno с введением в супрацилиарное пространство металлического имплантата при глаукоме различной этиологии. Вестник офтальмологии. 2019; 135 (3): 10–9.
7. Johnson M, Mclaren JW, Overby DR. Unconventional aqueous humor outflow: A review. Exp Eye Res. 2017; (158): 94–111.
8. Carreon T, van der Merwe E, Fellman RL, Johnstone M, Bhattacharya SK. Aqueous outflow — A continuum from trabecular meshwork to episcleral veins. Prog Retin Eye Res. 2017; (57): 108–33.
9. Фролов М. А., Фролов А. М., Казакова К. А. Комбинированные методы лечения при сочетании катаракты и глаукомы. Вестник офтальмологии. 2017; 133 (4): 42–6.
10. Yucel Y, Gupta N. Lymphatic drainage from the eye: A new target for therapy. Prog Brain Res. 2015; 220: 185–98.
11. Kammer JA, Mundy KM. Suprachoroidal Devices in Glaucoma Surgery. Middle East Afr Ophthalmol. 2015; 22 (1): 45–52.
12. Tanito M, Chihara E. safety and effectiveness of gold glaucoma micro shunt for reducing intraocular pressure in Japanese patients with open angle glaucoma. Jpn J Ophthalmol. 2017; 61 (5): 388–94.
13. Grisanti S, Grisanti S, Garcia-Feijoo J, Dick HB, Munoz-Negrete FJ, Arrondo E, et al. Supraciliary microstent implantation for open-angle glaucoma: multicentre 3-year outcomes. BMJ Open Ophthalmol. 2018; 22 (1): e000183.
14. Краснов М. М. Микрохирургия глауком, 2-е издание. М.: Медицина; 1980; 248 с.
15. Shaarawy TM, Grehn F, Sherwood MB, editors. Guidelines on design and reporting of glaucoma surgical trials. World Glaucoma Association. Amsterdam: Kugler publications, 2008; 2009.
16. Колесникова Л. Н., Панцырева Л. П., Свирин А. В. Дилятация супрахориоидального пространства в комбинации с циклодиализом. Вестник офтальмологии. 1976; 4: 18–20.
17. Demeler U. Direct cyclopexy following operative and traumatic cyclodialysis. Fortschr Ophthalmol. 1984; 81: 466–8.
18. Кумар В., Фролов М. А., Душина Г. Н., Шрадка А. С., Беззаботнов А. И. Обратный меридиональный циклодиализ ab interno в хирургическом лечении глаукомы различной этиологии: отдаленные результаты. Национальный журнал глаукома. 2018; 17 (4): 63–73.
19. Фролов М. А., Рябей А. В., Фролов А. М., Аль Хатиб Н. С. Результаты модифицированной синустрабекулэктомии с базальной иридэктомией, дренированием передней камеры и супрахориоидального пространства аутосклерой при первичной открытоугольной глаукоме. Точка зрения. Восток — запад, научно-практический журнал. 2018; (3): 23–6.
20. Figus M, Lazzeri S, Fogagnolo P, Laster M, Martinelli P, Nardi M. Supraciliary shunt in refractory glaucoma. Br J Ophthalmol. 2011; 95 (11): 1537–41.
21. Hueber A, Roters S, Jordan JF, Konen W. Retrospective analysis of the success and safety of Gold Micro Shunt Implantation in glaucoma. BMC Ophthalmol. 2013; (13): 35.
22. Agnifili L, Costagliola C, Figus M, Lezzi G, Piattelli A, Carpineto, et al. Histological findings of failed gold micro shunts in primary open-angle glaucoma. Graefes Arch Clin Exp Ophthalmol. 2012; 250 (1): 143–9.
23. Hoeh H, Vold SD, Ahmed IK, Anton A, Rau M, Singh K, et al. Initial Clinical Experience with the CyPass Micro-Stent: Safety and Surgical Outcomes of a Novel Supraciliary Microstent. J Glaucoma. 2016; 25 (1): 106–12.
24. Grisanti S, Margolina E, Hoeh H, Rau M, Erb C, Kersten-Gomez, et al. Supraciliary microstent for open-angle glaucoma: clinical results of a prospective multicenter study. Ophthalmologe. 2014; 111 (6): 548–52.
25. Perez CI, Chansangpetch S, Hsia YC, Lin SC. Use of Nd: YAG laser to recanalize occluded Cypass Micro-Stent in the early post-operative period. Am J Ophthalmol Case Rep. 2018; (10): 114–6.
26. Gigon A, Shaarawy T. The Suprachoroidal Route in Glaucoma Surgery. J Curr Glaucoma Pract. 2016; 10 (1): 13–20.
27. Рябцева А. А., Югай М. П. Изменение внутриглазного давления в ранние сроки после факоэмульсификации катаракты. Точка зрения. Восток — запад, научно-практический журнал. 2014; (1): 84
28. DeVience E, Chaudhry S, Saeedi OJ. Effect of intraoperative factors on IOP reduction after phacoemulsification. Int Ophthalmol. 2017; 37 (1): 63–70.
29. Анисимов С. И., Анисимова С. Ю., Дроздова Г. А., Ларионов Е. В., Рогачева И. В. Патофизиологические аспекты использования нового биологического материала ксенопласт в хирургическом лечении глаукомы. Национальный журнал глаукома. 2008; (2): 40–5.
30. Анисимова С. Ю., Анисимов С. И., Рогачева И. В. хирургическое лечение рафрактерной глаукомы с использованием нового, стойкого к биодеструкции коллагенового дренажа. Национальный журнал глаукома. 2006; (2): 51–6.

GUT MICROBIOTA OF HEALTHY NEWBORNS: NEW DIAGNOSTIC TECHNOLOGIES — NEW OUTLOOK ON THE DEVELOPMENT PROCESS

Priputnevich TV[1], Isaeva EL[1], Muravieva VV[1], Gordeev AB[1] ✉, Zubkov VV[1], Timofeeva LA[1], Mesyan MK[1], Shubina E[1], Makarov VV[2], Yudin SM[2]

[1] National Medical Research Center for Obstetrics, Gynecology and Perinatology named after Academician V. I. Kulakov, Moscow, Russia

[2] Center for Strategic Planning and Management of Medical and Biological Health Risks, Moscow, Russia

Currently, there are no criteria allowing to adequately assess composition and volume of the newborns' gut microbiota, which prevents early detection of the pathological processes and appropriate intervention. This study aimed to apply the methods of culturomics, proteomics and molecular genetic technologies to investigate the development of gut microbiota in healthy newborns delivered in the city of Moscow both vaginally and through a cesarean section. We examined 66 children, 33 of them delivered vaginally and 33 by cesarean section. The luminal bacterial flora samples were collected on the 1st, 7th and 30th days of life. There were 136 species of microorganisms belonging to 40 genera identified. We established that cesarean section slows down normal development of the gut microflora: through the follow-up period (1 month of life), gut microbiocenosis in such children did not yield the results on par with those registered in children born vaginally. Bifidobacteria were significantly more common in the vaginal delivery group: 84% of 10^9–10^{12} CFU/g versus 33% of 10^5–10^{12} CFU/g in the cesarean section group. At the same time, the former group had significantly less clostridia (33.3% and 65.4%, respectively) and lactose-negative *Escherichia coli* strains (2.4 and 19.4%, respectively) than the latter group.

Keywords: microbiota, newborns, gut microbiota

Author contribution: Priputnevich TV — study planning, organization of microbiological tests, data interpretation; Isaeva EL and Muravieva VV — conducting microbiological tests, draft authoring; Gordeev AB — data analysis and interpretation; Zubkov VV — study planning, feces samples collection organization; Timofeeva LA and Mesyan MK — feces collection; Shubina E — sequencing; Makarov VV and Yudin SM — study planning.

Compliance with ethical standards: the study was approved by the Ethics Committee of National Medical Research Center for Obstetrics, Gynecology and Perinatology named after Academician V. I. Kulakov (meeting minutes № 4 of April 12, 2018). Parents of all children included in the study signed the voluntary informed consent to participate in the study.

✉ **Correspondence should be addressed:** Alexey B. Gordeev
Akademika Oparina, 4, Moscow, 117997; gordeew@vega.protres.ru

Received: 28.08.2019 **Accepted:** 11.09.2019 **Published online:** 28.09.2019

DOI: 10.24075/brsmu.2019.063

МИКРОБИОТА КИШЕЧНИКА ЗДОРОВЫХ НОВОРОЖДЕННЫХ ДЕТЕЙ: НОВЫЕ ТЕХНОЛОГИИ ДИАГНОСТИКИ — НОВЫЙ ВЗГЛЯД НА ПРОЦЕСС СТАНОВЛЕНИЯ

Т. В. Припутневич[1], Е. Л. Исаева[1], В. В. Муравьева[1], А. Б. Гордеев[1] ✉, В. В. Зубков[1], Л. А. Тимофеева[1], М. К. Месян[1], Е. Шубина[1], В. В. Макаров[2], С. М. Юдин[2]

[1] Национальный медицинский исследовательский центр акушерства, гинекологии и перинатологии имени академика В. И. Кулакова, Москва, Россия

[2] Центр стратегического планирования и управления медико-биологическими рисками здоровью, Москва, Россия

В настоящее время не существует критериев адекватной оценки качественного и количественного состава микробиоты кишечника новорожденных детей, что не дает возможности выявить на ранних сроках патологический процесс и скорректировать его. Целью исследования было изучить становление микробиоты кишечника у здоровых новорожденных в городе Москве, рожденных самопроизвольно и путем операции кесарева сечения, с помощью методов культуромики, протеомики и молекулярно-генетических технологий. Обследовано 66 детей: 33 ребенка, рожденных самопроизвольно, и 33 — путем операции кесарева сечения. Образцы просветной микрофлоры собирали на первые, седьмые и 30-е сутки жизни. Выделено 136 видов микроорганизмов, относящихся к 40 родам. Показано, что кесарево сечение тормозит процесс нормального становления микрофлоры кишечника, и в течение изучаемого периода (первого месяца жизни) микробиоценоз кишечника у таких детей не достигает показателей у детей, рожденных самопроизвольно. Статистически достоверно в группе самопроизвольных родов преобладали бифидобактерии (частота их встречаемости в титре 10^9–10^{12} КОЕ/г составила 84% против 33% при титре 10^5–10^{12} КОЕ/г в группе кесарева сечения). В то же время у детей, рожденных самопроизвольно, по сравнению с детьми, рожденными путем кесарева сечения, отмечена статистически достоверно более низкая частота обнаружения клостридий (33,3 и 65,4% соответственно) и лактозоотрицательных штаммов *Escherichia coli* (2,4 и 19,4% соответственно).

Ключевые слова: микробиота, новорожденные, микробиота кишечника

Информация о вкладе авторов: Т. В. Припутневич — планирование исследования, организация микробиологических исследований, интерпретация данных; Е. Л. Исаева и В. В. Муравьева — проведение микробиологических исследований, подготовка черновика рукописи; А. Б. Гордеев — анализ и интерпретация данных; В. В. Зубков — планирование исследования, организация сбора проб фекалий; Л. А. Тимофеева и М. К. Месян — сбор проб фекалий; Е. Шубина — проведение секвенирования; В. В. Макаров и С. М. Юдин — планирование исследования.

Соблюдение этических стандартов: исследование одобрено этическим комитетом НМИЦ АГП им. В. И. Кулакова (протокол заседания № 4 от 12 апреля 2018 г.). Родители всех детей, включенных в исследование, подписали добровольное информированное согласие на участие в исследовании.

✉ **Для корреспонденции:** Алексей Борисович Гордеев
ул. Академика Опарина, д. 4, г. Москва, 117997; gordeew@vega.protres.ru

Статья получена: 28.08.2019 **Статья принята к печати:** 11.09.2019 **Опубликована онлайн:** 28.09.2019

DOI: 10.24075/vrgmu.2019.063

Today, the nature of microbial colonization of the human intestine, including that of the newborns, has changed significantly. The reasons are the growing number of complicated pregnancies, stressful situations, poor environmental conditions and uncontrolled intake of antibiotics.

An in-depth study of the gut microbiota that implies application of the methods offered by culturomics, high-tech isolated microorganisms identification (MALDI-TOF MS, 16S rRNA gene sequencing) and metagenomic analysis can yield an expanded outlook of its species diversity.

Against this background, the currently adopted gut microbiota standards (composition and volume) [1–3] require revision. To date, there are no clearly defined criteria for the newborns' gut microbiota assessment, the criteria that would allow timely interventions addressing the problems detected and early measures arresting pathological processes, such as necrotizing enterocolitis in premature babies. Very few researchers undertook statistical processing of the data describing composition and volume of the newborns' gut microbiota [4, 5].

This study aimed to apply the methods of culturomics, proteomics and molecular genetic technologies to investigate the development of gut microbiota in healthy newborns delivered in the city of Moscow both vaginally and by a cesarean section.

METHODS

A cohort of healthy full-term newborns was selected for this prospective study. The cohort was randomized by blocks, which yielded two groups of children:

1) group I — 33 children delivered vaginally;

2) group II — 33 children born by caesarean section.

The inclusion criteria were as follows: gestational age 38–40 weeks; Apgar score of 8–9 points (first and fifth minutes of life); body weight over 2800 g. Blood and urine of the newborns were tested for infectious pathologies or other factors that could affect development of the gut microbiota. All children were breastfed; feeding formulas were used in isolated cases only. No mother had a prolonged latency period; 3 women took antibiotics during pregnancy; 4 women had cervical incompetence (6%). In the surgical delivery cases the women received amoxicillin/clavulanic acid for prevention purposes before and during surgery.

The feces were collected from the newborns three times: on the 1st day, at the end of the 1st week and at the end of the 1st month of life. The samples of meconium obtained during the first bowel movement or feces collected from a sterile diaper and put into a sterile plastic container were delivered to the laboratory within 2 hours; plating was performed immediately upon delivery.

We studied the gut microbiota using an extended range of selective and non-selective culture media. The incubation was done in aerobic, microaerophilic and anaerobic conditions.

Following the generally adopted methods [3, 6], we plated meconium and feces on the following culture media. Isolation of the facultative anaerobic and aerobic microorganisms: Colombian blood agar, Brilliance chromogenic medium, Salmonella Shigella Agar, Sabouraud Dextrose Agar (Oxoid; Great Britain), mannitol salt agar (Himedia; India), *Streptococcus agalactiae* detection and differentiation medium (CHROMagar; France), Enterococcus Agar, Endo Agar (GITsPM i B; Russia). Lactobacilli culturing: Lactobacillus Agar (GITsPM i B; Russia). Obligate anaerobes isolation: Bifidobacterium Agar (Himedia; India), pre-reduced Schaedler Agar with necessary additives, Anaerobic Agar, Perfringens Agar, Iron Sulphite Agar, *Clostridium difficile* selective Agar (Oxoid; UK). To culture microaerophiles, we used a CO_2 incubator (Jouan; France) with the CO_2 concentration of 5%. To culture obligate anaerobes, we used an anaerobic box (Jouan; France) filled with a three-component gas mixture (N_2 — 80%; CO_2 — 10%; H_2 — 10%). Thioglycol broth (Oxoid; Great Britain) enabled sterility control.

The microorganisms were identified with the help of a MALDI-TOF AutoFlex III time-of-flight mass spectrometer powered by the MALDI BioTyper v3.0 software (Bruker Daltoniks; Germany). At SCORE > 2.0, the culture was marked as identified on the species level (high probability of identification). At SCORE 1.7 to 2.0, the culture was considered identified at the genus level.

When the SCORE was below 2.0, i.e. the strain was hard to identify, we did the 16S rRNA gene sequencing. The Proba-CiTo (DNA-Technology; Russia) reagent set enabled extraction of the DNA. We used two DNA fragments for sequencing: an amplicon of ~440 bp (positions 339–785 of the 16S rRNA gene) and an amplicon of ~1340 bp (positions 42–1380 of the 16S rRNA gene). These were amplified using the DTprime detecting amplifier (DNA-Technology; Russia). For sequencing, we employed a 3130 Genetic Analyzer (Applied Biosystems; USA) and used the BigDye™ Terminator v3.1 Cycle Sequencing Kit (Applied Biosystems; USA) following the protocol provided by the manufacturer. For species identification, the BLAST software package (National Center for Biotechnology Information; USA), freely available on the Internet, was used.

To determine differences in the frequency of occurrence of microorganisms depending on the mode of delivery, we applied the Fisher's exact test during statistical processing of the data. Median and interquartile range were used as descriptive statistics to characterize the degree of microbial contamination.

RESULTS

At the 1st time point we examined 66 children, 33 in each group. The meconium of every 5th child was sterile; in group II such a situation was observed twice as often as in group I (9 and 4 cases, respectively; $p > 0.05$). The non-sterile meconia featured diverse microflora (63 species; the average species diversity index was 3.8 species per child). The bacteria isolated most often (in 60% of the vaginally delivered babies, titer of 10^2–10^3 CFU/g, and in 70% of the cesarean section babies, titer of 10^2–10^4 CFU/g) were gram-positive facultative anaerobic microorganisms of 10 genera: *Staphylococcus*, *Streptococcus*, *Enterococcus*, *Micrococcus*, *Gemella*, *Globicatella*, *Granulicatella*, *Rothia*; *Corynebacterium*, *Bacillus*. It is noteworthy that in 12.2% of the group II children and in 6.1% of the group I children we detected *Staphylococcus aureus* (*S. aureus*). *Escherichia coli*, which normally makes up a significant part of the normal intestinal flora, was isolated thrice as often in the vaginally born babies (24.2% and 9.1%; $p > 0.05$). Same is true about other enterobacteria (27% and 15%, respectively; $p > 0.05$). Only one baby had *Pseudomonas aeruginosa* (group II).

Lactobacilli and bifidobacteria play the most important role in the development of the newborn's gut microbiota. These microorganisms were found as early as in the first day of life. The size of the lactobacilli colonies was significantly greater in group I (18% and 3%, respectively; $p > 0.05$); the lactobacilli forming those colonies were *Lactobacillus crispatus* and *Lactobacillus jensenii*, which are among the dominant species in the vaginal microbiota of healthy women. Bifidobacteria were also isolated more often in the sampled taken from the group I babies (9% and 3%, respectively; $p > 0.05$); the bacteria were *Bifidobacterium bifidum*, *B. longum*, *B. adolescentis*. Only 1 baby (group I) had bacteroids detected in the first day of life. Other anaerobes (veillonella, prevotella and campylobacter) were isolated almost exclusively in group II.

Through the first week of the study, some parents refused to continue participation and some children contracted an infectious disease. Therefore, at the 2nd time point we examined 52 babies, 25 from group I and 27 from group II.

Compared to the 1st time point, the average species diversity index increased almost 3-fold and reached 9.4 species per child. As in the first day of life, both groups

had facultative anaerobic microorganisms (9 genera) detected most often. Their titer increased considerably: in the vaginal delivery group it was 10^7–10^{11} CFU/g, in the cesarean section group — 10^7–10^{12} CFU/g; the frequency of occurrence was 100% in both groups. *S. aureus* became a more common bacterium: we isolated it in 44% of the group I babies and in 55.6% of the group II babies. The diversity of enterococci expanded from two to six species: *Enterococcus faecalis*, *E. durans*, *E. faecium*, *E. gilvus*, *E. avium*, *E. gallinarum*. Same as in the first day of life, *E. faecalis* dominated gut microbiota of the majority of participants, colonizing the intestines of 80% of the group I children and 88.9% of the group II children.

The range of gram-negative facultative anaerobic bacteria present extended from 6 to 15 species (*Enterobacteriaceae*). *E. coli* was still detected more often in the vaginally born babies (64% in group I and 44.4% in group II; $p > 0.05$). The frequency of isolation of other enterobacteria was approximately the same in both groups.

The composition of lactobacilli species extended with *L. paracasei*, *L. curvatus*, *L. gasseri*, *L. fermentum*, *L. rhamnosus.* It should be noted that the species of lactobacilli dominating vaginal microbiota of healthy women (*L. crispatus*, *L. jensenii* и *L. gasseri*) were only found in the group I children.

We registered statistically significant differences in the representation of bifidobacteria. In group I such were detected in 84% of samples with the titer of 10^9–10^{12} CFU/g, and in group II the figure was only 33%, with the titer of 10^5–10^{12} CFU/g ($p < 0.05$). The number of bifidobacteria species grew from 3 to 7: *B. adolescentis*, *B. breve*, *B. dentium*, *B. catenulatum*, *B. bifidum*, *B. longum*, *B. animalis*. Some were detected only on one of the groups: *B. adolescentis* and *B. catenulatum* (group I exclusively) and *B. dentium* and *B. animalis* (group II exclusively).

By the seventh day of life, microbiota became significantly more diverse, adding 11 new genera of other obligate anaerobes: *Bacteroides*, *Parabacteroides*, *Veillonella*, *Clostridium*, *Fusobacterium*, *Ruminococcus*, *Eubacterium*, *Eggerthella*, *Actinomyces*, *Collinsella*, *Propionibacterium*. The bacteroids represented by *Bacteroides fragilis*, *B. ovatus*, *B. vulgatus*, *B. uniformis*, *Parabacteroides distasonis* were only detected in children born vaginally. We registered no significant difference in the frequency of detection of clostridia (*Clostridium perfringens*, *C. butyricum*, *C. innocuum*, *C. tertium*). One baby from group II had *C. difficile*. Veilonella colonies grew larger in both groups.

Thus, by the 7th day of life microbiota of the participants featured significantly more species of various genera, both facultatively anaerobic and obligate anaerobic. Bifidobacteria, lactobacilli and bacteroids were prevalent in group I.

At the 3rd time point we examined 50 children, 24 from group I and 26 from group II. The average species diversity index was 9.4 species per child. As in the earlier periods, gram-positive facultative anaerobic bacteria (7 genera) were the most common. The frequency of detection of *S. aureus* remained largely unchained compared to the 7th day in group I (58.3%) and significantly increased in group II (76.9%). There were 2 new species of enterococci detected: *E. casseliflavus* and *E. raffinosus*.

As for the composition of gram-negative facultative anaerobic microflora, we isolated 11 *Enterobacteriaceae* species and 1 species of non-fermenting bacteria, *Stenotrophomonas maltophilia*. *E. coli* were still detected more often in the vaginally born babies (75% in group I and 61.5% in group II; $p > 0.05$). Samples from the group II children had other enterobacteria slightly more often (66.7% and 73%, respectively; $p > 0.05$).

The number of lactobacilli expanded to 15 species with *L. reuteri*, *L. casei*, *L. vaginalis*, *L. brevis*, *L. helveticus*, *L. acidophilus*; we detected twice as many species in group I. As for the bifidobacteria, there was only 1 new species detected, *B. ruminantium*. The most common were *B. longum* (58.3% in group I and 26.9% in group II) and *B. bifidum* (33.3 and 34.6%, respectively).

The new obligate anaerobes discovered were *Sutterella* and *Peptoniphilus*. Except for 1 case, bacteroids (6 species) — *B. fragilis*, *B. thetaiotaomicron*, *B. vulgatus*, *B. uniformis*, *B. cellulosilyticus*, *Parabacteroides distasonis*, — were detected in vaginally delivered babies exclusively.

We started seeing a statistically significant difference in the frequency of detection of clostridia (*C. perfringens*, *C. butyricum*, *C. tertium*, *C. ramosum*, *C. paraputrificum*, *C. difficile*): 33.3% of children in group I and 65.4% in group II ($p < 0.05$). There were twice as many species of clostridia in group II. One child from group II had *C. difficile*.

Candida yeast was found in both groups only on the 30th day of life; less than 10% of children had them.

Thus, regardless of the method of delivery, on the 30th day of life the gut microbiota featured multicomponent microbial associations of facultative and obligate anaerobes. At the same time, certain differences between obligate and transient microbiota components became obvious. The composition of lactobacilli was more diverse (almost twice as many species) in babies delivered vaginally, the species detected more often in their samples were those inhabiting vagina of healthy women. Bacteroids were predominantly isolated in the same group I children, while clostridia, with greater variety of species, were more peculiar to the C-section babies. The conditionally pathogenic facultative anaerobes (*S. aureus* and enterobacteria, with the exception of *E. coli*) more often colonized children by a cesarean section.

The hemolytic strains of *Enterococcus sp*. and *E. coli* occurred with the same frequency in both groups: *Enterococcus sp*. — 8.3% in each group, and *E. coli* — 9.5 and 9.7%, respectively. Lactose-negative strains of *E. coli* were isolated in the group II children 8 times more often than in group I, which is a significant difference (19.4 and 2.4%, respectively; $p < 0.05$).

Overall, we isolated and identified 136 species of microorganisms of 40 genera: *Staphylococcus*, *Streptococcus*, *Corynebacterium*, *Micrococcus*, *Enterococcus*, *Rothia*, *Bacillus*, *Neisseria*, *Haemophilus*, *Gemella*, *Globicatella*, *Granulicatella, Escherichia, Klebsiella, Raoultella, Kluyvera, Enterobacter, Citrobacter, Proteus, Morganella, Pantoea, Pseudomonas, Stenotrophomonas, Candida, Lactobacillus, Bifidobacterium, Bacteroides, Propionibacterium, Veillonella, Clostridium, Ruminococcus, Eggertella, Fusobacterium, Eubacterium, Actinomyces, Collinsella, Prevotella, Campylobacter, Peptoniphilus, Sutterella.*

Identification of genera of 36 isolated bacteria (SCORE < 2.0) required 16S rRNA sequencing. In most cases, sequencing results confirmed findings of the MALDI-TOF MS study. Only for 5 isolates 16S rRNA gene sequencing was the only method allowing reliable identification. In some cases with closely related microorganisms it was not possible to identify the species neither with sequencing nor with MALDI-TOF MS. These species were: Bifidobacterium kashiwanohense/ *Bifidobacterium pseudocatenulatum/Bifidobacterium catenulatum, Lactobacillus casei/Lactobacillus paracasei, Actinomyces naeslundii/Actinomyces viscosus, Actinomyces radingae/ Actinomyces ihumii*. Eleven isolates produced discrepancies in identification: for 7 of them, it was impossible to find out the genera correctly with the help of MALDI-TOF MS, and 4 presented problems with the species identification.

The table presents generalized data on the frequency of occurrence and degree of microbial contamination of the newborns' intestines depending on the method of delivery; the data allows preliminary characterization of the indicators peculiar to microflora of healthy children.

DISCUSSION

Until recently, it was believed that the gastrointestinal tract of a newborn remains sterile for the first 10–20 h (aseptic phase) [7], and the bacteria first to colonize the intestines of a vaginally delivered child are the lactobacilli from the mother's vaginal microflora [8–11]. However, some experimental research efforts gave rise to another point of view [12]. According to the recently published data, a fetus receives foundation of the gut microflora through bacterial translocation from his mother during the second half of pregnancy; some researchers argue sterility around the fetus [13–15]. In our study, we found that the meconium collected during first defecation in the first hours of life was unsterile in 53 of 66 newborns (80%), which does not exclude intrauterine colonization.

The published works state that the first hours and the first day of life are the time of active colonization, when the colonies of *Escherichia coli*, enterococci develop rapidly; the period is known as the growing colonization stage and its course is independent from the degree of maturity, perinatal fetus development conditions and the type of feeding [16–19]. The enterobacteria titer during that period reaches 10^9 CFU/g of feces [20], and the anaerobes — bifidobacteria, lactobacilli, bacteroids — are usually absent [21]. According to the data we obtained, the first hours of life were the time when the intestines were mainly colonized by the gram-positive cocci (*Staphylococcus spp*, *Streptococcus spp*), and the cesarean section babies had larger colonies than the vaginally delivered children (frequency of occurrence 70 and 60.6%, titers up to 10^4 and 10^3 CFU/g, respectively). During this period, enterobacteria and obligate anaerobic microorganisms were discovered rarely and with low titers. At the same time, already in the first hours of life microbiota of the vaginally born children featured more bifidobacteria and lactobacilli than that of babies delivered by a Caesarean section: 9 and 3%, respectively, and 18 and 3%, respectively. Bacteroids were detected only in 3% of children born vaginally. A possible reason for the discrepancy between our data and the results demonstrated by other authors is the fact that we aimed to obtain the sample biomaterial directly during the first act of defecation of the newborn.

Table. Frequency of occurrence, median and interquartile range of the degree of contamination of feces with microorganisms

Characteristic	1st day of life (*n* = 66)		7th day of life (*n* = 52)		1st month of life (*n* = 50)	
	Vaginal delivery	Cesarean section	Vaginal delivery	Cesarean section	Vaginal delivery	Cesarean section
E. coli						
Frequency of occurrence	24%	9%	64%	44.40%	70.80%	61.50%
Median (CFU/g)	10^2	10^2	10^8	10^9	10^9	10^9
Interquartile range (CFU/g)	10^2	10^2–10^3	10^8–10^9	10^8–10^{10}	10^8–10^{10}	10^8–10^{10}
Other enterobacteria						
Frequency of occurrence	27%	15%	68%	66.70%	66.70%	73%
Median (CFU/g)	10^3	10^3	10^9	10^9	10^9	10^9
Interquartile range (CFU/g)	10^2–10^4	10^2–10^3	10^8–10^{10}	10^9–10^{10}	10^8–10^{10}	10^9–10^{10}
Gram-positive facultative anaerobic and aerobic bacteria						
Frequency of occurrence	60.60%	70%	100%	100%	100%	100%
Median (CFU/g)	10^2	10^2	10^8	10^9	10^8	10^9
Interquartile range (CFU/g)	10^2	10^2–10^3	10^8–10^{10}	10^8–10^{10}	10^7–10^9	10^7–10^9
Bifidobacteria						
Frequency of occurrence	9%	3%	84%	33%	83.30%	53.80%
Median (CFU/g)	10^2	10^2	10^{11}	10^{10}	10^{11}	10^{10}
Interquartile range (CFU/g)	10^2–10^3	10^2	10^9–10^{11}	10^6–10^{11}	10^{10}–10^{12}	10^{10}–10^{11}
Lactobacilli						
Frequency of occurrence	18%	3%	28%	37%	58.30%	69%
Median (CFU/g)	10^2	10^2	10^8	10^8	10^8	10^8
Interquartile range (CFU/g)	10^2	10^2	10^6–10^{10}	10^6–10^{10}	10^5–10^{10}	10^7–10^{10}
Bacteroids						
Frequency of occurrence	3%	0	32%	0	25%	3.80%
Median (CFU/g)	10^2	0	10^9	0	10^{10}	10^9
Interquartile range (CFU/g)	10^2	0	10^9–10^{11}	0	10^{10}	10^9
Clostridia						
Frequency of occurrence	0	0	32%	40.70%	33.30%	65.40%
Median (CFU/g)	0	0	10^7	10^9	$10^{10.5}$	$10^{9.5}$
Interquartile range (CFU/g)	0	0	10^6–10^9	10^6–10^{10}	10^6–10^{11}	10^8–10^{10}

Further on, healthy babies have anaerobic and facultative anaerobic components of their microflora grow actively, the volumes reaching 10^5–10^7 CFU/g [15]. By the 6th day, aerobic and anaerobic parts of the microflora become balanced, then bifidobacteria and lactobacilli begin to develop rapidly and by the 2nd month of life they reach 10^9–10^{10} CFU/g. According to other researchers, days 3–5 mark the beginning of the microflora transformation stage, which results in bifidobacterial flora replacing other microorganisms. This is when bifidobacteria become the core (resident) microflora of the intestines [22–24]. The bifidoflora grows dominant by the 5–20th day of life [25]. Our discoveries are different: the total number of microorganisms increases, reaching $10^{10–12}$ CFU/g. This suggests that the facultative aerobic and obligate anaerobic components of the microbiota also achieve balance by the first week of life, but there are more various microorganisms colonizing the intestines. Another fact deserving a special note is that in the group II babies bifidobacteria did not colonize the gut actively while obligate anaerobes prevailed there (mainly veilonella, clostridia).

By the end of 1st month of life, both groups had the anaerobic part of microbiota taking leading positions; the dominant species were those of bifidoflora. Nevertheless, we detected bifidobacteria only in half of the babies delivered by the caesarean section, while in the vaginally born babies this indicator reached 83%.

The *B. longum subsp. infantis*, *B. animalis subsp. lactis*, *B. breve*, *B. bifidum* bacteria peculiar to the first year of life produce anti-inflammatory effect and contribute to the development of the Th1 immune response. In adults, the predominant strains are *B. longum subsp*. *longum*, *B. adolescentis*, *B. pseudocatenulatum*; they promote the Th2 immune response and prevail in the gut microbiota in case of obesity [24]. Besides, the genome of *B. longum subsp. infantis* has a cluster that encodes the synthesis of enzymes (sialidase, fucosidase, N-acetyl-β-hexosaminidase and β-galactosidase) capable of breaking down oligosaccharides to monosaccharides. [25]. Throughout life, bifidoflora remains prevailing and sterile, while other representatives of the obligate microflora can trigger a disease under certain conditions [13]. Our study revealed that it is not the most useful bifidobacteria that dominate the microbiota of the C-section newborns; in particular, they are not able to break down lactose (*B. animalis*, *B. dentium*, *B. ruminantium*).

CONCLUSIONS

Our results confirm that surgical delivery inhibits the normal process of gut microbiota development to a certain extent. In the future, we plan to continue accumulating information about the state of microbiota in this category of children and expand the scope of our research to include premature babies in order to determine the criteria reflecting normal gut microbiota of healthy full-term newborns. This study allowed establishing, and in the future — replenishing the collection of lactobacilli and bifidobacteria isolated from healthy full-term newborns with the aim to identify bacteria candidates for probiotic strains. Timely adequate assessment of the newborn's microbiota composition against the key biomarkers will allow targeted prevention of the immediate and long-term consequences of perinatal pathology in full-term and premature infants by prescribing an adequate composition of probiotics.

References

1. OST 91500.11.0004-2003. Protokol vedeniya bol'nykh. Disbakterioz kishechnika. Utv. Prikazom MZ RF № 231 от 09.06.2003. Moscow, 2003, 173 p.
2. Metodicheskiye rekomendatsii "Bakteriologicheskaya diagnostika disbakterioza kishechnika" Minzdrav RSFSR. 1977.
3. Metodicheskiye rekomendatsii "Mikrobiologicheskaya diagnostika disbakterioza kishechnika". Moskva, 2007.
4. Gronlund MM. Arvilommi H, Kero P, Lehtonen OP, Isolauri E. Importance of intestinal colonization in the maturation of humoral immunity in early infancy: a prospective follow up study of healthy infants aged 0-6 months. Arch Dis Child Fetal Neonatal. 2000; 83 (3): 186–92.
5. Levanova LA. Mikroekologiya kishechnika zhitelej Zapadnoj Sibiri, korrekciya disbioticheskih sostoyanij [dissertation]. M., 2003.
6. Shcherbakov PL, Nizhevich AA, Loginovskaya VV, Shcherbakova MYu, Kudriavtseva LV, Mitrokhin SD, et al. Mikroekologiya kishechnika u detey i yeye narusheniya. Farmateka. 2007; (14): 28–34.
7. Akoyev YuS. Funktsional'nyye osobennosti nedonoshennykh detey v rannem ontogeneze [dissertation]. M., 1999.
8. Kopanev YuA, Sokolov AL. Disbakterioz kishechnika: microbiologicheskiye, immunologicheskiye i klinicheskiye aspekty mikroekologicheskikh narusheniy u detey. M., 2002.
9. Stepurina OV. Pervichnoye infitsirovaniye rebenka. Infektsionnyye zabolevaniya detey i ekologiya cheloveka. Stavropol', 1999; 92–7.
10. Frolova NA. Osobennosti formirovaniya mikrobiotsenoza u detey rannego vozrasta v zavisimosti ot mikrobnogo peyzazha kishechnika materi [dissertation]. Smolensk, 2001.
11. Nikitenko VI, Tkachenko EI, Stadnikov AA. Translokatsiya bakteriy iz zheludochno-kishechnogo trakta — yestestvennyy zashchitnyy mekhanizm. Eksper i kiln gastroentorolog. 2004; (1): 48.
12. Funkhouser LJ, Bordenstein SR. Mom knows best: the universality of maternal microbial transmission. PLoS Biol. 2013; (11): e1001631.
13. Muglia LJ, Katz M. The enigma of spontaneous preterm birth. N Engl J Med. 2010; 362: 529–35.
14. Onderdonk AB, Hecht JL, McElrath TF, Delaney ML, Allred EN, Leviton A. Colonization of second-trimester placenta parenchyma. Am J Obstet Gynecol. 2008; 199: 51–2.
15. Solov'yeva IV, Belova IV, Tochilina AG, Efimov EI, Pozhidaeva AS. Formirovaniye mikroflory tolstoy kishki u detey. Mikrobiologicheskiy i epidemiologicheskiy vestnik Nizhegorodskogo universiteta imeni N. I. Lobachevskogo. 2012; (2–3): 93–9.
16. Fanaro S, Chierici R, Guerrini P, Vigi V. Intestinal microflora in early infancy: composition and development. Acta pediat. 2003; 91 (441): 48–55.
17. Orrhagt K, Nord CE. Factors controlling the bacterial colonization of the intestine in breastfed infants. Acta Pediatr. 1999; 88 (430): 47–57.
18. Edwards CA, Parret AM. Intestinal flora during the first months of life: new perspectives. Br J Nutr. 2002; 88 (11): 11–8.
19. Goldman AS. Modulation of the gastrointestinal tract of infants by human milk. Interfaces and interactions. An evolutionary perspective. J Nutr. 2000; 130 (2): 426–31.
20. Netrebenko OK. Pitaniye grudnogo rebenka i kishechnaya mikroflora. Pediatriya. 2005; (3): 53–57.
21. Tkachenko EI, Suvorova AN, editors. Disbioz kishechnika. Rukovodstvo po diagnostike i lecheniyu. SPb. InformMed, 2009; 276 p.
22. Shabalov NP. Neonatologiya. Moscow: Medpress-inform, 2004; p. 128–9.
23. Netrebenko OK. Pitaniye i razvitiye immuniteta u detey na raznykh vidakh vskarmlivaniya. Pediatriya. Zhurnal imeni G. N. Speranskogo. 2005; (6): 50–6.
24. Pechkurov DV, Turti TV, Belyaeva IA, Tjazheva AA. Intestinal

microflora in children: from formation disturbances prophylaxis to preventing non-infectious diseases. Pediatric pharmacology. 2016; 13 (4): 377–83.
25. Suvorov AN. Mikrobiota detey. Priroda. 2011; (8): 14–21.

Литература

1. ОСТ 91500.11.0004-2003. Протокол ведения больных. Дисбактериоз кишечника. Утв. Приказом МЗ РФ № 231 от 09.06.2003. Москва, 2003; 173 с.
2. Методические рекомендации «Бактериологическая диагностика дисбактериоза кишечника». Минздрав РСФСР. 1977.
3. Методические рекомендации «Микробиологическая диагностика дисбактериоза кишечника». Москва, 2007.
4. Gronlund MM. Arvilommi H, Kero P, Lehtonen OP, Isolauri E. Importance of intestinal colonization in the maturation of humoral immunity in early infancy: a prospective follow up study of healthy infants aged 0–6 months. Arch Dis Child Fetal Neonatal. 2000; 83 (3): 186–92.
5. Леванова Л.А. Микроэкология кишечника жителей Западной Сибири, коррекция дисбиотических состояний [диссертация]. М., 2003.
6. Щербаков П. Л., Нижевич А. А., Логиновская В. В., Щербакова М. Ю., Кудрявцева Л. В., Митрохин С. Д. и др. Микроэкология кишечника у детей и ее нарушения. Фарматека. 2007; (14): 28–34.
7. Акоев Ю. С. Функциональные особенности недоношенных детей в раннем онтогенезе [диссертация]. М., 1999.
8. Копанев Ю. А., Соколов А. Л. Дисбактериоз кишечника: микробиологические, иммунологические и клинические аспекты микроэкологических нарушений у детей. М., 2002.
9. Степурина О. В. Первичное инфицирование ребенка. Инфекционные заболевания детей и экология человека. Ставрополь, 1999; 92–7.
10. Фролова Н. А. Особенности формирования микробиоценоза у детей раннего возраста в зависимости от микробного пейзажа кишечника матери [диссертация]. Смоленск, 2001.
11. Никитенко В. И., Ткаченко Е. И., Стадников А. А. Транслокация бактерий из желудочно-кишечного тракта — естественный защитный механизм. Эксперимент. и клин. гастроэнтерол. 2004; (1): 48.
12. Funkhouser LJ, Bordenstein SR. Mom knows best: the universality of maternal microbial transmission. PLoS Biol. 2013; (11): e1001631.
13. Muglia LJ, Katz M. The enigma of spontaneous preterm birth. N Engl J Med. 2010; 362: 529–35.
14. Onderdonk AB, Hecht JL, McElrath TF, Delaney ML, Allred EN, Leviton A. Colonization of second-trimester placenta parenchyma. Am J Obstet Gynecol. 2008; 199: 51–2.
15. Соловьева И. В., Белова И. В., Точилина А. Г., Ефимов Е. И., Пожидаева А.С. Формирование микрофлоры толстой кишки у детей. Микробиологический и эпидемиологический вестник Нижегородского университета им. Н. И. Лобачевского. 2012; (2–3): 93–9.
16. Fanaro S, Chierici R, Guerrini P, Vigi V. Intestinal microflora in early infancy: composition and development. Acta pediat. 2003; 91 (441): 48–55.
17. Orrhagt K, Nord CE. Factors controlling the bacterial colonization of the intestine in breastfed infants. Acta Pediatr. 1999; 88 (430): 47–57.
18. Edwards CA, Parret AM. Intestinal flora during the first months of life: new perspectives. Br J Nutr. 2002; 88 (11): 11–8.
19. Goldman AS. Modulation of the gastrointestinal tract of infants by human milk. Interfaces and interactions. An evolutionary perspective. J Nutr. 2000; 130 (2): 426–31.
20. Нетребенко О. К. Питание грудного ребенка и кишечная микрофлора. Педиатрия. 2005; (3): 53–7.
21. Ткаченко Е. И., Суворова А. Н., редакторы. Дисбиоз кишечника. Руководство по диагностике и лечению. СПб. ИнформМед, 2009; 276 с.
22. Шабалов Н. П. Неонатология. М.: Медпресс-информ, 2004; с.128–29.
23. Нетребенко О. К. Питание и развитие иммунитета у детей на разных видах вскармливания. Педиатрия. Журнал им. Г. Н. Сперанского. 2005; (6): 50–6.
24. Печкуров Д. В., Турти Т. В., Беляева И. А., Тяжева А. А. Микробиота кишечника у детей: от профилактики нарушений становления к предупреждению неинфекционных заболеваний. Педиатрическая фармакология. 2016; 13 (4): 377–83.
25. Суворов А. Н. Микробиота детей. Природа. 2011; (8): 14–21.

PREDICTION OF BACTERIAL VULVOVAGINITIS IN GIRLS AT DIFFERENT TANNER STAGES OF SEXUAL DEVELOPMENT

Kazakova AV[1] ✉, Uvarova EV[2], Limareva LV[1], Trupakova AA[1], Mishina AI[1]

[1] Samara State Medical University, Samara, Russia

[2] Kulakov Federal Research Center for Obstetrics, Gynecology, and Perinatology, Moscow, Russia

At present, there is a paucity of research studies that comprehensively investigate the factors causing vulvovaginitis in young females. The aim of this work was to propose an algorithm for predicting the risk of vulvovaginitis in young girls and adolescents. The study recruited 252 healthy girls, who were stratified into a few groups depending on their sexual development on the Tanner scale. The composition of vaginal microbiota was determined in all the participants using real-time polymerase chain reaction (PCR); distribution of allele and genotype frequencies was assessed for the polymorphic variants of genes coding for pro- and anti-inflammatory cytokines. Based on the obtained data, we created a functional model for predicting the risk of vulvovaginitis in girls at different stages of sexual development. Favorable risk factors for Tanner I girls included predominance of obligate anaerobes in vaginal microbiota and the polymorphic IL10 variant (C-819T) homozygous for TT. The sensitivity of the model was 80%, its specificity was 78%. Favorable risk factors for prepubertal and pubertal girls included predominance of aerobes in the composition of vaginal microbiota and the presence of the TT allele in the polymorphic IL10 gene variant (C-3953T). The sensitivity of the model was 58.3%, whereas specificity, 94.1%. This study provides the rationale conforming with the principles of evidence-based medicine for using prevention measures in the groups at risk for vulvovaginitis at young age. The proposed measures allowed us to reduce the relapse rate of bacterial vulvovaginitis threefold.

Keywords: vulvovaginitis, teenagers, prediction, prevention, evidence-based medicine

Author contribution: Kazakova AV — study concept and design, data acquisition and analysis, manuscript draft; Uvarova EV — study concept and design, manuscript revision; Limareva LV — study concept and design, manuscript revision; Trupakova AA, Mishina AI — data acquisition and analysis, manuscript draft.

Compliance with ethical standards: the study was approved by the Ethics Committee of Samara State Medical University (Protocol № 5 dated April 20, 2018). Informed consent was obtained from the parents of the study participants.

✉ **Correspondence should be addressed:** Anna V. Kazakova
Lesnaya, 31, kv. 40, Samara, 443110; amigo14021980@yandex.ru

Received: 27.09.2019 **Accepted:** 17.10.2019 **Published online:** 29.10.2019

DOI: 10.24075/brsmu.2019.070

СПОСОБ ПРОГНОЗИРОВАНИЯ БАКТЕРИАЛЬНОГО ВУЛЬВОВАГИНИТА У ДЕВОЧЕК В ЗАВИСИМОСТИ ОТ СТАДИИ ПОЛОВОГО РАЗВИТИЯ СОГЛАСНО ШКАЛЕ ТАННЕРА

А. В. Казакова[1] ✉, Е. В. Уварова[2], Л. В. Лимарева[1], А. А. Трупакова[1], А. И. Мишина[1]

[1] Самарский государственный медицинский университет, Самара, Россия

[2] Научный центр акушерства, гинекологии и перинатологии имени В. И. Кулакова, Москва, Россия

На современном этапе мало научных работ по всестороннему изучению факторов, приводящих к вульвовагиниту у девочек. Целью исследования было разработать программу прогнозирования риска вульвовагинита у девочек в детском и подростковом возрасте. В исследовании приняли участие 252 здоровые девочки, которых разделили на группы в зависимости от стадии полового развития по Таннеру. У всех было проведено определение состава микрофлоры влагалища методом полимеразной цепной реакции (ПЦР) в режиме реального времени и распределение частот аллелей и генотипов полиморфных вариантов генов провоспалительных и противовоспалительных цитокинов. На основании полученных данных разработана рабочая модель по прогнозированию развития вульвовагинитов у девочек с учетом стадии полового развития. Благоприятными факторами для девочек на I стадии полового развития были преобладание облигатных анаэробов в микробиоте влагалища и гомозигота ТТ полиморфного варианта гена IL10 (С-819Т). Чувствительность модели составила 80%, специфичность — 78%. Для девочек в препубертатном и пубертатном периодах — преобладание аэробов в микробиоте влагалища и гомозигота ТТ полиморфного варианта гена IL10 (С-3953Т). Чувствительность модели составила 58,3%, специфичность — 94,1%. С позиции доказательной медицины обоснована необходимость профилактических мероприятий в группах риска по развитию вульвовагинитов в детском возрасте, позволяющая снизить частоту рецидивов бактериального вульвовагинита в 3 раза.

Ключевые слова: вульвовагинит, подростки, прогнозирование, профилактика, доказательная медицина

Информация о вкладе авторов: А. В. Казакова — концепция и дизайн исследования, сбор и обработка материала, статистическая обработка, написание и редактирование статьи; Е. В. Уварова — концепция и дизайн исследования, редактирование рукописи; Л. В. Лимарева — концепция и дизайн исследования, редактирование рукописи; А. А. Трупакова, А. И. Мишина — сбор и обработка материала, написание статьи.

Соблюдение этических стандартов: исследование одобрено этическим комитетом Самарского государственного медицинского университета (протокол № 5 от 20 апреля 2018 г.). Родители всех участников исследования подписали добровольное информированное согласие на анкетирование и медицинское вмешательство.

✉ **Для корреспонденции:** Анна Владимировна Казакова,
ул. Лесная, д. 31, кв. 40, г. Самара, 443110; amigo14021980@yandex.ru

Статья получена: 27.09.2019 **Статья принята к печати:** 17.10.2019 **Опубликована онлайн:** 29.10.2019

DOI: 10.24075/vrgmu.2019.070

In recent years, there have been reports of declining health statistics and the growing incidence of reproductive and gynecological disorders in children and adolescents [1–4]. Due to its high prevalence in children of all ages, genital inflammation is regarded as a clinically important problem [5–7]. Vulvovaginitis is the most common type of inflammatory genital conditions (84.2%) in girls under 10 years of age [8–10].

In young females, the main susceptibility factors include hormonal changes, lifestyle, poor intimate hygiene, and genetically determined features of immune response [11–14]. Early age of sexual initiation is one of the factors disrupting reproductive health and provoking dysbiosis of vaginal microbiota [15]. A greater threat is posed by self-medication practices and delays in seeking medical advice.

Local immunity response affects the composition of vaginal microbiota and plays a leading role in driving inflammation [16]; however, the mechanisms maintaining immune tolerance remain understudied [17,18].

Hygiene is an important aspect of sexual education. However, although hygiene practices are well-established and based on solid scientific evidence, hygiene habits differ across regions and among individuals with different social background. Unlike genetic factors that affect physical development and shape immune response, intimate hygiene and reproductive behavior can be modified to improve health. New approaches are needed to predict and prevent the risk of vulval and vaginal inflammation in young females.

The aim of this study was to develop a program for predicting the risk of vulval and vaginal inflammation in girls at different stages of sexual development. For that, we identified social, hygienic, clinical, and molecular-genetic prognostic markers of vulvovaginitis; proposed a prognostic model for predicting vulvovaginitis in girls; assessed the clinical effect of original prevention measures against vulval and vaginal inflammation in girls at different stages of sexual development.

METHODS

The study was conducted at the Outpatient Pediatric Department № 1 (Samara City Clinic № 13) from February 2013 to August 2016. The study recruited 252 healthy girls presenting for an annual check-up at the Clinic. All participants were stratified into a few groups according to their age. Age intervals reflected the stages of sexual development on the Tanner scale. Considering that the composition of vaginal microbiota in young girls is age-dependent, prognostic models were built for different sexual development stages: group 1 included 74 Tanner I girls and group 2, 178 Tanner II–V girls.

The following inclusion criteria were applied: age from 2 to 17 years, the absence of health complaints; no somatic or gynecological disorders; normal physical, psychological and sexual development.

Exclusion criteria were as follows: the use of antibacterial drugs in a month preceding the examination; acute inflammatory diseases at the time of examination and swab collection.

All girls and their mothers were interviewed using a questionnaire. Questions were asked about hygiene habits of mothers and their daughters and sexual behavior of the participants. Additionally, we studied 226 vaginal and 226 buccal swabs obtained from the girls.

Before the tests, complaints were taken, physical (height, weight, BMI) and sexual development (Tanner stage, external genital examination) was evaluated. Intimate hygiene practices were also assessed.

Swabs were collected from vaginal vestibule mucosa or the posterior fornix through hymenal rings using a standard swab kit. DNA of opportunistic microorganisms (OMs) was assayed in real-time PCR using a Femoflor-17 reagent kit (DNA-Technology; Russia) for profiling the composition of genitourinary microbiota. The following parameters were assessed: quality control of sample collection (SCQC); total bacterial mass (TBM); the presence of mollicutes (*Mycoplasma hominis, Ureaplasma spp.*), yeast (*Candida spp.*), bacteria (*Lactobacillus spp., Enterobacterium spp., Streptococcus spp., Staphylococcus spp., Gardnerella vaginalis / Prevotella bivia / Porphyromonas spp., Eubacterium spp., Sneathia spp. / Leptotrichia spp. / Fusobacterium spp., Megasphaera spp. / Veillonella spp. / Dialister spp., Lachnobacterium spp. / Clostridium spp., Mobiluncus spp. / Corinebacterium spp., Peptostreptococcus spp., Atopobium vaginae*), and pathogens (*Mycoplasma genitalium*). SCQC was valid in all cases, confirming the objectivity of the subsequent results analysis.

Considering the immune mechanisms underlying vulval and vaginal inflammation, we studied the distribution of allele and genotype frequencies for the following polymorphic variants of anti- and pro-inflammatory cytokine genes using PCR: IL1β (T-31C), IL1β (T-511C), IL1β(C-3953T), IL1β (G-1473C) in the IL1β gene; IL6 (C-174G) in the IL6 gene; TNFα (G-308A) in the TNFα gene; IL10 (G-1082A), IL10 (C-592A), IL10 (C-819T) in the IL10 gene; TGFβ1 (Arg25Pro) in the $TGF\beta_1$ gene in order to identify the role of polymorphisms of immune response genes in the development and clinical course of the pathology.

Decision trees were constructed using the classification and regression tree algorithm (CART). Briefly, each decision tree node had two children. In each step, the rule generated by the node split the dataset into two subsets: the one where the rule was satisfied and the other where it was not. The computer algorithm selected the attribute on which the node was split, determined the splitting value and decided when to stop tree bulding. The optimal rule was selected using the function for splitting quality assessment based on the Gini index [19].

The following groups of attributes were used to build our decision trees:

– information about vaginal microbiota obtained with the Femoflor kit (expressed as gram-equivalents and as percentage relative to TBM);

– results of molecular-genetic tests of polymorphic variants of genes coding for the selected cytokines;

– information about hygiene habits obtained from questionnaires (intimate washing, showering, changing underwear regularly, etc.).

Additionally, we calculated the ratio of lactobacilli (aerobes) to obligate anaerobes.

Testing the proposed recommendations on prevention

The obtained data were used to develop a set of prevention measures. To test their effect, we conducted a prospective study that enrolled 167 girls. The main group (n = 52) was given original recommendations proposed in this work; the control group (n = 115) received standard recommendations from a pediatric gynecologist. The girls were followed up for one year; then, the obtained data were statistically analyzed in compliance with the principles of evidence-based medicine [20].

Statistical analysis

The obtained data were saved to and processed in Microsoft Excel. Statistical analysis was performed using the SPSS 21 software (IBM SPSS Statistics; USA, license 20130626-3). The applied methods of descriptive statistics included calculation of the arithmetic mean and its deviation ($M \pm m$) or, in case of skewed distribution, the median and the quartile range. Information about the analyzed microorganisms was saved to a table; we specified the number of girls who had the identified species and the mean concentration of the microorganism expressed as a decadic logarithm (lg). Mean values were calculated only for the subgroup of girls who had the microorganism. For such variables as past infections, hygiene practices and genotypes, contingency tables were constructed and Pearson's chi-squared was calculated.

The quality of classification was assessed using ROC-curves and evidence-based medicine criteria: sensitivity and specificity.

RESULTS

Considering that the composition of vaginal microbiota depends on age, we built models for predicting the risk of vulvovaginitis in 2 groups of girls at different Tanner stages: group 1 (Tanner 1) and group 2 (Tanner II–V).

The prognostic model for Tanner I girls is shown in Fig. 1. The presence of the following two prognostic markers was considered a favorable risk factor: predominance of obligate anaerobes in the composition of vaginal microbiota and the polymorphic IL10 variant (C-819T) homozygous for TT. If any of these two conditions was not satisfied or lactobacilli dominated the composition of vaginal microbiota or there was at least one C allele in the IL10 gene, this led to an increased risk of vulvovaginitis in girls from group 1.

The quality of prediction was assessed by constructing a contingency table for observed and predicted outcomes (Table 1). Nine predictions were false-positive (vulvovaginitis was predicted by the model but the girl turned out to be healthy). Three predictions were false-negative. In group 1, the sensitivity of the applied method was 80%, whereas specificity — 78%.

Based on the constructed decision tree, the prediction algorithm for Tanner I girls was as follows:

1. If the proportion of aerobes was > 34%, then the risk of vulvovaginitis was estimated as probable. If the proportion of aerobes was ≤ 34%, the algorithm proceeded to step 2.

2. If locus 819 of the IL10 gene was homozygous for the TT allele, then the risk of vulvovaginitis was considered minimal. If this locus was homozygous for the C allele (the CC genotype) or heterozygous (the CT genotype), then the risk of vulvovaginitis was estimated as high.

The prognostic model for predicting the risk of vulvovaginitis in Tanner II–V girls is shown in Fig. 2. Favorable risk factors in prepubertal and pubertal girls included aerobic predominance in the composition of vaginal microbiota and the presence of the TT allele in the polymorphic IL10 gene variant (C-3953T). If any of these two conditions was not satisfied (the smaller proportion of aerobes, the presence of at least one C allele in the IL10 gene), then an increased risk of vulvovaginitis in girls from group 2 was inferred. The sensitivity of the prognostic models was 58.3%, whereas specificity, 94.1%.

The prediction algorithm for Tanner II–V girls was as follows:

1. If the aerobic content expressed as genomic equivalents was ≤ 6.15, the algorithm proceeded to step 2. If the aerobic content expressed as genomic equivalents was > 6.15, the algorithm proceeded to step 4.

2. If the IL10 (C-592A) gene was homo- or heterozygous for at least one A allele, the risk of vulvovaginitis was estimated as minimal. If the polymorphic IL10 (C-592A) gene carried the CC genotype, the algorithm proceeded to step 3.

3. If a girl showered every day, she was at minimum risk for vulvovaginitis. If showering was not regular, the risk for vulvovaginitis was estimated as high.

4. If the IL1β (C-3953T) gene had the TT genotype, the risk for vulvovaginitis was minimal. If this gene had the CT or CC genotype, we proceeded to step 3.

It is known that a substitution of the T allele for the C allele at position -3953 in the IL1β gene results in a decreased production of proinflammatory IL1β and is clinically associated with a weaker immune response to an antigen. In combination with inadequate hygiene practices, this factor can be decisive in triggering inflammation.

When the A allele is substituted for the C allele at position -592 of the IL10 gene, the production of IL10 increases. IL10 is an anti-inflammatory cytokine; its overproduction during immune response to infection can undermine the effect of immune defense mechanisms. Although IL10 overproduction is determined genetically, the decision tree demonstrates that this factor exerts its negative impact only in case of poor hygiene practices.

Summing up, the use of decision trees allowed us to create a convenient and functional prognostic model for assessing the risk of vulvovaginitis and to analyze different allele combinations and their interplay.

Based on the reliable risk factors identified by our regression model, we proposed the following prevention measures for the girls over 16 years of age at risk for vulvovaginitis.

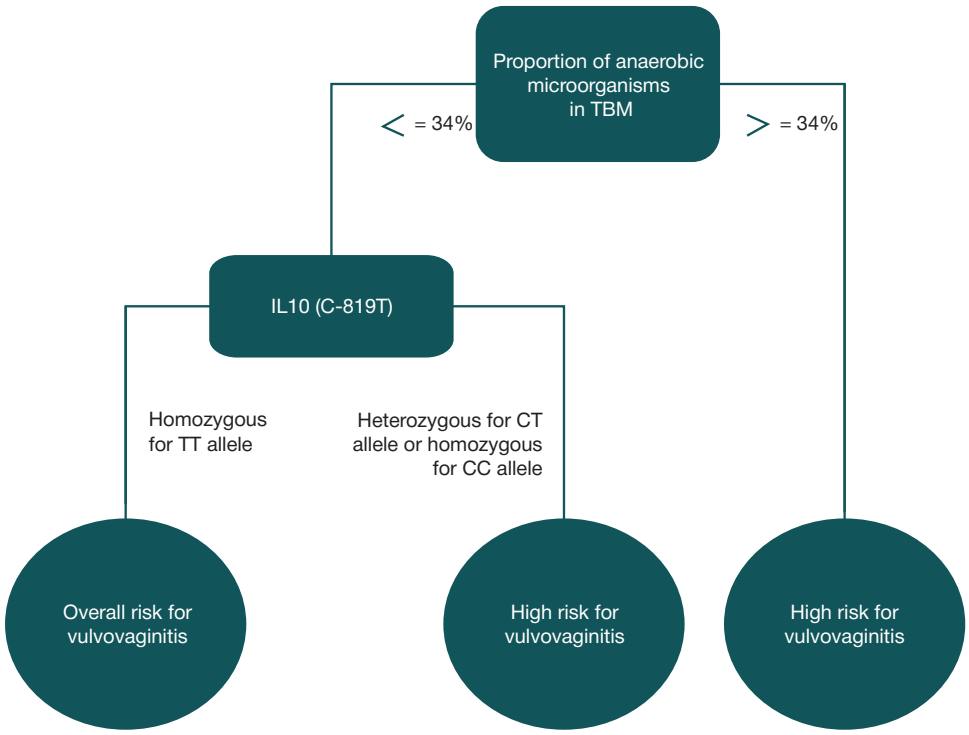

Fig. 1. The algorithm for assessing the risk of bacterial vulvovaginitis in Tanner I girls

Table 1. Quality of prediction

Observed	Predicted by the model		Total
	Healthy	Vulvovaginitis	
Healthy	32	9	41
Vulvovaginitis	3	12	15
Total	35	21	56

Tanner I girls were recommended 1) seeking medical advice with medical professionals immediately if genitourinary or ENT infections were noticed; 2) showering daily and changing underwear regularly; 3) washing the intimate area twice a day; 4) seeing a gynecologist once a year.

Tanner II–V girls were recommended 1) seeking medical advice with an allergist and regular check-ups in case of any allergies; 2) showering daily and changing underwear regularly; 3) washing the intimate area twice a day; 4) sexual initiation not earlier than 17 years; 5) safe sexual behavior: using reliable methods of contraception, sticking to one sex partner; 6) seeing a gynecologist once a year.

To assess the effect of our original prevention measures, we calculated the values for a number of quantitative indicators according to the recommendations by Kotelnikov GP and Shpigel AS [20]. A contingency table was constructed for additional prevention measures and relapses (Table 2).

Study results are shown in Tables 3 and 4. The 2 main indicators used to calculate the effect of prevention measures were relapse rates in the main (treatment) and control groups (RRM, RRC):

$$RRM = a / (a + b);$$
$$RRC = c / (c + d).$$

95% CI for RRM and RRC was calculated using the Wilson method.

RRM was 17.3% (95% CI: 9.4–29.7%); RRM, 34.8% (95% CI: 26.7–43.9%); $p = 0.035$ (Pearson's χ^2 was applied).

The difference between the relapse rates in the main and control groups was estimated using the values of relative and absolute risk reduction (RRR, ARR).

RRR represented the decrease in the relapse rate in the main group relative to the control group:

$$RRR = (RRC – RRM) / RRC.$$

ARR represented the difference between the relapse rates in the main and control groups:

$$ARR = RRC – RRM.$$

95% CI for RRR was calculated using the method proposed by M. Gardner and D. Altman; 95% CI for ARR was calculated using the method proposed by L. Bjerre and J. LeLorier [21, 22].

In this study, the relapse rate in the main group dropped by 17.5% (95% CI: 2.7–29.5%), i.e., twofold:

$$RRR = (34.8 – 17.3) / 34.8 \times 100\% = 50.2\%.$$

OR for the relapse rate with CI calculated according to J. Bland and D. Altman, was 0.39 (95% CI: 0.17–0.89).

Subsequently, we calculated the number of patients (NP) who had to follow the proposed prevention strategy in order to prevent the poor outcome in one patient. NP equals the reciprocal of ARR (if ARR is expressed as percentage, then NP=100% / ARR); its CI is reciprocals of the upper and lower limits of 95% CI: ARR.

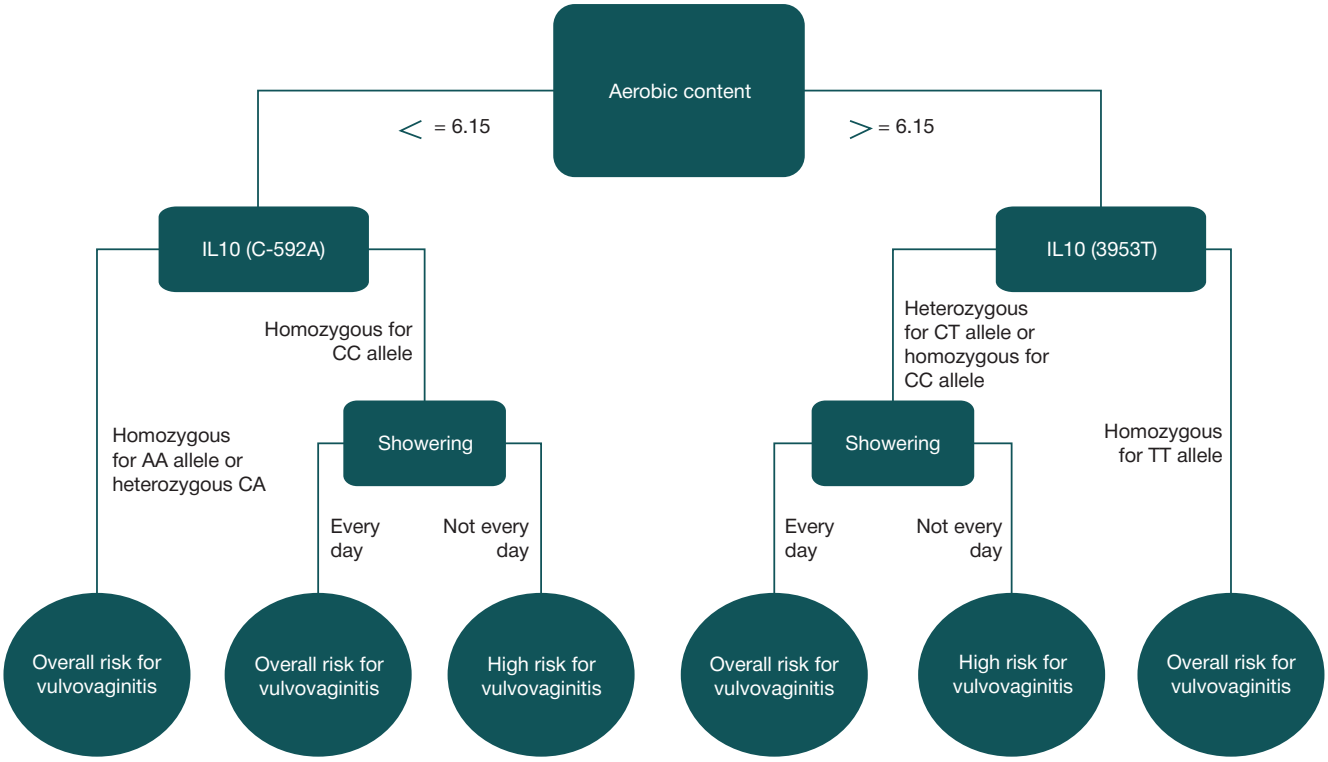

Fig. 2. The algorithm for assessing the risk of non-specific genital inflammation in Tanner II–V girls

Table 2. The contingency table

Groups	Relapse	No relapse	Total
Main group— prevention measures proposed in the study	*a*	*b*	*a* + *b*
Control group — follow-up observation	*c*	*d*	*c* + *d*
Total	*a* + *c*	*b* + *d*	*a* + *b* + *c* + *d*

Note: *a* — relapse, *b* — no relapse, *c* — relapse, *d* — no relapse.

Table 3. Outcomes of the proposed prevention measures

Groups	Effect of prevention measures		Total
	Relapse of vulvovaginitis	No relapse observed	
Main group: prevention measures applied	9	43	52
Control group: observation	40	75	115
Total	49	118	167

Table 4. Indicators of intervention effect

Indicator	Abbreviation	Value, %
Relapse rate in the main group	RRM	17.3 (9.4–29.7)
Relapse rate in the control group	RRC	34.8 (26.7–43.9)
Relative risk reduction	RRR	50.2 (5.1–73.9)
Absolute risk reduction	ARR	17.5 (2.7–29.5)
Number of patients to be treated	NP	6 (3–38)
Relative risk	RR	0.5 (0.26–0.95)
Odds ratio	OR	0.39 (0.17–0.89)
χ^2 with Yates' correction	χ^2	4.47
p	*p*	0.035

$$NP = 100\% / CAP = 100\% / 17.5\% = 6.$$

This means that if 6 girls at risk for vulvovaginitis strictly follow our recommendations, then at least one of them will not develop vulvovaginitis within a year. It should be noted that for our sample size, CI for NP is 3 to 38 individuals.

Comparison of relapse rates in the group that was given original recommendations and the statistics on the prevalence of vulvovaginitis in the population confirmed the positive effect of the proposed prevention strategy. Relapses occurred in 17.4% of the girls form the group at risk for the pathology (Clopper–Pearson 95% CI was 8.6–31.4%). In the follow-up period, 6 girls developed clinical symptoms of nonspecific vulvovaginitis; the vaginal swabs obtained from 3 of those 6 girls revealed bacterial contamination. Those figures differed significantly ($p < 0.001$) from the population data; the latter suggest that on average, relapses of lower genital tract inflammation in this age group occur in 60% of cases [23, 24].

DISCUSSION

The obtained data are consistent with the results of another study demonstrating that, as a rule, vulvovaginitis is caused by nonspecific factors and that adequate hygiene practices have the best prevention effect against bacterial vulvovaginitis [25].

The importance of good feminine hygiene products and adequate intimate hygiene practices is emphasized in another study reporting that 25% of the respondents use vaginal douching, 29% use sprays, and 19%, topical antiseptics in order to prevent STD, which increases the risk of vaginal microbiota dysbiosis [26].

A cross-sectional study conducted in Slovakia has identified the most common intimate hygiene malpractices in female adolescents and young women between 15 and 22 years of age, including total hair removal in the intimate area (95%), bad hygiene before and after intercourse (38%), wearing a damp bathing suit instead of changing it to a dry one (58.06%), wearing unsuitable underwear. Younger respondents (15 to 19 years) and women with a lower educational status had worse hygiene habits that could be associated with unawareness of the related intimate health problems [27].

The analysis of the literature on the dysbiosis of vaginal microbiota at young age reveals no consensus on the predictors of this pathology.

Studies of vaginal microbiota covering its age-related aspects are scarce and do not often account for the stage of reproductive system development a participant is undergoing at the moment.

The role of polymorphisms and the expression of cytokine genes in driving the pathology is understudied.

There is a need for a comprehensive study of endogenous (vaginal microbiota, polymorphisms of immune response genes, somatic health) and exogenous factors (behavior) contributing to and driving vulvovaginal inflammation.

CONCLUSIONS

1. The proposed models for predicting genital inflammation account for Tanner stages of sexual development and can be used in girls between 2 and 17 years of age to decide on the treatment or prevention strategy. 2. This study provides the rationale conforming with the principles of evidence-based medicine for using prevention measures in the groups at risk for vulvovaginitis at young age. These measures allow reducing the relapse rate of bacterial vulvovaginitis threefold. 3. The proposed algorithm can be further improved using modern software and the personalized approach for the identification of groups at risk.

References

1. Alvarez-Olmos MI, et al. Vaginal lactobacilli in adolescent: presence and relationship to local and systemic immunity, and to bacterial vaginosis. Sex Transm Dis. 2004; (31): 393–400.
2. Amjadi F, et al. Role of the innate immunity in female reproductive tract. Adv Biomed Res. 2014; (3): 1.
3. Attieh E, Maalouf S, Roumieh D, et al. Feminine hygiene practices among female patients and nurses in Lebanon. Reproductive Health. 2016; 13 (1): 59.
4. Beyiter I, Kavukcu S. Clinical presentation, diagnosis and treatment of vulvovaginitis in girls: a current approach and review of the literature. World J Pediatr. 2017; 13 (2): 101–5.
5. Kazakova A. V. Programma profilaktiki bakterial'nogo vul'vovaginita u devochek v zavisimosti ot stadii polovogo razvitija [dissertacija]. Samara, 2019. Russian.
6. Prilepskaya VN, Letunovskaya AB, Donnikov AE. Mikrobiocenoz vlagalishha i polimorfizm genov citokinov kak marker zdorov'ja zhenshhiny. Ginekologija. 2015; (2): 4–13. Russian.
7. Altun I, Cinar ND, Dede C. Hygiene behaviour in university students in Turkey. J Pak Med Assoc. 2013; 63 (5): 585–9.
8. Grinevich EV. Harakteristika mikrobiocenozov vlagalishha, kishechnika i mochevyvodjashhih putej pri vul'vovaginitah u devochek rannego vozrasta v zavisimosti ot razlichnyh faktorov riska [dissertacija]. Smolensk, 2005. Russian.
9. Kazakova AV, Spiridonova NV, Uvarova EV, Komarova MV, Bezrukova AA. Mnogomernyj analiz prediktorov patologicheskih vydelenij iz polovyh putej v zavisimosti ot obraza zhizni studentok. Reproduktivnoe zdorov'e detej i podrostkov. 2016; (6): 90–7. Russian.
10. Chebotareva YuYu, Kostoeva ZA, Grigorjan AA. Anatomo-funkcional'nye osobennosti reproduktivnoj sistemy pri vul'vovaginitah u chasto bolejushhih detej. Kubanskij nauchnyj medicinskij vestnik. 2013; (1): 178–81. Russian.
11. Karlsson CL, Molin G, Cilio CM, et al. The pioneer gut microbiota in human neonates vaginally born at terma pilot study. Pediatr Res. 2011; (70): 282–6.
12. Kayserova J, et al. Serum immunoglobulin free light chains in severe forms of atopic dermatitis. Clin Immunol. 2010; (71): 312–6.
13. Kestřánek J, Jílek P, Matula V, et al. Jaký je aktuální stav diagnostiky vulvovaginálního dyskomfortu v České Republice? Česká Gynekologie. 2013; 78 (6): 522–7.
14. Mitchell C, Moreira C, Fredricks D, et al. Detection of fastidious vaginal bacteria in women with HIV infection and bacterial vaginosis. Infectious Diseases in Obstetrics and Gynecology. 2009; (12) Access mode: https://www.ncbi.nlm.nih.gov/pmc/articles/PMC2777244/. (Date of access: 22.10.19).
15. Zhizhko EV, Chiganovoj SD. Molodaja sem'ja: problemy i perspektivy social'noj podderzhki. Krasnojarsk: RUMC JuO, 2011; 145 s. Russian.
16. Fischer GO. Chronic vulvitis in prepubertal girls. Aust J Dermatology. 2010; (51): 118–23.
17. Lewis WG, Robinson LS, Perry J, et al. Hydrolysis of secreted sialoglycoprotein immunoglobulin A (IgA) in ex vivo and biochemical models of bacterial vaginosis. J Biol Chem. 2012; 287 (3): 2079–89.
18. Ott MA, Ofner S, Fortenberry JD. Beyond douching: use of feminine hygiene products and STI risk among young women. J Sex Med. 2009; (6): 1335–40.
19. Kohreidze NA, Gurkin YuA, Kutusheva GF, i dr. Vul'vovaginit v rannem detstve. SPb., 2017; 23 s. Russian.
20. Zijadullaev UH. Sostojanie immuniteta pri kandidoznom vul'vovaginite u devochek podrostkov. Problemy reprodukcii. 2014; (2): 32–4. Russian.
21. Gardner MJ, Altman DG. Statistics with confidence. BMJ publications. Reprint. 1994: 51–52.
22. Bjerre LM, LeLorier J. Expressing the magnitude of adverse effects in case-control studies: “the number of patients needed to be treated for one additional patient to be harmed”. BMJ. 2000; (320): 503–6.
23. Zdravoohranenie v Rossii. 2017: Statisticheskij sb. Rosstat. Moskva, 2017; 170 s. Dostupno po ssylke: [http://www.gks.ru/free_doc/doc_2017/zdrav17.pdf]. Russian.
24. Kirillova EN, Pavlyukova SA, Akulich NS. Vul'vovaginit u detej. Medicinskij zhurnal. 2017; (2): 151–3. Russian.
25. Brabin L, Roberts SA, Fairbrother E, et al. Factors affecting vaginal pH levels among female adolescents attending genitourinary medicine clinics. Sex Transm Infect. 2005; (81): 483–7.
26. Brotman RM, Erbelding EJ, Jamshidi RM, et al. Findings associated with recurrence of bacterial vaginosis among adolescents attending sexually transmitted diseases clinics. J Pediatr Adolesc Gynecol. 2007; (20): 225–31.
27. Donders GG, et al. Vaginal cytokines in normal pregnancy. American journal of obstetrics and gynecology. 2003; (189): 1433–8.

Литература

1. Alvarez-Olmos MI, et al. Vaginal lactobacilli in adolescent: presence and relationship to local and systemic immunity, and to bacterial vaginosis. Sex Transm Dis. 2004; (31): 393–400.
2. Amjadi F, et al. Role of the innate immunity in female reproductive tract. Adv Biomed Res. 2014; (3): 1.
3. Attieh E, Maalouf S, Roumieh D, et al. Feminine hygiene practices among female patients and nurses in Lebanon. Reproductive Health. 2016; 13 (1): 59.
4. Beyiter I, Kavukcu S. Clinical presentation, diagnosis and treatment of vulvovaginitis in girls: a current approach and review of the literature. World J Pediatr. 2017; 13 (2): 101–5.
5. Казакова А. В. Программа профилактики бактериального вульвовагинита у девочек в зависимости от стадии полового развития [диссертация]. Самара, 2019.
6. Прилепская В. Н., Летуновская А. Б., Донников А. Е. Микробиоценоз влагалища и полиморфизм генов цитокинов как маркер здоровья женщины. Гинекология. 2015; (2): 4–13.
7. Altun I, Cinar ND, Dede C. Hygiene behaviour in university students in Turkey. J Pak Med Assoc. 2013; 63 (5): 585–9.
8. Гриневич Е. В. Характеристика микробиоценозов влагалища, кишечника и мочевыводящих путей при вульвовагинитах у девочек раннего возраста в зависимости от различных факторов риска [диссертация]. Смоленск, 2005.
9. Казакова А. В., Спиридонова Н. В., Уварова Е. В., Комарова М. В., Безрукова А. А. Многомерный анализ предикторов патологических выделений из половых путей в зависимости от образа жизни студенток. Репродуктивное здоровье детей и подростков. 2016; (6): 90–7.
10. Чеботарева Ю. Ю., Костоева З. А., Григорян А. А. Анатомо-функциональные особенности репродуктивной системы при вульвовагинитах у часто болеющих детей. Кубанский научный медицинский вестник. 2013; (1): 178–81.
11. Karlsson CL, Molin G, Cilio CM, et al. The pioneer gut microbiota in human neonates vaginally born at terma pilot study. Pediatr Res. 2011; (70): 282–6.
12. Kayserova J, et al. Serum immunoglobulin free light chains in severe forms of atopic dermatitis. Clin Immunol. 2010; (71): 312–6.
13. Kestřánek J, Jílek P, Matula V, et al. Jaký je aktuální stav diagnostiky vulvovaginálního dyskomfortu v České Republice? Česká Gynekologie. 2013; 78 (6): 522–7.
14. Mitchell C, Moreira C, Fredricks D, et al. Detection of fastidious vaginal bacteria in women with HIV infection and bacterial vaginosis. Infectious Diseases in Obstetrics and Gynecology. 2009; (12) Access mode: https://www.ncbi.nlm.nih.gov/pmc/articles/PMC2777244/. (Date of access: 22.10.19).
15. Жижко Е. В., Чигановой С. Д. Молодая семья: проблемы и перспективы социальной поддержки. Красноярск: РУМЦ ЮО, 2011; 145 с.
16. Fischer GO. Chronic vulvitis in prepubertal girls. Aust J Dermatology. 2010; (51): 118–23.

17. Lewis WG, Robinson LS, Perry J, et al. Hydrolysis of secreted sialoglycoprotein immunoglobulin A (IgA) in ex vivo and biochemical models of bacterial vaginosis. J Biol Chem. 2012; 287 (3): 2079–89.
18. Ott MA, Ofner S, Fortenberry JD. Beyond douching: use of feminine hygiene products and STI risk among young women. J Sex Med. 2009; (6): 1335–40.
19. Кохреидзе Н. А., Гуркин Ю. А., Кутушева Г. Ф. и др. Вульвовагинит в раннем детстве. СПб., 2017; 23 с.
20. Зиядуллаев У. Х. Состояние иммунитета при кандидозном вульвовагините у девочек подростков. Проблемы репродукции. 2014; (2): 32–4.
21. Gardner M J, Altman DG. Statistics with confidence. BMJ publications. Reprint. 1994: 51–52.
22. Bjerre LM, LeLorier J. Expressing the magnitude of adverse effects in case-control studies: “the number of patients needed to be treated for one additional patient to be harmed”. BMJ. 2000; (320): 503–6.
23. Здравоохранение в России. 2017: Статистический сб. Росстат. Москва, 2017; 170 с. Доступно по ссылке: [http://www.gks.ru/free_doc/doc_2017/zdrav17.pdf].
24. Кириллова Е. Н., Павлюкова С. А. , Акулич Н. С. Вульвовагинит у детей. Медицинский журнал. 2017; (2): 151–3.
25. Brabin L, Roberts SA, Fairbrother E, et al. Factors affecting vaginal pH levels among female adolescents attending genitourinary medicine clinics. Sex Transm Infect. 2005; (81): 483–7.
26. Brotman RM, Erbelding EJ, Jamshidi RM, et al. Findings associated with recurrence of bacterial vaginosis among adolescents attending sexually transmitted diseases clinics. J Pediatr Adolesc Gynecol. 2007; (20): 225–31.
27. Donders GG, et al. Vaginal cytokines in normal pregnancy. American journal of obstetrics and gynecology. 2003; (189): 1433–8.

PHYSIOLOGICAL MECHANISMS OF THE LOW-INTENSITY LASER RADIATION IMPACT ON THE HIGHLY QUALIFIED ATHLETES' SPECIAL PHYSICAL PERFORMANCE

Bruk TM[1], Terekhov PA[1]✉, Litvin FB[1], Verlin SV[2]

[1] Smolensk State Academy of Physical Culture, Sport and Tourism, Smolensk, Russia

[2] Rehabilitation Center of the State School of the Olympic reserve, Bronnitsy, Moscow region, Russia

In the context of strengthening the fight against doping and limiting the use of synthetic pharmaceuticals, the effective remedies to increase physical performance and accelerate the recovery of athletes are being sought. One of such remedies is exposure to low-level laser radiation (LLLR, LLLT). The study was aimed to investigate the physiological response of highly qualified female rowers' functional systems to the LLLR irradiation course. To monitor the body of athletes, we used laser Doppler flowmetry (LDF), mathematical analysis of heart rate, neuroenergy mapping, as well as pedagogical testing using the Concept 2 simulator. After irradiation of the neck in the projection of the carotid arteries with pulsed infrared LLLR, the blood perfusion rate increased by 38% ($p < 0.05$) and cell oxygen utilization rate increased by 48% ($p < 0.05$). The decrease in the hemoglobin oxygen saturation by 16% ($p < 0.05$) was also observed. Due to LLLT, the activity of the autonomous regulation mechanism increased with an increase in the total power of the heart rate variability spectrum (TP) by 41% ($p < 0.05$), and in high-frequency power (HF) by 73% ($p < 0.05$). The influence of central mechanism decreased with a decrease in amplitude mode (AMo) by 71% ($p < 0.05$), and in stress-index (SI) by 175% ($p < 0.05$). Irradiation by LLLR promoted the efficiency of oxygen delivery to certain cerebral cortex areas with the increase of SPL. After LLLT, the speed of 2000 meters distance "passing" by athletes also increased by 3.32% ($p > 0.05$). The discovered effects of LLLT allow one to expand the range of physiotherapeutic agents that enhance the special physical performance of athletes and accelerate recovery.

Keywords: LLLR (LLLT), heart rate variability, microcirculation, neuroenergy mapping, athletes, physical performance

Author contribution: Bruk TM — analysis of brain function (neuroenergy mapping), laser therapy; Terekhov PA — physical fitness assessment, statistical analysis of the results, manuscript writing; Litvin FB — study of microcirculation and heart rate variability, manuscript writing; Verlin SV — selection of study participants.

Compliance with ethical standards: the study was approved by the Local Ethics Committee of Smolensk State Academy of Physical Culture, Sport and Tourism (protocol № 67 dated September 9, 2018). Informed consent was obtained from all study participants.

✉ **Correspondence should be addressed:** Pavel A. Terekhov
Kirova, 42 A, kv. 11.04, Smolensk, 214018; terechov_86@mail.ru

Received: 30.09.2019 **Accepted:** 21.10.2019 **Published online:** 30.10.2019

DOI: 10.24075/brsmu.2019.071

ФИЗИОЛОГИЧЕСКИЕ МЕХАНИЗМЫ ВОЗДЕЙСТВИЯ НИЗКОИНТЕНСИВНОГО ЛАЗЕРНОГО ИЗЛУЧЕНИЯ НА СПЕЦИАЛЬНУЮ ФИЗИЧЕСКУЮ РАБОТОСПОСОБНОСТЬ ВЫСОКОКВАЛИФИЦИРОВАННЫХ СПОРТСМЕНОВ

Т. М. Брук[1], П. А. Терехов[1]✉, Ф. Б. Литвин[1], С. В. Верлин[2]

[1] Смоленская государственная академия физической культуры, спорта и туризма, Смоленск, Россия

[2] Медико-восстановительный центр Государственного училища олимпийского резерва, Бронницы, Московская область, Россия

В условиях ужесточения борьбы с допингом и ограничения использования синтетических фармпрепаратов ведется поиск эффективных средств для повышения физической работоспособности и ускорения восстановления спортсменов. Одним из таких средств является воздействие низкоинтенсивным лазерным излучением (НИЛИ). Целью настоящего исследования было изучение физиологического ответа функциональных систем высококвалифицированных гребцов-академистов (женщины) на курсовое воздействие НИЛИ. Для наблюдения за организмом спортсменок использовали лазерную допплеровскую флоуметрию (ЛДФ), математический анализ сердечного ритма, нейроэнергокартирование, а также педагогическое тестирование с использованием тренажера Concept 2. После освечивания шеи в области проекции сонных артерий импульсным инфракрасным НИЛИ наблюдали повышение показателя перфузии крови на 38% ($p < 0,05$), показателя утилизации кислорода клетками на 48% ($p < 0,05$), а также снижение показателя сатурации гемоглобина кислородом на 16% ($p < 0,05$). В результате применения НИЛИ происходило повышение активности автономного механизма регуляции с ростом мощности спектра колебаний ритма сердца (TP) на 41% ($p < 0,05$), мощности высокочастотных колебаний (HF) — на 73% ($p < 0,05$), росло влияние центрального механизма со снижением амплитуды моды (AMo) на 71% ($p < 0,05$), индекса напряжения (ИН) — на 175% ($p < 0,05$). Воздействие НИЛИ способствовало повышению эффективности доставки кислорода в отдельные области коры больших полушарий с ростом уровня постоянных потенциалов (УПП). Благодаря воздействию НИЛИ на 3,32% ($p > 0,05$) выросла скорость «прохождения» спортсменками дистанции 2000 м. Обнаруженные эффекты применения НИЛИ позволяют расширить спектр физиотерапевтических средств, способствующих повышению специальной физической работоспособности спортсменов и ускорению восстановления.

Ключевые слова: НИЛИ, вариабельность сердечного ритма, микроциркуляция, нейроэнергокартирование, спортсмены, работоспособность

Информация о вкладе авторов: Т. М. Брук — анализ функционального состояния мозга (нейроэнергокартирование), проведение лазерных процедур; П. А. Терехов — оценка специальной физической подготовленности, статистическая обработка результатов, подготовка рукописи; Ф. Б. Литвин — изучение процессов микрогемоциркуляции, вариабельности сердечного ритма, подготовка рукописи; С. В. Верлин — отбор участников исследования.

Соблюдение этических стандартов: исследование одобрено этическим комитетом ФГБОУ ВО «СГАФКСТ» (протокол № 67 от 9 сентября 2018 г.). Все спортсменки подписали добровольное информированное согласие на участие в исследовании.

✉ **Для корреспонденции:** Павел Александрович Терехов
ул. Кирова, д. 42 А, кв. 11.04, г. Смоленск, 214018; terechov_86@mail.ru

Статья получена: 30.09.2019 **Статья принята к печати:** 21.10.2019 **Опубликована онлайн:** 30.10.2019

DOI: 10.24075/vrgmu.2019.071

To achieve record levels, highly qualified athletes work at the limit of the body's functional capabilities, which often lead to homeostasis impairment. One of the ways to preserve homeostasis is to expand the adaptive boundaries of organs and systems that provide the response to training and competitive physical loads, which ensures the achievement of an adaptive result [1].

According to literature data, as a result of low-level laser radiation (LLLR) absorption, energy is transformed into various biological reactions, which trigger the processes of self-regulation and self-healing of impaired homeostasis [2–5]. In particular, under the influence of LLLT, antioxidant defense enzymes are activated, cell metabolism is enhanced, biomembranes are stabilized. The effect of LLLR on the elasticity of erythrocyte membranes facilitates the red blood cells penetration into the capillaries of the microvascular bed, and the stimulation of the energy metabolism aerobic phase involving the incompletely deoxidized glycolysis metabolites and lipid oxidation products as well as the indirect membrane mechanism, leads to oxygen saturation of the venous blood and improves microcirculation [6]. At the same time, the influence of LLLT on microcirculatory-tissue relations remains understudied [7].

Laser therapy is an essential component of modern biomedical support of the elite sport at almost all stages of athletes' training. Comprehensive monitoring of the athlet's body using a complex of informative and reproducible methods for rapid assessment of body state (biochemical and hematological indicators, laser Doppler flowmetry (LDF) data, heart rate variability (HRV), neuroenergy mapping (NEM) data, etc.) allows one to correct the athlete's homeostasis for adequate formation of fatigue not going beyond the pathology side and for acceleration of the recovery processes.

Researchers revealed the ability of LLLT to improve the physical performance of athletes of various qualifications involved in different sports. LLLR irradiation of biologically active points leaded to an increase in the aerobic performance indicator in 80% of football players with a subsequent increase in the amount of mechanical work performed [8]. A significant increase in the absolute and relative values of PWC170 after LLLT was obtained in athletes of cyclic sports. Short-term exposure to LLLR did not cause significant changes in the biochemical composition of the blood, but increased the activity of parasympathetic influences on the heart rhythm [9, 10]. The humoral-hormonal status of the athletes' body changed due to LLLT. In particular, an increase in the concentration of beta-endorphin, glucocorticoids, triiodothyronine, thyroxine in game sports athletes and cross-country skiers was revealed [11, 12].

The systemic mechanisms that provide the effects of laser stimulation as a part of the complex training program of hockey players are described. Positive structural and functional changes in the body of hockey players and swimmers lead to a marked improvement of the physical fitness [13, 14].

The study was aimed to investigate the physiological response of highly qualified female rowers' functional systems to the LLLR irradiation course in the special preparatory period of the annual cycle of sports training. The objectives of the study were as follows: assessment of the LLLT effect on the microcirculation system, detection of the heart rate regulation changes, investigation of the effect on the metabolic activity of the cerebral cortex neurons, evaluation of the highly qualified athletes' physical performance.

METHODS

The study was conducted in October 2018. Twenty four highly qualified female rowers studying at the State School of the Olympic reserve (Bronnitsy, Moscow region) participated in the study which was carried out at the training center.

The participants were divided into two groups: treatment group (TG) and control group (CG). The treatment group included 12 athletes. Inclusion criteria: Master of Sports (MS) qualification level, membership in the Moscow Region combined team. Exclusion criteria: low qualification of athletes, the acute phase of the disease. The control group included 12 athletes (MS) not qualified for the combined team. Representatives of both groups used the single training program.

The study included two phases. At the first phase of the study, we evaluated the functional state of individual body systems and the physical fitness of the TG and CG athletes before LLLT. Then, the athletes of both groups in their weekly training cycle performed a special training program to prepare for the competition season.

The TG athletes were exposed to LLLT during 7 days in the morning before training. Their necks were irradiated neck symmetrically on both sides in the region of the carotid triangle using Uzor-A-2K 2-channel therapeutic laser unit (Voskhod; Russia). The laser radiation wavelength was 0.89 ± 0.02 μm; pulse mode; pulse repetition frequency 1500 Hz; 10 minute exposure time. The CG athletes were through the fake LLLT without turning on the emitting heads of the Uzor-A-2K unit. After laser therapy the studied indices were registered again.

The athletes' heart rate variability (HRV) was evaluated using the Varicard 2.51 complex (Ramena; Russia). The recording of cardiointervalogram lasting 5 minutes was carried out using the standard method in a sitting position. The following HRV parameters were evaluated: heart rate (HR), indicators characterizing the activity of autonomous (total power of the heart rate variability spectrum (TP), high-frequency power (HF) and central (low-frequency power (LF), very-low-frequency power (VLF), amplitude mode (AMo) regulatory mechanisms, indicator of the prevalence of central regulatory mechanisms over autonomous (stress-index, SI).

The LAKK-M (Lazma; Russia) multifunctional laser diagnostic system was used as a recording instrument for studying microcirculation. After that the microcirculation parameter (PM) was analyzed in perfusion units (PU). The time-frequency analysis of blood flow oscillations was performed using the wavelet analysis LDF3.0.2.384 software (Lazma; Russia). The active mechanism contribution to the formation of vascular tone was estimated by the amplitude of sympathetic (As), myogenic (Am) and endothelial (Ae) oscillations (PU). The contribution of passive mechanism was estimated by the amplitude of respiratory (Ar) and cardiac (Ac) oscillations (PU). The optical tissue oximetry method was used for evaluation of blood oxygen saturation level (SO_2, %) and specific oxygen consumption rate (U, p.d.u.). The steady potentials level (SPL) parameter was used for assessment of the brain tissue metabolic activity in the frontal, parietal, occipital, right and left temporal lobes.

For topographic mapping of brain electrical activity the 5-channel Neuro-KM complex was used (STATOKIN; Russia) according to standard method [15]. The time of 2000 meter distance "passing" using the Concept 2 Model D (PM5; China) rowing simulator was the indicator of special physical fitness. The test was performed indoors, in the gym with constant temperature and illumination intensity.

Statistical analysis of the results was carried out using the IBM SPSS Statistics 19 software for Windows (StatSoft, Inc.; USA). The Mann–Whitney U-test was used to compare the studied indicators in the TG and CG athletes. To compare the indicators in TG athletes and CG athletes who experienced the imaginary effect of LLLT, as well as with the indicators of athletes after laser therapy, the Wilcoxon signed-rank test was used. The differences were considered significant at $p < 0.05$.

RESULTS

Percutaneous laser stimulation combined with standard training loads promotes the expansion of the body functional capabilities at various organization levels (from cellular to systemic). We studied the dynamics of the processes that occurred in the microvascular beds after the course of LLLT.

In the TG athletes, the perfusion level significantly increased by 38% compared to baseline ($p < 0.05$). At the same time, in the CG athletes the microcirculation parameter increased by 5% ($p > 0.05$) (Table 1). The 14% decrease in SO_2 in the microvascular beds together with a tendency to SO_2 increase by 2% in the CG was the evidence of oxygen metabolism biostimulation in the TG athletes due to LLLT ($p < 0.05$). A significant increase by 49% in the estimated rate of oxygen utilization by tissues was an indicator of oxygen diffusion from blood into the tissue ($p < 0.05$). In the CG athletes the same indicator demonstrated almost no growth (1%, $p > 0.05$).

In our study, the myocyte tone decreased by 53% ($p < 0.05$) in the TG athletes, thereby increasing the lumen of the microvascular bed vessels. In addition, arterioles widened the lumen due to the decrease in the activity of the autonomic nervous system sympathetic nerves, the ends of which innervate smooth muscle cells of the blood vessel wall middle layer. According to the wavelet analysis, the indicator of sympathetic tone was reduced by 40% ($p < 0.05$). As a result of LLLT, the throughput of the microvascular bed exchange link increased due to vasodilation of microvessels of various diameters.

At the autonomic nervous system (ANS) level, the course of LLLT reduced the activity of the sympathetic region, while increasing the effect of the ANS parasympathetic region on the heart, which provided trophotropic recovery effect (Table 2). As a result, stress-index reduced by 174%, AMo reduced by 48% ($p < 0.05$). The TP index significantly increased by 41%. Certain spectrum parameters increased as well (LF by 121% and HF by 73%, $p < 0.05$). Noteworthy is the 75% increase in the VLF index, which reflects the function of cortical-humoral centers.

Without physiotherapy, during training in the CG athletes, sympathetic influences maintained high activity with a tendency to reduce the effect of the vagus nerve on the heart rhythm. High sympathoadrenal system activity promoted energy deficiency. In TG athletes, during the recovery period between training sessions, tissue anabolism increased due to LLLT, thus providing high functional readiness of the body for training activities. At the same time, increased catabolism maintained in the CG athletes caused the fatigue accumulation due to the under-recovery of the body after another training session.

LLLT indirectly stimulates functional adaptive changes in the cerebral cortex neurons. After the course of LLLT the TG athletes demonstrated enchanced metabolic activity of brain tissue in the studied areas, which was evidenced by the growth of steady potential level (SPL) value. Compared to baseline

Table 1. Blood microcirculation in highly qualified female rowers at various stages of the study (M ± *m*)

№	Index	Group	Study phase		$p < 0.05$
			I	II	
1	PM, PU	TG	12.92 ± 1.61	17.86 ± 2.05	*
		CG	11.50 ± 1.34	12.07 ± 1.80	
		p	> 0.05	**< 0.05	
2	SO_2. %	TG	80.2 ± 4.04	69.1 ± 3.72	*
		CG	81.2 ± 4.56	82.9 ± 5.17	
		p	> 0.05	**< 0.05	
3	U, p.d.u.	TG	1.87 ± 0.10	2.79 ± 0.16	*
		CG	1.68 ± 0.08	1.70 ± 0.12	
		p	> 0.05	**< 0.05	
4	Ac, PU	TG	13.25 ± 1.84	18.01 ± 2.59	*
		CG	15.38 ± 2.34	13.79 ± 1.83	
		p	> 0.05	> 0.05	
5	Ar, PU	TG	20.06 ± 2.93	22.57 ± 3.12	
		CG	17.84 ± 2.50	23.19 ± 4.01	
		p	> 0.05	> 0.05	
6	Am, PU	TG	25.70 ± 3.10	39.41 ± 4.80	*
		CG	26.24 ± 4.42	27.11 ± 3.86	
		p	> 0.05	**< 0.05	
7	As, PU	TG	31.93 ± 2.72	44.69 ± 4.90	*
		CG	29.13 ± 3.15	30.42 ± 3.16	
		p	> 0.05	**< 0.05	
8	Ae, PU	TG	35.78 ± 4.96	58.00 ± 5.70	*
		CG	30.85 ± 3.75	33.55 ± 4.28	
		p	> 0.05	**< 0.05	

Note: PM — microcirculation parameter; SO_2 — blood oxygen saturation in skin tissue; U — oxygen consumption; Ac — cardiac PM oscillations; Ar — respiratory PM oscillations; Am — myogenic PM oscillations; As — sympathetic PM oscillations; Ae — endothelial PM oscillations; ** — differences between groups; * — intragroup differences; $p < 0.05$.

(Table 3), there was an increase in the SCP indicator by 94% in the frontal lobe, by 109% in the parietal lobe, by 33% in the occipital lobe and 29% in the left temporal lobe ($p < 0.05$).

The steady potential values after LLLT were distributed according to the dome-shaped curve principle (Table 3). In the CG athletes, maximum SPL values were registered in occipital (Oz) and left temporal (Ts) lobes. Thus, the dome-shaped distribution of energy consumption by the brain was violated, i.e. some deformation occured.

In the CG rowers, the SPL value tended to increase during the study, the differences were not significant.

Thus, the energy metabolism of neurons in the studied regions of cerebral cortex increased after the course of LLLT.

For correct assessment of the effectiveness of the LLLT use as a remedy for recovery it is advisable to evaluate the physical fitness level. In our study we evaluated the physical fitness level using testing with the Concept 2 rowing simulator. The time needed by the highly qualified female rowers to "pass" the 2000 meters distance at various phases of the study is presented in Table 4. At the first phase (baseline) no significant differences between two groups were revealed. The CG athletes "passed" the distance in 456.55 ± 3.55 s, and the TG rowers "passed" the distance in 454.07 ± 2.43 s ($p > 0.05$).

The course of LLLT stimulated the body of the TG athletes increasing the speed of "passing" the 2000 meter distance up to 435.63 ± 2.34 s, which was 3.32% less than baseline ($p < 0.01$). In the CG rowers, the time needed for "passing" the distance remained almost unchanged (453.02 ± 3.34 s) ($p > 0.05$). Thus, combined with the standard training process, the course of LLLT leaded to an increase in the special physical performance of female rowers during the special preparatory period of the sports training annual cycle.

DISCUSSION

The analysis of the obtained data demonstrated that the course of LLLT improved the microhemocirculation system function. We detected a significant perfusion increase, indicating an enchancement of metabolic activity at the cellular and tissue levels. An increase in the microcirculation intensity is associated with vasodilation, regulation in the microcirculation system is provided by external and internal mechanisms [16–18].

Of the internal mechanisms, the maximum contribution to the increase of the microvascular bed vessels capacity is provided by the endothelial component. Endotheliocytes take part in the formation of the vasodilation response which leads to the reduction of the microvascular tone by 62% ($p < 0.05$). The trigger stimulus arising in response to LLLT is the release of vasodilator, nitric oxide (NO) by Ca^{2+}-dependent endothelial cells, which is a precursor of the endothelium-derived relaxing factor (EDRF) [19]. Myogenic vasodilation is due to a decrease in the smooth muscle cells tone of the vascular wall.

In smooth muscle cells, LLLT leads to an increase in the level of intracellular cAMP in the cytosol, leading to activation of calcium ATPase, a decrease in calcium ions level in the cytoplasm, and relaxation of vascular smooth muscle cells [20].

The pronounced effect of laser photostimulation is associated with the effect of low-intensity radiation on

Table 2. Heart rate variability in highly qualified female rowers at various stages of the study (M ± *m*)

№	Index	Group	Study phase		$p < 0.05$
			I	II	
1	HR, bpm	TG	75.66 ± 3.20	66.94 ± 2.04	*
		CG	77.17 ± 3.18	75.67 ± 3.25	
		p	> 0.05	**< 0.05	
2	AMo, %	TG	40.10 ± 3.55	26.52 ± 2.41	*
		CG	37.92 ± 0.91	38.55 ± 0.88	
		p	> 0.05	**< 0.05	
3	SI, p.d.u.	TG	167.02 ± 19.53	60.73 ± 6.38	*
		CG	126.27 ± 13.87	123.94 ± 13.64	
		p	> 0.05	**< 0.05	
4	TP, ms^2	TG	3793.11 ± 522.24	5340.14 ± 701.02*	*
		CG	1564.17 ± 209.46	1598.62 ± 213.95	
		p	**< 0.05	**< 0.05	
5	HF, ms^2	TG	967.95 ± 130.74	1671.85 ± 175.12	*
		CG	877.50 ± 120.29	581.31 ± 70.37	
		p	> 0.05	**< 0.05	
6	LF, ms^2	TG	889.65 ± 153.29	1965.54 ± 233.56	*
		CG	473.67 ± 50.07	477.00 ± 50.29	
		p	> 0.05	**< 0.05	
7	VLF, ms^2	TG	967.75 ± 150.62	1693.76 ± 195.17	*
		CG	519.50 ± 79.60	426.57 ± 61.58	
		p	> 0.05	**< 0.05	

Note: HR — heart rate; AMo — amplitude mode; SI — stress index; TP — total power of the heart rate variability spectrum; HF — high-frequency power; LF — low-frequency power; VLF — very-low-frequency power; ** — differences between groups; * — intragroup differences; $p < 0.05$.

metabolism. Oxidation of energy materials (glucose, pyruvate, lactate) increases, leading to improvement of microcirculation and oxygen utilization in tissues [21]. According to the data obtained, the mixed blood hemoglobin saturation with oxygen of the microvascular bed decreases, the specific oxygen consumption of tissues increases, which facilitate metabolism and provide energy production in the form of ATP in the cells [22]. An increase in the cells functional activity occurs primarily due to calcium-dependent increase in the redox potential of mitochondria, an increase in their functional activity, and ATP synthesis [23–26]. In mitochondria, LLLT accelerates the electron transfer along the respiratory pathway [26].

According to PK Anokhin's functional systems theory, structural and functional components of different level and localization are involved in the implementation of the adaptive effect by the organism. Local improvement of homeostasis at the tissue microcirculation level is a component of the vegetative balance restructuring at the system level [27]. Under the influence of high-intensity physical activity, the optimal ratio between the sympathetic and parasympathetic ANS links is violated in favor of the predominance of sympathicotonia, reflecting the imbalance of the reciprocal regulatory effects of the ANS on the athlete's cardiac system. In such conditions, a pronounced tension of the compensatory mechanisms of the athlete's cardiovascular system is observed, which is associated with distress [28].

It was found that LLLT changes the activity of the neural pathways involved in the regulation of cardiac activity. Some authors note that LLLT activates the calcium-dependent mechanisms [29]. Calcium is an intracellular mediator of a number of hormones, primarily mediators of CNS and ANS [30], suggesting the involvement of laser-induced effects in neurohumoral regulation. At the end of the laser therapy course, the activity of the ANS sympathetic division decreases, the contribution of the parasympathetic division increases, and the total intensity of regulatory processes decreases. In general, LLLT promotes the deployment of trophotropic processes aimed at preserving energy and plastic resources.

It is well known that sports activity gives results only when the athlete's skill is refined to automatism, that is, with minimal participation from the central regulatory systems. A system with relatively autonomous links, due to the independence of its elements, is more flexible, which facilitates its adaptation to changing environmental conditions, including adaptation to sports activity [31]. An increase in the number of the sinus node degrees of freedom helps the body to achieve a functional optimum to cope the load. As a result, SI reduces by 174% ($p < 0.05$). The spectral parameters dynamics indicates a transition to a higher level of adaptive capabilities ensuring the athlete's body resistance to training loads. Thus, the growth rate of the activity of the autonomous heart rhythm control (HF) pathway increases by 73%, and of the central (LF) by 121%. At the same time, the contribution of cortical-humoral control centers (VLF) is enhanced by 75% against the background of bradycardia. Such a spectrogram reflects the high functional capabilities of the athlete's body [32].

An increase in the functional reserve of the body after a course of LLLT has been noted earlier [33–34]. Laser radiation regulates restoration of the vegetative balance and restrains the activity of the sympathoadrenal system [35]. The evidence was obtained of the relationship between the increased relative power of a heart rhythm spectrum in the VLF frequency range with a change in the frequency and time parameters of the brain rhythmic activity [36]. Rhythmic activity was detected in the frontal, parietal and occipital lobes of the brain.

Table 3. Steady potentials level (mV) in certain areas of cerebral cortex of highly qualified female rowers at various stages of the study (M ± *m*)

№	Index	Group	Study phase		$p < 0.05$
			I	II	
1	Frontal lobe (Fz)	TG	7.129 ± 0.384	13.851 ± 0.531	*
		CG	5.214 ± 0.312	5.915 ± 0.334	
		p	> 0.05	**< 0.05	
2	Parietal lobe (Cz)	TG	7.277 ± 0.390	15.239 ± 0.745	*
		CG	7.315 ± 0.411	7.854 ± 0.425	
		p	**< 0.05	> 0.05	
3	Occipital lobe (Oz)	TG	9.724 ± 0.404	12.954 ± 0.525	*
		CG	8.057 ± 0.354	8.948 ± 0.477	
		p	> 0.05	> 0.05	
4	Left temporal lobe (Ts)	TG	10.121 ± 0.334	13.063 ± 0.526	*
		CG	10.289 ± 0.351	11.973 ± 0.382	
		p	> 0.05	> 0.05	

Note: TG — treatment group; CG — control group; ** — differences between groups; * — intragroup differences; $p < 0.05$.

Table 4. Time of 2000 meter distance "passing" using the Concept 2 simulator by highly qualified female rowers at various stages of the study (M ± *m*)

№	Index	Group	Study phase		$p < 0.05$
			I	II	
1	Time of 2000 meter distance "passing" using the Concept 2 simulator, s	TG	454.07 ± 2.43	435.63 ± 2.34	*
		CG	456.55 ± 3.55	453.02 ± 3.34	
		p	> 0.05	**< 0.01	

Note: TG — treatment group; CG — control group; ** — differences between groups; * — intragroup differences; $p < 0.05$.

Some researchers suggest that normal energy exchange is mainly characterized by the dome-shaped curve, in which the maximum potential values are recorded in the central lead (Cz) and gradually decrease to the periphery [37]. Obviously, an SPL shift in the occipital and left temporal lobes may be associated with an increase in the functional activity of nonspecific reticular-limbic-cortical neural pathways [38].

An imbalance of regulatory influences from the higher nervous activity, depending on the brain and its cortex, leads to a violation of the speed of conditioned reflex reactions, a violation of the interaction between the first and second signaling systems, accompanied by emotional and behavioral deviations [39]. However, the adaptation mechanisms of athlete's cortical neurons under the influence of extremely high physical activity remain understudied. The results of our study on the metabolic activity of neurons in certain areas of the cerebral cortex after the course of LLLT demonstrate an improvement in the steady potential level by 1.3–2 times.

The structural and functional adaptation changes in the body arising under the influence of LLLT promote the improvement of physical performance and physical fitness of highly qualified rowers. The interaction of low-energy laser radiation with the body allows one to create a highly effective method of using laser therapeutic units in a set of remedies for improvement of special physical performance, physical fitness and overall athletic performance of athletes [40].

CONCLUSION

Our study results demonstrated that exposure to LLLR improved the functional state of the athlete's body and increased the effectiveness of sports training at the preparatory stage. The systemic response to LLLT was associated with perfusion increase in the exchange link of microvascular bed, facilitation of the diffusion of oxygen from blood into tissues and an increase in the efficiency of oxygen consumption in the cell. To a large extent, additional influx of blood from the main vessels ensured the microcirculation increase. After the course of LLLT, the increase of metabolic activity of neurons in certain areas of the cerebral cortex was observed. Thus, the adaptive stability of the body increase due to laser therapy, its functional capabilities expand, which helps to improve the athletes' special physical performance and accelerate the recovery process.

References

1. Anokhin PK. Printsipial'nye voprosy obshchey teorii funktsional'nykh sistem. Printsipy sistemnoy organizatsii funktsiy. M.: Nauka», 1973; p. 5–61.
2. Kuznetsova TN, Pavlov SE. Metodika primeneniya fizioterapevticheskikh sredstv (nizkoenergeticheskikh IK-lazerov) v trenirovochnom protsesse plovtsov. Metodicheskaya razrabotka dlya prepodavateley, aspirantov i studentov RGAFK. M.: RGAFK, 1997; 52 p.
3. Dorovskikh VA, Borodin EA, Borodina GP et al. Vliyanie nizkoenergeticheskikh lazerov na svobodnoradikal'noe okislenie glyukozo-6-fosfat degidrogenazy i katalazy eritrotsitov. V sbornike: Materialy Mezhdunarodnogo kongressa "Lazer i zdorov'e–99"; Moskva, 1999; 435–6.
4. Kozel AI, Popov GK. Mekhanizm deystviya lazernogo oblucheniya na tkanevom i kletochnom urovne. Vestnik RAMN. 2000; 2: 41–3.
5. Ulashchik VS. Analiz mekhanizmov pervichnogo deystviya nizkointensivnogo lazernogo izlucheniya na organizm. Zdravookhranenie (Minsk). 2016; 6: 41–51.
6. Potemkin LA. Mediko-biologicheskoe obespechenie i kvantovaya meditsina sporta vysshikh dostizheniy. M.: Izd-vo ZAO "MILTA-PKP GIT", 2001; 135 p.
7. Krupatkin AI, Sidorov VV. Funktsional'naya diagnostika sostoyaniya mikrotsirkulyatorno-tkanevykh sistem: Kolebaniya, informatsiya, nelineynost'. Rukovodstvo dlya vrachey. M.: LIBROKOM, 2014; 498 p.
8. Bogoslova TV. Vliyanie nizkointensivnogo lazernogo izlucheniya na fizicheskuyu rabotosposobnost' studentov instituta fizicheskoy kul'tury [dissertatsiya]. Yaroslavl', 2004.
9. Osipova NV. Sravnitel'naya kharakteristika vliyaniya nizkointensivnogo lazernogo izlucheniya na uroven' fizicheskoy rabotosposobnosti studentov razlichnykh spetsializatsiy sportivnogo vuza [dissertatsiya]. SPb., 2008.
10. Prokopyuk ZN. Ustoychivost' organizma sportsmenov k gipoksii i ee korrektsiya nizkointensivnym lazernym vozdeystviem [dissertatsiya]. Smolensk, 2010.
11. Lifke MV. Dinamika gormonal'nogo statusa sportsmenov razlichnoy kvalifikatsii, vypolnyayushchikh fizicheskuyu nagruzku umerennoy moshchnosti na fone lazernogo vozdeystviya [dissertatsiya]. Kursk, 2009.
12. Volkova AA. Vliyanie nizkointensivnogo lazernogo izlucheniya na funktsional'noe sostoyanie organizma lyzhnikov-gonshchikov, [dissertatsiya]. Smolensk, 2011.
13. Pavlov SE., Razumov AN, Pavlov AS. Laser stimulation in medical and biological provision of qualified sportsmen training. Moscow: Publishing house "Sport", 2017; 536 p.
14. Pavlov SE, Pavlov AS, Petrov AA. Osobennosti dinamiki chrednegruppovykh pokazateley dispersionnykh kharakteristik funktsionirovaniya miokarda khokkeistov, ispol'zovavshikh v predstartovoy podgotovke metod lazernoy stimulyatsii sportivnoy rabotosposobnosti. V sbornike: Olimpiyskiy byulleten' № 15, sost. Mel'nikova NYu, Treskin AV, Leonteva NS, Nikiforova AYu; M.: Izd-vo ZAO "Olimpiyskaya panorama", 2014; 247–51.
15. Fokin VF, Ponomareva NV, Kuntsevich GI. Elektrofiziologicheskie korrelyaty skorosti dvizheniya krovi po sredney mozgovoy arterii zdorovogo cheloveka. Vestnik RAMN. 2013; (10): 57–60.
16. Bollinger A. Is high–frequency flux motion due to respiration or to vasomotion activity? In: A. Bollinger et al. Vasomotion and flow motion. Prog Appl Microcirculation. Basel, Karger. 1993; 20: 52–8.
17. Fagrell B. Problems using laser Doppler on the skin in clinical practice. Laser Doppler.– London – Los Angeles – Nicosia: Med – Orion Rublishing Company. 1994; 49–54.
18. Fedorovich AA. VEB-kapillyaroskopiya — novye vozmozhnosti monitorirovaniya kapillyarnogo krovotoka v kozhe cheloveka. V sbornike: Materialy XII mezhdunarodnoy nauchnoy konferentsii "Mikrotsirkulyatsiya i gemoreologiya"; 01–03 iyulya 2019 g.; Yaroslavl': Kantsler 2019: 11.
19. Murrey RK et al. Harper's Biochemistry. Appleton & Lange, 1996; 700 p.
20. Daniolos A, Lerner AB, Lerner MR. Action of light on frog pigment cells in culture. Rigment Cell Res. 1990; 3(1): 38–43.
21. Tambovskiy AN, Sidorenko TA. Nekotorye rezul'taty primeneniya vnetrenirovochnogo sredstva v protsesse podgotovki grebtsov. Uchenye zapiski universiteta imeni P.F. Lesgafta. 2015; 5 (123): 182–85.
22. Karu TY. Pervichnye i vtorichnye kletochnye mekhanizmy lazernoy terapii. V knige: Moskvin SV, Buylin VA, redaktory. Nizkointensivnaya lazernaya terapiya. M.: Tekhnika, 2000; p. 71–94.
23. Maltsev AP. Mekhanizmy deystviya lazernogo izlucheniya na prokarioticheskie kletki. Mezhdunarodnyy studencheskiy nauchnyy vestnik. 2016; (6): 23.
24. Filippin L, Magalhães PJ, Di Benedetto G et al. Stable interactions between mitochondria and endoplasmic reticulum allow rapid accumulation of calcium in a subpopulation of mitochondria. J Biol Chem. 2003; 278 (40): 39224–34.

25. Schaffer M, Sroka R, Fuchs C et al. Biomodulative effects induced by 805 nm laser light irradiation of normal and tumor cells. Journal of Photochemistry and Photobiology B: Biology. 1997; 40 (3): 253–57.
26. Eliseenko VI. Mekhanizmy vzaimodeystviya nizkoenergeticheskogo lazernogo izlucheniya IK-spektra s biologicheskimi tkanyami V sbornike: Lazery i aeroiony v meditsine pod red. Evstigneeva AR, Kaplana MA; Kaluga–Obninsk, 1997: 71–2.
27. Krupatkin AI. Neinvazivnaya otsenka tkanevogo dykhaniya u cheloveka s ispol'zovaniem veyvlet-analiza kolebaniy saturatsii krovi kislorodom i krovotoka v mikrososudakh kozhi. Fiziologiya cheloveka. 2012; 38 (4): 67–73.
28. Gavrilova EA, Larintseva OS. Faktory riska vnezapnoy serdechnoy smerti sportsmenov na raznykh etapakh sportivnoy podgotovki po dannym kardiologicheskogo obsledovaniya. Sportivnaya meditsina: nauka i praktika. 2018; 2: 33–6.
29. Moskvin SV, Fedorova TA, Foteeva TS. Plazmaferez i lazernoe osvechivanie krovi. M.-Tver': OOO «Izd-vo «Triada», 2018; 416 p.
30. Grenner D. Gormony, reguliruyushchie metabolizm kal'tsiya. V knige: R Marri, D Grenner et al, redaktory. Biokhimiya cheloveka, tom 2. M.: Mir, 1993; p. 193–204.
31. Bayevsky RM. Cybernetic analysis of heart rate control processes. Actual problems of physiology and pathology of blood circulation. Moscow: Medicine, 1976; 161.
32. Zhemaytite DI. Vegetativnaya reaktsiya sinusovogo uzla serdtsa i zdorovykh i bol'nykh. Analiz serdechnogo ritma. Vil'nyus: Mosklas, 1982; p. 522.
33. Bruk TM, Terekhov PA, Osipova NV, Zyukin AV. Effektivnost' vozdeystviya kompleksnogo primeneniya fizicheskikh i ergogennykh sredstv na pokazateli spetsial'noy fizicheskoy podgotovlennosti i anaerobnoy rabotosposobnosti vysokokvalifitsirovannykh sportsmenov. Vestnik Rossiyskoy voenno-meditsinskoy akademii. 2019; 1 (65): 113–9.
34. Tambovskiy AN. Sidorenko TA, Yurev YuN, Shurmanov EG. Vliyanie kompleksa fizioterapevticheskikh sredstv na organizm sportsmenov. Uchenye zapiski universiteta imeni PF Lesgafta. 2015; (5): 123.
35. Elizarov NA. Adaptatsionnaya kardioprotektsiya fizicheskimi faktorami v lechenii i profilaktike ishemicheskoy bolezni serdtsa [dissertatsiya]. M., 2007.
36. Eremeeva OV. Physiological features of the effects of biofeedback of brain potentials in athletes with dominance of metabolic heart rate modulator [dissertation]. Arkhangelsk, 2012.
37. Jo H-G, Schmitd S, Inacker E, Markowiak M, Hinterberger Th. Meditation and attention: A controlled study on long-term meditators in behavioral performance and event-related potentials of attentional control. International Journal of Psychophysiology. 2016; 99: 33–9.
38. Muller TA, Shilov SN. Osobennosti urovnya aktivatsii lobnoy kory i neyrometabolizma golovnogo mozga u detey 7–10 let s SDVG. Vestnik Novosibirskogo gosudarstvennogo pedagogicheskogo universiteta. 2017; 7 (5): 193–206.
39. Moskvin SV, Kochetkov AV. Effektivnye metodiki lazernoy terapii. M.–Tver': Triada, 2016; 80 p.
40. Pavlov SE, Pavlova TN. Tekhnologiya podgotovki sportsmenov. MO, Shchelkovo: Izdatel' Markhotin PYu, 2011; 344 p.

Литература

1. Анохин П. К. Принципиальные вопросы общей теории функциональных систем. Принципы системной организации функций. М.: Наука, 1973; с. 5–61.
2. Кузнецова Т. Н., Павлов С. Е. Методика применения физиотерапевтических средств (низкоэнергетических ИК-лазеров) в тренировочном процессе пловцов. Методическая разработка для преподавателей, аспирантов и студентов РГАФК. М.: РГАФК, 1997; 52 с.
3. Доровских В. А., Бородин Е. А., Бородина Г. П. и др. Влияние низкоэнергетических лазеров на свободнорадикальное окисление глюкозо-6-фосфат дегидрогеназы и каталазы эритроцитов. В сборнике: Материалы Международного конгресса «Лазер и здоровье–99»; Москва, 1999; 435–436.
4. Козель А. И., Попов Г. К. Механизм действия лазерного облучения на тканевом и клеточном уровне. Вестник РАМН. 2000; 2: 41–3.
5. Улащик В. С. Анализ механизмов первичного действия низкоинтенсивного лазерного излучения на организм. Здравоохранение (Минск). 2016; (6): 41–51.
6. Потемкин Л. А. Медико-биологическое обеспечение и квантовая медицина спорта высших достижений. М.: Изд-во ЗАО «МИЛТА-ПКП ГИТ», 2001; 135 с.
7. Крупаткин А. И., Сидоров В. В. Функциональная диагностика состояния микроциркуляторно-тканевых систем: Колебания, информация, нелинейность. Руководство для врачей. М.: ЛИБРОКОМ, 2014; 498 с.
8. Богослова Т. В. Влияние низкоинтенсивного лазерного излучения на физическую работоспособность студентов института физической культуры [диссертация]. Ярославль, 2004.
9. Осипова Н. В. Сравнительная характеристика влияния низкоинтенсивного лазерного излучения на уровень физической работоспособности студентов различных специализаций спортивного вуза [диссертация]. СПб., 2008.
10. Прокопюк З. Н. Устойчивость организма спортсменов к гипоксии и ее коррекция низкоинтенсивным лазерным воздействием [диссертация]. Смоленск, 2010.
11. Лифке М. В. Динамика гормонального статуса спортсменов различной квалификации, выполняющих физическую нагрузку умеренной мощности на фоне лазерного воздействия [диссертация]. Курск, 2009.
12. Волкова А. А. Влияние низкоинтенсивного лазерного излучения на функциональное состояние организма лыжников-гонщиков [диссертация]. Смоленск, 2011.
13. Павлов С. Е., Разумов А. Н., Павлов А. С. Лазерная стимуляция в медико-биологическом обеспечении подготовки квалифицированных спортсменов. М.: Спорт, 2017; 536 с.
14. Павлов С. Е., Павлов А. С., Петров А. А. Особенности динамики среднегрупповых показателей дисперсионных характеристик функционирования миокарда хоккеистов, использовавших в предстартовой подготовке метод лазерной стимуляции спортивной работоспособности. В сборнике: Олимпийский бюллетень № 15, сост. Мельникова Н. Ю., Трескин А. В., Леонтьева Н. С., Никифорова А. Ю.; М.: Изд-во ЗАО «Олимпийская панорама», 2014; 247–51.
15. Фокин В. Ф., Пономарёва Н. В., Кунцевич Г. И. Электрофизиологические корреляты скорости движения крови по средней мозговой артерии здорового человека. Вестник РАМН. 2013; (10): 57–60.
16. Bollinger A. Is high–frequency flux motion due to respiration or to vasomotion activity? In: A. Bollinger et al. Vasomotion and flow motion. Prog. Appl. Microcirculation. Basel, Karger. 1993; 20: 52–58.
17. Fagrell B. Problems using laser Doppler on the skin in clinical practice. Laser Doppler.– London – Los Angeles – Nicosia: Med – Orion Publishing Company. 1994; 49–54.
18. Федорович А. А. ВЭБ-капилляроскопия — новые возможности мониторирования капиллярного кровотока в коже человека. В сборнике: Материалы XII международной научной конференции «Микроциркуляция и гемореология»; 01–03 июля 2019 г.; Ярославль: Канцлер 2019: 11.
19. Murrey RK et al. Harper's Biochemistry. Appleton & Lange, 1996; 700 p.
20. Daniolos A, Lerner AB, Lerner MR. Action of light on frog pigment cells in culture. Pigment Cell Res. 1990; 3 (1): 38–43.
21. Тамбовский А. Н., Сидоренко Т. А. Некоторые результаты применения внетренировочного средства в процессе подготовки гребцов. Ученые записки университета имени П.Ф. Лесгафта. 2015; 5 (123): 182–85.
22. Кару Т. Й. Первичные и вторичные клеточные механизмы лазерной терапии. В книге: Москвин С. В., Буйлин В. А.,

редакторы. Низкоинтенсивная лазерная терапия. М.: Техника, 2000; с. 71–94.
23. Мальцев А. П. Механизмы действия лазерного излучения на прокариотические клетки. Международный студенческий научный вестник. 2016; (6): 23.
24. Filippin L, Magalhães PJ, Di Benedetto G et al. Stable interactions between mitochondria and endoplasmic reticulum allow rapid accumulation of calcium in a subpopulation of mitochondria. J Biol Chem. 2003; 278 (40): 39224–34.
25. Schaffer M, Sroka R, Fuchs C et al. Biomodulative effects induced by 805 nm laser light irradiation of normal and tumor cells. Journal of Photochemistry and Photobiology B: Biology. 1997; 40 (3): 253–57.
26. Елисеенко В. И. Механизмы взаимодействия низкоэнергетического лазерного излучения ИК-спектра с биологическими тканями В сборнике: Лазеры и аэроионы в медицине под ред. Евстигнеева А. Р., Каплана М. А; Калуга–Обнинск, 1997; 71–2.
27. Крупаткин А. И. Неинвазивная оценка тканевого дыхания у человека с использованием вейвлет-анализа колебаний сатурации крови кислородом и кровотока в микрососудах кожи. Физиология человека. 2012; 38 (4): 67–73.
28. Гаврилова Е. А., Ларинцева О. С. Факторы риска внезапной сердечной смерти спортсменов на разных этапах спортивной подготовки по данным кардиологического обследования. Спортивная медицина: наука и практика. 2018; (2): 33–6.
29. Москвин С. В., Федорова Т. А., Фотеева Т. С. Плазмаферез и лазерное освечивание крови. М.–Тверь: ООО «Изд-во «Триада», 2018; 416 с.
30. Греннер Д. Гормоны, регулирующие метаболизм кальция. В книге: Р. Марри, Д Греннер и др., редакторы. Биохимия человека, том 2. М.: Мир, 1993; с. 193–204.
31. Баевский Р. М. Кибернетический анализ процессов управления сердечным ритмом // Актуальные проблемы физиологии и патологии кровообращения. М.: Медицина, 1976; 161 с.
32. Жемайтите Д. И. Вегетативная реакция синусового узла сердца и здоровых и больных. Анализ сердечного ритма. Вильнюс: Москлас,1982; с. 522.
33. Брук Т. М., Терехов П. А., Осипова Н. В., Зюкин А. В. Эффективность воздействия комплексного применения физических и эргогенных средств на показатели специальной физической подготовленности и анаэробной работоспособности высококвалифицированных спортсменов. Вестник Российской военно-медицинской академии. 2019; 1 (65): 113–9.
34. Тамбовский А. Н., Сидоренко Т. А., Юрьев Ю. Н., Шурманов Е. Г. Влияние комплекса физиотерапевтических средств на организм спортсменов. Ученые записки университета имени П. Ф. Лесгафта. 2015; (5): 123.
35. Елизаров Н. А. Адаптационная кардиопротекция физическими факторами в лечении и профилактике ишемической болезни сердца [диссертация]. М., 2007.
36. Еремеева О. В. Физиологические особенности эффектов биоуправления потенциалами мозга у спортсменов с доминированием метаболического модулятора сердечного ритма [диссертация]. Архангельск, 2012.
37. Jo H-G, Schmitd S, Inacker E, Markowiak M, Hinterberger Th. Meditation and attention: A controlled study on long-term meditators in behavioral performance and event-related potentials of attentional control. International Journal of Psychophysiology. 2016; (99): 33–9.
38. Муллер Т. А., Шилов С. Н. Особенности уровня активации лобной коры и нейрометаболизма головного мозга у детей 7–10 лет с СДВГ. Вестник Новосибирского государственного педагогического университета. 2017; 7 (5): 193–206.
39. Москвин С. В., Кочетков А. В. Эффективные методики лазерной терапии. М.–Тверь: Триада, 2016; 80 с.
40. Павлов С. Е., Павлова Т. Н. Технология подготовки спортсменов. МО, Щелково: Издатель Мархотин П. Ю., 2011; 344 с.